

POLITECNICO DI TORINO

**Corso di Laurea Magistrale
in Ingegneria dei Materiali**

Tesi di Laurea Magistrale

**Comportamento termico dei materiali polimerici per
automotive**



Relatori

Prof.ssa Dr.ssa Roberta Bongiovanni

Dott. Ing. Alessandro Melillo

Candidato

Giovana Correzola Pinto

2018

Acknowledgements

First, I would like to thank both, my thesis advisor, Prof. Roberta Bongiovanni, and my tutor at Dayco Europe, Eng. Alessandro Melillo, for leading, guiding, teaching and helping me every time I had a problem or a question about my research and writing.

Besides Alessandro Melillo, my sincere thanks also go to everyone from Dayco, specially the laboratory technicians Nicola de Simone and Sergio Pioselli. Thank you for being every day there by my side, for the talks and the laughs, for all the coffee and hot chocolate during the coffee breaks, and mainly for everything you thought me during these months. This thesis wouldn't be possible without the three of you.

My profound gratitude also to everyone I had the pleasure to meet and to get to know better during these two years of double degree. All my roommates from both years, my classmates, my Brazilian fellows and all my friends from AEGEE, who made me feel at home in this foreign country and who I can happily say became my Italian family. Each one of you was important in a way or another, not only for this achievement but for making these two years unforgettable. And for this, each one of you will always have a special place in my heart.

Finally, a special thanks to all my family, my parents, my siblings and my boyfriend. Only you know how was the journey to arrive here, you accompanied me through all the obstacles and the successes, and you allowed this dream to become true. Without you all by my side, I wouldn't have become the person I am today, and I wouldn't have been able to pursue my dreams and to accomplish my goals. This thesis is the final chapter of one of the most important and remarkable parts of my life, and I would like to dedicate it to you. You gave me all the means and the support to make it become real and, for this, my most profound and sincere thank you.

Summary

Acknowledgements	ii
1. Introduction	1
2. State of the art on materials for automotive tensioners	2
2.1. Automotive tensioners.....	2
2.2. Materials for automotive tensioners	5
2.3. Thermal characterization of polymers: Differential Scanning Calorimetry (DSC).....	14
2.4. Thermal characterisaiont of polymers: Thermogravimetric Analysis (TGA).....	26
3. Experimental.....	31
3.1. Materials.....	31
3.2. Methods	37
3.2.1. Differential Scanning Calorimetry (DSC).....	37
3.2.2. Thermogravimetric Analysis (TGA)	46
3.2.3. Statistical Analysis with Minitab 18 Software.....	49
4. Results and discussion	52
4.1. DSC - Melting Temperatures	52
4.2. DSC - Content Determination	60
4.3. TGA – Content Determination.....	62
4.4. Statistical Evaluation of the Content Determination	64
5. Conclusions	73
6. Bibliography	74
7. Appendix A	77
8. Appendix B	81
9. Appendix C	82
10. Appendix D	91
11. Appendix E	93
11.1. LM481-17	93
11.2. LM482-17	96
11.3. LM483-17	99
11.4. LM484-17	102
11.5. LM485-17	105
11.6. LM486-17	108
11.7. LM487-17	112

11.8.	LM488-17	115
11.9.	LM489-17	118
11.10.	LM490-17	122
11.11.	LM491-17	126
11.12.	LM492-17	129
11.13.	LM493-17	132
11.14.	LM494-17	136
11.15.	LM495-17	140
11.16.	LM496-17	143
11.17.	LM497-17	147
11.18.	LM498-17	150
11.19.	LM499-17	153
11.20.	LM500-17	157
11.21.	LM501-17	160
11.22.	LM502-17	163
11.23.	LM503-17	166
11.24.	LM504-17	169

1. Introduction

This manuscript consists of a summary and an explanation of the activities carried out during the training period at the R&D Laboratory of Materials at Dayco Europe S.r.l., in Ivrea (Italy). Dayco is a multinational company present in more than 18 countries around the world. It is a global leader in the Original Equipment Market, overseeing research, design, manufacturing and distribution of essential engine products, drive systems and services for automobiles, trucks, construction, agriculture and industry.

The scope of this M.Sc. thesis is the study of physical and chemical properties of the plastic components, mainly spring bushings, produced by Dayco Europe S.r.l., through the performance of several thermal analyses.

In order to understand the properties required during the application of this component, to address the choice of material and to monitor its degradation, the manuscript first presents an introduction to timing belt and accessory tensioners, and their function in an automotive engine. Then, there is an introduction to materials applied in the field, as well as to their main properties, advantages and disadvantages.

The focus of the report, however, is set on the polymeric material used at Dayco Europe S.r.l., supplied by DSM with the commercial name of Stanyl® TW371, that is composed by polyamide (PA46) and polytetrafluorethylene (PTFE). Besides discussing the main properties that allowed this blend to be used in several components and applications inside the automotive sector. The work also brings the still existing issues that regard its degradation and high tendency to absorb moisture.

In addition, it describes the different techniques of thermal analysis and how they can be used to study some important properties of polymers used in the automotive industry. The focus, in this case, is centered on the Differential Scanning Calorimetry (DSC), that was used both to identify the material constituents, by measuring the melting peak temperatures, and to determine their content.

The melting peak temperatures were measured for three groups of samples; the results were analyzed from a statistical point of view, using the statistical software Minitab. It could be confirmed that the utilized method is reproducible.

Thermogravimetric Analysis (TGA), was also performed to determine the composition of a material: results were compared with DSC data and found consistent.

2. State of the art on materials for automotive tensioners

2.1. *Automotive tensioners*

Inside all automotive engines it is possible to distinguish two kinds of tensioner, a main belt tensioner and an accessory tensioner. In general, the tensioner is a device that has the function to ensure that a single long belt, which passes around the engine pulleys, delivers the right amount of tension to them, in a way that they can move properly and drive the engine components, so that everything works as it should. The timing belt tensioner gives the tension to the belt that transmits the rotational movement from the crankshaft to the camshaft, while the accessory tensioner is responsible for powering the single belt that drives the pulleys of the cooling fan, the alternator, the power steering and the air conditioning compressor.

So, considering the scope of a tensioner, the four functional parameters that define the performance of this engine component are: torque, damping, offset and parallelism.

Figure 2.1 shows where the timing belt tensioner is placed inside an automotive engine, while Figure 2.2 brings a schematic exploded view of all its components and their functions, that are indicated through different colors, according to the four parameters previously cited.

The torque is generated by a main spring, fitted in an arm. Therefore, this torque gives the required tension to the belt through a pulley that is forced against it and remains under tension. When subjected to the tension, the belt responds with transitory forces generated by the engine; these forces are damped due to the friction generated in the interface between the metal and the plastic components. So, the damping is necessary to dissipate the vibrations induced on the belt by the engine and therefore to guarantee a certain level of stability.

The offset, instead, is the distance between the engine plane and the pulley; while the parallelism is the angular misalignment between the motor and pulley plane. So, the components that have an influence on the offset and the parallelism have the function to maintain their values within acceptable limits that allow the correct placement of belt during the exercise conditions of the engine.

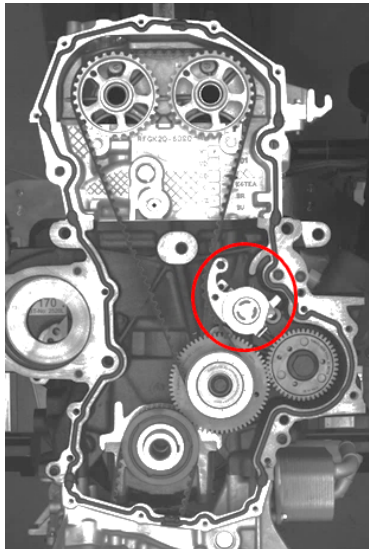


Figure 2.1: Timing belt tensioner system of an engine, with the timing belt tensioner evidenced inside the red circle.

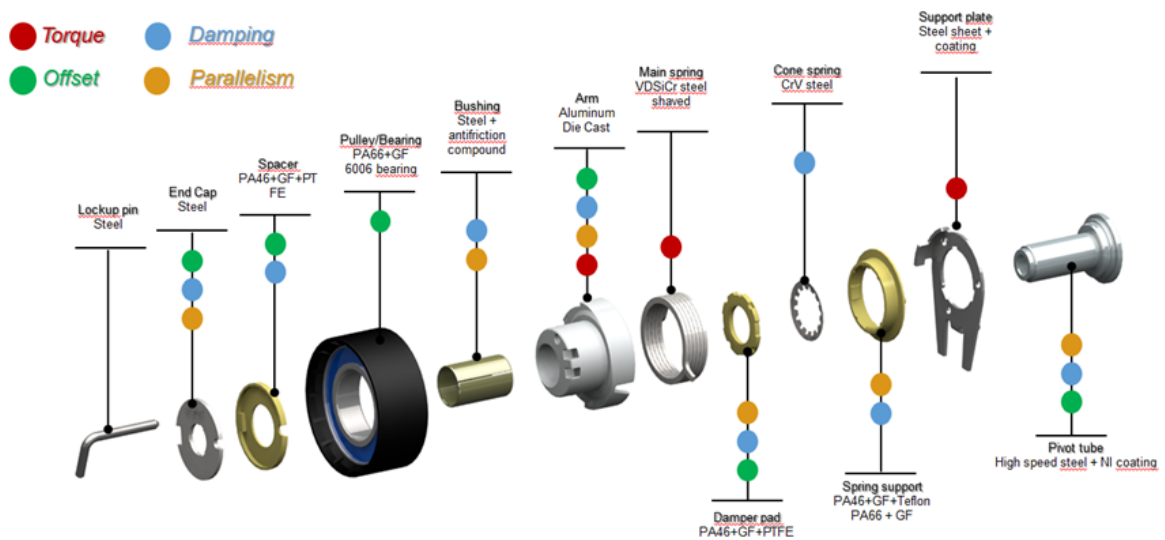


Figure 2.2: Schematic exploded view of all components of a timing belt tensioner and their functions.

The accessory drive tensioners, on the other hand, guarantee the proper operation of the belt connected to the accessory pulleys. But also in this case they are characterized by the four parameters previously cited: torque, parallelism (alignment), damping and offset.

Figure 2.3 shows where the accessory tensioner is placed inside an automotive engine and to which pulleys it is connected; while Figure 2.4 brings a schematic exploded view of all its components and their functions.

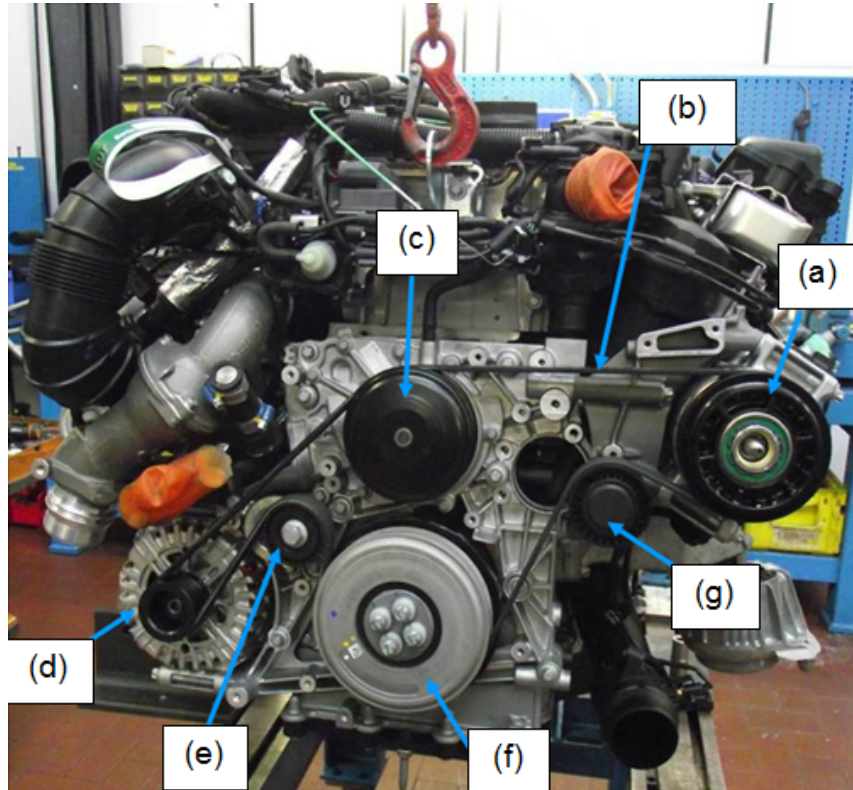


Figure 2.3: (a) Air conditioner pulley; (b) Belt; (c) Water pump pulley; (d) Alternator pulley; (e) Accessory belt tensioner; (f) Crankshaft pulley with decoupler; (g) Accessory tensioner.

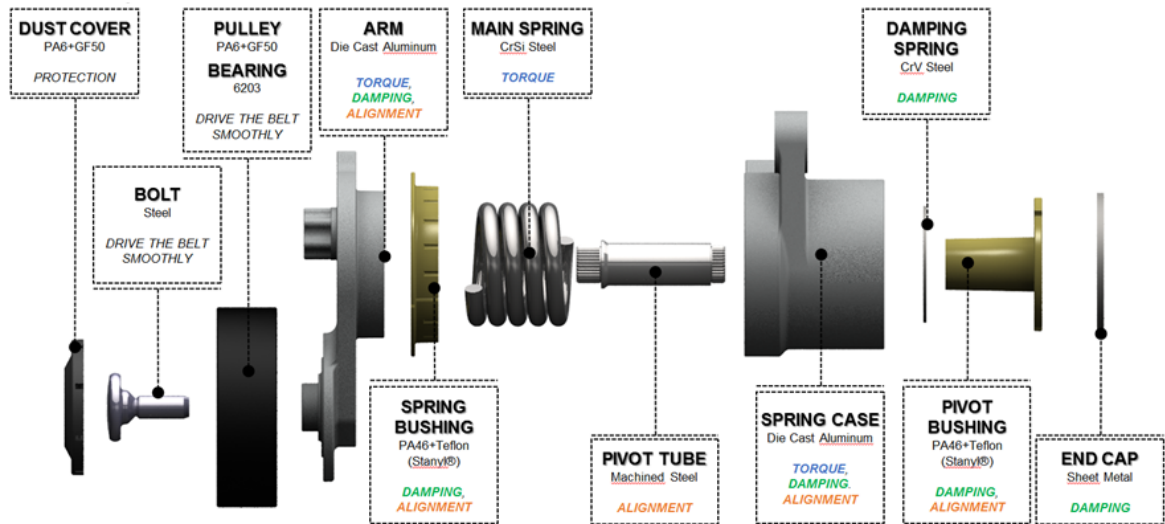


Figure 2.4: Schematic exploded view of all components of an accessory tensioner and their functions.

2.2. *Materials for automotive tensioners*

As showed in Figure 2.2 and Figure 2.4, the production of a tensioner involves the use of a wide range of materials, such as die cast aluminum, steel of several types, and also a variety of polymers, that can be used by their own, or combined with other polymers and additives, like glass fiber for example.

The focus of this M.Sc. thesis, however, is on the physical and chemical properties of the polymers used in the production of automotive tensioners, mainly on the plastic spring bushing component of the accessory tensioners produced by Dayco Europe S.r.l.

The plastic spring bushing is placed between the arm and the main spring of the tensioner, that is in charge of generating the torque that will put the belt in tension. Considering this, its main functions are to provide an interface between the two metal components, allowing their relative movement and damping the transitory forces induced by the engine. Its use is related to the advantages of requiring less lubricant and reducing the vibration and the noise. But to play this role in an efficient way, there are some main properties that are required from the chosen material, such as:

- High heat resistance and thermal stability
- High creep resistance
- High wear, abrasion and friction resistance

Considering these required characteristics, the two groups of materials most largely used, not only for spring bushings but also on other polymeric components of automotive tensioners, are the polyamides (PA) and the polytetrafluorethylene (PTFE), that can be combined between each other to form a blend, or with additives and reinforcing agents, as showed in Figure 2.2 and Figure 2.4, and listed below:

- Spring bushing – polyamide PA46 + PTFE
- Dust cover – polyamide PA6 + glass fiber
- Pivot bushing – polyamide PA46 + PTFE
- End cap spacer and spring support – polyamide PA46 + PTFE + glass fiber
- Pulley – polyamide PA66 + glass fiber

The polyamide resins are a semi crystalline thermoplastic commercially known as Nylon, that are characterized by the presence of an amide group (-CO-NH-) in the main chain. Their basic repeating unit is represented in Figure 2.5.^{[1]-[3]}



Figure 2.5: Generic repeating unit of the polyamides.

The polyamides are obtained from the reaction of polymerization by condensation, that consists of a chemical reaction between the functional groups of the two monomers, with the formation of the repeat unit and the production of a byproduct, such as water. Usually, in this reaction, the rate of conversion is extremely high and at the beginning of the process almost all the monomers are consumed or

transformed in dimers, for example. On the other hand, the rate of chain growth is relatively low compared to the other type of polymerization, by addition.^[4]

This family of polymers can exhibit several structures according to the number of methylene groups and can be classified considering the ratio between this number and the number of amide linkages/groups. Many polyamides are named PAXY, in which X and Y are the amount of carbon atoms on each side of the amide bond, considering the repeat unit. Some common types of polyamides are PA6, PA66, PA11, PA12, PA610, PA612 and PA46.

Figure 2.6 shows the example of the polyamide PA66, produced through the reaction between an amine and a carboxylic acid.^{[4], [5]}

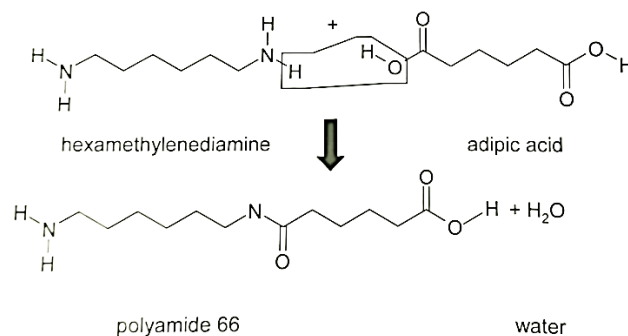


Figure 2.6: Polycondensation process of the PA66.^[5]

On the other hand, the polytetrafluorethylene (PTFE), also known commercially as Teflon, is also a thermoplastic resin, but it is obtained from the polymerization by addition of the tetrafluoroethylene monomer. This type of polymerization consists of three stages – initiation, propagation and termination. Two characteristics of this mechanism of polymerization are the relatively rapid chain growth and the presence of monomer units until the end of the process.^[4]

In the first step, the carbon-carbon bond of the monomer is broken, by a free-radical from a catalyst, the absorption of heat or light, by UV radiation or by electrochemical and mechanical methods, creating an active monomer unit. The second step is the propagation, in which the active monomer reacts with other monomer unit, adding it to the molecular active chain and making it grows gradually by the addition of repeat units, that are attached one at a time. The third and final step is the termination, in which two active centers from different chains react between each other to form one large chain or two chains, one of them with a double bond.^{[4], [6]}

The PTFE polymerization by addition process is showed in Figure 2.7. In this case the polymerization occurs due to the addition of a free-radical initiator, that can be a peroxide, a ferrous sulfate or even oxygen.

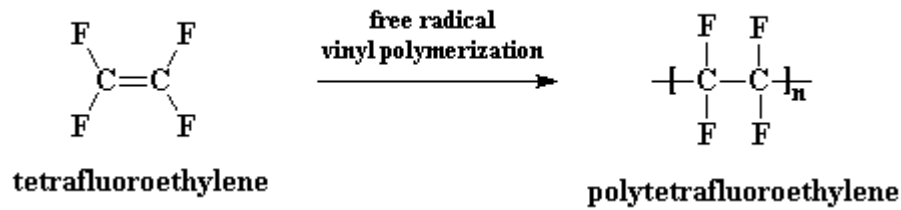


Figure 2.7: Free-radical polyaddition of the tetrafluoroethylene in order to produce the PTFE.^[7]

Also, as mentioned before, both polymers are semi crystalline thermoplastics, that are known for containing linear and branched polymer chains, that are not crosslinked and are joined together only due to weak intermolecular forces (Van der Waals). Usually, on heating, the thermoplastic polymers soften and melt, making themselves capable of being molded and recycled. While on cooling, they become rigid and crystallize, presenting a behavior that depends on the degree of crystallization of the polymer.^{[4], [5]}

The ability to deform, melt and flow is related to the intermolecular forces, that allow the chains to easily turn and stretch under load. Also, the properties of thermoplastic polymers are strongly dependent of the temperature, specially of the glass transition temperature (T_g) and the melting temperature (T_m). T_g is the critical temperature characteristic of the amorphous region of the polymer: on cooling, the T_g corresponds to the point in which occurs the transformation from a liquid to a rubbery material, and finally to a rigid one. So, as shown in Figure 2.8, under the T_g thermoplastics are rigid, on the T_g they become leathery and then with the increasing temperature they become rubbery and liquid.^{[4], [5]}

AT higher temperature than T_m the crystalline phase is lost. In cooling it is restored: the lowest the cooling rate, the highest the degree of crystallinity.^[4]

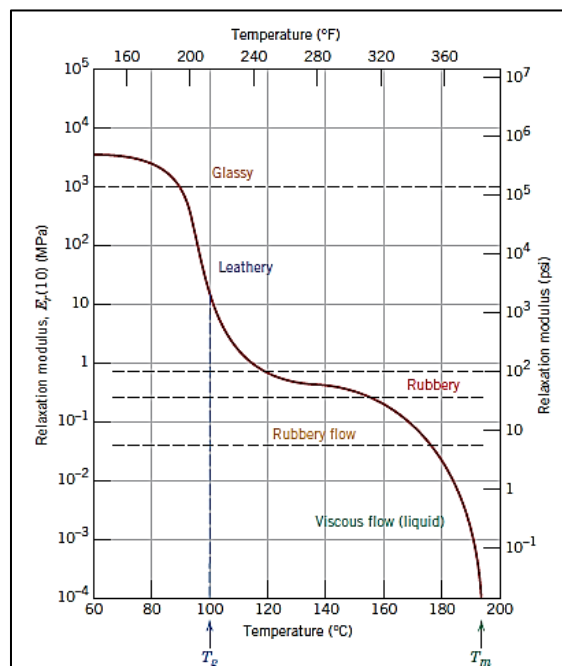


Figure 2.8: Behavior of thermoplastic polymers in function of temperature.^[4]

In Figure 2.9 is possible to analyze the deformation behavior of thermoplastics due to the application of a stress. At the first stage they undergo an instantaneously linear elastic deformation, because of reversible elastic stretches of the entangled chains. But this deformation is also influenced by shifts of entire sections of chains, that are reversible in a long period of time, characterizing a non-linear region of elastic deformation. This phenomenon is also called viscoelasticity, and determines an elastic deformation that is not relaxed immediately after the removal of the stress. Then, if the material is subjected to mechanical forces above the elastic limit (yield point), the macromolecules undergo permanent plastic deformation. In this kind of strain, the chains are disentangled, stretched and oriented parallel to each other, leading to a lateral contraction of the material and the formation of a neck. Finally, this last phenomena reinforce the material and leads to a final increase of the tensile stress before the rupture.^{[4], [5]}

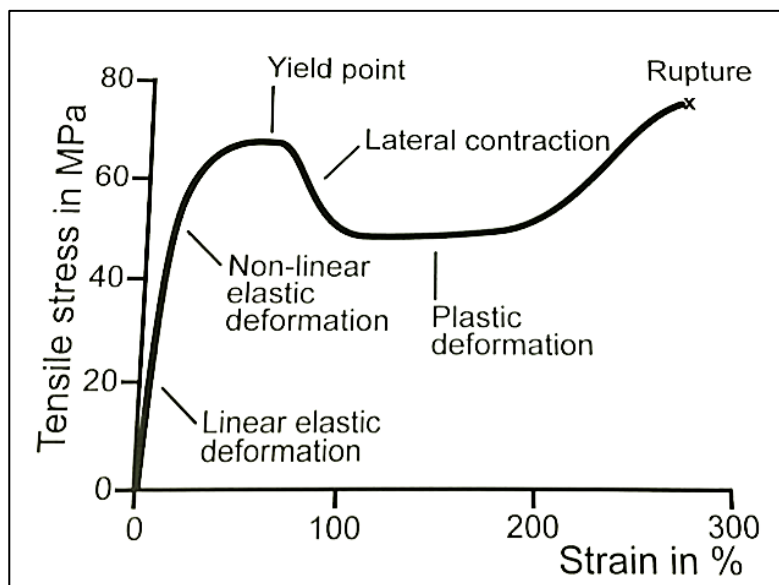


Figure 2.9: Tensile stress-strain curve of thermoplastics.^[5]

The viscoelasticity behavior, previously cited, is typical of thermoplastic materials and is described as the combination of viscous fluids and elastic solids behavior. So, for low temperatures or for stress applied extremely rapid (short period of time), the thermoplastic polymer behaves as an elastic solid, in which the deformation is independent of time and occurs instantaneously when the load is applied or released, as shown in Figure 2.10(b). However, for high temperatures or for stress applied during a long period of time, these materials present a viscous fluids behavior, in which the strain is dependent of time and increases gradually as a response of the load applied. Besides that, once the load is released, the deformation does not recover totally, as seen in Figure 2.10(d).^{[4], [5]}

Therefore, a viscoelastic material will have both, an elastic and a viscous behavior. With the application of a stress, it will respond immediately with an elastic deformation, that later will keep increasing in time due to the viscous behavior. Then, when the stress is released, a fraction of the deformation will instantaneously decrease, and the rest will keep decreasing in time, but it will never return to the original shape again, as shown in Figure 2.10(c).^[4]

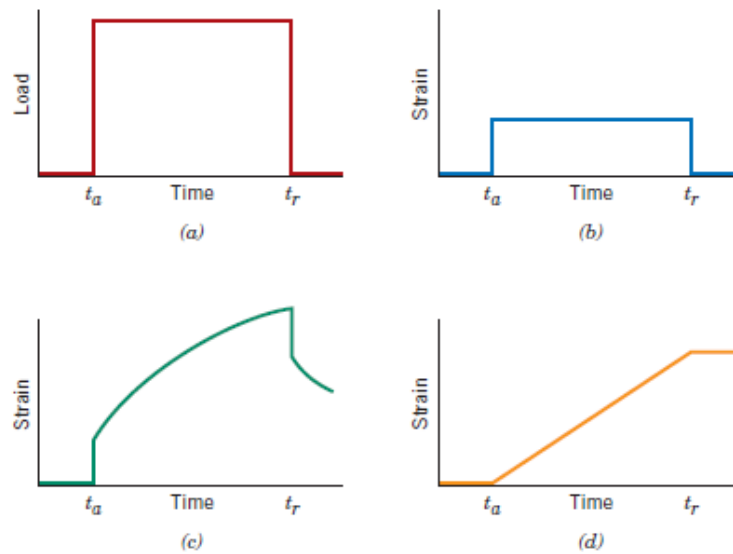


Figure 2.10: The graphs show, when a stress is applied (a), the deformation behavior of elastic solids (b), viscoelastic polymers (c) and viscous fluids (d).^[4]

The phenomena of time-dependent deformation during a constant stress level is called viscoelastic creep. It increases with increasing stress and temperature, and decreases with increasing crystallinity.^[5]

So, considering everything that was said, some important properties of the polyamides that led to its choice for tensioners are:

- High heat resistance
- Excellent creep behavior
- High chemical and oxidative stability
- Good abrasion, wear and friction resistance

Considering the PTFE, on the other hand, it is very famous for its low friction coefficient and low degree of stickiness, that make it the most common thermoplastic internal lubricant. This means that it is very effective to add some amount of PTFE into a polymer matrix in order to have a significant reduction of wear rates and frictional characteristics.

The datasheets of the PTFE and the most common types of polyamide can be found in Appendix A.

The main issue still related to the use of polyamides is the moisture absorption from the environment due to the presence of the amide group (-CONH-) with which the water is bound by hydrogen bonds (N-H).^[1]

The level of water absorption by the polyamides depends on some parameters such as:

- Polyamide type (Ratio Methylene/Amide groups)

Higher the ratio CH₂/NHCO, lower the moisture absorption. This is because there are more hydrophobic methylene groups than amide groups, that can easily bound with water trough hydrogen bonds. So, for example, the moisture absorption of PA46 is much higher compared to PA66 (see Figure 2.11).^[2]

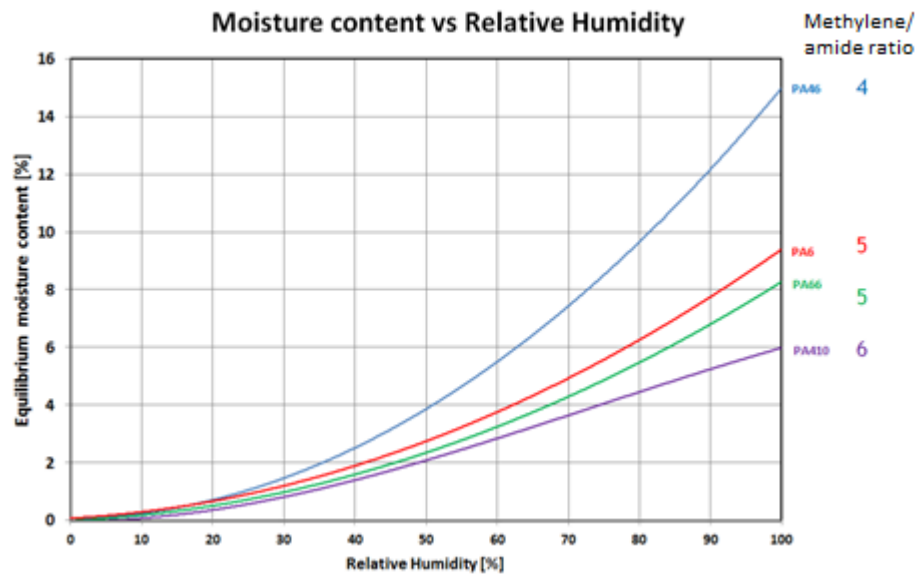


Figure 2.11: Comparison of the moisture absorption of PA46, PA6, PA66 and PA410.^[2]

- Crystallinity - Higher the crystallinity, lower the moisture absorption. This is because the moisture absorption occurs in the amorphous phase, so higher the crystalline phase, lower the probability of absorbing water.^{[2], [8]}
- Density of amorphous phase - Lower the density of the amorphous phase, higher the free volume and higher the moisture absorption.^[9]
- Polyamide content in compound - Higher the polyamide content in the compound, higher the moisture absorption.^[8]
- Environmental conditions - Higher the environmental temperature and humidity, higher the moisture absorption.^[8]
- Thickness - Thinner the component, higher the moisture absorption.^[8]

The moisture absorption by the polyamides can lead to its degradation, which is the term given to all the process that lead to an irreversible modification of the material's structure, affecting its physical and mechanical properties. Some common degrading agents are: temperature, oxygen, UV radiation, chemical agents, water or moisture, ozone, γ -ray, microorganisms and atmospheric pollutants. And some macroscopic factors that can be visually recognized as result of a degradation process are: loss of color on the surface, loss of lucidity, appearance of white spots, formation of cracks and their propagation to the final break.^[10]

There aren't so many studies about how exactly does the degradation of the polyamide by water occurs, but there are some proposed mechanisms that are presented below.

The first possible mechanism of degradation is showed in Figure 2.12, in which a molecule of PA6 reacts with water. The molecule of water breaks two amide bonds (-CO-NH-) and form a separate chain with an amine group in one side and a carboxyl acid in the other side. So, there is both a loss of functional and structural properties.

There is also the possibility that this new chain dehydrates and evolves cyclic amide structure.^[11]

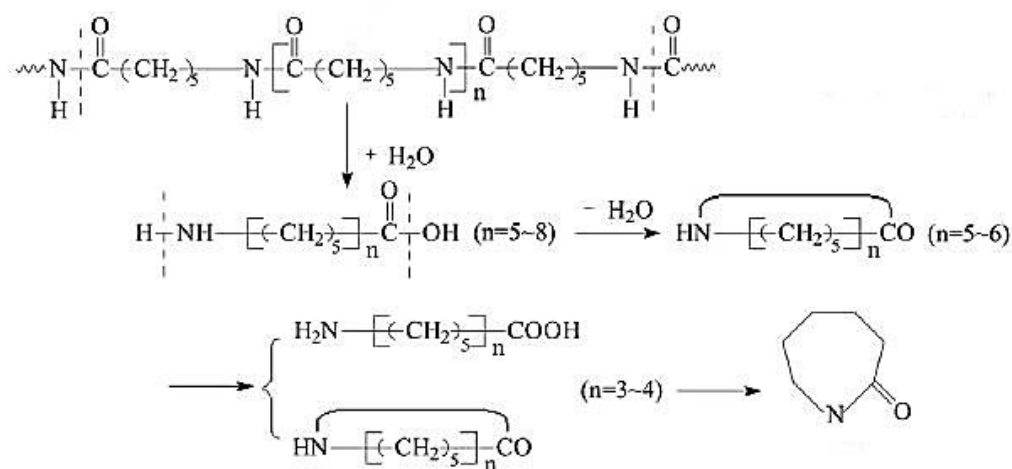


Figure 2.12: Proposed mechanism of degradation by water of PA6.^[11]

The degradation mechanism of the PA66 can be described by an analogue reaction, but in this case the original chain is split in two separated chains in which one has only carboxyl acid groups and the other one has only amine groups, as seen in Figure 2.13.^[12]

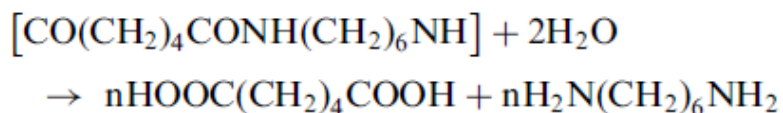


Figure 2.13: Proposed mechanism of degradation by water of PA66.^[12]

In addition, in all cases the breaking of the amide bond (-CO-NH-) is favored under acid conditions, like shown in Figure 2.14 and in Figure 2.15, that shows the example of the degradation of Kevlar in the presence of HCl.^[12]

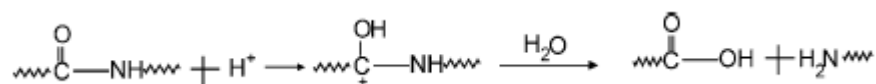


Figure 2.14: Degradation of polyamides under acid condition in the presence of water.^[12]

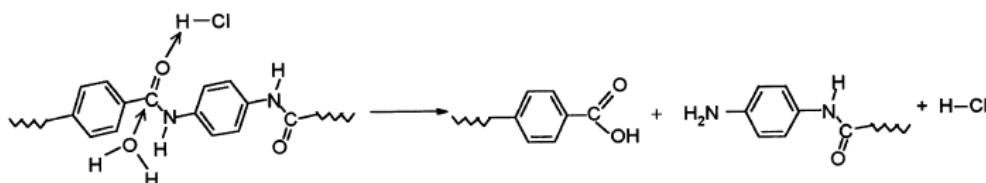


Figure 2.15: Proposed mechanism for the degradation of Kevlar in the presence of water and HCl.^[13]

Some effects of the moisture absorption that can lead to a degradation of the material and to a lower performance are:

- Processing problems

The moisture absorption can change the mechanical properties of the material, leading, at room temperature, to lower stiffness and strength, while increasing toughness. Figure 2.16 shows the variation of the shear modulus of PA46 with different degree of moisture absorption as a function of temperature.^[2]

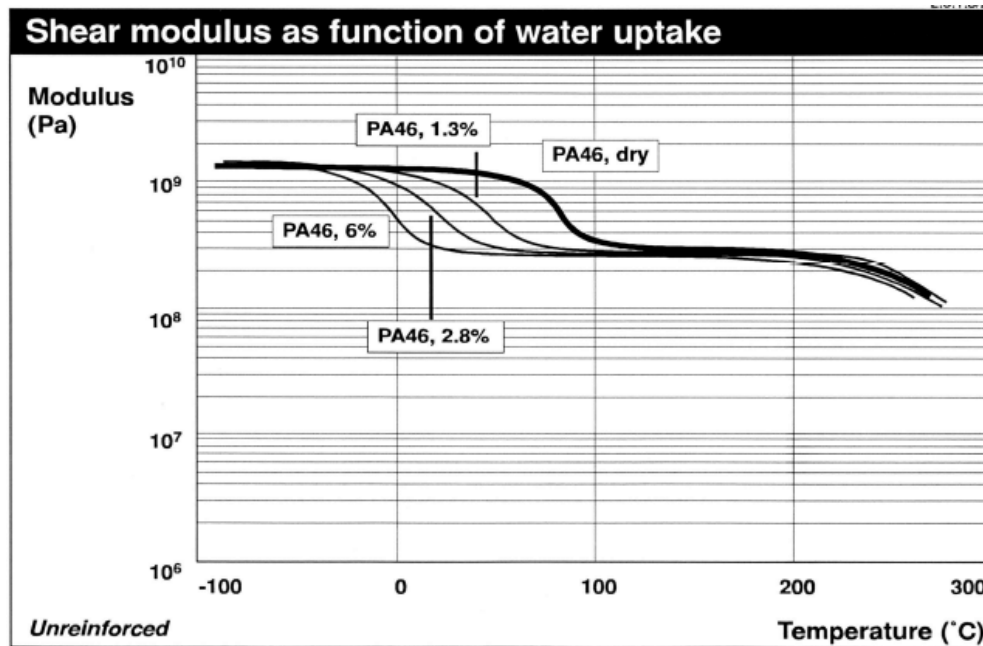


Figure 2.16: Variation of the shear modulus of PA46 with different degree of moisture absorption as a function of temperature.^[2]

- Dimensional change

The dimensional changes of a component due to the absorption of water occur in all three directions, but it is particularly critical in thickness. It also affects the coefficient of linear expansion and the mold shrinkage in the direction of flow. So it is important to know the percentage by which the component will swell before designing the mold.^[14]

Finally, when considering it as the main component of the spring bushings, this dimensional change is one of the main causes of failure, because it exposes the steel interface to the environment, increasing the risk of corrosion.

- Modification of the Tg

As the water softens the glassy amorphous phase, the moisture absorption tends to plasticize the polymer and reduce significantly its glass transition temperature (Tg), that shifts to lower temperatures (see Figure 2.17).^{[2],[15]}

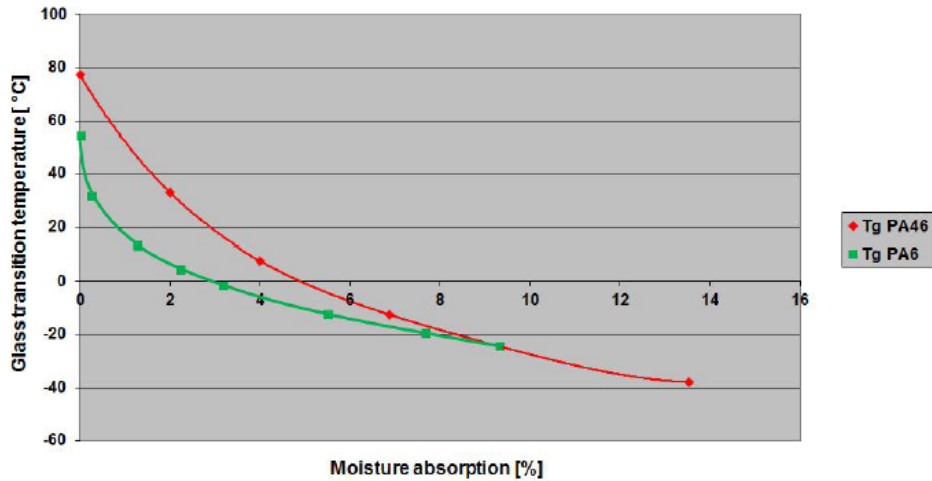


Figure 2.17: Glass transition temperature of PA46 and PA6 as a function of moisture absorption.^[2]

So, to reduce the moisture uptake of these materials and its corresponding effects, it is suitable to subject the final product to a heat treatment called annealing. The annealing is an irreversible heat treatment of the final product, that is performed at high temperatures ($T > 100^{\circ}\text{C}$) and can increase the crystallinity of the polymer and the density of the amorphous phase, reducing the moisture absorption of the material. This reduction depends on the annealing time and temperature and can reach up to a factor of three. As shown in Figure 2.18, higher the temperature and the time of annealing, higher the reduction of moisture absorption.^{[9], [16], [17]}

The most recommended annealing condition, according to DSM, that is the supplier of the polyamides used at Dayco Europe S.r.l., is at a temperature of 230°C for 2 hours under nitrogen atmosphere. However, when a nitrogen atmosphere is not available, it is suitable to perform it at temperatures below 200°C for times longer than 3 hours under air, that is the process used by Dayco to produce the components studied in this project.^[9]

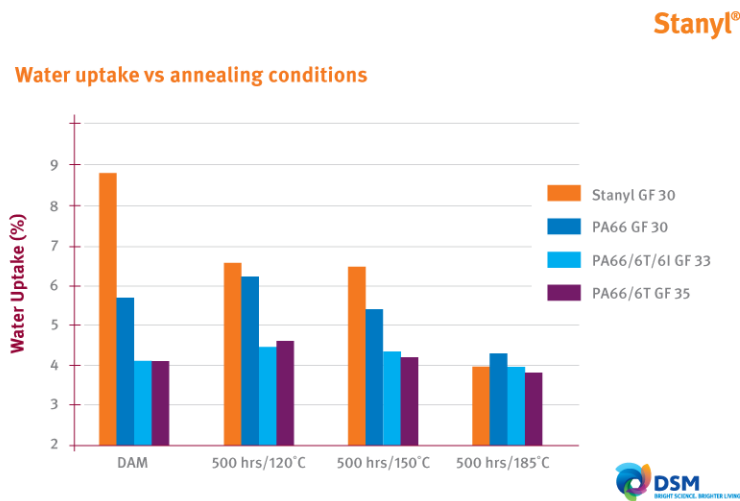


Figure 2.18: Comparison of the reduction of moisture absorption of different polyamides under different annealing conditions: Dry-As-Molded (DAM); after 500hrs at 120°C ; after 500hrs at 150°C ; and after 500hrs at 185°C .^[17]

Besides the reduction of the water uptake, the annealing can also cause some modifications in the material properties, such as:

- Increase in the molecular weight
- Increase in stiffness, yield strength and fatigue, creep and abrasion resistance
- Increase in resistance to salts
- Decrease in elongation, toughness and impact properties
- Decrease in wear resistance, if carried out under air.^{[9], [16]}

Finally, when talking about heat treatments and the application of polymers inside an automotive engine, one should also pay attention to another very common mechanism of degradation of these materials, the thermal degradation.

The thermal degradation involves all the processes in which the temperature is the main degrading agent, and it occurs when the energy provided by the environment is sufficient to split the chemical bonds of the molecule, i.e. when it is sufficient to exceed the activation energy, that is equal to the energy of the bond itself. The most common bonds in polymers (C-C, C-H, C-N, C-O...) break down into temperatures between 150 and 500 °C. Besides the temperature, the degradation process is also influenced by the heating rate used to reach that temperature.^[10]

Usually, at lower temperatures there is a loss of functional properties, in which there are rearrangements or chemical reactions (elimination, condensation, cyclization) of the lateral substituents, while the main chain remains untouched. However, at higher temperatures the main chain starts to split and to form free-radicals, leading to a decrease of the degree of polymerization and to the formation of monomer or chain fragments. In this case, a loss of structural properties is observed. The breaking of the main chain can occur in different ways according to the type of polymer. Vinyl polymers, produced by polyaddition undergo a primary dissociation of the carbon-carbon bond; while high polar polymers with functional groups in the main chain, produced by polycondensation, undergo an ionic dissociation.^{[10], [12]}

2.3. Thermal characterization of polymers: Differential Scanning Calorimetry (DSC)

The Differential Scanning Calorimetry technique measures the heat flow in a sample, in comparison with a reference crucible, when both are heated, cooled or held in a constant temperature. It is capable of detect endothermic and exothermic effects, measure transition and reaction enthalpies, and determine peak temperatures and specific heat capacity, that can be used to determine some important properties such as:

- Fusion or melting temperature and enthalpy
- Crystallization behavior and supercooling
- Solid-solid and glass transitions
- Degradation and chemical reactions
- Oxidation decomposition and stability.^{[5], [18]}

According to the literature, the sample preparation for a DSC analysis must be done paying attention to some aspects such as:

- Thermal contact

The optimum thermal contact between sample and crucible is necessary in order to reduce the thermal gradients, avoid the smearing of sharp effects and increasing the repeatability of the results. In order to achieve the optimal conditions, there are some standard ways of lying the different kinds of sample inside the crucible. For example, fine powders and liquids must be distributed uniformly at the bottom of the crucible; samples with an irregular side must be lied with the flat side facing downward; irregular and tough materials must be milled into fine powder; and so on.^{[5], [19]}

- External contamination

The contamination can happen either with the sample or with its decomposition products, and it must be avoided in all cases. In addition to the contamination of the crucible, it is also important to never place the sample material directly in contact with the sensor, or it will also contaminate and cause even worse artifacts.^{[5], [19]}

- Atmosphere influence

It is important to control the atmosphere gas composition and the interaction between sample and gas. The atmosphere influence can vary according to crucible used. Some possibilities are the use of an open crucible, a self-generated atmosphere or an hermetically sealed crucible.^[5]

In the first possibility, the sample comes into contact with the atmosphere inside the equipment, and the measurement is performed under isobaric conditions. In this case, the sample evaporates before the boiling point is reached, as seen in Figure 2.19, that brings some typical DSC measurement curves. Since there is always the risk of contamination and damaging of the measurement cell, the crucible can be covered with a lid in which a hole is made, creating a self-generated atmosphere. The hole allows a restricted gas exchange, that is necessary to determine the boiling point of the liquid and to prevent its prematurely evaporation. Finally, if the sample is hermetically sealed in the crucible, there is an endothermic evaporation and a high increase in pressure, due to the formation of decomposition products. So in this case there is no boiling point.^[5]

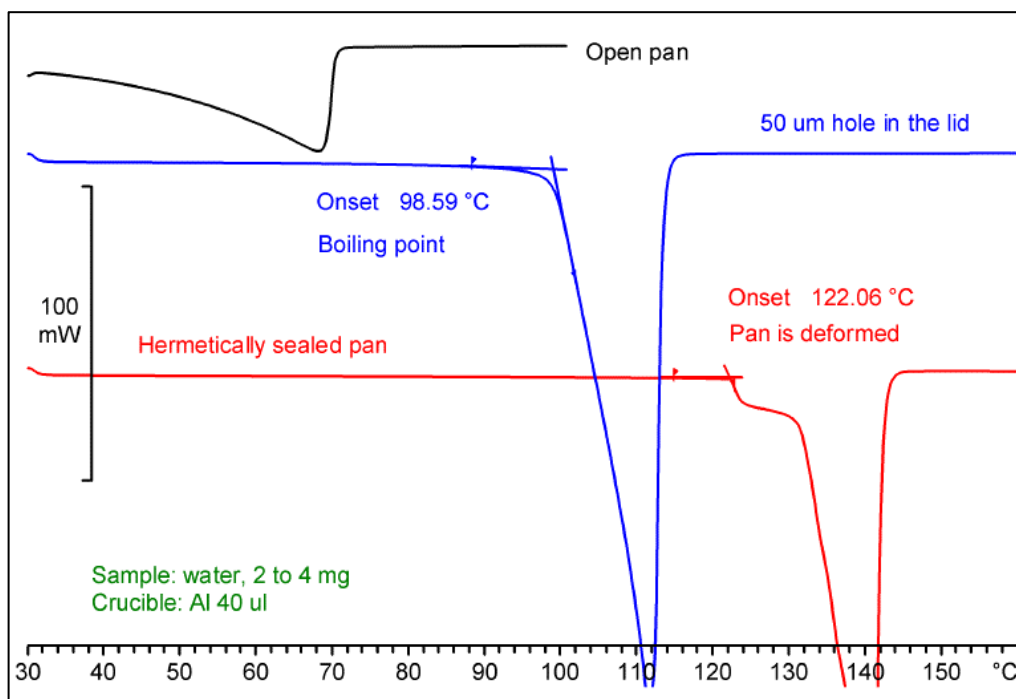


Figure 2.19: DSC curves of water in different atmospheres.^[19]

Then after the measurement, it is always recommended to weight the sample and compare the value with the initial one to see if there was some kind of reaction or decomposition. The degradation of the sample due to the extreme conditions of the measurement can also be evaluated from its visual aspect.

Finally, the standard weight of the samples used in the DSC analysis are:

- Organic samples – 5 to 10 mg
- Inorganic samples – 10 to 50 mg
- Unknown or dangerous samples – 0.5 to 1 mg.^[19]

Besides the sample, it is also important to pay attention to the chosen crucible. The crucibles are used to contain the sample and avoid its direct contact with the DSC sensor. Some aspects taken into consideration before choosing the crucible material are:

- The crucible material must be inert, i.e. it can't react with the sample in any way during the whole process of measurement.
- Crucible of non-inert material can be used only if the aim is the study of the sample's reactivity.
- The crucible material must have a melting temperature much higher than the range of temperature used to study the sample.
- Both sample and reference crucibles must be from the same material.^{[5]. [19]}

The most common crucibles are shown in Figure 2.20:

- Standard 40 μ L aluminum crucible – it is the most used crucible, because aluminum is largely inert, but as it can in some cases react, usually it is heated at 400°C for 10 minutes before the beginning of the measurement to form a protective oxide layer.

- Light 20 μL aluminum crucible – used for films and powdered samples to give an improved peak separation.
- 30, 70 and 150 μL platinum crucibles
- 40 μL gold crucible
- 120 μL middle pressure (2 MPa) steel crucible
- High pressure (15 MPa) steel/gold crucible – used to study chemicals reactions, because it certifies that the sample will reach the reaction temperature, instead of evaporate as it would happen in the aluminum crucible.^{[5], [19]}

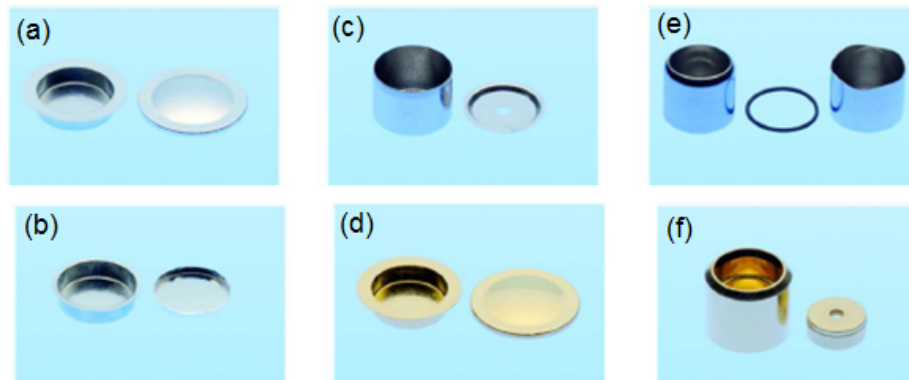


Figure 2.20: Different types of crucibles that can be used in the DSC measurement.^[19]

The results obtained from the DSC can be evaluated through the study of the measurement curve in order to determine and calculate the parameters of interest, such as: characteristic temperatures; enthalpy changes; specific heat capacity; composition and purity; conversion curves, and so on.

First of all, according to literature, an endothermic peak will correspond to a melting process if:

- There is no significant reduction of sample's mass.
- There are visual effects of melting process, like melt pool.
- The peak's half-width is significantly less than 10K.^[5]

As showed in Figure 2.21, some possible endothermic peaks are:

- a) Pure substance – the low-temperature side of the peak is a practically a straight line (because the melting temperature is a constant) and the melting point is given by the onset temperature, that is the extrapolated temperature determined by the intersection between the tangent to baseline and the tangent to the low temperature side of the peak.
- b) Substance with eutectic impurities – there are two peaks, the first one corresponding to the eutectic transition and the second one to the melting process. The eutectic peak increases with increasing impurity and can also not be observed if it is amorphous. In this case the melting point is given by the peak temperature.
- c) Semi crystalline plastic – impure and polymeric substances exhibit a concave low-temperature side and broader melting peaks due to the size distribution of the crystallites. Also in this case the melting point is given by the peak temperature.

- d) Exothermic decomposition on melting
- e) Endothermic decomposition on melting
- f) Liquid crystals – it is similar to pure substance's peaks, but it can present small sharp peaks due to mesophase transitions.^{[5], [20]}

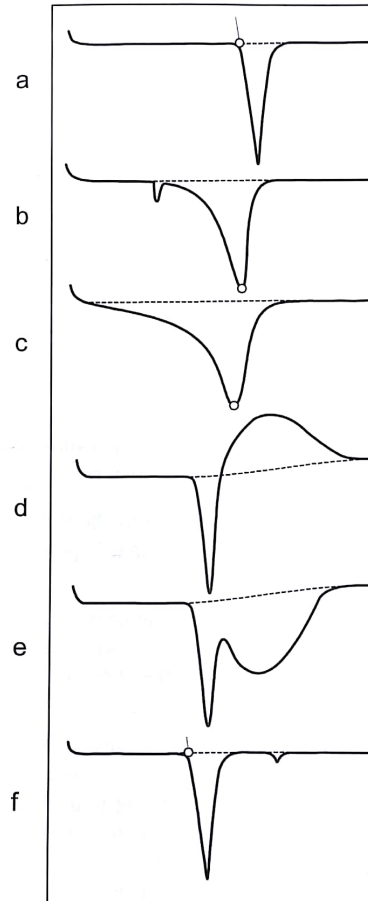


Figure 2.21: Possible endothermic peaks in a DSC analysis.^[5]

On the other hand, the glass transition of an amorphous material leads to an increase of its specific heat capacity, shifting the DSC curve in the endothermic direction (downwards). The glass transition usually covers a temperature range of 10 to 30K and is not characterized by a peak, but by a step. The exception is the relaxation peak that sometimes may occur if the sample has been stored for a long time below the T_g . Other two important characteristics are the fact that the radius of curvature at the onset is much higher than at the end set, and the curve slopes in the endothermic direction before the transition but is almost horizontal afterward. All these characteristics are shown in Figure 2.22.^{[4], [5], [20]}

- a) Glass transition
- b) Glass transition with enthalpy relaxation
- c) Reverse transition – the enthalpy relaxation peak is not observed
- d) Curie transition.^{[5], [20]}

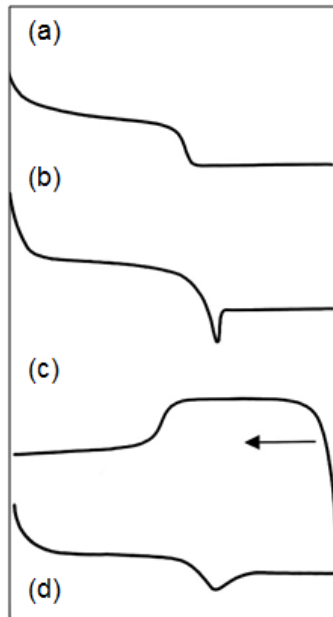


Figure 2.22: Possible DSC peaks for the glass transition.^[5]

The characteristic temperatures of a DSC analysis are obtained by the intersection points between baselines and tangents drawn on the curve, in correspondence of thermal effects' peaks and steps, as shown in Figure 2.23.^[5]

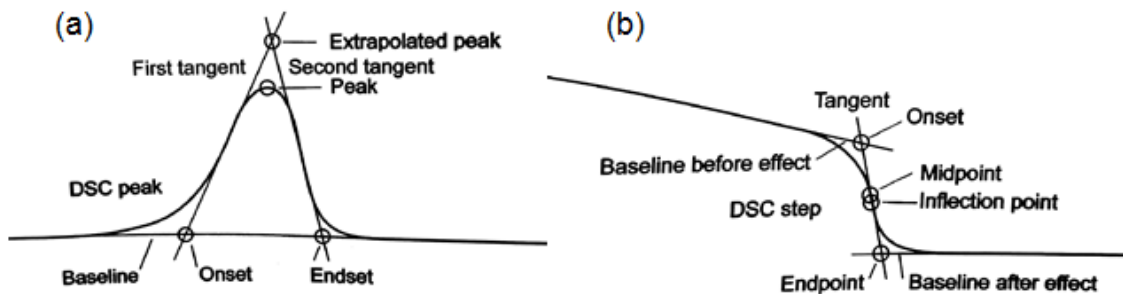


Figure 2.23: Characteristic points of DSC peak-like (a) and step-like (b) deviations.^[5]

- **Peak:** Deviation of an ideal straight line of the curve, that corresponds to a thermal effect. The peak height is given by the greatest vertical distance of a point on the measurement curve from the corresponding baseline point. The peak height is given in the selected ordinate unit, while the peak temperature corresponds to the abscise value of that point.^[5]
- **Onset:** It is given by the point of intersection of the baseline before the thermal effect and the first tangent (tangent to the low-temperature side of the peak). The onset point determines the extrapolated starting temperature of the thermal effect.^[5]
- **End set:** It is given by the point of intersection of the baseline after the thermal effect and the second tangent (tangent to the high-temperature side of the peak). The end set point determines the extrapolated end temperature of the thermal effect.^[5]

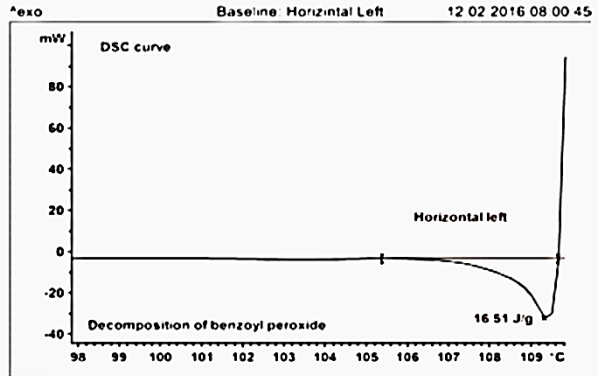
- Extrapolated peak: Corresponds to the point of intersection of the first and second tangents.^[5]
- Baseline: The baselines, as the name says, are the ideal straight lines that represent the base of a peak and are interpolated in a way that they leave the DSC curve tangentially before the thermal effect and rejoin it, also tangentially, after the thermal effect. But practically they are not always straight, and they can be drawn in many ways according to the shape of the curve and to the thermal effect to be evaluated. An important aspect is that they can't cross the measurement curves or be discontinuous. An overview of the main types of baseline is shown in Table 2.1.^{[5], [21]}

Table 2.1: Overview of possible baseline types.^{[5], [21]}

Baseline Type	Description and Applications	Example
Line	Default straight baseline. Typical of thermal effects with constant increase of c_p , or with a constant value of c_p .	
Tangential left	Extension of the tangent to the curve before the thermal effect. Used when melting peaks are followed by decomposition effects.	
Tangential right	Extension of the tangent to the curve after the thermal effect. Typical of the melting process of semi crystalline polymers with significant c_p temperature function below the melting range.	

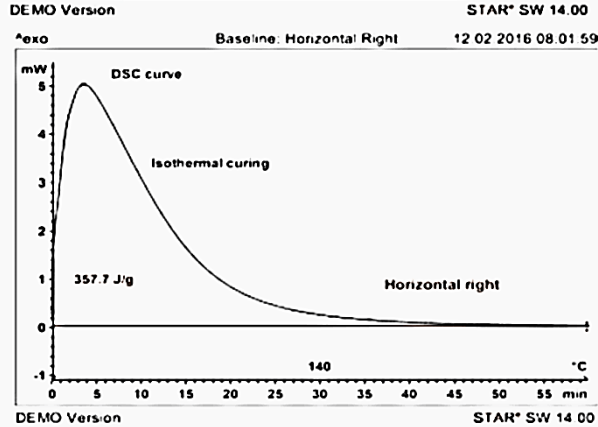
Horizontal left

Extension of the horizontal line of the curve before the thermal effect. Typical of substance's decomposition effects.



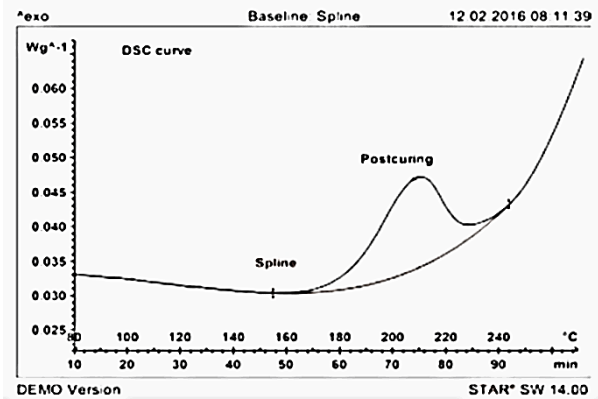
Horizontal right

Extension of the horizontal line of the curve after the thermal effect. Used for isothermal reactions, melting of plastics and DSC purity determination.



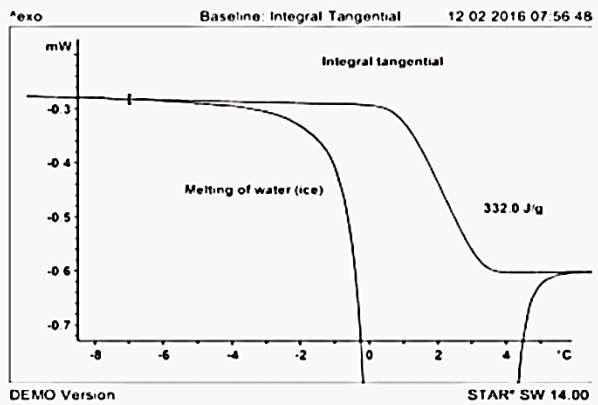
Spline

Used with overlapping effects, it is based on the tangents left and right, and it is manually interpolated using a flexible ruler.



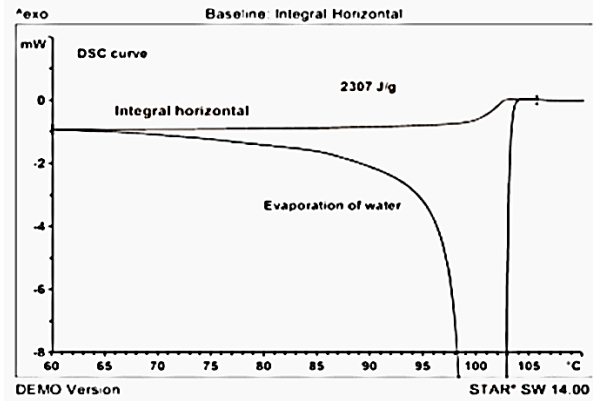
Integral tangential

It is obtained through an iterative process that calculates and normalizes an integral between a trial baseline and the measured curve, always basing on the tangents left and right. Used when the c_p temperature function is different before and after the thermal effect.



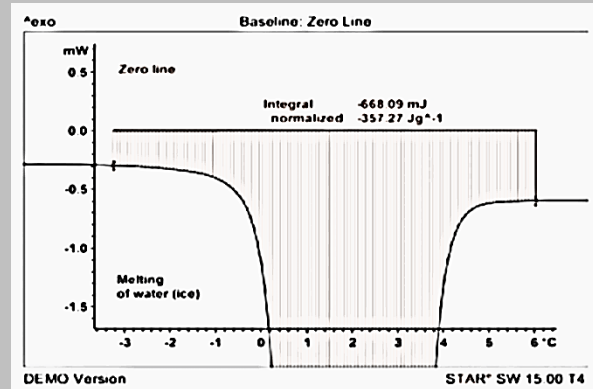
Integral horizontal

It is also obtained through the iterative process, and it is used with samples whose heat capacity undergoes a significant change, e.g. through vaporization and decomposition. The baseline always begins and ends horizontally.



Zero line

Horizontal line that intersects the ordinate at the zero point. It requires subtraction of a blank curve. Used for the determination of transition enthalpies including sensible heat.



- Midpoint: The midpoint is characteristic of steps on the measurement curve and can be defined in different ways, as shown in Figure 2.24. [5], [19], [22]

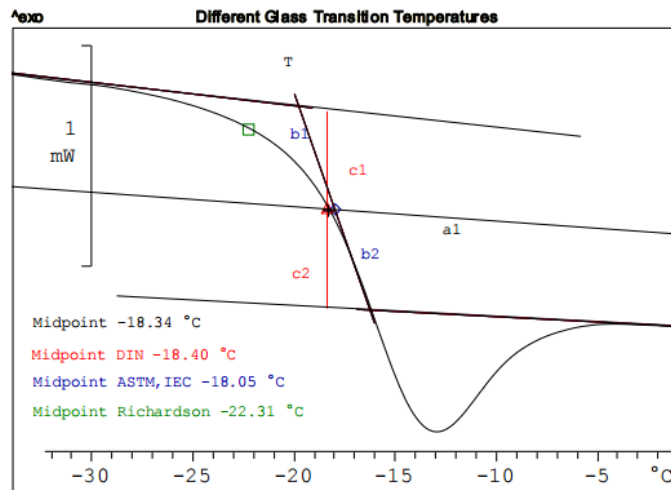


Figure 2.24: Methods for calculating the midpoint of a step on the DSC measurement curve. [22]

- Mettler (ISO) – it uses the bisector, a1, of the angle between the tangents to the onset and to the end set (above and below the glass transition). The midpoint is the intersection of this line with the measured curve.

- DIN – it is the point at which the measured curve is equidistant between the upper and lower tangents ($c1 = c2$). $c1$ is the distance between the measured curve and the tangent to the onset (below the glass transition). $c2$ is the distance between the measured curve and the tangent to the end set (above the glass transition).
- ASTM – a tangent is drawn at the point of inflection of the measured curve, and the midpoint is the mean value between onset and end set of this inflectional tangent ($b1 = b2$).
- Richardson – it considers the areas underlying the extrapolated tangents to the measurement curve, as shown in Figure 2.25.^{[5], [19], [22]}

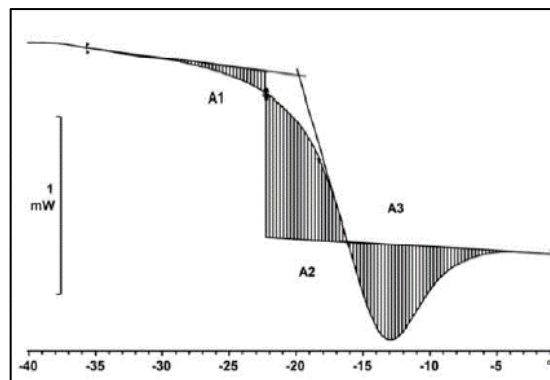


Figure 2.25: Calculation of the midpoint through the Richardson method.^[5]

In addition, these methods can also be used to calculate the step height, that gives information about the material composition. For example, a step height of 0,5 J/gK is typical of an amorphous polymer, while lower values are a result of the presence of crystals and glass fibers, for example.^[19]

- Inflection point: Point in which occurs the inflection of the curve.
- Glass transition:

The glass transition is exhibited on the DSC measurement curve as a step-like thermal effect, because it changes the mobility of the molecules and the c_p of the sample. In addition to the step, an endothermic relaxation peak can or cannot be observed, depending on the heating rate used.^[5]

Usually the glass transition is characterized by the glass transition temperature (T_g), the height of the c_p step (Δc_p) and the width of the glass transition (Δt). The T_g is calculated as the temperature at the midpoint of the step, that can be determined by the methods previously explained (see Figure 2.24), that influence also the calculus of the step height. The width of the glass transition, on the other hand, is calculated as the difference between the onset and the end set temperatures, as shown in Figure 2.26.^[5]

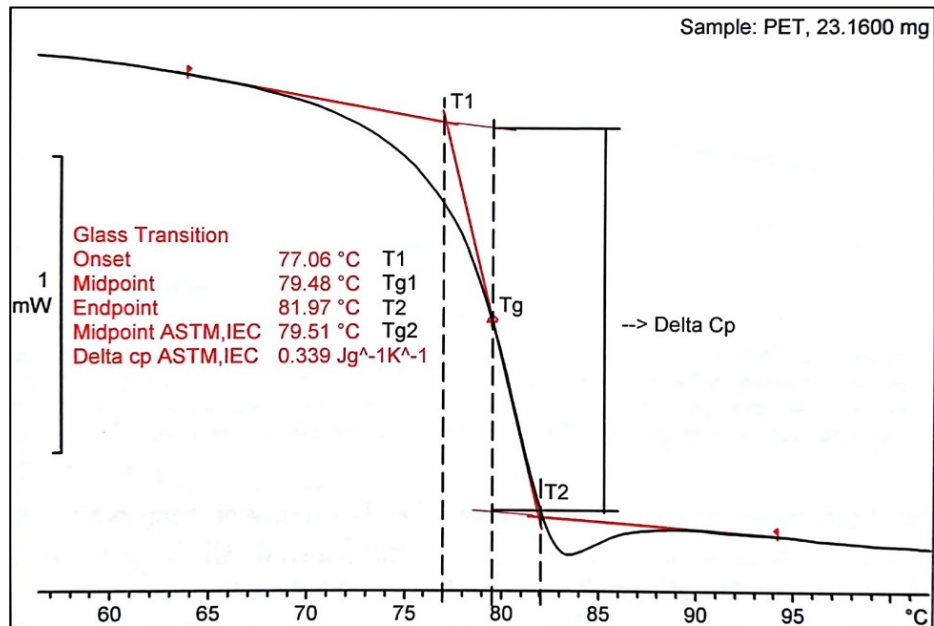


Figure 2.26: Main parameters used to characterize the glass transition effect.^[5]

So, considering the DSC analysis, the procedure to calculate the T_g involves first the selection of the optional results and standard test method (midpoint determination method), the setting of the evaluation range (that will be the baseline limits), and the choice of the evaluation method, that can be either the glass transition evaluation or the glass transition with relaxation peak evaluation. With these parameters, the DSC software is able to calculate the two tangential baselines, the bisector of the angle between the two baselines and the inflectional tangent at the point of greatest slope, that will be used to determine and calculate the parameters of interest.^[5]

It is also important to remember that the glass transition is not a thermodynamic fixed point, it depends on the heating and cooling rate, on the thermal and mechanical history of the sample and on the method used to determine it.^{[4], [5]}

Some factors that can influence the glass transition are:

- Crystallinity – increasing crystallinity leads to a smaller step height, a higher T_g and a broader width.
- Crosslinking and molar mass – the increase of these parameters shifts the T_g to higher temperatures.
- Additives – the presence of plasticizers shifts T_g to lower temperatures, while the presence of fillers decreases the step height.
- Blends and copolymers – compatible blends give one T_g in the interval between the T_g of its pure components, while an incompatible blend gives two separated transitions.
- Chemical modification – it can lead to changes in the T_g, step height and transition width.^{[4], [5]}

- Enthalpy:

As shown in Equation 2.1, the enthalpy change of a sample from T₁ to T₂ corresponds exactly to the quantity of heat converted and can be calculated as the

integral of the heat flow with respect to time, either if the DSC curve is plotted against time or temperature. Graphically the area integrated corresponds to the area between the DSC measurement curve and the chosen baseline.^[5]

$$\Delta H = \int_1^2 \phi dt = \int_1^2 \frac{dH}{dt} dt \quad (2.1)$$

For the correct determination and integration of the peak area, is necessary to define the type of baseline, to select the desired results and to define the evaluation range, i.e. the integration and the baseline limits. All the possible results of a DSC integration can be observed in Figure 2.27.^[5]

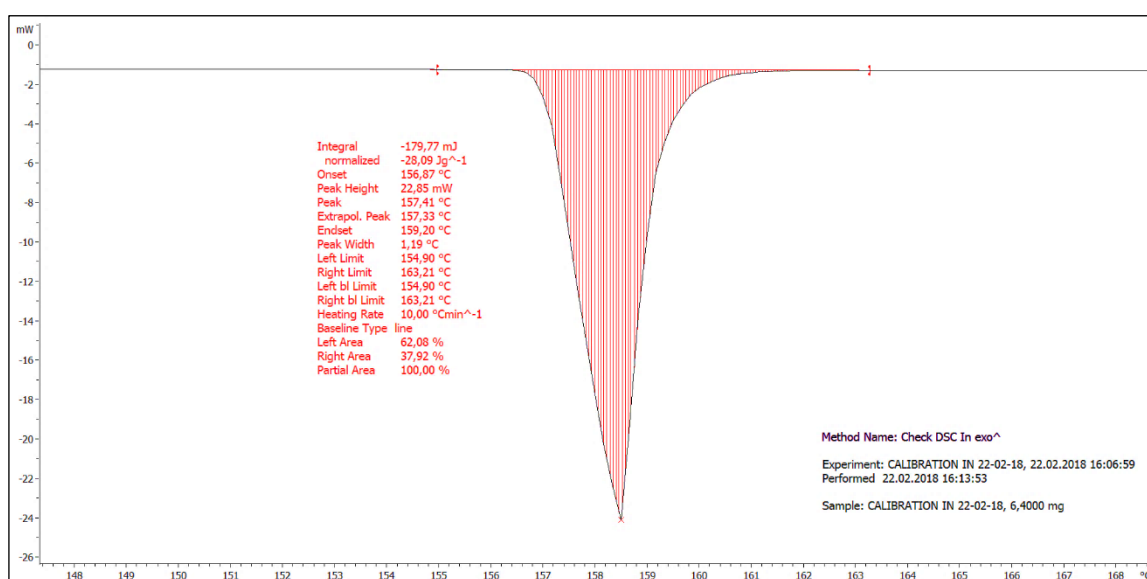


Figure 2.27: Complete set of results obtained from a DSC peak integration.^[5]

- Content determination

As explained before, the DSC peak areas are proportionally to the content (C) of the component of interest, that have undergone a physical or chemical transition. The proportionality constant is the transition or reaction enthalpy (ΔH), as shown in Equation 2.2.^[5]

$$C = \frac{\Delta H_{measured}}{\Delta H_{100\%}} 100\% \quad (2.2)$$

Some components that can be measured in this way are freezable free water, peroxides, moisture, degree of cure of thermosets α -quartz and the degree of crystallinity, for example.^[5]

2.4. Thermal characterisation of polymers: Thermogravimetric Analysis (TGA)

The TGA is a thermoanalytical technique that uses a thermogravimetric analyzer to measure the mass of a sample as a function of the sample's temperature or the time (in an isothermal measurement). It is important to say that actually the instrument measures the weight of the sample, as a force, and then convert it to its mass.^{[5], [23], [24]}

The results of a TGA measurement are displayed in a TGA curve in which mass is plotted against temperature or time, allowing the study of the sample's decomposition processes and the quantitative determination of its individual constituents. In addition, it is common to display also the DTG curve, i.e. the first derivative of the TGA curve with respect to temperature or time, that shows the rate of mass variation. Figure 2.28 shows typical TGA/DTG curves, in which each variation of the sample's mass is observed as a step on the TGA curve and as a peak on the DTG curve.^{[5], [23], [24]}

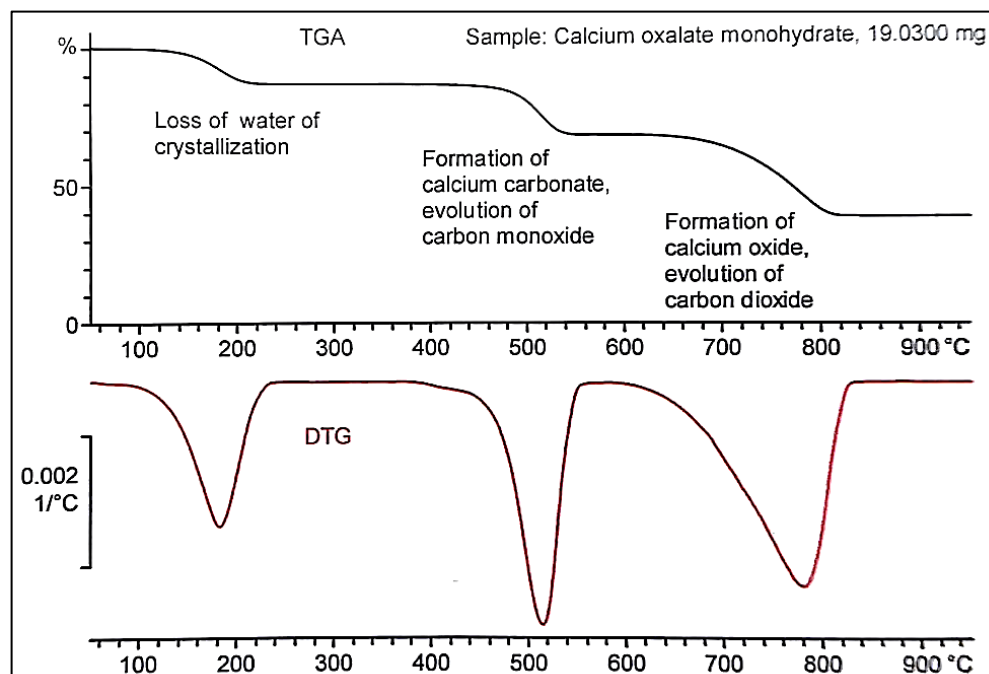


Figure 2.28: Example of typical TGA (Thermogravimetric Analysis) and DTG (Differential Thermogravimetric) curves.^[5]

Some thermal effects that can lead to a gain or a loss of mass in the sample are:

- Evaporation of volatile constituents
- Oxidation of metals
- Oxidative decomposition of organic substances
- Thermal decomposition (pyrolysis)
- Heterogeneous chemical reactions
- Change of magnetic field in ferromagnetic materials.^[5]

Finally, the main parameters that can be determined by a TGA analysis are: composition, thermal stability, decomposition, stoichiometry and kinetics of reactions, evaporation, adsorption and desorption processes...^{[5], [19], [24]}

According to the literature, the sample preparation for the TGA must be done with a consistent and reproducible method, because both the sample's morphology and its mass influence the results of the measurement. The morphology can affect the heat transfer within the sample and change the diffusion rate of reaction products, while the mass used determines the rate of mass loss of the sample (see Figure 2.29).^{[5], [19]}

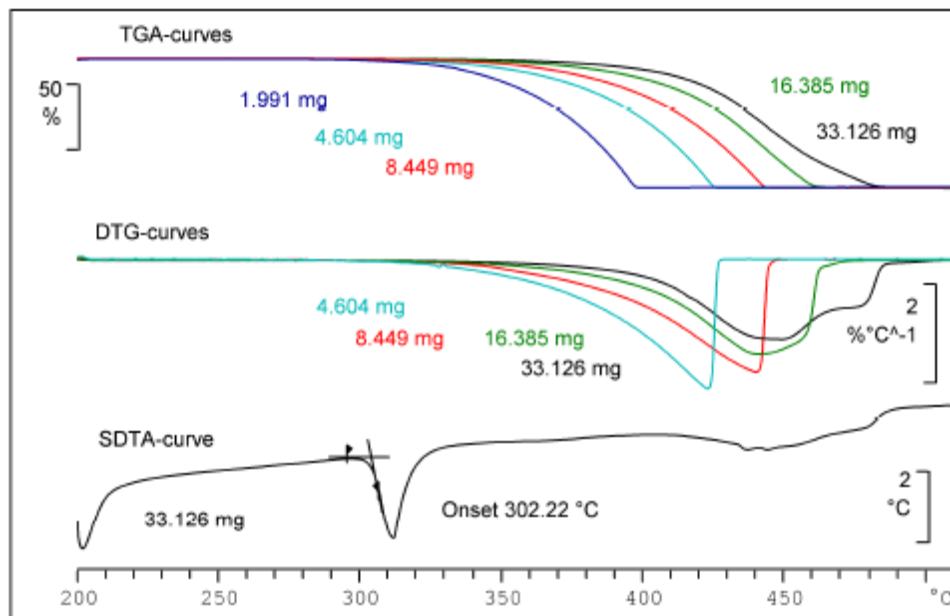


Figure 2.29: Influence of the sample's mass on the heating rate and the TGA/DTG curves obtained. The graph also shows the SDTA curve, that stands to Single Differential Thermal Analysis and calculates the difference between the measured temperature of the sample and a reference temperature given by the temperature program of the software.^[19]

The weight of the sample can be measured using an external separated balance (optimizes time), the TGA balance (ensure weight stability), or using an automatic weight with a sample robot (for a large number of samples).^[19]

So, some factors that always need to be respected are:

- The sample should be representative of the bulk of the analyzed material.
- The mass of the sample should be sufficient to achieve the precision required for the test.
- The sample should be changed as little as possible by the sample preparation process.
- The sample should not be contaminated.^[5]

Regarding the crucibles used in the TGA measurement, these are quite similar to those used in the DSC analysis. As this analysis requires an open system, the crucibles can be used either totally opened or in a self-generated atmosphere, i.e. sealed with a lid on which a very small hole is made. This last method is more suitable because, as the hole is made immediately before the start of the measurement, it prevents the sample from eventually contaminations. However it has

the disadvantage of shifting the mass loss to higher temperatures, due to an increase in the pressure, delaying the start of the reactions.^[5]

Some factors that are required when choosing a crucible are:

- The crucible's material should not react with the sample.
- The crucible should ensure the thermal contact with the sample; i.e. it cannot allow the sample to move.
- The crucible should reduce the temperature gradients in the sample.
- For a better thermal conductivity, it is suitable the use of a metal crucible.^[5]
^[19]

The main types of crucibles are shown in Figure 2.30.

- a) Alumina – found in several dimensions; they can be used in the whole temperature range (until 1600°C) without problems. The lid can also be in alumina with a hole, or even in aluminum for unstable samples.
- b) Platinum – with a great thermal conductivity; they are suitable for high temperature measurements. A sapphire disk is inserted between the crucible and its holder, because both are made of Pt, and they can sticky irreversible together. Besides this, as Pt is not always inert, it is also used as a catalyst for combustion reactions, for example.
- c) Sapphire – with an excellent thermal stability; they are commonly used with high melting point metals.^[5] ^[19]



Figure 2.30: Examples of types of crucibles. From the left to the right, alumina, platinum and sapphire crucibles.^[19]

In general, the evaluation of a TGA measurement curve consists in the determination and calculation of height of the observed steps. But this can be a problem when dealing with successive and partly overlapping effects. This is why it is very recommended to present the results also on a DTG curve, because it is easier to distinct the peaks.^[5]

The determination of the steps can be done both manually and automatically, always respecting the rule that the sum of all steps plus the residual mass is equal to the sample's initial mass (100%).^[5]

As shown in Figure 2.31, the steps can be separated by their corresponding baselines, that are always horizontal and tangent to the measurement curve. So the step height will be the distance between two successive baselines.^[5]

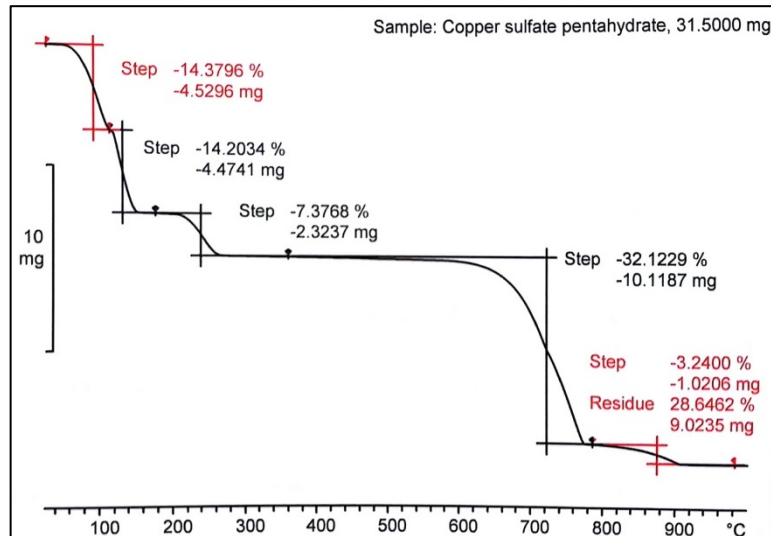


Figure 2.31: Step separation in a TGA measurement curve, using horizontal baselines. ^[5]

On the other hand, if the decomposition steps are extremely sharp, the tangential baseline method is used for the determination and separation of the steps, as shown in Figure 2.32. ^[5]

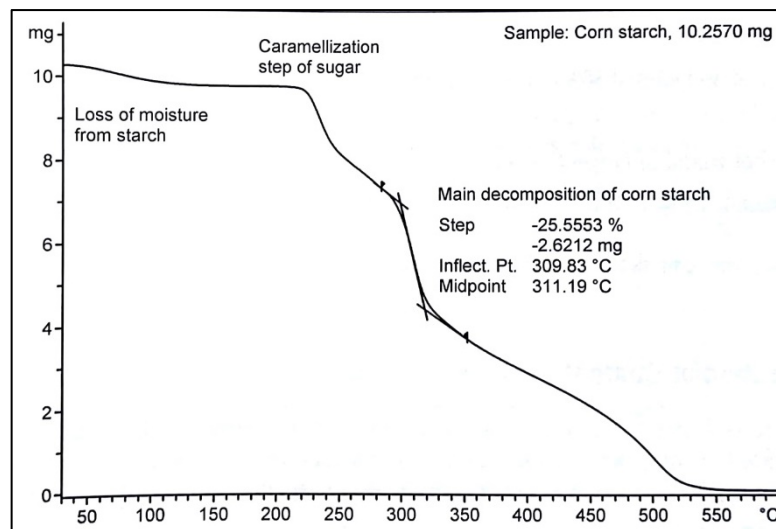


Figure 2.32: Step separation in a TGA measurement curve, using tangential baselines. ^[5]

Once the steps are defined, it is possible to obtain the following parameters, that are used to calculate the content and check the stoichiometry of the reactions.

- Residual mass at the end of a step
- Tangential onset and end set
- Point of inflection and midpoint at 50% of the step height
- Heating rate
- Sample temperature and segment time. ^[5]

Then, the step height can be used to determine a constituent content. The possible cases are:

- Constituent of interest is totally consumed during the measurement. It is the easiest case and the percentage content (G) is calculated as the ratio between the mass loss (Δm) and the initial mass (m_o), as shown in Equation 2.3. ^[5]

$$G(\%) = \frac{\Delta m}{m_o} \cdot 100\% \quad (2.3)$$

- Constituent of interest is part of a stoichiometry reaction and undergoes a partial loss of mass. In this case some other parameters need to be considered such as the molar mass of the eliminated gas (M_{gas}), the molar mass of the original constituent of interest (M) and the number of moles of gas eliminated for each mole of sample material (n), like shown in Equation 2.4. ^[5]

$$G(\%) = \frac{\Delta m}{m_o} \cdot \frac{M}{n \cdot M_{gas}} 100\% \quad (2.4)$$

- Constituent of interest is part of a non-stoichiometric reaction or a group of complex reactions and require an empirical determination of its content. It is done by calculating an empirical reference step (R_{emp}), determined through the TGA analysis of a reference sample of known content under the same measurement conditions. As shown in Equation 4.7, it is given by the ratio between the mass loss step (Δm_r in %) and the product of the sample's mass (m) and the content of the reference sample (G_o in %). ^[5]

$$R_{emp} = \frac{\Delta m_r}{m \cdot G_o} \quad (2.5)$$

So, once the empirical reference step is calculated, it can be used to determinate the empirical content of the constituent of interest, as shown in Equation 2.6. ^[5]

$$G(\%) = \frac{\Delta m}{m_o \cdot R_{emp}} \cdot 100\% \quad (2.6)$$

3. Experimental

3.1. Materials

The most common material used to produce spring bushings in Dayco's laboratories around the world is a blend of polyamide PA46 and polytetrafluoroethylene (PTFE), nominally in the proportion of 85% and 15% respectively. This material is supplied by DSM and it is commercially known as Stanyl® TW371. The material certificate can be found in Appendix B, while Table 3.1 and Table 3.2 show the main properties of the polyamide PA46 and the polytetrafluoroethylene (PTFE) used in the blend.

Table 3.1: Description of PA46. ^{[2], [25]}

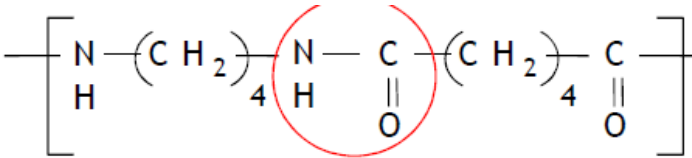
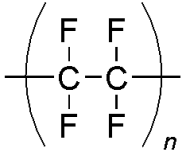
PA46	
Commercial name	Stanyl®
Ratio methylene/amide	4
Molecular structure	
Tm (°C)	290-295
Tg (°C)	80-94
Decomposition Temperature (°C)	-
Crystallinity (%)	70-80
Density (g/cm³)	1.18-1.21
Young's Modulus (MPa)	3300
Coef. of Linear Thermal Expansion (*10⁻⁶/K)	70-80
Specific Heat Capacity (J/(g.K))	2.1 – 2.8
Thermal Conductivity (W/(m.K))	0.3
Melting Enthalpy (J/g)	83.6

Table 3.2: Description of PTFE. ^{[1], [25], [26]}

PTFE	
Molecular structure	
Tm (°C)	325-330
Tg (°C)	125-130
Decomposition Temperature (°C)	576-585
Crystallinity (%)	70-80
Density (g/cm³)	2.13-2.23
Young's Modulus (MPa)	400-750
Coef. of Linear Thermal Expansion (*10⁻⁶/K)	100-150
Specific Heat Capacity (J/(g.K))	1.0
Thermal Conductivity (W/(m.K))	0.23-0.25
Melting Enthalpy (J/g)	41-82

In this project, 24 specimens of plastic spring bushings from the same production lot of the same supplier were analyzed through both a Differential Scanning Calorimetry (DSC) and a Thermogravimetric Analysis (TGA) in order to control the variation of the chemical composition, physical properties and dimensions. The samples were named, and will be referred in this project, following Dayco's laboratory codes from LM481-17 to LM504-17, as shown in Figure 3.1 and listed in Table 3.3.



Figure 3.1: Plastic spring bushing samples LM481-17 to LM504-17.

Considering the sampling for the DSC, a total of 72 samples were taken. Three samples from each one of the 24 spring bushings subjected to test, that were divided in three groups, called Group 1, 2 and 3. The First Group had already been taken and analyzed by Dayco's R&D Laboratory technician Nicola De Simone; while the Second and Third Groups were analyzed during the execution of this thesis.

Then, each sample was submitted to a DSC analysis, that also in this case was divided in three groups. So, to summarize, the performed DSC analyses were:

- Analysis 1 – analysis of samples from Group 1, named from LM481-17-1 to LM504-17-1, previously performed by Dayco's R&D Laboratory technician Nicola De Simone.
- Analysis 2 – analysis of samples from Group 2, named from LM481-17-2 to LM504-17-2, performed during the execution of this thesis at Dayco's R&D Laboratory in Ivrea, Italy.
- Analysis 3 – analysis of samples from Group 3, named from LM481-17-3 to LM504-17-3, performed during the execution of this thesis at Dayco's R&D Laboratory in Ivrea, Italy.

The sampling for the TGA, on the other hand, was made in the laboratory of Dayco, in Ivrea, where a sample of each one of the 24 spring bushings was taken, without having its weight measured, and was delivered for analysis in the laboratory of Dayco in Chieti.

Regarding the dimensional parameters of the plastic spring bushings, Figure 3.3 shows their technical drawing with the nominal values of all the dimensional measurements. In addition, the thickness of all 24 specimens were measured, in 6 different points, in order to see its variation. These points are showed in Figure 3.2 and correspond all to section C of Detail Z in Figure 3.3, that is the wear zone of interest and has a nominal thickness of $1,5 \pm 0,05$ mm. In Appendix C it is possible to find a photo of each plastic spring bushing back and forward, and also the values of thickness measured in all six points showed in Figure 3.2.

Table 3.3 shows both, the weight of the 72 samples taken and divided in Groups 1, 2 and 3, and also the average value of thickness.

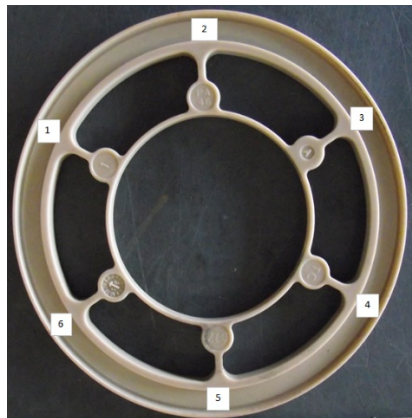


Figure 3.2: Points of the wear zone in which the thickness was measured for all 24 plastic spring bushing samples.

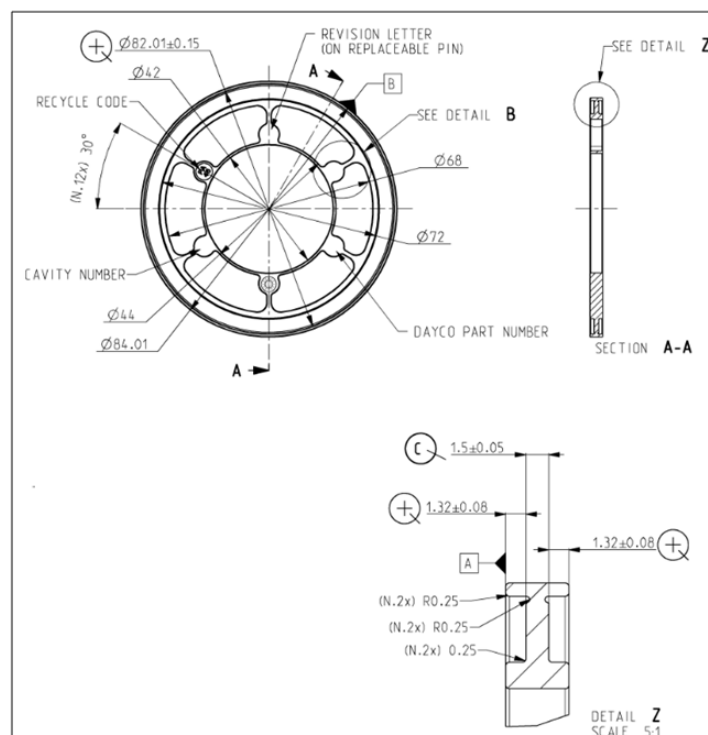


Figure 3.3: Technical drawing number TC072AA of the spring bushings used in 21757081 Volvo engines.

Table 3.3: Measured average thickness and weight of the 72 samples that will be analyzed through the DSC in Analyses 1, 2 and 3.

Samples	Average Thickness [mm]	Weight of samples for DSC Analyses 1, 2 and 3		
		Group 1 [mg]	Group 2 [mg]	Group 3 [mg]
LM481-17	1,455	7,6	6,7	5,8
LM482-17	1,455	6,5	7,4	7,8
LM483-17	1,456	5,1	5,8	8,9
LM484-17	1,458	7,6	8,2	7,9
LM485-17	1,460	8,7	8,1	5,8
LM486-17	1,464	8,5	5,9	7,1
LM487-17	1,466	7,0	6,8	7,6
LM488-17	1,462	5,8	5,9	5,4
LM489-17	1,458	7,5	7,2	5,8
LM490-17	1,463	8,7	7,0	5,1
LM491-17	1,466	7,4	6,1	8,6
LM492-17	1,458	8,3	6,9	7,1
LM493-17	1,456	5,6	8,2	8,2
LM494-17	1,465	7,3	8,3	7,2
LM495-17	1,456	5,9	8,1	7,0
LM496-17	1,456	5,5	7,8	8,3
LM497-17	1,464	6,3	7,1	6,7
LM498-17	1,456	8,9	6,7	6,3
LM499-17	1,453	7,8	8,7	8,3
LM500-17	1,456	9,2	8,8	7,2
LM501-17	1,460	7,1	7,6	7,6
LM502-17	1,461	9,5	7,1	8,3
LM503-17	1,460	5,0	7,0	7,2
LM504-17	1,456	6,8	9,5	7,4

So, considering the procedure explained in Section 2.3, the preparation of the 72 samples for DSC Analyses 1, 2 and 3 was performed following the steps described below.

- With the help of a cutting plier, three samples from each plastic spring bushing were properly taken, labeled and saved in separated glass recipients, as shown in Figure 3.4.



Figure 3.4: Sample preparation method. It is possible to see the original spring bushing component, the two small samples extracted with the use of a cutting plier, the glass recipients in which the samples were stored and the corresponding labels used to identify them.

- All the 72 samples were then weighted using a high precise balance with a resolution of 0.0001g (see Figure 3.5). The weights measured are shown in Table 3.3 and will later be used as an input in the STAR^e software, to calculate the enthalpy.



Figure 3.5: Left- glass recipients properly labeled with the corresponding sample. Right - high precise balance used to weight the samples.^[18]

- Each sample was then placed inside an Aluminum 40 μ L crucible (code ME-26763), that was closed with the corresponding lid and sealed with a Mettler Toledo's crucible sealing press. To seal the crucible, one just needs to place it on the crucible holder of the sealing press and turn the press handle 360° (see Figure 3.6).

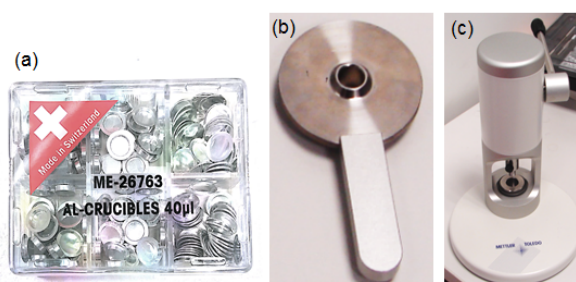


Figure 3.6: (a) Aluminum 40 μ L crucibles and lids; (b) Crucible holder; (c) Mettler Toledo's crucible sealing press.^[18]

- After sealed, the crucible's lid was pierced with a needle (see Figure 3.7) in order to allow the exit of the gas during the experiment, and to create the self-generated atmosphere. It is suitable to pierce the lid immediately before placing it inside the DSC analyzer, so that the risks of contamination will be reduced.



Figure 3.7: Needles used to make the hole on the crucible's lid.^[18]

- At this point the sample is ready to be analyzed. So, after starting the DSC equipment and setting the parameters of the desired measurement, it can be placed on the sensor disk, on the left side of the reference crucible. The procedure is shown in Figure 3.8.

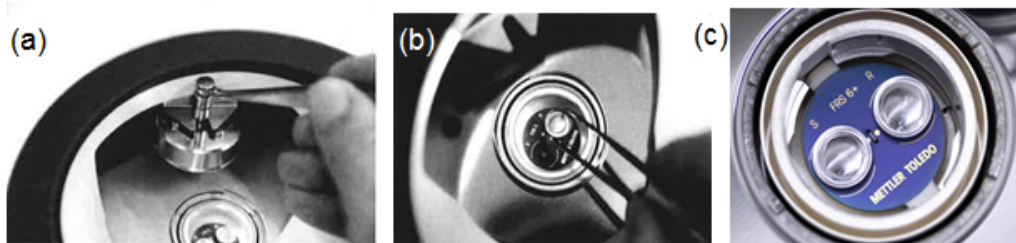


Figure 3.8: (a) Removal of the furnace cover; (b) Sample's crucible placement on the left side of the reference crucible; (c) Correct placement of the sample, where the sensor disk is marked with the letter S.^[18]

- Once both crucibles are on the sensor disk, inside the DSC furnace, it can be closed and the measurement can start.

The sampling for the TGA, on the other hand, was performed following the steps described below.

- In the DAYCO EUROPE SRL's laboratory in Ivrea, Italy, with the help of a cutting plier, a sample from each plastic spring bushing were properly taken, labeled from LM481-17 to LM504-17 and saved in separated glass recipients, as shown in Figure 3.9.



Figure 3.9: Preparation of the samples used in the TGA.

- The 24 samples were then sent to the DAYCO EUROPE SRL's laboratory in Chieti, Italy, where they were properly weighted and analyzed.

3.2. Methods

3.2.1. Differential Scanning Calorimetry (DSC)

The DSC equipment can be basically described as a heat flow measuring cell equipped with ceramic sensors. As shown in Figure 3.10, the equipment is composed by a very small furnace made of pure silver with electrical flat heater, and equipped with a Pt100 thermal sensor. Inside the furnace, a thin disk of glass ceramic material connects the silver plate with a star-shaped sensor disk (FRS5 or HSS7) equipped with 56 thermocouples that are responsible for measuring the heat flows of the sample and the reference crucible with an extremely high sensitivity and resolution. Besides these features there is also a cooling attachment, that can be an air cooling, a circulator cryostat, a liquid nitrogen...^[5]

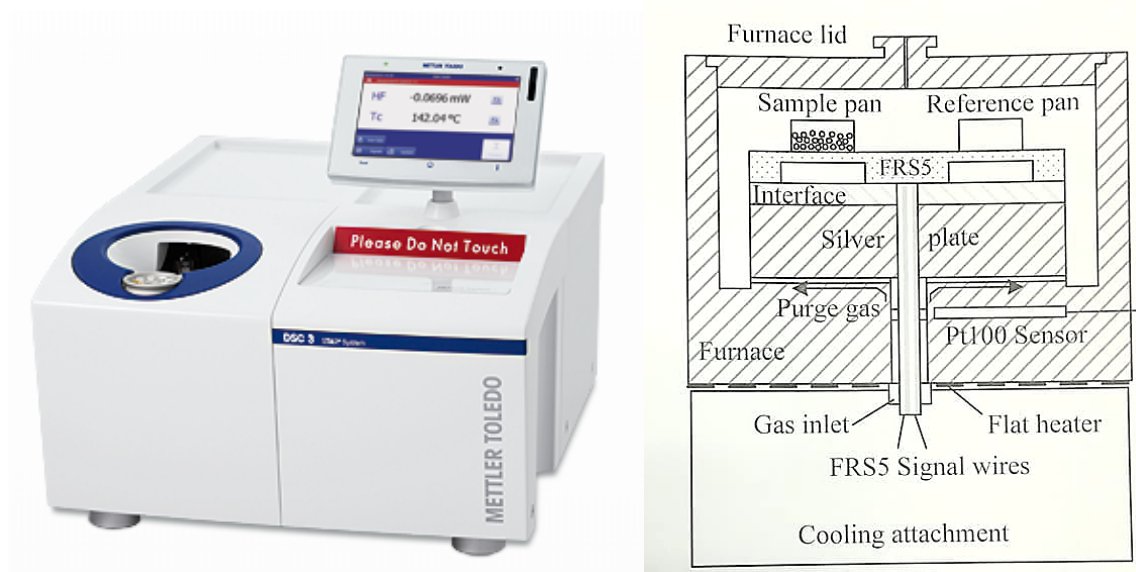


Figure 3.10: DSC equipment.^{[5], [27]}

The sample lies inside a crucible, that is sealed and placed exactly over the sensor disk, on the left side; while on the right side in placed the empty crucible of reference, as shown in Figure 3.11.^[19]

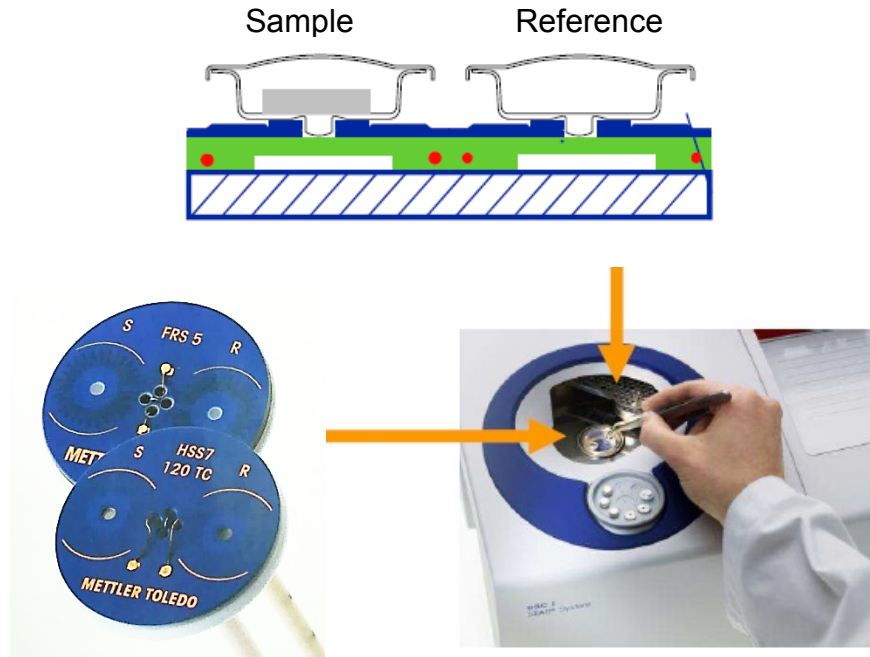


Figure 3.11: Detail of both sample and reference crucibles, and MultiSTAR FRS5 and HSS7 DSC sensors.^{[5]. [19]}

The heat flow (Φ) is measured by the FRS5 and HSS7 DSC sensors, that are equipped with circular thermal resistances (R_{th}) and several thermocouples located under each of the two crucible positions, as shown in Figure 3.11. The thermal resistance (R_{th}) creates the necessary condition for the heat to flow radially from the reference to the sample, causing a temperature difference that is measured by the thermocouples.^[5]

Also, to create the initial heat flow, from the furnace to the reference crucible, the furnace temperature (T_c) is increased by ΔT , calculated as the product between the heating rate (β) and a time constant (τ_{lag}), as shown in Equation 3.1.^[5]

$$\Delta T = T_c - T_R = \beta \cdot \tau_{lag} \quad (3.1)$$

During the measurement, ΔT is always controlled so that the reference temperature (T_R) remains constant and follows exactly the temperature input of the program.^[5]

Figure 3.12 shows the relation between the courses of the three analyzed temperatures during the measurement. At the beginning the temperature is exactly the same in the furnace and in both crucibles. However, it keeps this way only for a short time, because, as explained previously, the furnace temperature (T_c) is immediately increased by ΔT in order to create the heat flow that will raise both reference (T_R) and sample (T_s) temperatures. These two temperatures increase at the same rate until the melting temperature (T_f) of the sample is reached. At this point, the heat will no longer be used to raise sample's temperature, but to promote its fusion and phase transition. Then, once the transition is over, the curve returns to its normal course.^[5]

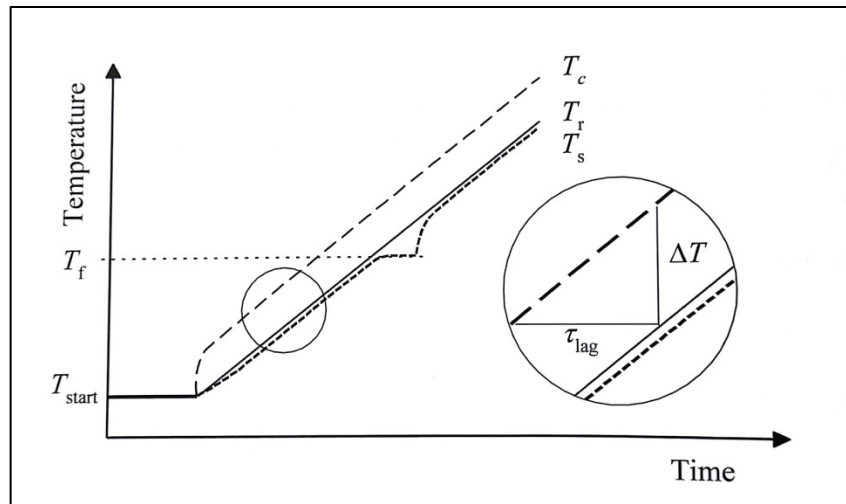


Figure 3.12: Relation between the three temperatures that influence the DSC analysis: furnace temperature (T_c), reference temperature (T_r) and sample temperature (T_s).^[5]

Considering that the sample crucible is placed on the left side and the reference crucible is placed on the right side, as shown in Figure 3.11, the heat flow to the sample is calculated as the difference between the heat flow on each side, like shown in Equation 3.2, in which Φ_l and Φ_r are respectively the heat flows on the left and right side.^[5]

$$\phi = \phi_l - \phi_r = \frac{T_s - T_c}{R_{th}} - \frac{T_r - T_c}{R_{th}} = \frac{T_s - T_r}{R_{th}} \quad (3.2)$$

In other words, as shown in Figure 3.13, the calculated heat flow corresponds exactly to the variation of enthalpy (ΔH) due to the phase transition of the sample.

So the graph ΔT versus Time/ T_R (Figure 3.13 (b)) shows the sensor signal, that is converted, using Equation 3.2, in the DSC signal, showed on the graph Heat flow versus Time/ T_R (Figure 3.13 (c)).^[5]

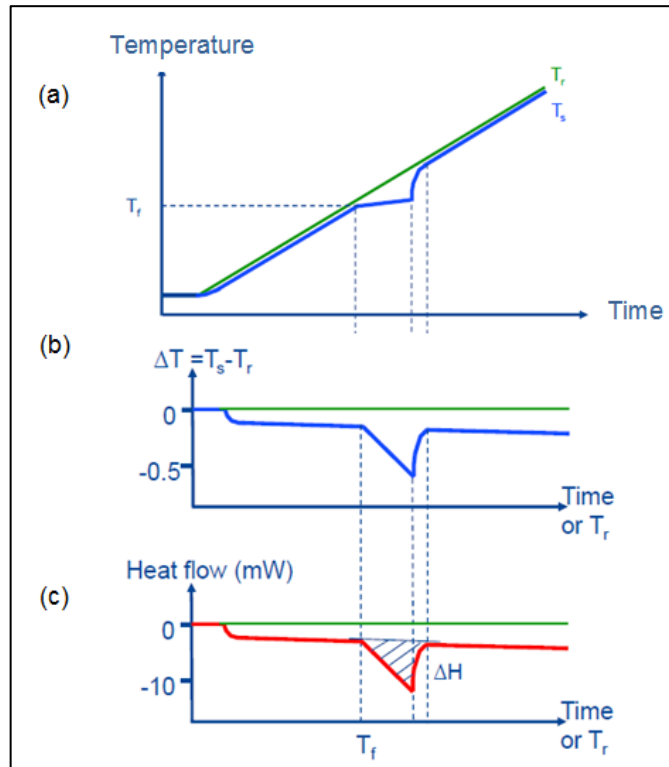


Figure 3.13: (a) Comparison between T_s and T_R over time; (b) Sensor signal that show the difference of temperature between sample and reference; (c) DSC signal with the calculation of the heat flow through the difference of enthalpy (ΔH) obtained from the peak integral.[19]

The Equation 3.2 can also be written in terms of the sensor signal or thermoelectric voltage (V) and of its calorimetric sensitivity (E), that is the product between the thermal resistance (R_{th}) and the thermocouple sensitivity (S), as shown in Equation 3.3.^[5]

$$\phi = \frac{V}{S \cdot R_{th}} = \frac{V}{E} \quad (3.3)$$

So finally, the formula used by the software to calculate the sample temperature is given by Equation 3.4.^[5]

$$T_s = T_R + \phi \cdot R_{th} = T_R + \phi \cdot \frac{E}{S} \quad (3.4)$$

Before starting the DSC analysis of interest, it was made a one-point calibration to ensure the temperature and heat flow accuracy of the measurement.

The calibration process consists in analyze a reference substance and compare the measured results with the tabled reference values. If the results are within the acceptable error limits, then the instrument is calibrated. Otherwise occurs an adjustment of its parameters so that deviation between both values become acceptable again.

In the DSC, the parameters that require calibration are:

- Temperature (T)
- Heating rate dependence of the temperature (T_{lag})
- Heat flow (Φ).^[5]

There are two methods of calibration and adjustment that can be used according to the range of temperature of interest, the one-point and the multi-point calibration methods.^[5]

The one-point calibration consists on the use of only one reference substance, for example indium, and it presents a high accuracy in small intervals of temperature ($\pm 50K$ around the melting point of the reference substance), but is not suitable for larger ones.^[5]

The multi-point calibration, on the other hand, is recommended for large temperature ranges, because it uses more than one reference substance to perform the calibration, so there are more melting peaks to be compared to reference values. Practically it is often done with two reference substances, but for highest accuracy three to five calibration points uniformly spread over the temperature range can be used. In general, the use of 2 or 3 reference substances certifies an accuracy temperature range calibration from 200 to 300°C; while the use of 4 or more substances improve this range to more than 400°C. Also, as all reference substances are placed inside the same crucible and are melted at different heating rates, to obtain clear results occurs to separate each substance with a very small piece of aluminum foil, so they do not touch one another.^[5]

As mentioned previously, for the scope of this thesis, it was performed a one-point calibration respecting the following steps of measurement:

- The measurement cell was purged with a gas flow rate of about 50 mL/min for the elimination of dust or residues from previous samples. Nitrogen, is the most common purge gas used, because it is inert in a range of temperature between room temperature and 600°C. However, for extremely precise measurement it is suitable the use of Helium, that also inert but has an excellent thermal conductivity, giving a better separation of the peaks. If the sample does not react with oxygen, it is possible the use of air below 100 to 200°C. And finally, if the aim is to study the oxidative behavior, the analysis is made with an oxygen atmosphere.^[5]
- Any eventual moisture from the measurement cell was removed by briefly heating it to 400°C.
- A sample of 6 mg \pm 10 μ g of indium was weighted and placed inside the standard aluminum crucible. If stored under appropriate conditions, the same crucible can be used for about 20 calibration cycles.
- The calibration measurement was performed three times. The In certifies the calibration of the instrument only in the temperature range from 100 to 200°C.
- If the deviations of the onset temperature and the specific enthalpy of the melting peak are within the error limits, the equipment may be used in this range of temperature without any problem.
- If the deviation is unacceptable, occurs an adjustment of the parameters and another calibration measurement.^[5]

Table 3.4 describes the sample and the parameters used, and the expected results for the sample melting temperature (onset temperature) and the heat flow (peak integral).

Table 3.4: Parameters used for the DSC calibration with a sample of In and the expected results for a calibrated instrument.^[12]

Sample	Indium
Sample weight	6.4 mg
Crucible	Aluminum 40 μ L, sealed and pierced
Heating rate	10 K/min
Starting temperature	120°C
End temperature	180°C
Purge gas	60 mL/min or 3.6 L/h N ₂
Cooling method	Air
Expected sample temperature	156.6°C \pm 0.3°C
Expected heat flow	-28.45 J/g \pm 1.0 J/g

Figure 3.14 shows the calibration curve obtained for the In sample. It exhibits an onset temperature of 156.87°C, that is within the accepted range of 156.3 and 156.9°C; and a normalized heat flow of -28.08 J/g, that is also among the limit values of -27.45 and -29.45 J/g.^[5] So according to this measurement, the DSC module is within the specifications, i.e. it is calibrated.

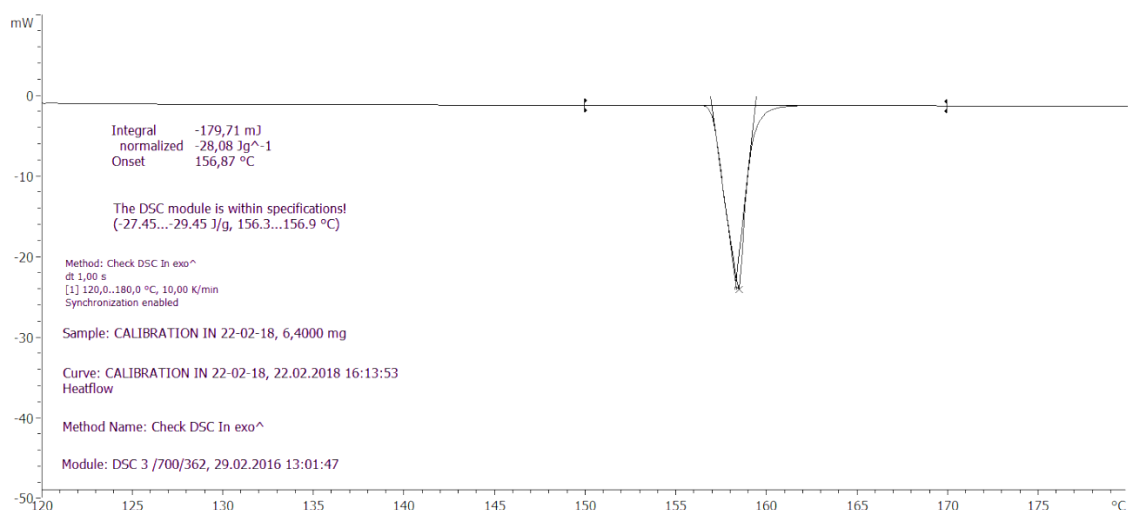


Figure 3.14: DSC calibration curve performed on 22-02-2018 with a sample of In (6.4 mg), using a temperature range from 120 to 180°C and a heat flow of 10K/min.

The complete certificates of the In sample and the calibration can be found in Appendix D.

So, once the sample is ready for the analysis, turn on the DSC with the power button located on the back of the machine and start the DSC software STAR. Go to 'Routine Editor' on the top left of the screen (see Figure 3.15) and select it to choose the desired measurement method. It is possible to create a new one selecting 'New' or to use an already existing method selecting 'Open' on the screen showed in Figure 3.16.

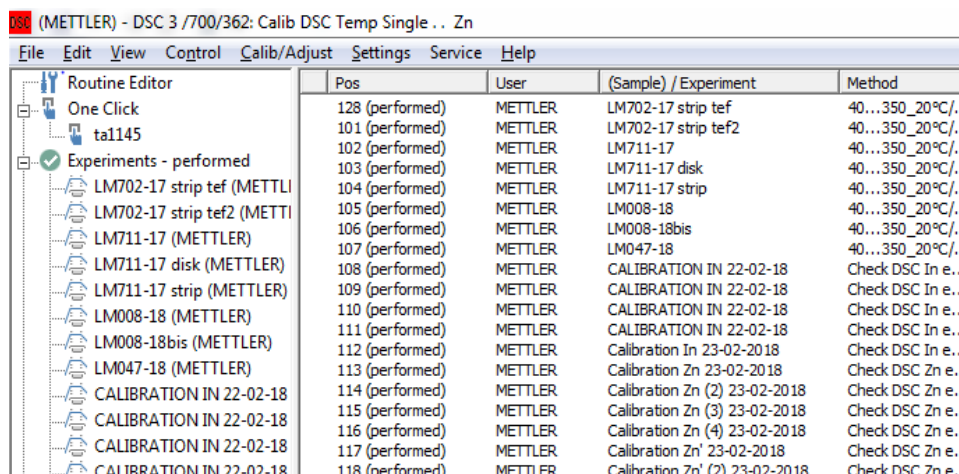


Figure 3.15: Display screen when the software STAR is started.

For the DSC analyses of the spring bushing samples in this thesis, the selected method was:

- Temperature range: 40 to 350°C,
- Heating rate: 20°C/min
- Purge gas flow rate: 50mL/min or 3L/h of N₂.

Once the method was chosen, there is a check of all test parameters. The test was identified with the measurement name in the field 'Sample Name' and the weight, measured for the corresponding sample, was introduced in the field 'Weight'.

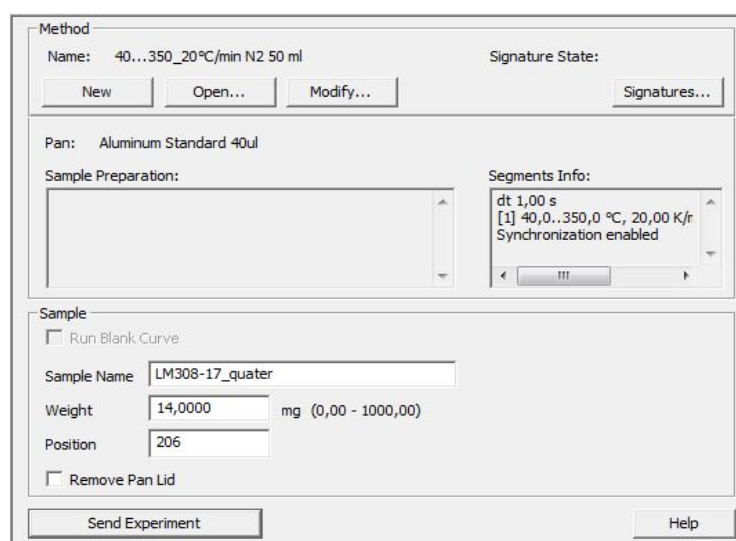


Figure 3.16: Parameters setting screen.

So, the measurement starts by clicking on 'Send Experiment' button and then clicking two times on 'OK' button. It is possible to follow the experiment through the curve that is showed on the screen.

For all the measurement curves, the thermal effects were analyzed and the corresponding melting temperatures (T_m) of each constituent were determined.

Besides the determination of the specific temperature of each thermal effect observed on the measurement curves, it was also made an attempt to calculate the content of each polymer through the integration of the melting peaks. Since the difficult part of this process is to find the better way of determining the baseline used for the integration and make sure to use the same one in all the measurements, one of the scopes of this thesis was to define a standard method and, if possible, to create an Evaluation Macro to do it automatically every time.

The method used to calculate the composition of the sample was the function Content Determination of the Evaluation Window present in the Mettler Toledo's Software Star^e. This function is based on the fact that, generally, the DSC peak areas are proportionally to the content (C) of the component of interest, that have undergone a physical or chemical transition. The proportionality constant is the transition or reaction enthalpy (ΔH), as shown in Equation 3.5.^[5]

$$C = \frac{\Delta H_{measured}}{\Delta H_{100\%}} 100\% \quad (3.5)$$

So, for this specific case, it consists on calculating the ratio between the enthalpy or heat of fusion measured in one of the melting peaks and the enthalpy of fusion of the corresponding pure substance.

In practice, considering the Mettler Toledo's Software Star^e, it consists on the following steps:

- Open the measurement curve in the Evaluation Window
- Select the melting peak of the substance of interest
- Click on DSC > Content at the top menu (see Figure 3.17)

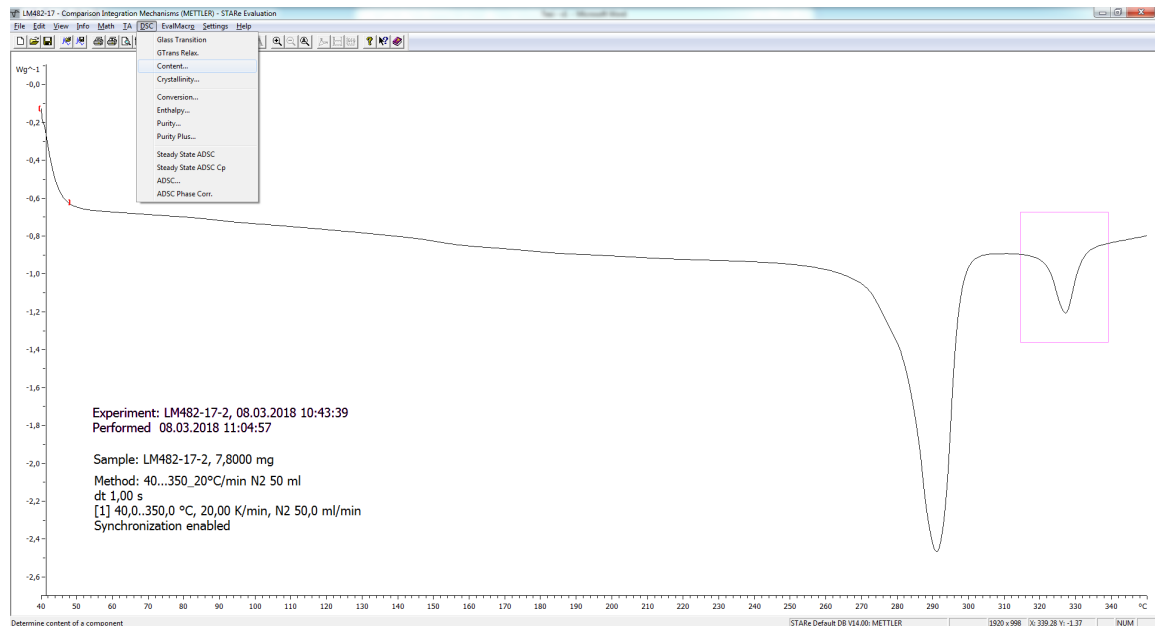


Figure 3.17: Display screen after the third step, in which the peak was selected and the menu DSC was opened.

- Insert the melting enthalpy of the pure substance in the newly opened window (see Figure 3.18)

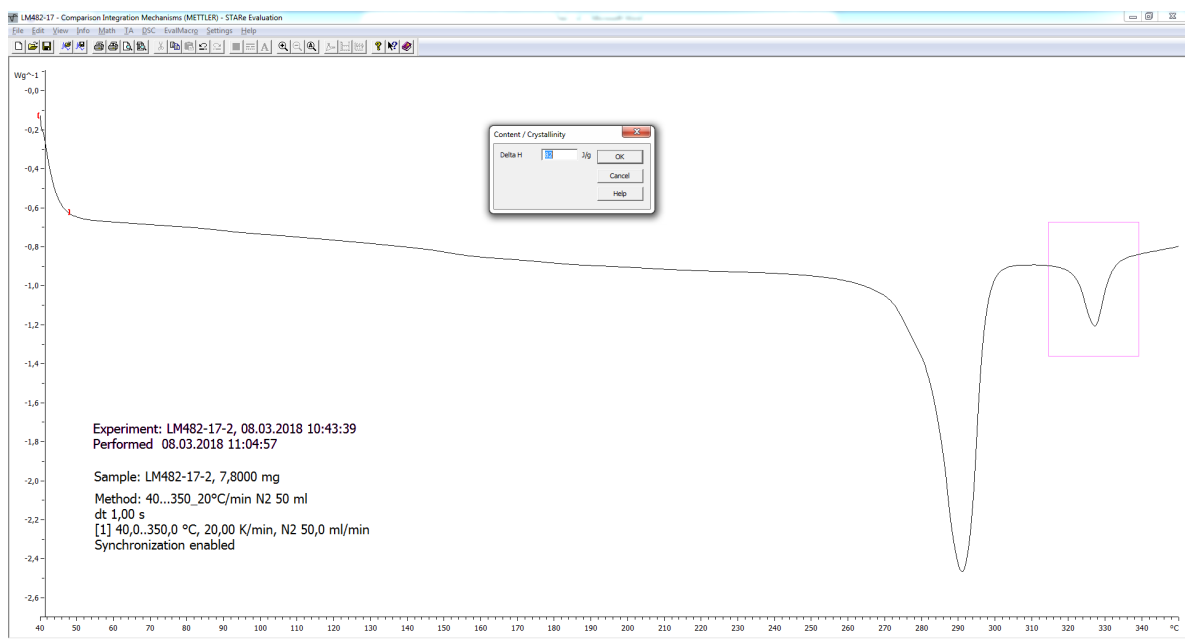


Figure 3.18: Display screen with the window to insert the melting enthalpy of the pure substance.

- Adjust the limits of the integration area, by dragging the up and downward flags to the desired position, and the baseline, by clicking in the top menu Settings > Baseline (see Figure 3.19).

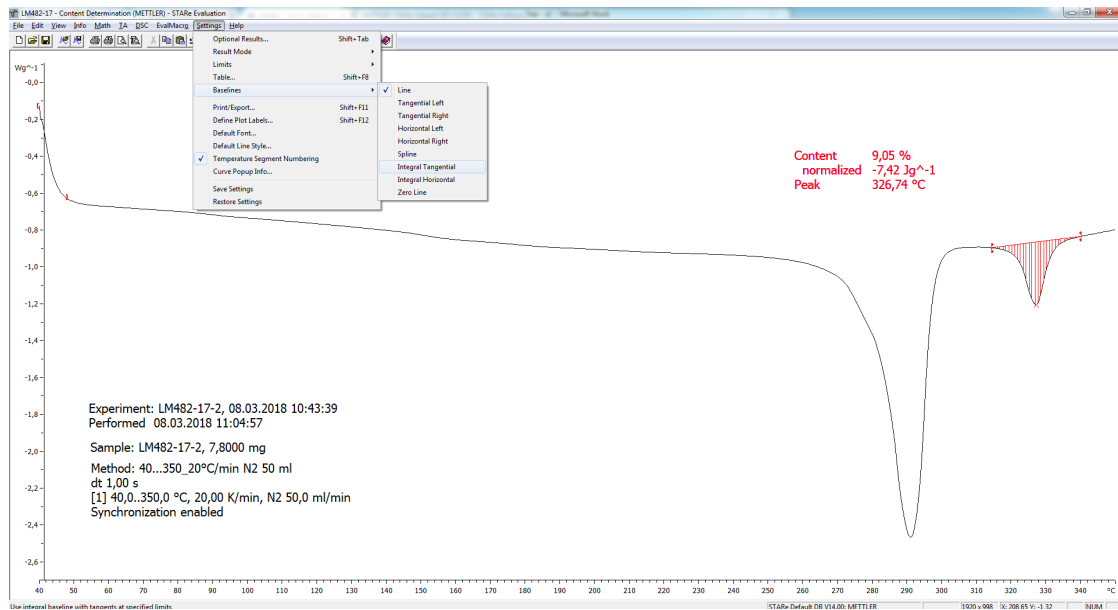


Figure 3.19: Display screen of the result, with the integration area identified in red, and the content of that substance determined.

The only difficulty of using this method is the requirement of the enthalpy of fusion of the pure material as input. This can be an issue because this parameter is not a constant and can vary significantly from one supplier to another, with the shape and dimension of the raw material, with its degree of crystallinity and with the method used to process it.

So, in this case, as the supplier did not provide any information about the precise value of the enthalpy of fusion of both polymers, it was chosen to determine the content of the PTFE, which values of enthalpy of fusion could be found in literature, and calculate the content of PA46 as the difference between 100% and the percentage of PTFE.

In literature it is possible to find mainly to values of enthalpy of fusion for the PTFE, one of about 82J/g for the 100% crystalline material, and one of about 41J/g, for the semi crystalline material.^{[28]–[30]}

3.2.2. Thermogravimetric Analysis (TGA)

The TGA equipment can be described as a high precision thermobalance on which the sample is gradually heated. As shown in Figure 3.20, its main components are the thermobalance with a sample crucible and a calibration weight, a furnace with a programmable control temperature and a sample purge gas that controls the environment, flowing over the sample and exiting through an exhaust. Also, it is suitable to purge the balance chamber with a protective gas in order to avoid the effects of heat radiation and the ingress of corrosive decomposition products.^{[5], [19], [24]}

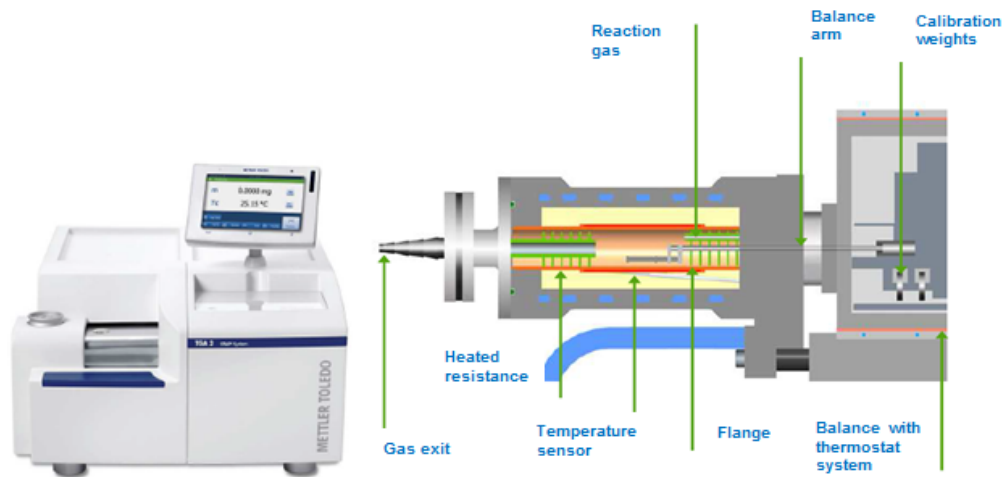


Figure 3.20: TGA analyzer.^[19]

During the sample loading, the balance usually is fixed and the furnace chamber is moved to allow the access to the balance. Considering this, there are some types of balance commonly used, such as the top loading balance (furnace chamber is moved upwards); suspension balance (furnace chamber is moved downwards); or horizontal arrangement (furnace chamber is moved horizontally). Besides that, balances can also provide different degrees of resolution, being classified as semi micro-balances (10 μ g), micro-balances (1 μ g) or even ultra-micro-balances (0,1 μ g).^{[5], [24]}

Before performing the measurement, it is important to choose the heating rate very carefully, because it not only can change the temperature range in which thermal effects occur, but it also causes a systematic deviation between the true sample temperature and the measured one. This last aspect is usually determined and corrected during the temperature calibration and adjustment. But when dealing with real samples with different thermal conductivities, a slight dependence on the heating rate is always expected and can be observed with a variation of the peak temperature.^[5]

Regarding the variation of the temperature region in which thermal effects may occur, the choice of an unsuitable heating rate can lead to an overlapping of reactions, that can remain undetected. For example, higher heating rates shift reactions to higher temperatures.^[5]

Another important parameter that needs to be properly set before the measurement is the furnace atmosphere, that is formed by a continuous inflow and outflow of different gases, that allow the material exchange between the sample and the environment. Otherwise it would be a closed system with no mass variation.^[5]

A protective gas is always suitable in order to protect the balance from the effects of heat radiation and the ingress of corrosive decomposition products. Usually dry inert gases, like nitrogen and argon, are used for this purpose.^{[5], [19], [23]}

In addition, there is a purge gas that flows over the sample and is responsible for the removal of the gaseous reaction products formed from the furnace chamber. It is common to use helium as purge gas, because it increases the heat transfer from the furnace to the sample.^{[5], [19], [23]}

It is also possible to have reactive gases interacting with the sample, such as air, oxygen (for the study of oxidation) and hydrogen (for the study of catalysis and reduction) diluted with argon. But these gases are used only in particular cases, and their residual presence in an inert atmosphere can damage the sample and the measurement. Some possible sources of residual oxygen are: contaminated purge gas, due to leaks in the gas supply tubing for example; adsorption of oxygen on the measuring cell; and ingress of atmospheric oxygen due to back diffusion at the purge gas outlet or to leaks.^{[5], [19], [23]}

Finally, a problem regarding the inflow and outflow of gases in the system is the pressure variation, that can lead to either an overpressure or a reduced one. The overpressure can be caused if the gas outlet valve is not opened, and it can lead to an explosion. So, for safety reasons, some TGA analyzers are already equipped with a system that limits the overpressure inside the furnace chamber to 10kPa, releasing it gradually if this limit is overpassed. On the other hand, the pressure reduction is recommended in some cases, for example to separate overlapping effects, and can be done using a vacuum pump.^[5]

In addition, as explained previously for the DSC analysis, a calibration of the instrument is always required to ensure that the obtained results are correct. In this case, the parameters of the TGA analyzer that are often checked are the values measured for the sample's mass and temperature. This is done using a reference sample, that allows the comparison of the measured values with the tabled ones. If there is no deviation or it is within the acceptable limits, the equipment is considered calibrated and suitable for other measurements. Otherwise, an adjustment is required and the parameters are changed in order to correct the deviation.

The balance calibration with reference masses is usually done automatically by the software when the measurement conditions are changed or during long periods of waiting.^[5]

The temperature calibration, on the other hand, can be performed either through a method based on Curie point transitions of certain ferromagnetic materials or through melting point standards of very pure samples, that is more accurate and uses DTA and SDTA signals. Both methods can be observed in Figure 3.21.^[5]

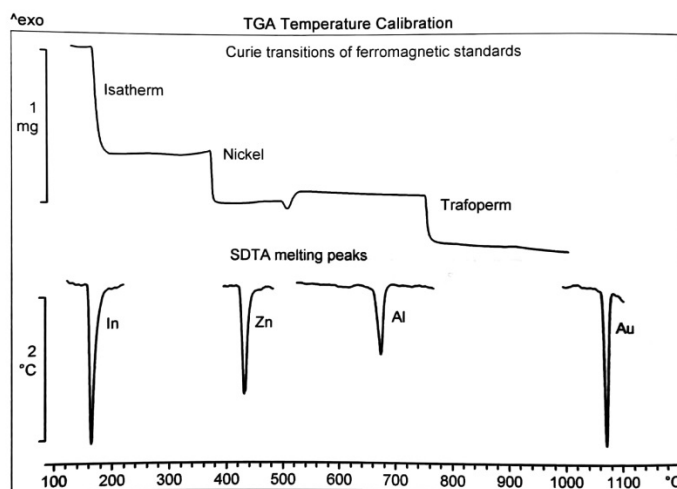


Figure 3.21: Temperature calibration methods of a TGA analyzer: using the Curie transition points of ferromagnetic materials (above) or melting point standards (below).^[5]

Taking all these points into consideration, the method used to perform the TGA analyses of the 24 samples of spring bushing, named from LM481-17 to LM504-17, respected the following steps:

- Hold for 5 minutes at 40°C
- Heat from 40 to 850°C at a heating rate of 10°C/min
- Heat from 850 to 900°C at a heating rate of 10°C/min
- Hold for 10 minutes at 900°C (to separate probably overlapping decomposition events)
- Hold for 1 minute at 900°C (to release the gas).

After the analysis and the obtainment of a measurement curve for each sample, the software could calculate the content of each polymer (PA46 and PTFE) and the content of residue by analyzing the height of the different steps and the percentage of weight loss.

3.2.3. Statistical Analysis with Minitab 18 Software

In addition, using Minitab 18 Software, also a statistical analysis of the obtained data was performed.

First, it was chosen to present the data in a Box Plot Graph, which is a graphical summary of the distribution of samples, and can be used to compare several distributions, their shape, central tendency and variability.^[31]

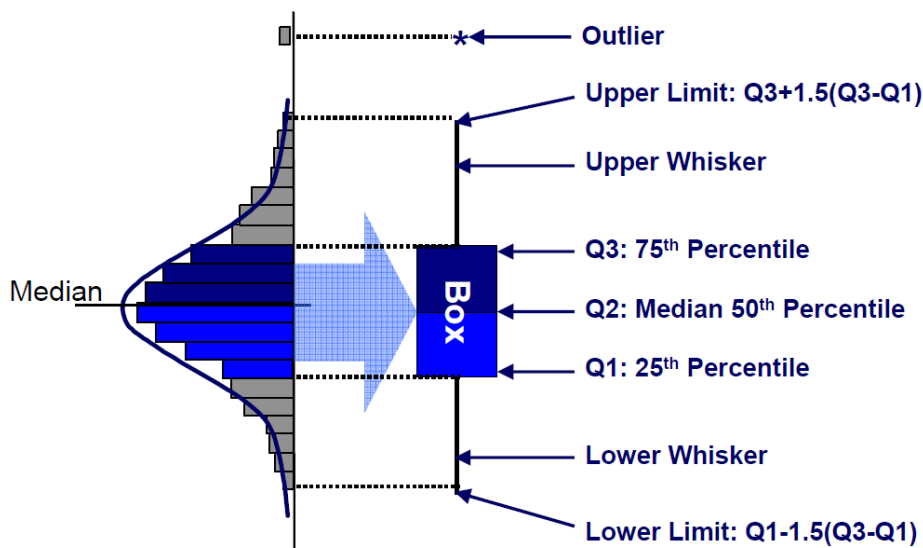


Figure 3.22: Main parameters of a Box Plot-Whisker Graph.^[32]

Figure 3.22 shows how to interpret a typical Box Plot Graph. It is represented as a block with whiskers, in which all the data are located within a range divided in four equal parts (each one with 25% of the data), that are limited by the quartiles.

- 1st Quartile (Q1): 25% of the data are less than or equal to this value. It determines the bottom line of the box.^{[32]–[36]}

- 2nd Quartile (Q2): It is the median value; i.e. 50% of the data are less than or equal to this value.^{[32]–[36]}
- 3rd Quartile (Q3): 75% of the data are less than or equal to this value. It determines the top line of the box.
- Interquartile range (IQR): is the central zone, represented by the box. It describes the spread of the data and can be given by the difference between the upper and lower quartiles (IQR = Q3 - Q1).^{[33]–[36]}
- Whiskers: are the lines below and above the box, and represent, respectively, the data range from the first quartile to the smallest data point within the lower limit and from the third quartile to the largest data point within the upper limit.^{[32], [36]}
- Outliers: data points beyond the lower and upper limits, i.e. the values that are below $Q1 - 1,5 * IQR$, and above $Q1 + 1,5 * IQR$.^{[32]–[36]}

Besides the Box Plot, it is also suitable to compare the groups of data in order to verify whether there is a significant statistical difference between them. In order to do so, the method followed was the one showed in Figure 3.23, in which first it was necessary to check if the samples have a normal distribution or not, for then perform the most suitable hypothesis test.

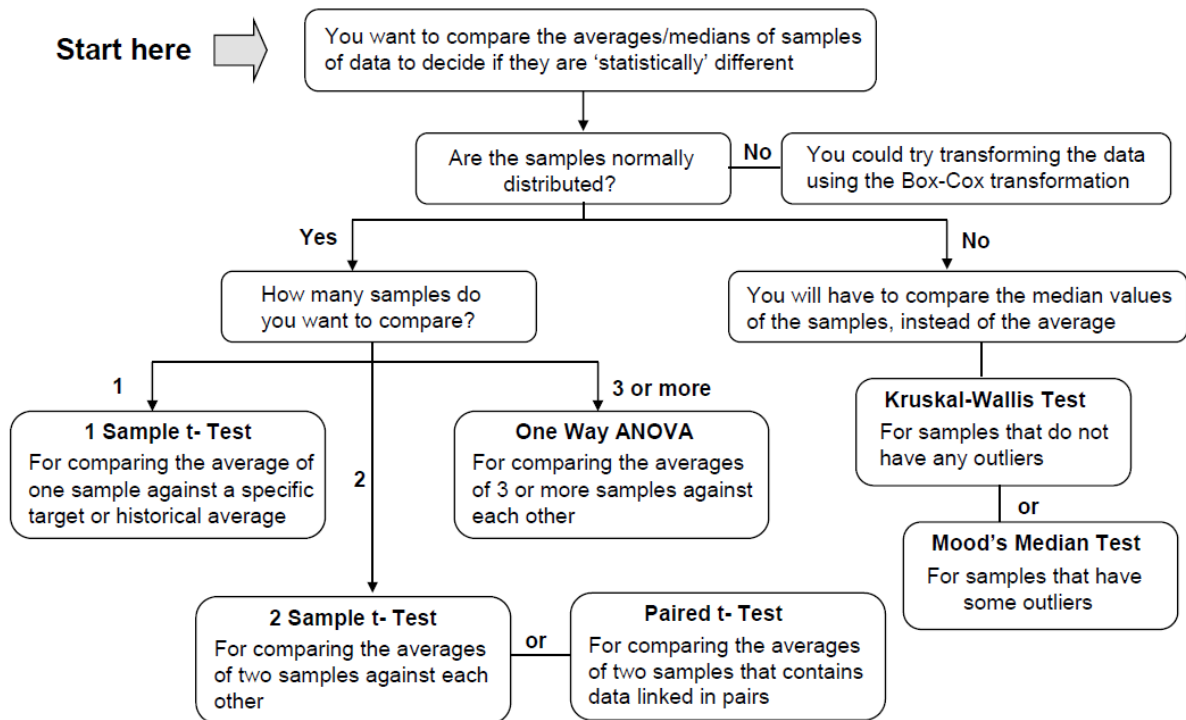


Figure 3.23: Scheme of possible hypothesis tests for mean and median.^[32]

The normal distribution can be evaluated using the Anderson Darling (AD) Hypothesis Test, that can be graphically represented with a Probability Plot. It takes into consideration the following statements, with a significance level (α or P-value) of 0,05; i.e. a confidence level of $1 - \alpha = 95\%$.

- Null Hypothesis (Ho) – the data are normally distributed ($\alpha > 0,05$)

- Alternative Hypothesis (H_a) – the data aren't normally distributed ($\alpha < 0,05$).^{[32], [36]}

If the data presents a normal distribution, it is possible to perform the Analysis of Variance (One-Way ANOVA) and tell whether there is a statistical difference between the samples or not. In this case, it is used a very similar hypothesis method, as showed next.

- Null Hypothesis (H_0) – all means are equal ($\alpha > 0,05$)
- Alternative Hypothesis (H_a) – not all means are equal ($\alpha < 0,05$)

So, if the significance level (α or P-value) is bigger than 0,05 or 5%, there is no statistical difference between the data, and all means are considered equal. Besides the P-value, some other parameters used in this test are explained below.^[37]

- Degree of Freedom (DF): number of independent elements in the sum of squares. $DF \text{ Factor} = N^\circ \text{ of Factors} - 1$.^[37]
- Sum of Squares (Adj. SS): total variation of the sum of square distances in the data, in which the distances are measured as the difference between each data point and the mean of all observations.^[37]
- Mean Squares (Adj. MS): calculated as the ratio between the sum of squares factor and the degree of freedom.^[37]
- F-value: ratio between the MS Factor, calculated between the mean of a factor and the mean of all observations, and the MS Error, calculated between an observation value and the mean of the observations of that factor.^[37]

On the other hand, if the data do not present a normal distribution, it is recommended to perform a test that compares the median values of the samples, instead of the average, as described in Figure 3.23. So, as the samples presented some outliers, it was performed the Mood's Median Test.

The Mood's Median Test is also based in a hypothesis method, and is used when the samples are not normally distributed and there are outliers. This analysis can both determine whether the medians of two or more groups differ and calculate a range of values that is likely to include the difference between population medians.^{[32], [36]}

So, also in this case, considering a confidence level of 95% ($\alpha = 5\%$), the two hypotheses are:

- Null Hypothesis (H_0) – The differences between the medians are not statistically significant ($\alpha > 0,05$)
- Alternative Hypothesis (H_a) – The differences between some of the medians are statistically significant ($\alpha < 0,05$)^{[32], [36]}

Some other parameters used in this test are:

- Degree of Freedom (DF): number of independent elements in the sum of squares. $DF \text{ Factor} = N^\circ \text{ of Factors} - 1$.^[37]
- Chi-Square: sum of the values calculated as the square of the difference between the observed and expected values for a cell, divided by the expected value for that cell. Higher the chi-square value, higher the difference between the observed and the expected values.^[37]

4. Results and discussion

4.1. DSC - Melting Temperatures

All the measurement curves obtained during the DSC analyses of the 72 samples taken from spring bushing components LM481-17 to LM504-17 can be seen in Appendix E, while the data are summarized, described and explained here.

As explained in Section 3.1, the samples were divided in Groups 1, 2 and 3 (see Table 3.3), and the DSC analyses of each group were called Analyses 1, 2 and 3.

All the measurement curves obtained exhibited an aspect like the one of sample LM481-17, showed in Figure 4.1, in which it is possible to observe the temperature range from 40 to 350°C in the x axis, and the variation of the heat flow normalized to mass [Wg^{-1}] in the y axis. At the top of the y axis it is also indicated the direction of the exothermic thermal effects. As it is directed upwards, the melting peaks will be showed downwards.

The curve presents an initial deflection due to the difference of heat capacity between the sample and the reference. Then, it continues practically constant until the polymer with the lower melting temperature (PA46) starts to melt. The melting of the PA46 will form a melting peak, that can be used to identify the melting temperature (peak temperature) and to calculate the content of the polymer. Then, as the temperature continues to increase, the PTFE starts to melt, and another melting peak is formed.

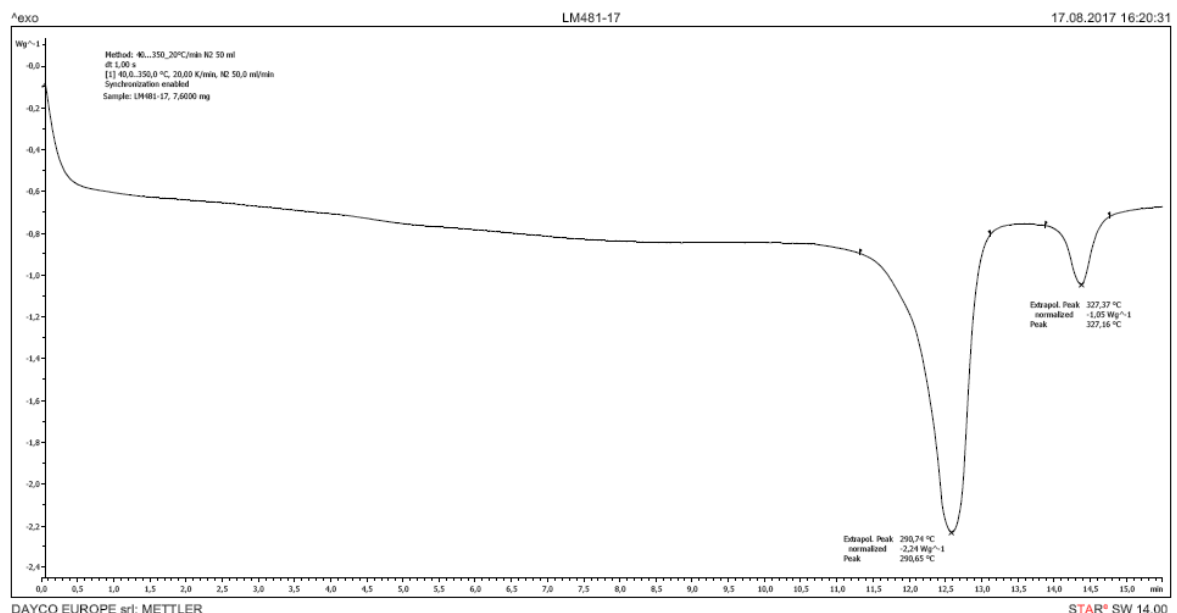


Figure 4.1: DSC analysis of LM481-17: there are two peaks. The peak with a temperature of 290,65°C is compatible with PA46 polyamide (peak between 290 and 295 °C) while the peak with a temperature of 327,16°C is compatible with PTFE (peak between 325 and 335 °C); there aren't any artifacts or other peaks that identify impurities.

Also, as expected for these polymers, in none of the curves it was possible to observe the glass transition, possibly because the amorphous fraction of the material is quite small. The expected values would be for PA46 polyamide between 70°C and 94°C, and for PTFE between 125 and 130°C.^[25]

So, the values of melting temperature obtained, from the DSC analyses, for the PA46 and the PTFE in Analyses 1, 2 and 3 are showed, respectively, in Table 4.1 and Table 4.2.

Considering the acceptable range of melting temperature for each polymer, it is possible to observe that in Analysis 1 (Group 1) all the samples showed T_m values that were compatible with those expected, that are between 290 and 295°C for PA46 and between 325 and 335°C for PTFE.^[25] The obtained melting peaks of PA46 presented a maximum value of 292,0°C and a minimum of 290,4°C, with an average of 291,1°C; while for the PTFE the maximum T_m was 328,2°C and the minimum 325,9°C, with an average of 327,0°C.

Observing the data obtained from Analysis 2 (Group 2), the measured melting peaks of PA46 presented maximum value of T_m of 291,9°C and a minimum one of 289,9°C, with an average of 290,8°C; while for the PTFE the maximum T_m was 327,7°C and the minimum 326,3°C, with an average of 327,0°C. So, with the exception of LM482-17-2, all of the samples presented values of T_m compatible with the acceptable range of both polymers.^[25]

Finally, considering the data obtained from Analysis 3 (Group 3), the melting peak of PA46 presented a maximum value of T_m of 292,0°C and a minimum one of 289,9°C, with an average of 290,8°C; while for the PTFE the maximum T_m was 328,5°C and the minimum 326,0°C, with an average of 327,2°C. So, in this case not all the samples presented values of T_m that were compatible with PA46, because sample LM482-17-3 exhibited a temperature of 289,9°C that is slightly below the accepted range from 290 to 295°C. Regarding the PTFE instead, all the resulting values were within the range from 325 to 335°C.^[25]

Table 4.1: Values of Tm obtained for the PA46 in each one of the performed analyses, with the respect average and standard deviation for each sample and for the whole set of 72 samples.

PA46					
Sample	Tm (°C) Analysis 1	Tm (°C) Analysis 2	Tm (°C) Analysis 3	Average Tm (°C)	Standard Deviation
LM481-17	290,7	290,8	290,9	290,8	0,11
LM482-17	291,0	289,9	289,9	290,3	0,66
LM483-17	290,7	291,3	290,8	290,9	0,30
LM484-17	290,6	291,1	291,1	290,9	0,27
LM485-17	291,2	290,9	290,8	290,9	0,20
LM486-17	291,5	290,8	290,5	290,9	0,49
LM487-17	292,0	290,7	290,9	291,2	0,69
LM488-17	290,8	291,5	290,5	290,9	0,49
LM489-17	291,0	290,6	290,8	290,8	0,19
LM490-17	290,4	290,6	290,9	290,6	0,22
LM491-17	291,0	291,4	291,1	291,1	0,22
LM492-17	290,9	290,0	290,6	290,5	0,44
LM493-17	292,0	291,1	291,2	291,4	0,52
LM494-17	290,6	291,9	291,2	291,2	0,62
LM495-17	290,9	290,9	290,6	290,8	0,15
LM496-17	291,3	290,8	291,1	291,1	0,24
LM497-17	290,8	290,7	290,3	290,6	0,26
LM498-17	291,1	290,7	291,3	291,0	0,31
LM499-17	291,0	290,8	290,8	290,8	0,09
LM500-17	290,6	291,1	290,5	290,7	0,30
LM501-17	291,7	290,6	292,0	291,4	0,75
LM502-17	291,1	290,5	290,5	290,7	0,37
LM503-17	291,7	290,9	290,9	291,1	0,46
LM504-17	291,6	290,0	290,6	290,7	0,79
			TOTAL	290,9	0,43

Table 4.2: Values of Tm obtained for the PTFE in each one of the performed analyses, with the respect average and standard deviation for each sample and for the whole set of 72 samples.

PTFE					
Sample	Tm (°C) Analysis 1	Tm (°C) Analysis 2	Tm (°C) Analysis 3	Average Tm (°C)	Standard Deviation
LM481-17	327,2	326,9	327,3	327,1	0,19
LM482-17	325,9	326,7	326,7	326,5	0,51
LM483-17	327,4	327,3	327,1	327,3	0,17
LM484-17	327,2	326,4	327,1	326,9	0,42
LM485-17	327,8	327,1	326,9	327,3	0,46
LM486-17	326,8	327,2	326,8	327,0	0,26
LM487-17	328,2	326,8	326,1	327,0	1,07
LM488-17	326,0	327,6	326,6	326,7	0,83
LM489-17	327,2	326,8	326,9	326,5	0,20
LM490-17	326,8	326,8	326,6	326,3	0,12
LM491-17	327,2	327,2	326,0	326,8	0,71
LM492-17	326,4	327,2	326,8	326,8	0,37
LM493-17	327,8	327,0	327,1	327,3	0,44
LM494-17	326,5	327,5	326,1	326,7	0,69
LM495-17	325,9	327,7	326,5	326,7	0,93
LM496-17	326,3	327,1	326,0	326,5	0,55
LM497-17	326,6	327,2	326,5	326,7	0,37
LM498-17	326,7	326,9	326,2	326,6	0,37
LM499-17	326,9	327,1	327,1	327,0	0,12
LM500-17	327,5	327,0	326,4	327,0	0,56
LM501-17	327,5	326,4	328,5	327,5	1,05
LM502-17	327,1	326,4	326,4	326,6	0,42
LM503-17	327,1	326,7	326,4	326,7	0,33
LM504-17	327,0	326,3	326,4	326,6	0,39
TOTAL				326,9	0,53

In addition, using Minitab Software, it was possible to analyze and present the data in a Boxplot Graph, as showed in Figure 4.2 for the PA46 and in Figure 4.3 for the PTFE.

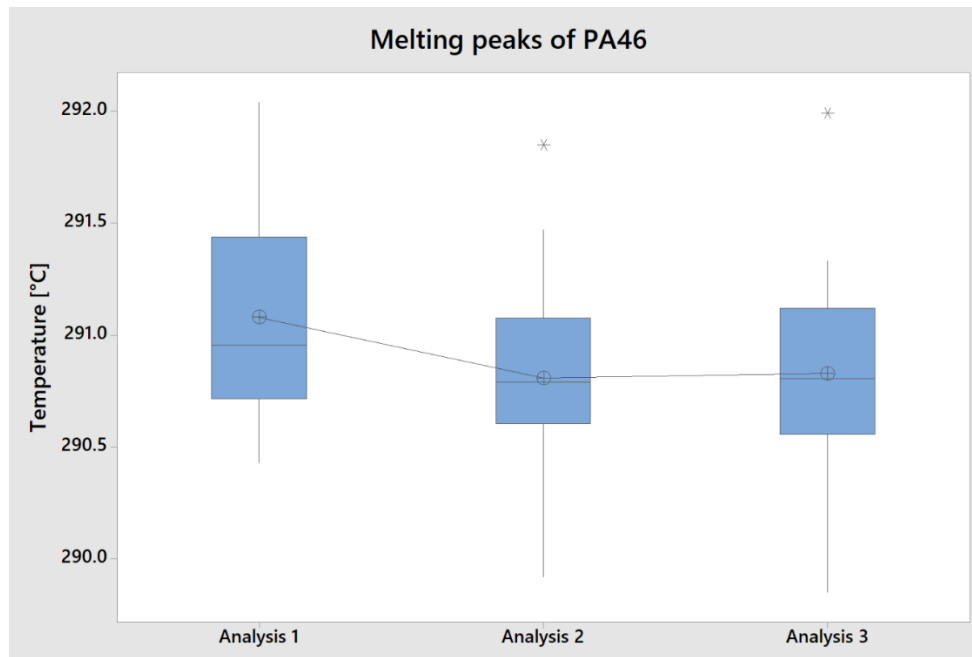


Figure 4.2: Graphical variation of the values of Tm obtained for the PA46 in each one of the performed analyses.

Table 4.3 shows the main parameters used to create the Box Plot Graph of PA46, showed in Figure 4.2, as well as the values obtained from them.

- N – number of samples in each one of the three analyses
- Mean – average value of melting temperature of the PA46
- SE Mean – standard error or deviation of the mean. It represents the deviation of the mean with different experiments conducted each time.[38]

$$SE\ Mean = \frac{StDEV}{\sqrt{N}} \quad (\text{Eq. 4.1})$$

- StDEV – standard deviation. It shows how spread out numbers are, and it can be calculated as showed in Equation 4.2, in which μ is the mean, N the number of samples, x_i each data point.[32], [39]

$$\sigma = \sqrt{\frac{1}{N-1} \sum_{i=1}^N (x_i - \mu)^2} \quad (\text{Eq. 4.2})$$

Table 4.3: Data used to create the boxplot graph of the melting peaks of PA46 of all three analyses.

Statistics PA46									
Variable	N	Mean	SE Mean	StDev	Minimum	Q1	Median	Q3	Maximum
Analysis 1	24	291,1	0,0924	0,453	290,4	290,7	291,0	291,4	292,0
Analysis 2	24	290,8	0,0916	0,449	289,9	290,6	290,8	291,1	291,9
Analysis 3	24	290,8	0,0841	0,412	289,9	290,6	290,8	291,1	292,0

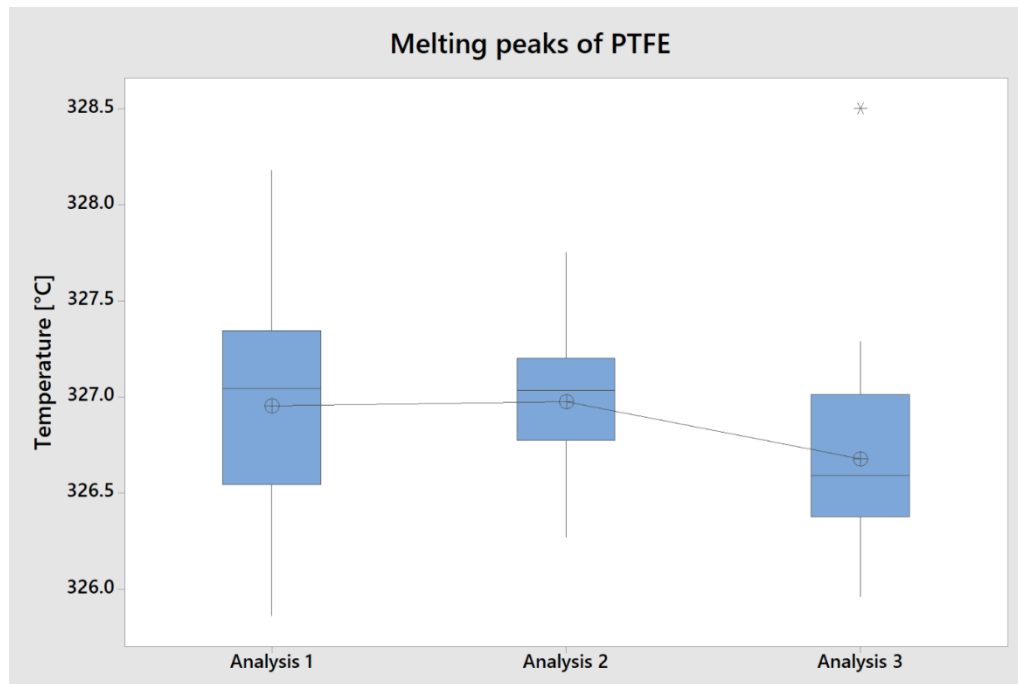


Figure 4.3: Graphical variation of the values of T_m obtained for the PTFE in each one of the performed analyses.

In the same way, Table 4.4 shows the main parameters used to create the Box Plot Graph of PTFE, showed in Figure 4.3, as well as the values obtained from them.

Table 4.4: Data used to create the box plot graph of the melting peaks of PTFE of all three analyses.

Statistics of PTFE									
Variable	N	Mean	SE Mean	StDev	Minimum	Q1	Median	Q3	Maximum
Analysis 1	24	327,0	0,124	0,607	325,9	326,5	327,0	327,3	328,2
Analysis 2	24	327,0	0,076	0,372	326,3	326,8	327,0	327,2	327,7
Analysis 3	24	326,7	0,11	0,538	326,0	326,4	326,6	327,0	328,5

So, as it is possible to see in the Box Plots Graphs, all three series of measurements show that the used methodology is reproducible.

In addition, in order to confirm this assessment, from a statistical point of view, it was also performed an Analysis of Variance (ANOVA). However, as explained in the previous chapter, the ANOVA can only be performed if the samples are normally distributed. So, Figure 4.4 and Figure 4.5 show, respectively, the Probability Plot (considering a normal distribution with a confidence interval of 95%) of Analyses 1, 2 and 3 for both the PA46 and the PTFE.

Among the results presented on each graph, the most important one is the P-value (significance level), that needs to be smaller than 0,05 or 5% so that the data can be considered normally distributed. Besides it, it is also suitable to take into consideration the Anderson Darling (AD) parameter, that measures how well the data points fit the normal distribution (their distance from the central line). Smaller values of AD parameter give evidence of better goodness of fit of normal distribution.

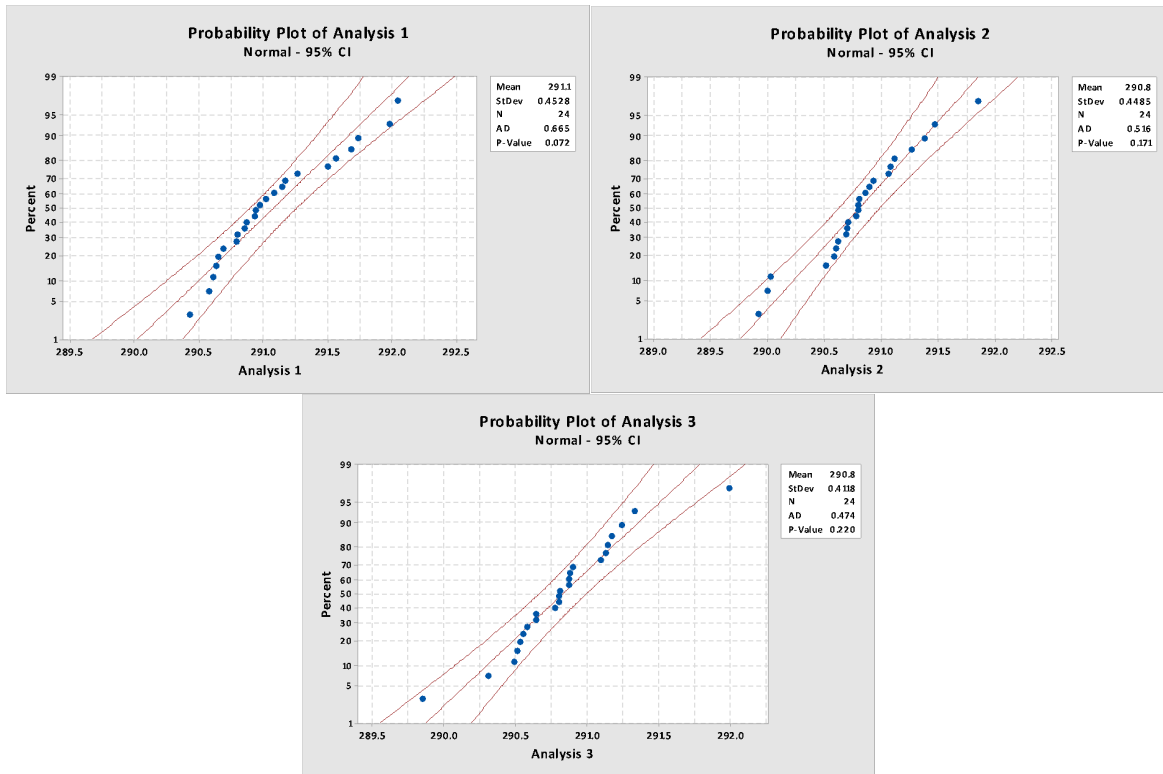


Figure 4.4: Probability Plots of Analyses 1, 2 and 3 for the PA46. The P-values are respectively 0.072, 0.171 and 0.220, that are all greater than 0.05 (5%).

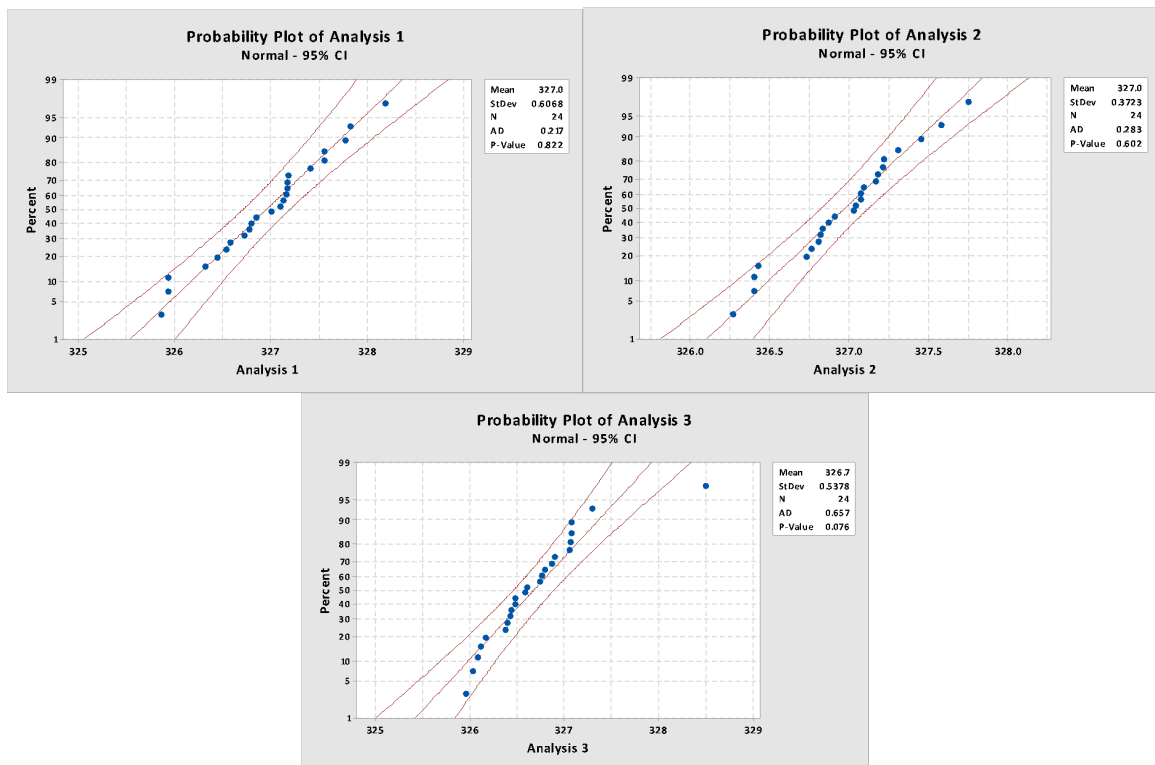


Figure 4.5: Probability Plots of Analyses 1, 2 and 3 for the PTFE. The P-values are respectively 0.822, 0.602 and 0.076, that are all greater than 0.05 (5%).

As the Probability Plots of both polymers confirmed that all the data are normally distributed (P-values > 0.05), it was possible to perform the ANOVA Test.

Table 4.5, Table 4.6 and Table 4.7 present the results of the Analysis of Variance of the polymer PA46. Also in this case, the main result is the P-value (in Table 4.6), that presented a value of 0.065, that is greater than 0.05, confirming that there is no statistical difference between all three factors (Analyses, 1, 2 and 3).

Table 4.5: It shows the number of factors analyzed in the ANOVA Test. There were 3 factors: Analysis 1, Analysis 2 and Analysis 3 of PA46.

Factor Information PA46		
Factor	Levels	Values
Factor	3	Analysis 1, Analysis 2, Analysis 3

Table 4.6: It shows the parameters used for the test, such as the calculated factor, error and total values of Degree of Freedom, Sum of Squares, Mean Squares, F-value and P-value. The P-value was calculated as 0,065.

Analysis of Variance PA46					
Source	DF	Adj SS	Adj MS	F-Value	P-Value
Factor	2	1.092	0.5459	2.84	0.065
Error	69	13.243	0.1919		
Total	71	14.335			

Table 4.7: It shows the number of observations (N) considered in each one of the three factors, the mean of each factor, the standard deviation and the limits of the 95% confidence interval.

Means PA46				
Factor	N	Mean	StDev	95% CI
Analysis 1	24	291.079	0.453	(290.901, 291.258)
Analysis 2	24	290.808	0.449	(290.630, 290.987)
Analysis 3	24	290.829	0.412	(290.650, 291.007)

In the same way, Table 4.8, Table 4.9 and Table 4.10 present the results of the ANOVA for the PTFE. Also in this case, the obtained P-value of 0.089 is greater than 0.05, confirming that there is no statistical difference between the factors.

Table 4.8: It shows the number of factors analyzed in the ANOVA Test. There were 3 factors: Analysis 1, Analysis 2 and Analysis 3 of PTFE.

Factor Information PTFE		
Factor	Levels	Values
Factor	3	Analysis 1, Analysis 2, Analysis 3

Table 4.9: It shows the parameters used for the test, such as the calculated factor, error and total values of Degree of Freedom, Sum of Squares, Mean Squares, F-value and P-value. The P-value was calculated as 0,089.

Analysis of Variance PTFE					
Source	DF	Adj SS	Adj MS	F-Value	P-Value
Factor	2	1.332	0.6660	2.51	0.089
Error	69	18.310	0.2654		
Total	71	19.642			

Table 4.10: It shows the number of observations (N) considered in each one of the three factors, the mean of each factor, the standard deviation and the limits of the 95% confidence interval.

Means PTFE				
Factor	N	Mean	StDev	95% CI
Analysis 1	24	326.953	0.607	(326.744, 327.163)
Analysis 2	24	326.975	0.372	(326.765, 327.185)
Analysis 3	24	326.676	0.538	(326.466, 326.886)

Therefore, it is possible to conclude that the utilized methodology is reproducible, because different measurements, performed in different periods by different operators, do not present statistical differences.

4.2. DSC - Content Determination

As explained in Section 3.2.1, it was performed an integration of the melting peak of the PTFE by using the Content Determination function, that compares the measured enthalpy of fusion with the one from the semi crystalline pure material (41J/g) in order to determine the approximate content of it. Then, once obtained the content of PTFE, the complementary content of PA46 can be calculated.

This method was performed in all three groups samples from LM481-17 to LM504-17, using the measurement curves from Analyses 1, 2 and 3. The measurement curves with the representation of the integration area are presented in Appendix E, while the results obtained are showed in Table 4.11.

It is possible to observe that Analyses 1, 2 and 3 presented quite similar results, with average contents of PA46 of 86.48, 86.24 and 85.96%, and average contents of PTFE of 13.52, 13.76 and 14.04%.

Table 4.11: Results of the content determination of PA46 and PTFE, obtained from the DSC measurement curves of Analyses 1, 2 and 3.

Sample	Analysis 1		Analysis 2		Analysis 3	
	%PTFE	%PA46	%PTFE	%PA46	%PTFE	%PA46
LM481-17	12,35	87,65	13,03	86,97	13,28	86,72
LM482-17	15,04	84,96	13,18	86,82	13,65	86,35
LM483-17	13,94	86,06	12,28	87,72	12,66	87,34
LM484-17	12,94	87,06	13,90	86,10	14,25	85,75
LM485-17	13,14	86,86	13,10	86,90	13,19	86,81
LM486-17	13,44	86,56	15,43	84,57	14,35	85,65
LM487-17	12,93	87,07	13,96	86,04	14,63	85,37
LM488-17	14,06	85,94	14,32	85,68	12,79	87,21
LM489-17	15,03	84,97	13,17	86,83	13,71	86,29
LM490-17	13,93	86,07	13,96	86,04	14,30	85,70
LM491-17	13,37	86,63	14,44	85,56	14,57	85,43
LM492-17	13,24	86,76	13,62	86,38	13,74	86,26
LM493-17	14,30	85,70	14,41	85,59	13,38	86,62
LM494-17	14,21	85,79	14,56	85,44	14,47	85,53
LM495-17	13,67	86,33	13,66	86,34	13,51	86,49
LM496-17	13,88	86,12	13,69	86,31	16,86	83,14
LM497-17	13,45	86,55	12,55	87,45	14,27	85,73
LM498-17	15,46	84,54	13,94	86,06	14,19	85,81
LM499-17	13,83	86,17	13,01	86,99	13,63	86,37
LM500-17	10,95	89,05	12,76	87,24	14,14	85,86
LM501-17	11,99	88,01	14,72	85,28	14,83	85,17
LM502-17	12,07	87,93	14,13	85,87	14,33	85,67
LM503-17	14,12	85,88	14,32	85,68	13,64	86,36
LM504-17	13,11	86,89	14,00	86,00	14,66	85,34
Max Value	15,46	89,05	15,43	87,72	16,86	87,34
Min. Value	10,95	84,54	12,28	84,57	12,66	83,14
Average Value	13,52	86,48	13,76	86,24	14,04	85,96
Standard Deviation	1,03	1,03	0,75	0,75	0,84	0,84

In addition, in order to create the Evaluation Macro and set an automatic process, the first part consisted in making all the evaluation according to the steps mentioned in Section 3.2.1. Then, once the results were obtained and everything was showed on the screen, the EvalMacro button at the top menu was selected and the 'Save EvalMacro As' option was chosen. Finally, it was necessary to insert the name of the Evaluation Macro.

So, with the Evaluation Macro saved, it is possible to calculate the content of each polymer automatically in the following way:

- Open the measurement curve in the Evaluation Window
- Select EvalMacro > Open EvalMacro.

- Select the name of the Evaluation Macro you want to open in the newly opened window.
- If the Evaluation Macro was properly saved, the program will automatically exhibit all the information about the experiment, the method of measurement and the sample, and it will automatically determine the baseline (Integral Tangential), calculate the integral of the PTFE melting peak and its content, by using the set value of 41J/g for the enthalpy of fusion of the semi crystalline pure material.

4.3. TGA – Content Determination

All the measurement curves obtained during the TGA analyses of the 24 samples taken from spring bushing components LM481-17 to LM504-17 can be seen in Appendix E, while a comparison of them is showed in the thermogram of Figure 4.6.

The thermogram shows the percentage of weight, on axis y, and the time, in minutes, on axis x. When the measurement starts, the sample has 100% of its weight, that decreases depending on the reactions and thermal effects to which the sample is subjected with the increase of temperature.

So, it is possible to see that in the first 15 minutes there is no loss of mass, which means that the material didn't undergo any reaction. Then, there is a small deviation of the baseline, that is probably due to the presence of moisture, that evaporates. After that it is possible to see two significant steps, that refer respectively to the decomposition of PA46 and PTFE. Finally, at the end of the measure there is always a small percentage of mass, that corresponds to either additives that didn't undergo any decomposition process, or ashes produced from the material decomposition.

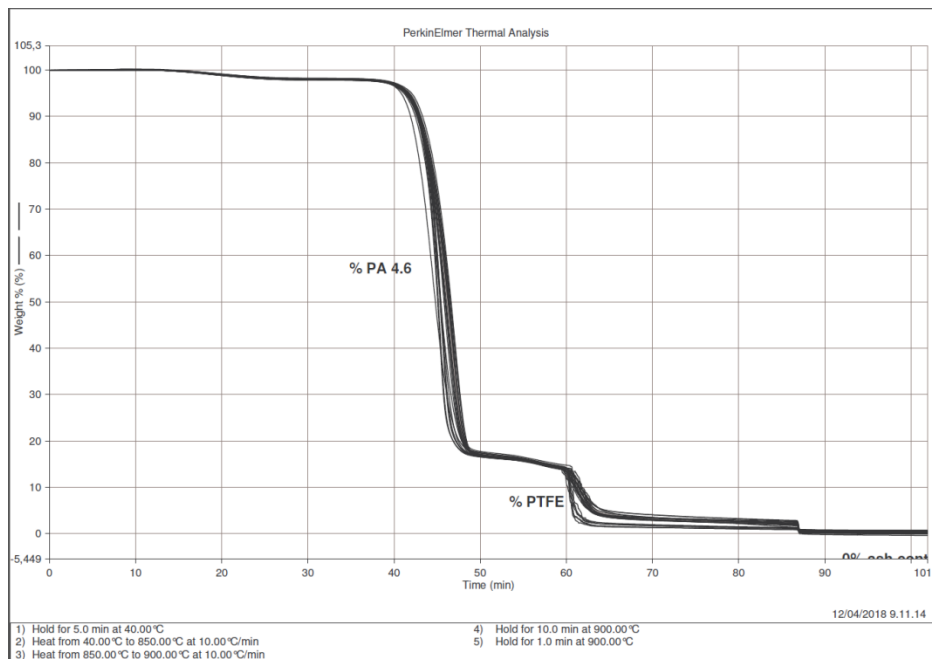


Figure 4.6: TGA measurement curves of samples LM481-17 to LM504-17. It is possible to recognize the steps formed during the decomposition of PA46 and PTFE due to the loss of weight.

Table 4.12 summarizes the content values obtained from the TGA analyses for both polymers, PA46 and PTFE, and it also brings the content of residue found in the sample. The maximum value of PA46 content was 83,8398% and the minimum was 82,72%, with an average of 83,46%; while for the PTFE the maximum content was 15,18% and the minimum 12,90%, with an average of 13,78%.

The analysis also identified some residue at the end of the experiment, that presented a maximum content of 3,93% and a minimum of 0,71%, with an average value of 2,46%.

Table 4.12: Results of the content values (%) of PA46, PTFE and residue obtained from the TGA analyses of the 24 samples (from LM481-17 to LM504-17).

Sample	PA46 (%)	PTFE (%)	Residue (%)	Sum (%)
LM481-17	83,56	13,48	2,96	100,00
LM482-17	83,31	13,19	3,38	99,88
LM483-17	83,39	13,35	2,97	99,71
LM484-17	83,80	13,31	3,30	100,41
LM485-17	83,05	12,90	3,93	99,88
LM486-17	83,01	13,99	3,04	100,04
LM487-17	83,76	14,53	1,24	99,53
LM488-17	83,02	15,18	1,63	99,83
LM489-17	83,84	14,80	0,95	99,59
LM490-17	83,77	14,94	0,71	99,42
LM491-17	83,73	14,94	0,81	99,48
LM492-17	83,06	13,44	3,23	99,73
LM493-17	83,19	13,53	2,93	99,65
LM494-17	83,59	13,50	2,64	99,73
LM495-17	83,64	12,92	2,95	99,51
LM496-17	82,72	13,23	3,34	99,29
LM497-17	83,78	13,00	3,05	99,83
LM498-17	83,29	13,43	2,94	99,66
LM499-17	83,80	13,38	2,48	99,66
LM500-17	83,49	13,19	2,77	99,45
LM501-17	83,47	13,67	2,67	99,81
LM502-17	83,45	13,62	2,84	99,91
LM503-17	83,71	14,59	1,03	99,32
LM504-17	83,53	14,56	1,24	99,33
Max Value	83,84	15,18	3,93	102,96
Min. Value	82,72	12,90	0,71	96,33
Average Value	83,46	13,78	2,46	99,69
Standard Deviation	0,32	0,71	0,96	1,99

The residue present at the end of the measurement is usually associated to the ashes from the decomposition process of the polymers and to inert substances, like

additives and fillers, that did not react within the temperature range used and remained intact after the measurement.

These residues are not seen in the DSC analyses because of two main reasons:

- The range of temperature used in the DSC measurement is only able to melt the material, without causing its decomposition, so there isn't any formation of ashes.
- The range of temperature used in the DSC measurement is not high enough to melt the inert substances presented in the material, so it is not possible to observe a corresponding melting peak.

4.4. Statistical Evaluation of the Content Determination

Once the content of each polymer was determined using both the DSC and the TGA, it is suitable to analyze the results under a statistical point of view to mainly check two important points:

- whether the content determination through the DSC can be considered trustful and reproducible.
- which is the statistical difference between the results obtained from each one of the three analyses, using the DSC, and the results from the TGA.

All the values of content determined, both through the DSC (Analyses 1, 2 and 3) and the TGA, for the PA46 are showed, in Table 4.13.

As showed before, it is possible to see that the average contents obtained from the DSC are quite similar (86.48, 86.24 and 85.96% respectively), while the average obtained from the TGA is slightly below (83,46%). However, considering the average of all fours measurements, for each one of the 24 samples, it is possible to observe that the values give a total average of 85,53%of content of PA46 (see Table 4.13), that can be considered exactly the nominal content of PA46 present in the Stanyl® TW371 material, which is 85%.

Table 4.13: Values of content obtained for the PA46 in each one of the performed analyses.

Content PA46						
Sample	Analysis 1	Analysis 2	Analysis 3	TGA	Average	Standard Deviation
LM481-17	87,65	86,97	86,72	83,56	86,22	1,82
LM482-17	84,96	86,82	86,35	83,31	85,36	1,58
LM483-17	86,06	87,72	87,34	83,39	86,13	1,96
LM484-17	87,06	86,10	85,75	83,80	85,68	1,37
LM485-17	86,86	86,90	86,81	83,05	85,90	1,91
LM486-17	86,56	84,57	85,65	83,01	84,95	1,53
LM487-17	87,07	86,04	85,37	83,76	85,56	1,39
LM488-17	85,94	85,68	87,21	83,02	85,46	1,76
LM489-17	84,97	86,83	86,29	83,84	85,48	1,35
LM490-17	86,07	86,04	85,70	83,77	85,40	1,09
LM491-17	86,63	85,56	85,43	83,73	85,34	1,20
LM492-17	86,76	86,38	86,26	83,06	85,62	1,71
LM493-17	85,70	85,59	86,62	83,19	85,27	1,47
LM494-17	85,79	85,44	85,53	83,59	85,09	1,01
LM495-17	86,33	86,34	86,49	83,64	85,70	1,38
LM496-17	86,12	86,31	83,14	82,72	84,57	1,91
LM497-17	86,55	87,45	85,73	83,78	85,88	1,56
LM498-17	84,54	86,06	85,81	83,29	84,93	1,28
LM499-17	86,17	86,99	86,37	83,80	85,83	1,40
LM500-17	89,05	87,24	85,86	83,49	86,41	2,35
LM501-17	88,01	85,28	85,17	83,47	85,48	1,88
LM502-17	87,93	85,87	85,67	83,45	85,73	1,83
LM503-17	85,88	85,68	86,36	83,71	85,41	1,17
LM504-17	86,89	86,00	85,34	83,53	85,44	1,43
Total					85,53	1,55

In order to analyze these data and check whether there are significant differences, it was made a Box Plot Graph, using the Minitab Software, as showed in Figure 4.7. The Box Plot confirms the difference between the averages of Analyses 1, 2 and 3, and the TGA, which was already expected due to the factor that the results were obtained from different analyses, that were performed using different methods of measurement. Besides this, it is also possible to see that there are some outliers in Analyses 1 and 3.

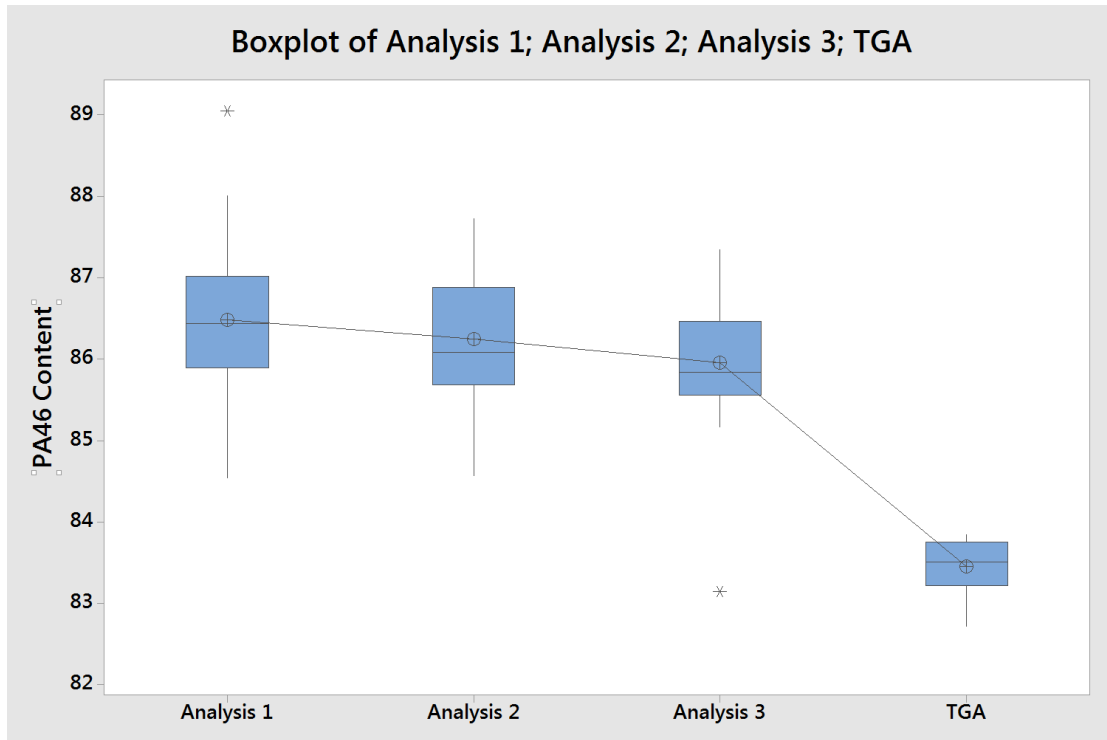


Figure 4.7: Graphical variation of the values of content obtained for the PA46 in each one of the performed DSC analyses and in the TGA.

In addition, each one of the four factors were analyzed through a Probability Plot in order to check whether the data have a normal distribution.

Figure 4.8, Figure 4.9, Figure 4.10 and Figure 4.11 show, respectively, the Probability Plots of Analyses 1, 2, 3 and the TGA. As all the measured P-values were greater than 0,05 (5%), all the data can be considered normally distributed with a confidence level of 95%.

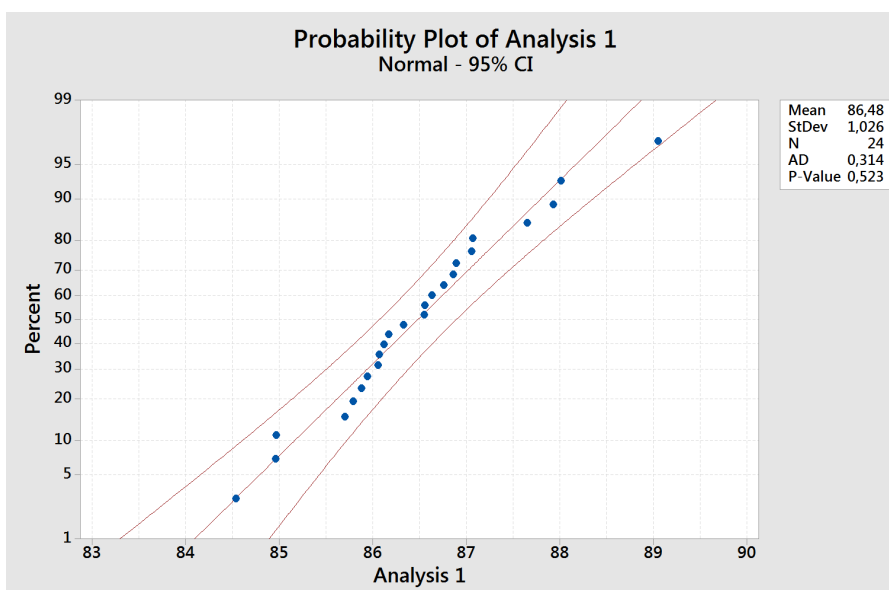


Figure 4.8: Probability Plot of Analysis 1 for the PA46. In this case, the data is normally distributed, because the P-value measured was 0.523 (P-value > 0.05).

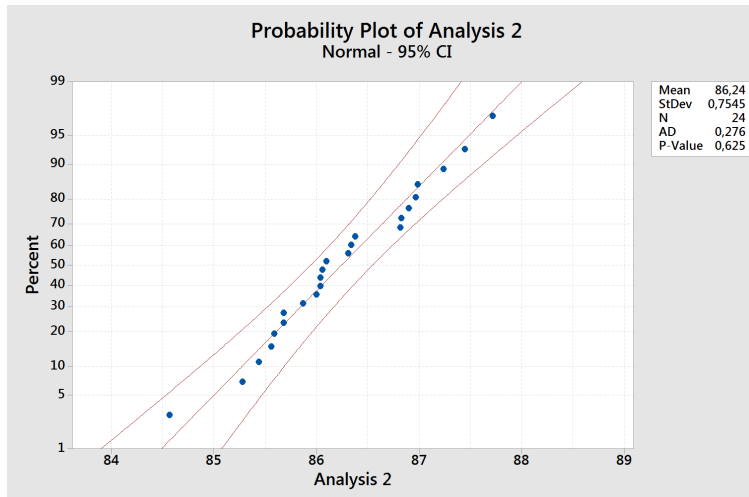


Figure 4.9: Probability Plot of Analysis 2 for the PA46. In this case, the data is normally distributed, because the P-value measured was 0.625 (P-value > 0.05).

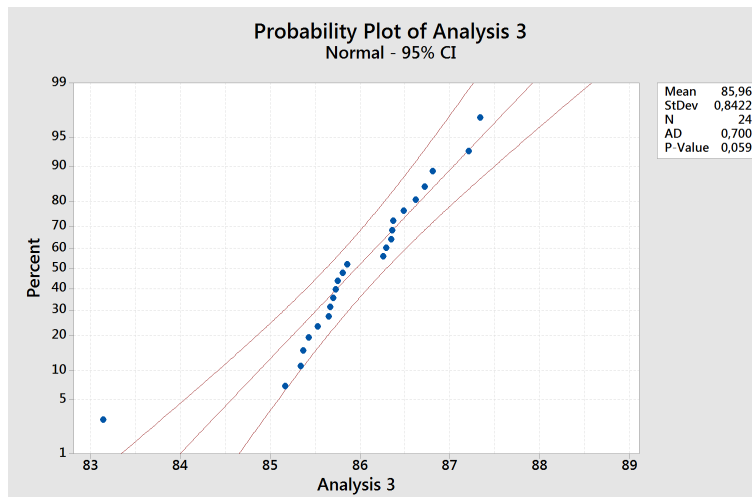


Figure 4.10: Probability Plot of Analysis 3 for the PA46. In this case, the data is normally distributed, because the P-value measured was 0.059 (P-value > 0.05).

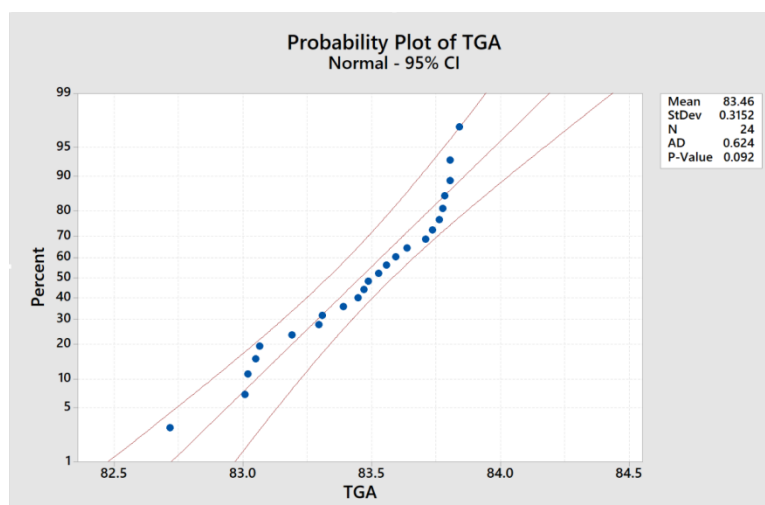


Figure 4.11: Probability Plot of the TGA for the PA46. In this case, the data is normally distributed, because the P-value measured was 0.092 (P-value > 0.05).

Therefore, as all the factors were normally distributed, an Analysis of Variance (ANOVA) was performed in order to calculate the statistical difference between the DSC and TGA results.

Table 4.14, Table 4.15 and Table 4.16 present the results of the Analysis of Variance of the polymer PA46. In this case, the P-value (showed in Table 4.15), presented a value of 0.000, that is smaller than 0.05, confirming that there is a statistical difference between all four factors (TGA and Analyses 1, 2 and 3). This difference was already expected, due to the factor that the results were obtained from different analyses, that were performed using different methods of measurement.

Table 4.14: It shows the number of factors analyzed in the ANOVA Test. There were 4 factors: Analysis 1, Analysis 2, Analysis 3 and TGA of PA46.

Factor Information PA46		
Factor	Levels	Values
Factor	4	Analysis 1, Analysis 2, Analysis 3, TGA

Table 4.15: It shows the parameters used for the test, such as the calculated factor, error and total values of Degree of Freedom, Sum of Squares, Mean Squares, F-value and P-value. The P-value was calculated as 0,000.

Analysis of Variance PA46					
Source	DF	Adj SS	Adj MS	F-Value	P-Value
Factor	3	141,56	47,1871	77,66	0,000
Error	92	55,90	0,6076		
Total	95	197,46			

Table 4.16: It shows the number of observations (N) considered in each one of the four factors, the mean of each factor, the standard deviation and the limits of the 95% confidence interval.

Means PA46				
Factor	N	Mean	StDev	95% CI
Analysis 1	24	86,481	1,026	(86,165; 86,797)
Analysis 2	24	86,244	0,754	(85,928; 86,560)
Analysis 3	24	85,957	0,842	(85,641; 86,273)
TGA	24	83,4561	0,3152	(83,1401; 83,7721)

Finally, since there is a difference, it is suitable to calculate the minimum and maximum differences that one can find between the performed analyses, based in the content ranges showed in Table 4.16 for a confidence interval of 95%.

- Minimum difference: $85,6 - 83,8 = 1,8\%$
- Maximum difference: $86,8 - 83,1 = 3,7\%$
- Error range between DSC and TGA: (1,8; 3,7)

In the same way, all the values of content determined, both through the DSC and the TGA, for the PTFE are showed in Table 4.17, in which it is possible to see that content average value of PTFE obtained from the TGA (13.78%) is very similar to the averages of Analyses 1, 2 and 3, that are respectively 13.52, 13.76 and 14.04%. This can also be confirmed by the low value of standard deviation of 0,73. In addition, it is also possible to see the total average value, considering all fours measurements for each one of the 24 samples, which gives a value of 13,77%. This value is slightly below the nominal content of PTFE present in the Stanyl® TW371 material, which is 15%.

Table 4.17: Values of content obtained for the PTFE in each one of the performed analyses.

Content PTFE						
Sample	Analysis 1	Analysis 2	Analysis 3	TGA	Average	Standard Deviation
LM481-17	12,35	13,03	13,28	13,48	13,03	0,49
LM482-17	15,04	13,18	13,65	13,19	13,77	0,88
LM483-17	13,94	12,28	12,66	13,35	13,06	0,74
LM484-17	12,94	13,90	14,25	13,31	13,60	0,59
LM485-17	13,14	13,10	13,19	12,90	13,08	0,13
LM486-17	13,44	15,43	14,35	13,99	14,30	0,84
LM487-17	12,93	13,96	14,63	14,53	14,01	0,78
LM488-17	14,06	14,32	12,79	15,18	14,09	0,99
LM489-17	15,03	13,17	13,71	14,80	14,18	0,89
LM490-17	13,93	13,96	14,30	14,94	14,28	0,47
LM491-17	13,37	14,44	14,57	14,94	14,33	0,67
LM492-17	13,24	13,62	13,74	13,44	13,51	0,22
LM493-17	14,30	14,41	13,38	13,53	13,91	0,52
LM494-17	14,21	14,56	14,47	13,50	14,18	0,48
LM495-17	13,67	13,66	13,51	12,92	13,44	0,35
LM496-17	13,88	13,69	16,86	13,23	14,42	1,65
LM497-17	13,45	12,55	14,27	13,00	13,32	0,73
LM498-17	15,46	13,94	14,19	13,43	14,26	0,86
LM499-17	13,83	13,01	13,63	13,38	13,46	0,35
LM500-17	10,95	12,76	14,14	13,19	12,76	1,34
LM501-17	11,99	14,72	14,83	13,67	13,80	1,32
LM502-17	12,07	14,13	14,33	13,62	13,54	1,02
LM503-17	14,12	14,32	13,64	14,59	14,17	0,40
LM504-17	13,11	14,00	14,66	14,56	14,08	0,71
				Total	13,77	0,73

Figure 4.12 presents the Box Plot Graph of the corresponding data, obtained using the Minitab Software. Also, in this case, it is possible to see the presence of some outliers in Analyses 1 and 3, that are the complementary values of the correspondent outliers observed in the PA46 results.

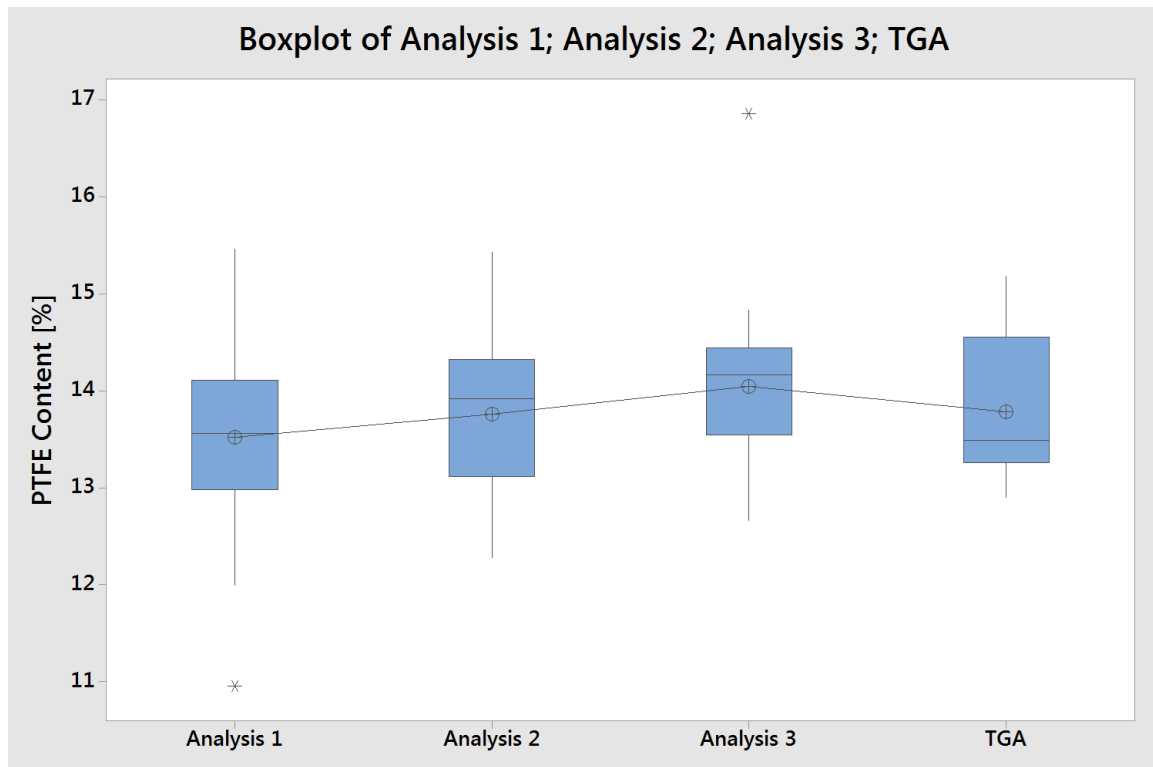


Figure 4.12: Graphical variation of the values of content obtained for the PTFE in each one of the performed DSC analyses and in the TGA.

In addition, following the same steps of the PA46, each one of the four factors were analyzed through a Probability Plot in order to check whether the data have a normal distribution.

Figure 4.13, Figure 4.14 and Figure 4.15 show, respectively, the Probability Plots of Analyses 1, 2, and 3 for the PTFE. As all the measured P-values were greater than 0.05 (5%), all the data can be considered normally distributed with a confidence level of 95%.

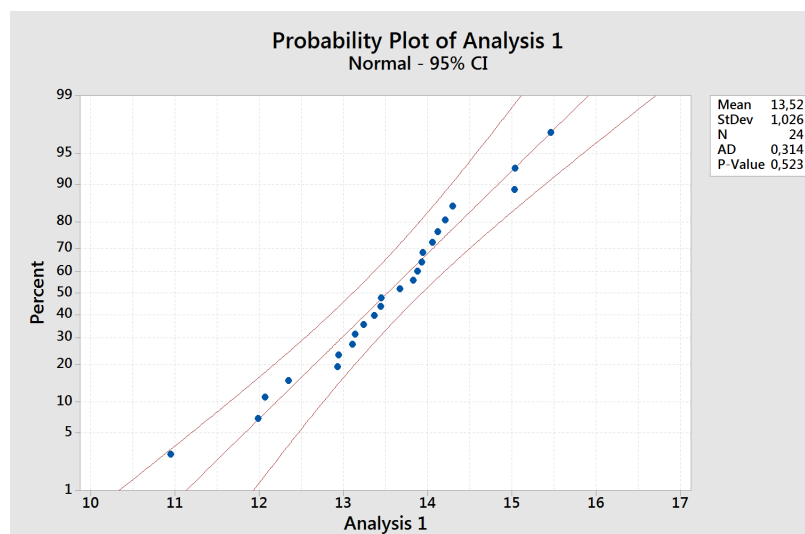


Figure 4.13: Probability Plot of Analysis 1 for the PTFE. In this case, the data is normally distributed, because the P-value measured was 0.523 (P-value > 0.05).

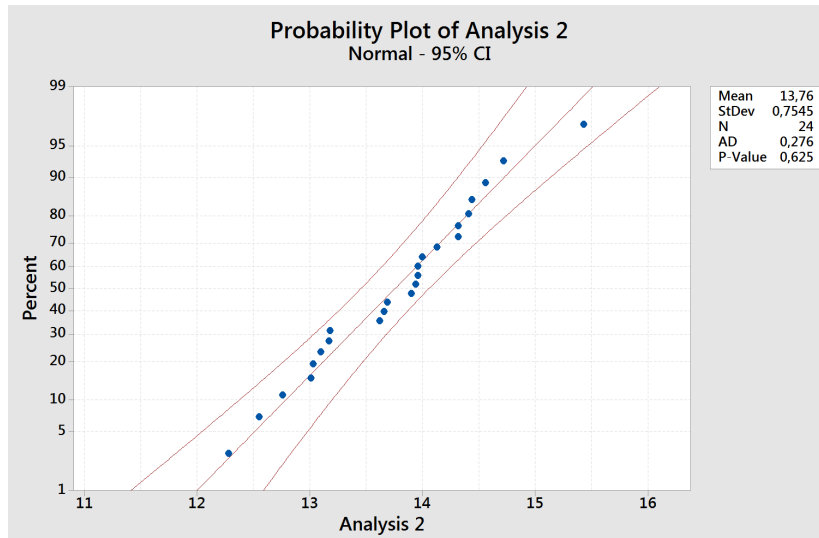


Figure 4.14: Probability Plot of Analysis 2 for the PTFE. In this case, the data is normally distributed, because the P-value measured was 0.625 (P-value > 0.05).

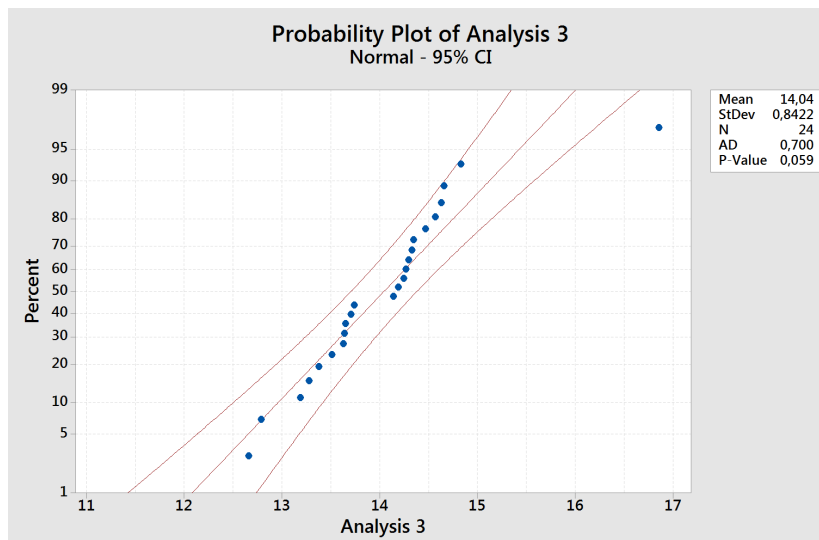


Figure 4.15: Probability Plot of Analysis 3 for the PTFE. In this case, the data is normally distributed, because the P-value measured was 0.059 (P-value > 0.05).

The results of the PTFE content obtained from the TGA, on the other hand, could not be adapted to a normal distribution (P-value < 0.05), because, as showed in the Probability Plot and in the Histogram in Figure 4.16, there are practically two families of data.

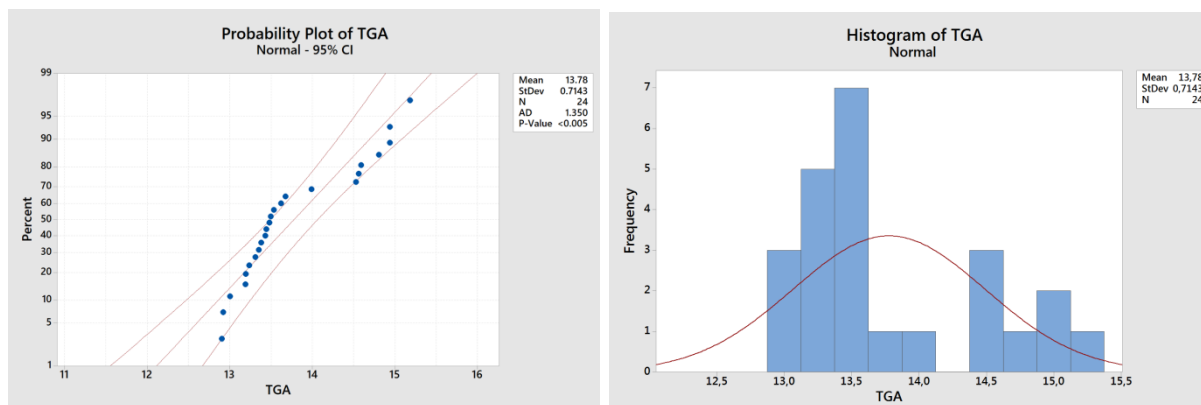


Figure 4.16: Probability Plot and Histogram of the content of PTFE obtained from the TGA. It does not present a normal distribution (P-value < 0.05).

Therefore, since not all the analyzed factors (Analysis 1, 2, 3 and TGA) are normally distributed, the Mood's Median Test was performed in order to calculate the statistical difference between the DSC and TGA results.

Table 4.18 and Table 4.19 present the results of the Mood's Median Test for the PTFE. In this case, the P-value (in Table 4.18) presented a value of 0.172, that is greater than 0.05, confirming that for this polymer there is no statistical difference between the results obtained from Analyses 1, 2, 3 and the TGA.

Table 4.18: It shows the number of observations (N) considered in each one of the four factors, the mean of each factor, the standard deviation and the limits of the 95% confidence interval.

Mood median test for Response			
Chi-Square = 5,00	DF = 3	P-value = 0,172	Overall median = 13,68

Table 4.19: It shows the median of each factor, the number of observations (N) that are below and above the overall median, the interquartile range (Q3-Q1) and the limits of the 95% confidence interval.

Factor	N≤	N>	Median	Q3-Q1	Individual 95,0% CIs
Analysis 1	13	11	13,56	1,12	(13.1348, 13.9608)
Analysis 2	10	14	13,92	1,20	(13.1783, 14.1629)
Analysis 3	9	15	14,16	0,90	(13.6383, 14.3335)
TGA	16	8	13,49	1,30	(13.3429, 14.0837)

Therefore, it is possible to conclude that a P-value of 0,172 gives confidence that there isn't a statistical difference between the two methods of analysis. This result is different from the result of ANOVA because in this case it is utilized a less robust statistic test that compare median and not average values.

5. Conclusions

The melting temperature, obtained from the DSC analyses confirmed that it is possible to identify the polymers present in the material. The methodology is reproducible, because different measurements, performed in different periods by different operators, did not present statistical differences.

Regarding the content determination of the polymer blends through the DSC, this work proved that it is possible to be done; it can be performed using different procedures and it can be set to be performed automatically through an Evaluation Macro.

The comparison between the results from the DSC, the TGA and the nominal contents of the product shows that the variations between them are about 3%. It is important to note that this variation is quite small considering the use of different techniques, that aim to measure different properties in function of temperature, and use different parameters (balance, sample weight, heat flow, atmosphere...) and different methods of calculating and obtaining their results.

Therefore, as the objective of this work was to find out whether it is possible to obtain an indicative idea of the content of the analyzed material through the DSC, it is possible to conclude that the results were very satisfactory, the mentioned methods can be considered trustful and reproducible, and can indeed be used for analyses in the daily life of the R&D Laboratory of Materials at Dayco, Ivrea.

Finally, some improvements that could be studied for a future work are:

- The content determination of the PA 46 by the integration using the literature value of 8,6J/g and the comparison of the results with the ones obtained from the complement to 100% using the PTFE content value.
- The obtainment of the melting enthalpy of the pure substances from the suppliers, in order to measure a more precise value of content for each polymer.
- Weight the crucible-sample system before and after the measurement, in order to be able to identify also the presence of humidity and possible volatile substances.
- Perform a chemical analysis of the residues from the TGA, in order to identify their composition and their origin.

6. Bibliography

- [1] Wear and Friction of Materials - Tribological Characteristics of Engineering Thermoplastics (Stanyl, Plaslube and Nylatron). DSM Engineering Plastics.
- [2] "Polyamides of DSM," presented at the DSM-Dayco Tech Day, 29-Sep-2014.
- [3] "Polyamides." [Online]. Available: <http://www.essentialchemicalindustry.org/polymers/polyamides.html>. [Accessed: 31-May-2018].
- [4] W. D. Callister and D. G. Rethwisch, Materials science and engineering. Hoboken, NJ: Wiley, 2011.
- [5] D. M. Wagner and G. Widmann, Thermal Analysis in Practice - Collected Applications Handbook. Schwerzenbach, Switzerland: Mettler Toledo, 2009.
- [6] A. Myśliński, "Materials and Instructions for Experiments no. 2 and 5 - Basic Technology of polymers," Faculty of Chemistry, University of Warsaw, Warsaw, 2017.
- [7] "Polytetrafluoroethylene." [Online]. Available: <http://pslc.ws/macrog/ptfe.htm>. [Accessed: 01-Mar-2018].
- [8] "Moisture Absorption in Durethan Polyamide Parts - Product Information." Lanxess Energizing Chemistry, May-2005.
- [9] "Annealing to enhance material properties - Reduction of moisture uptake," presented at the DSM - Dayco Tech Day, 16-Nov-2015.
- [10] "Dispense di polimeri avanzati, degradazione e riciclo dei polimeri," Corso di Laurea Magistrale in Ingegneria Dei Materiali, Politecnico di Torino, Torino, 2017.
- [11] W. Wang, L. Meng, and Y. Huang, "Hydrolytic degradation of monomer casting nylon in subcritical water," Polym. Degrad. Stab., vol. 110, pp. 312–317, Dec. 2014.
- [12] L. Meng, Y. Zhang, Y. Huang, M. Shibata, and R. Yosomiya, "Studies on the decomposition behavior of nylon-66 in supercritical water," Polym. Degrad. Stab., vol. 83, no. 3, pp. 389–393, Mar. 2004.
- [13] Z. Czégény and M. Blazsó, "Thermal decomposition of polyamides in the presence of poly(vinyl chloride)," J. Anal. Appl. Pyrolysis, vol. 58–59, pp. 95–104, Apr. 2001.
- [14] Stanyl PA46 - General Information on applications, processing and properties. DSM Engineering Plastics, 2002.
- [15] "Nylon 6 - Influence of Water on Mechanical Properties and Tg." PerkinElmer, 2007.
- [16] "Stanyl - General Information on Properties." DSM Engineering Plastics, Sep-2004.

- [17] "Moisture resistance." [Online]. Available: http://www.dsm.com/products/stanyl/en_US/product-info/properties/moisture.html. [Accessed: 02-Mar-2018].
- [18] A. Melillo, "Istruzione tecnica per l'utilizzo del Calorimetro Differenziale a Scansione," Dayco Europe S.r.l, IT 03-16, Aug. 2017.
- [19] F. Lodroni and E. Girotti, "Good Thermal Analysis Practice (GTAP) - Consigli e suggerimenti per Analisi Affidabili," presented at the Mettler Toledo, 2017.
- [20] D. J. Schawe, D. R. Riesen, J. Widmann, D. M. Schubnell, and U. Jorimann, "Usercom 11 - Information for users of Mettler Toledo thermal analysis system." Mettler Toledo GmbH, Analytical.
- [21] D. M. Nijman, Thermal Analysis in Practice - Tips and Hints - Introductory Handbook, vol. 2. Schwerzenbach, Switzerland: Mettler Toledo, 2013.
- [22] M.-T. I. I. all rights reserved, "Evaluation Possibilities for the Glass Transition." [Online]. Available: https://www.mt.com/hk/en/home/supportive_content/matchar_apps/MatChar_HB401.html. [Accessed: 13-Mar-2018].
- [23] D. A. Hammer, Thermal Analysis of Polymers - Selected Applications Handbook. Schwerzenbach, Switzerland: Mettler Toledo, 2013.
- [24] "FAQ Beginners Guide to Thermogravimetric Analysis (TGA)." PerkinElmer, 2015.
- [25] Netzsch-Gerätebau GmbH, "Thermal Properties of Polymer Materials at a Glance." [Online]. Available: <https://www.openpr.com/news/189753/Thermal-Properties-of-Polymer-Materials-at-a-Glance.htm>. [Accessed: 01-Mar-2018].
- [26] Calvero, Chemical structure of poly(tetrafluoroethylene). 2006.
- [27] M.-T. I. I. all rights reserved, "DSC 3 - Differential Scanning Calorimeter." [Online]. Available: https://www.mt.com/ch/en/home/products/Laboratory_Analytics_Browse/TA_Family_Browse/DSC/DSC_3.html. [Accessed: 15-Feb-2018].
- [28] V. F. Sciuti, C. C. Melo, L. B. Canto, and R. B. Canto, "Influence of Surface Crystalline Structures on DSC Analysis of PTFE," Mater. Res., vol. 20, no. 5, pp. 1350–1359, Jul. 2017.
- [29] T. B. Douglas and A. W. Harman, "Relative enthalpy of polytetrafluoroethylene from 0 to 440°C," Journal of Research of the National Bureau of Standards, vol. 69A, p. 9, 1965.
- [30] J. Blumm, A. Lindemann, M. Meyer, and C. Strasser, "Characterization of PTFE Using Advanced Thermal Analysis Techniques," Int. J. Thermophys., vol. 31, no. 10, pp. 1919–1927, Oct. 2010.
- [31] "What is a boxplot?" [Online]. Available: <http://support.minitab.com/en-us/minitab/17/topic-library/basic-statistics-and-graphs/graphs/graphs-that-compare-groups/boxplots/boxplot/>. [Accessed: 23-Apr-2018].
- [32] G. Della Role, "Corso Six Sigma per Black Belts - Fase di Analyze," presented at the Machiper, Jan-2011.

[33] "What are quartiles?" [Online]. Available: <http://support.minitab.com/en-us/minitab/17/topic-library/basic-statistics-and-graphs/graphs/graphs-that-compare-groups/boxplots/quartiles/>. [Accessed: 23-Apr-2018].

[34] "Box Plot Diagram to Identify Outliers." [Online]. Available: <http://www.whatissixsigma.net/box-plot-diagram-to-identify-outliers/>. [Accessed: 23-Apr-2018].

[35] "Basic Stats in R - Boxplot," Biost@ts. [Online]. Available: <https://biostats.w.uib.no/7-boxplot/>. [Accessed: 23-Apr-2018].

[36] D. C. Montgomery and G. C. Runger, Applied statistics and probability for engineers, 3rd ed. New York: Wiley, 2003.

[37] "Methods and formulas for the analysis of variance in One-Way ANOVA." [Online]. Available: <https://support.minitab.com/en-us/minitab/18/help-and-how-to/modeling-statistics/anova/how-to/one-way-anova/methods-and-formulas/analysis-of-variance/>. [Accessed: 01-May-2018].

[38] "Standard Error of the Mean." [Online]. Available: <https://explorable.com/standard-error-of-the-mean>. [Accessed: 01-May-2018].

[39] "Standard Deviation Formulas." [Online]. Available: <http://www.mathsisfun.com/data/standard-deviation-formulas.html>. [Accessed: 01-May-2018].

[40] "Polymer Data Base." [Online]. Available: <http://www.polymerprocessing.com/polymers/index.html>. [Accessed: 07-Mar-2018].

7. Appendix A

Table 7.1 Description of PA6. [2], [25]

PA6	
Commercial name [DSM]	Akulon K/F
Ratio methylene/amide	5
Molecular structure	
Tm (°C)	225-235
Tg (°C)	50-80
Decomposition Temperature (°C)	435
Crystallinity (%)	30-40
Density (g/cm³)	1.12-1.15
Young's Modulus (MPa)	2800
Coef. of Linear Thermal Expansion (*10⁻⁶/K)	80-90
Specific Heat Capacity (J/(g.K))	1.59-1.70
Thermal Conductivity (W/(m.K))	0.22-0.33
Melting Enthalpy (J/g)	190

Table 7.2: Description of PA66. [2], [25]

PA66	
Commercial name [DSM]	Akulon S
Ratio methylene/amide	5
Molecular structure	
Tm (°C)	225-265
Tg (°C)	70-90
Decomposition Temperature (°C)	430-473
Crystallinity (%)	50
Density (g/cm³)	1.13-1.16
Young's Modulus (MPa)	3000
Coef. of Linear Thermal Expansion (*10⁻⁶/K)	35-45
Specific Heat Capacity (J/(g.K))	1.67-1.70
Thermal Conductivity (W/(m.K))	0.24-0.33
Melting Enthalpy (J/g)	185

Table 7.3: Description of PA11. [2], [25], [40]

PA11	
Commercial name [DSM]	Nylon 11
Ratio methylene/amide	10
Molecular structure	$- \left[\overset{\text{H}}{\underset{ }{\text{N}}} - \overset{\text{O}}{\parallel}{\text{C}} - (\text{CH}_2)_{10} \right] -$
Tm (°C)	185
Tg (°C)	40-50
Decomposition Temperature (°C)	-
Crystallinity (%)	-
Density (g/cm³)	1.03-1.05
Young's Modulus (MPa)	1400
Coef. of Linear Thermal Expansion (*10⁻⁶/K)	85-120
Specific Heat Capacity (J/(g.K))	1.26
Thermal Conductivity (W/(m.K))	0.23-028
Melting Enthalpy (J/g)	224

Table 7.4: Description of PA12. [2], [25], [40]

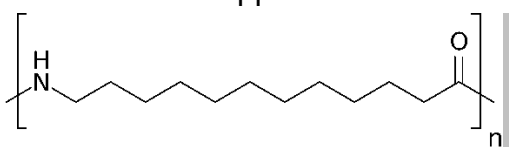
PA12	
Commercial name [DSM]	Nylon 12
Ratio methylene/amide	11
Molecular structure	
Tm (°C)	170-180
Tg (°C)	40-50
Decomposition Temperature (°C)	464
Crystallinity (%)	-
Density (g/cm³)	1.01-1.04
Young's Modulus (MPa)	1400
Coef. of Linear Thermal Expansion (*10⁻⁶/K)	120-140
Specific Heat Capacity (J/(g.K))	1.17-1.26
Thermal Conductivity (W/(m.K))	0.22-0.24
Melting Enthalpy (J/g)	95

Table 7.5: Description of PA610. [2], [25], [40]

PA610	
Commercial name [DSM]	Nylon 6,10
Ratio methylene/amide	7
Molecular structure	$- \left[\overset{\text{H}}{\underset{ }{\text{N}}} - (\text{CH}_2)_6 - \overset{\text{H}}{\underset{ }{\text{N}}} - \overset{\text{O}}{\parallel} \text{C} - (\text{CH}_2)_8 - \overset{\text{O}}{\parallel} \text{C} \right] -$
Tm (°C)	210-230
Tg (°C)	50-80
Decomposition Temperature (°C)	-
Crystallinity (%)	-
Density (g/cm³)	1.07-1.09
Young's Modulus (MPa)	2700
Coef. of Linear Thermal Expansion (*10⁻⁶/K)	70-90
Specific Heat Capacity (J/(g.K))	1.6
Thermal Conductivity (W/(m.K))	0.2
Melting Enthalpy (J/g)	117-227

Table 7.6: Description of PA612. [2], [25], [40]

PA612	
Commercial name [DSM]	Nylon 6,12
Ratio methylene/amide	8
Molecular structure	$- \left[\overset{\text{H}}{\underset{ }{\text{N}}} - (\text{CH}_2)_6 - \overset{\text{H}}{\underset{ }{\text{N}}} - \overset{\text{O}}{\parallel} \text{C} - (\text{CH}_2)_{10} - \overset{\text{O}}{\parallel} \text{C} \right] -$
Tm (°C)	210-220
Tg (°C)	55-65
Decomposition Temperature (°C)	-
Crystallinity (%)	-
Density (g/cm³)	1.06
Young's Modulus (MPa)	2100-2250
Coef. of Linear Thermal Expansion (*10⁻⁶/K)	-
Specific Heat Capacity (J/(g.K))	1.67-1.88
Thermal Conductivity (W/(m.K))	-
Melting Enthalpy (J/g)	1.06

Table 7.7: Description of PA46.^{[2], [25]}

PA46	
Commercial name [DSM]	Stanyl [®]
Ratio methylene/amide	4
Molecular structure	
Tm (°C)	290-295
Tg (°C)	80-94
Decomposition Temperature (°C)	-
Crystallinity (%)	70-80
Density (g/cm³)	1.18-1.21
Young's Modulus (MPa)	3300
Coef. of Linear Thermal Expansion (*10⁻⁶/K)	70-80
Specific Heat Capacity (J/(g.K))	2.1
Thermal Conductivity (W/(m.K))	0.3
Melting Enthalpy (J/g)	83.6

Table 7.8: Description of PTFE.^{[1], [25], [26]}

PTFE	
Molecular structure	
Tm (°C)	325-330
Tg (°C)	125-130
Decomposition Temperature (°C)	576-585
Crystallinity (%)	70-80
Density (g/cm³)	2.13-2.23
Young's Modulus (MPa)	400-750
Coef. of Linear Thermal Expansion (*10⁻⁶/K)	100-150
Specific Heat Capacity (J/(g.K))	1.0
Thermal Conductivity (W/(m.K))	0.23-0.25
Melting Enthalpy (J/g)	40-82

9. Appendix C

Table 9.1: Thickness measurements, in mm, of all 24 spring bushing samples (LM481-17 to LM504-17) in the 6 different wear points showed in Figure 3.2

Positions	1	2	3	4	5	6	Average
LM481-17	1,450	1,452	1,454	1,466	1,457	1,449	1,455
LM482-17	1,451	1,451	1,455	1,458	1,464	1,448	1,455
LM483-17	1,451	1,452	1,453	1,468	1,463	1,451	1,456
LM484-17	1,453	1,455	1,462	1,466	1,462	1,449	1,458
LM485-17	1,452	1,460	1,461	1,463	1,466	1,456	1,460
LM486-17	1,453	1,465	1,465	1,470	1,472	1,46	1,464
LM487-17	1,452	1,466	1,471	1,480	1,471	1,458	1,466
LM488-17	1,456	1,459	1,472	1,468	1,465	1,453	1,462
LM489-17	1,450	1,457	1,463	1,465	1,458	1,457	1,458
LM490-17	1,457	1,463	1,462	1,470	1,471	1,453	1,463
LM491-17	1,455	1,467	1,473	1,475	1,465	1,462	1,466
LM492-17	1,451	1,459	1,461	1,462	1,464	1,452	1,458
LM493-17	1,450	1,453	1,455	1,461	1,464	1,451	1,456
LM494-17	1,460	1,461	1,465	1,469	1,477	1,456	1,465
LM495-17	1,452	1,452	1,460	1,458	1,460	1,451	1,456
LM496-17	1,452	1,458	1,457	1,459	1,461	1,451	1,456
LM497-17	1,459	1,461	1,470	1,475	1,468	1,451	1,464
LM498-17	1,451	1,452	1,458	1,460	1,464	1,452	1,456
LM499-17	1,449	1,450	1,455	1,457	1,459	1,447	1,453
LM500-17	1,453	1,453	1,457	1,463	1,461	1,450	1,456
LM501-17	1,451	1,457	1,465	1,469	1,463	1,452	1,460
LM502-17	1,451	1,457	1,467	1,464	1,473	1,454	1,461
LM503-17	1,455	1,460	1,464	1,466	1,466	1,450	1,460
LM504-17	1,451	1,454	1,457	1,463	1,460	1,451	1,456

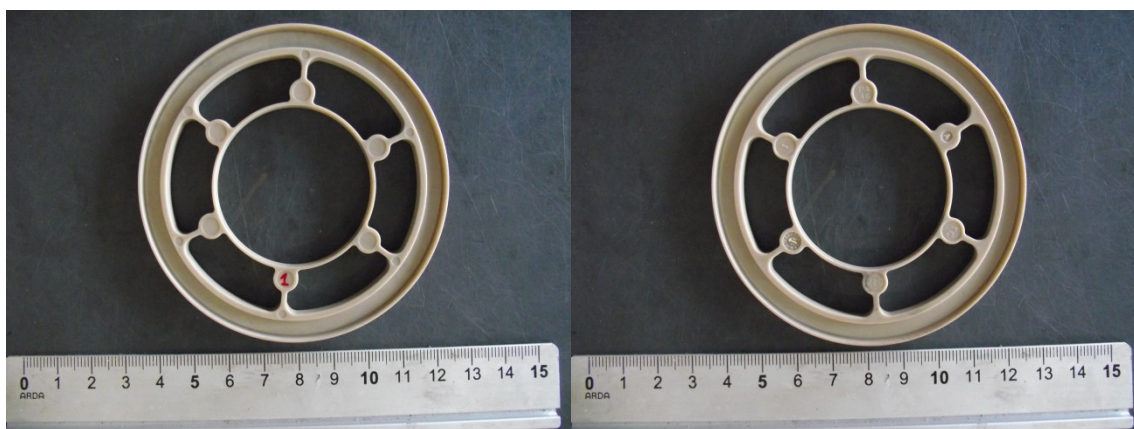


Figure 9.1: Sample LM481-17.

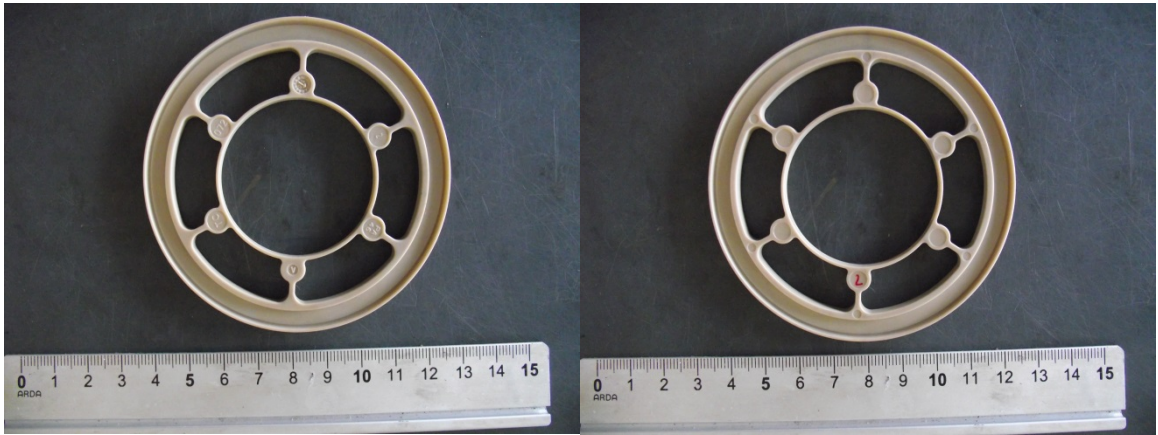


Figure 9.2: Sample LM482-17.

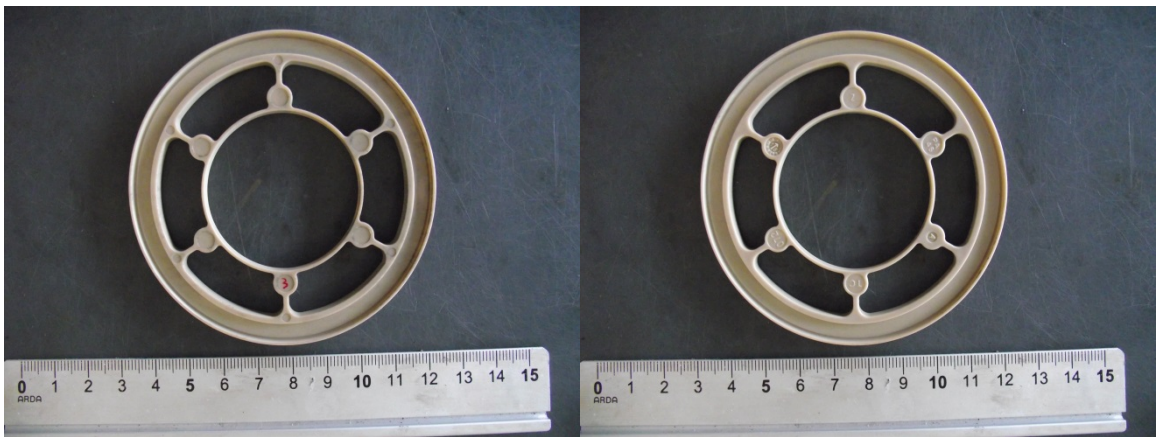


Figure 9.3: Sample LM483-17.



Figure 9.4: Sample LM484-17.

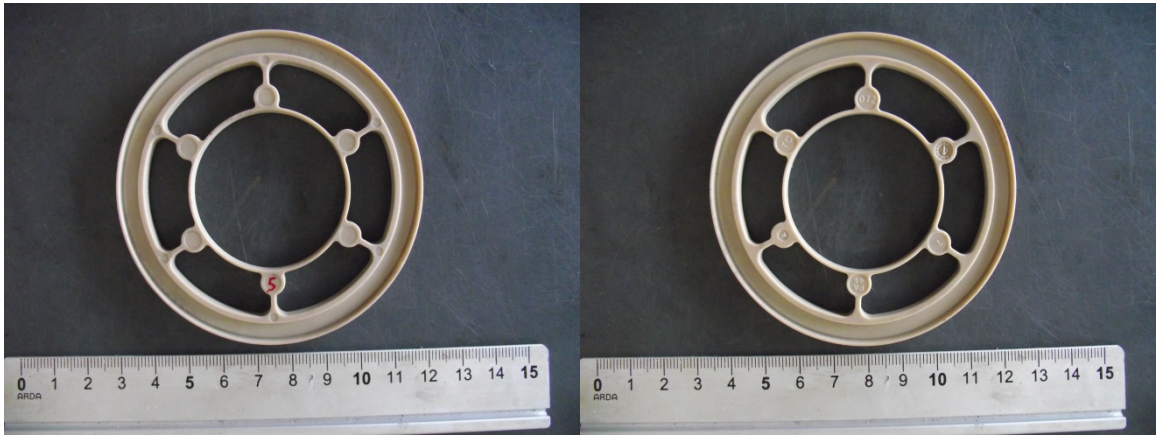


Figure 9.5: Sample LM485-17.

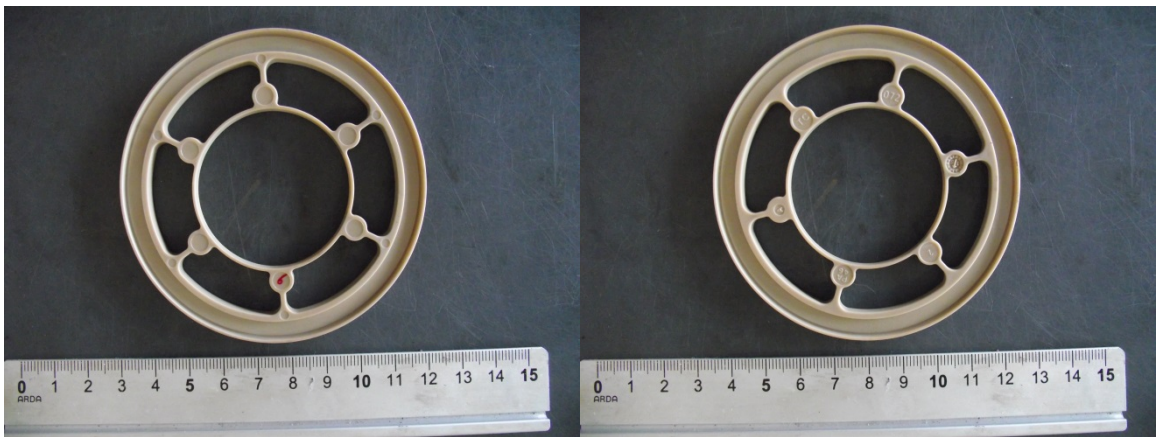


Figure 9.6: Sample LM486-17.

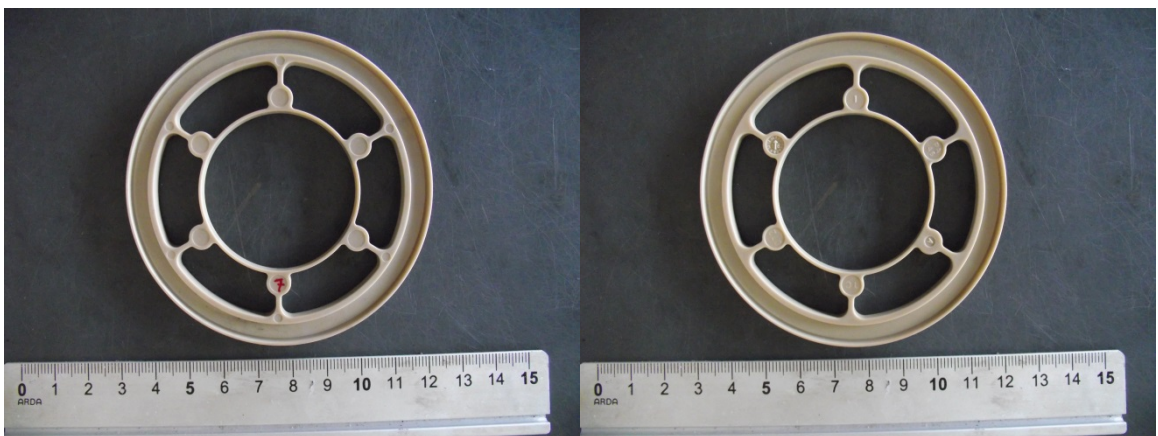


Figure 9.7: Sample LM487-17.

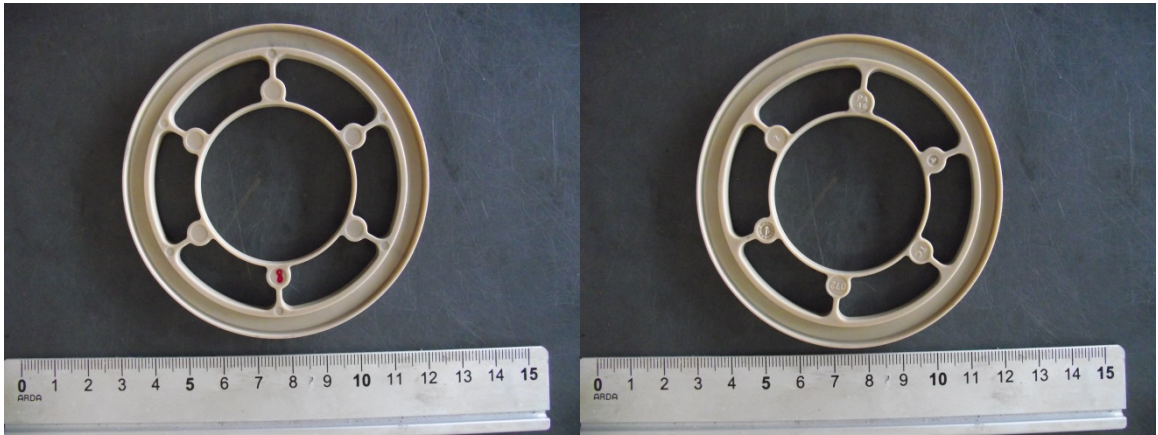


Figure 9.8: Sample LM488-17.



Figure 9.9: Sample LM489-17.

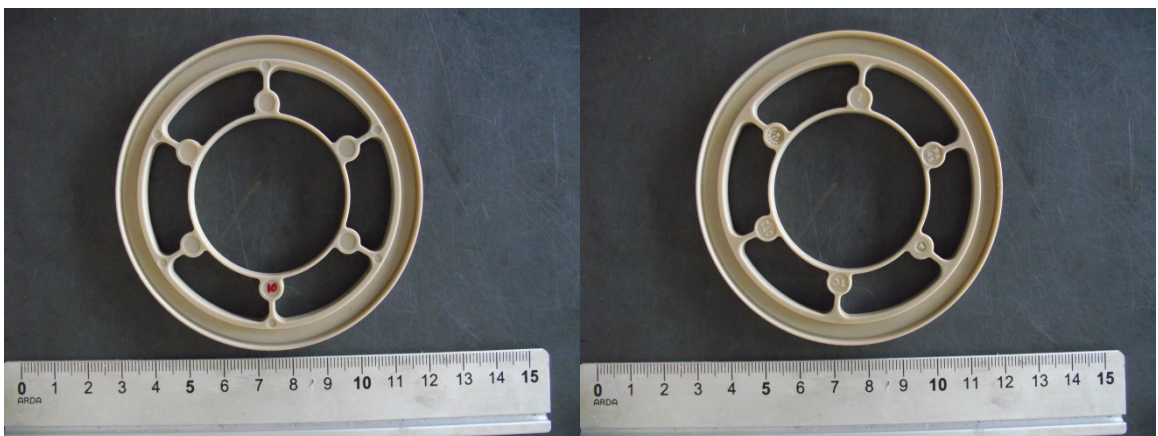


Figure 9.10: Sample LM490-17.

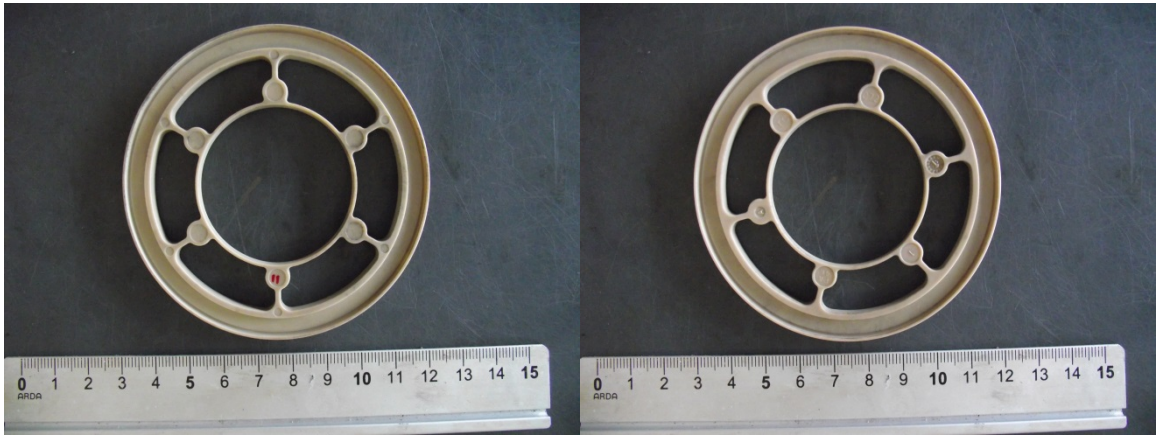


Figure 9.11: Sample LM491-17.

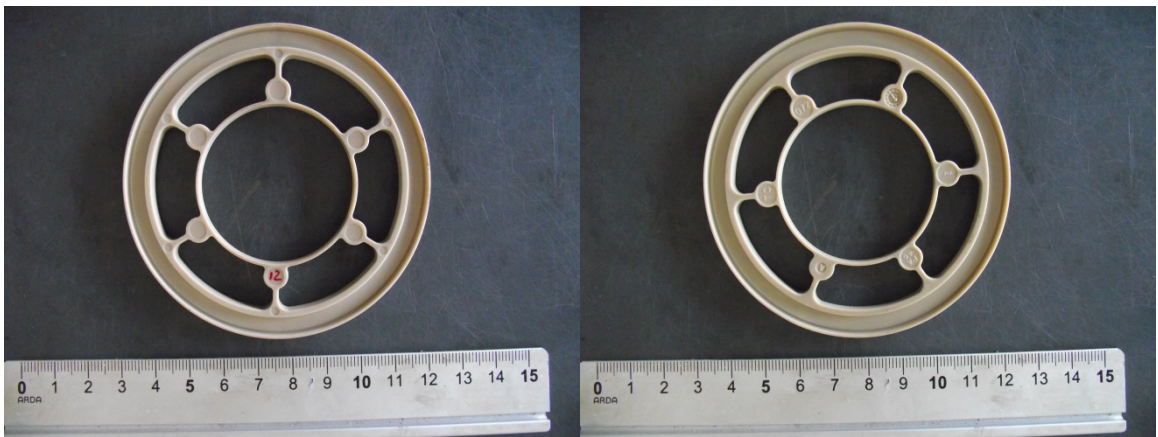


Figure 9.12: Sample LM492-17.

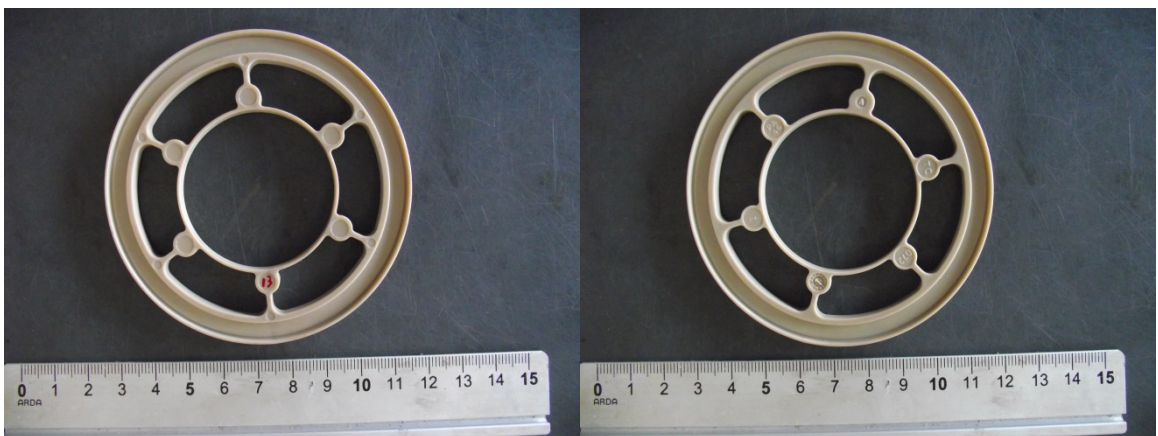


Figure 9.13: Sample LM493-17.



Figure 9.14: Sample LM494-17.

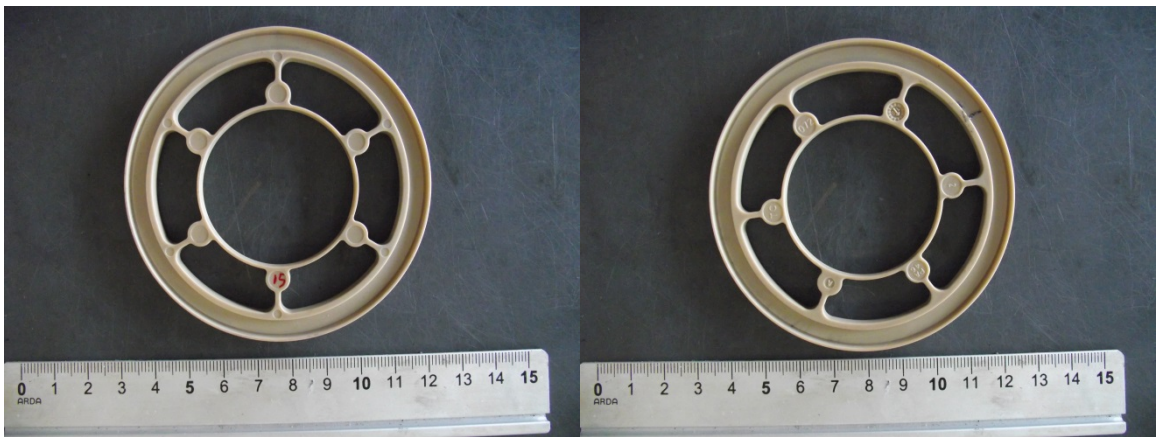


Figure 9.15: Sample LM495-17.

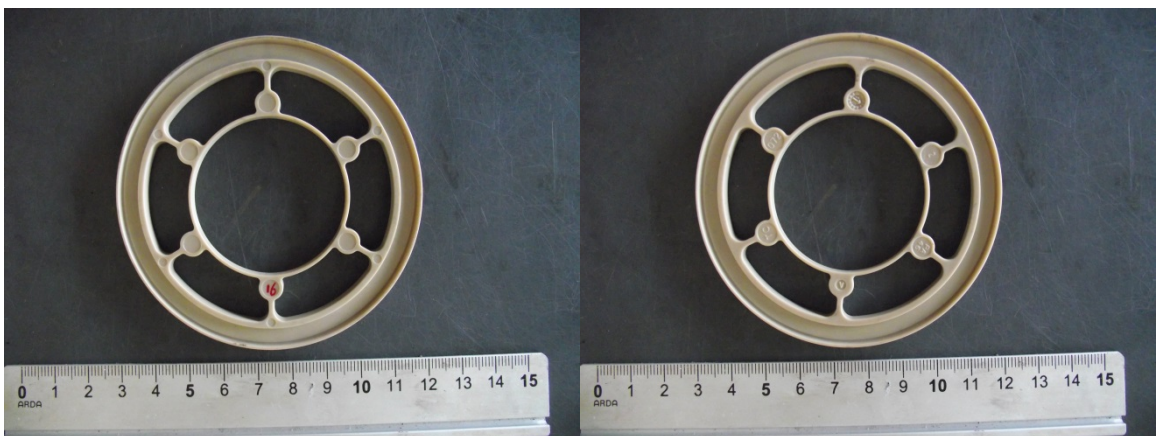


Figure 9.16: Sample LM496-17.

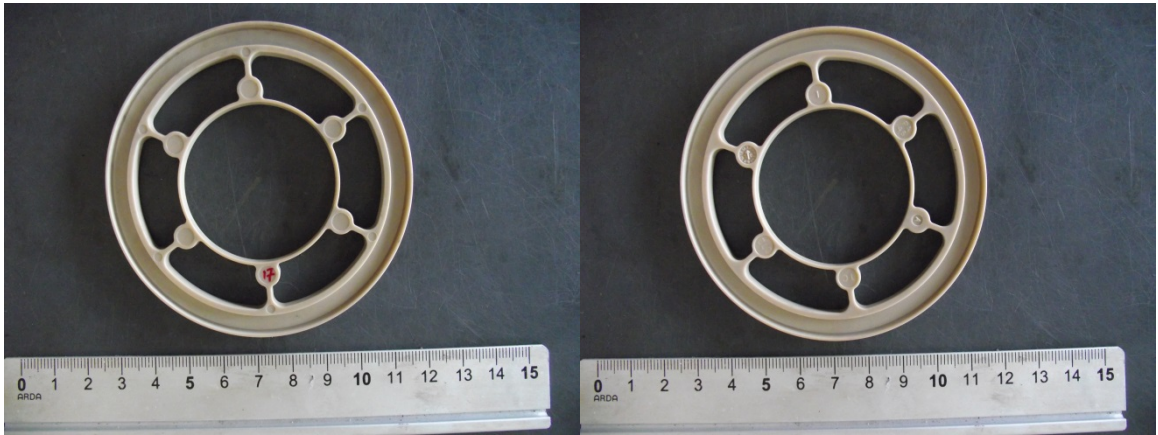


Figure 9.17: Sample LM497-17.

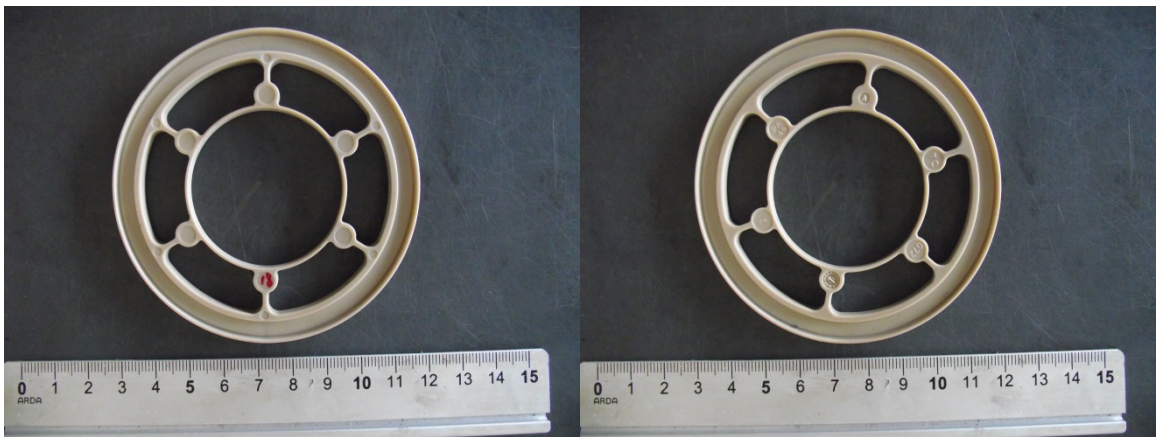


Figure 9.18: Sample LM498-17.

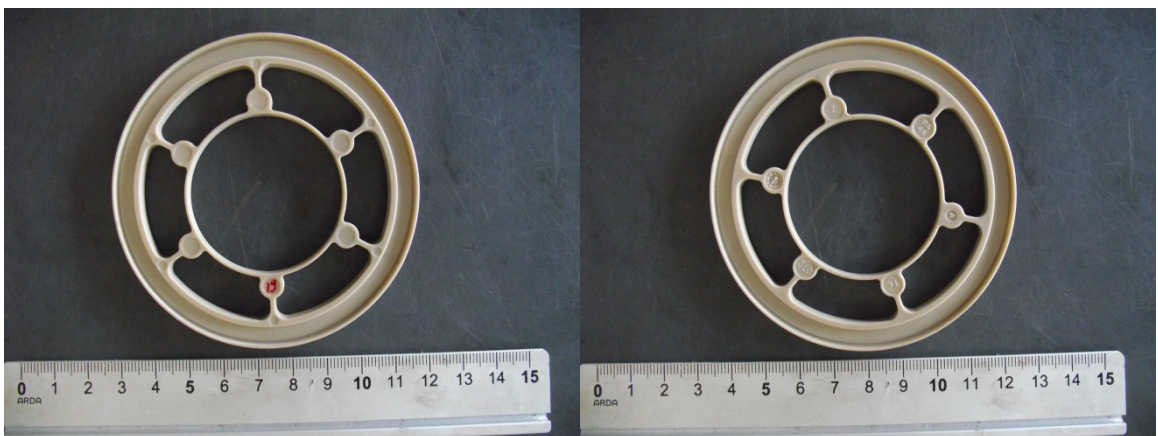


Figure 9.19: Sample LM499-17.

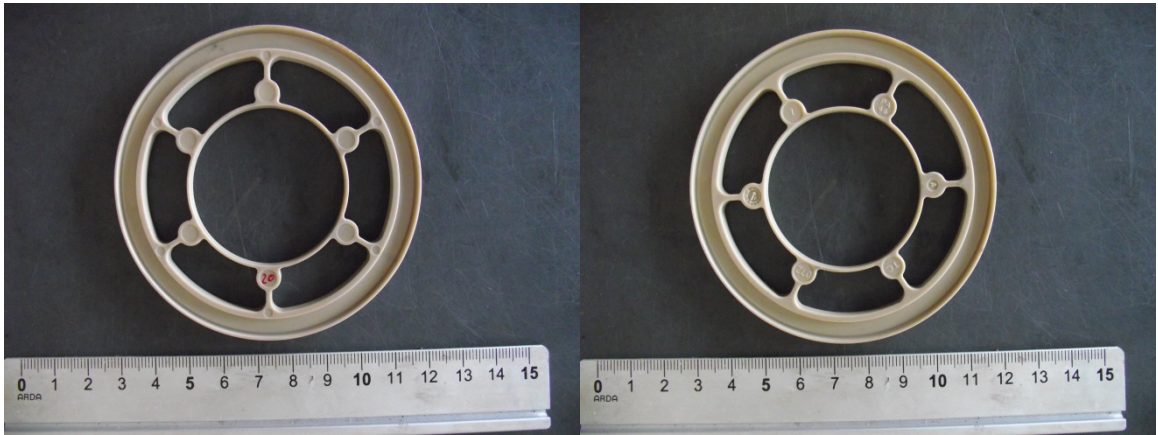


Figure 9.20: Sample LM500-17.

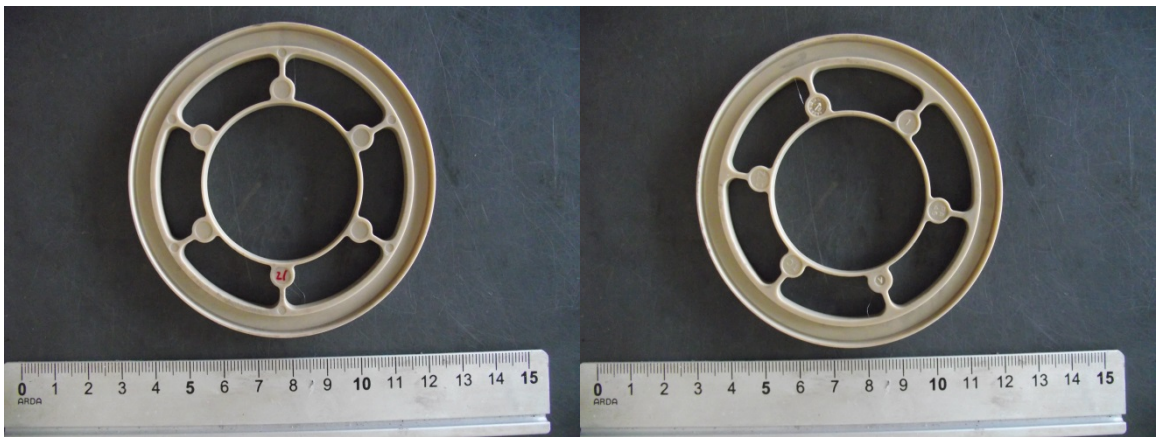


Figure 9.21: Sample LM501-17.

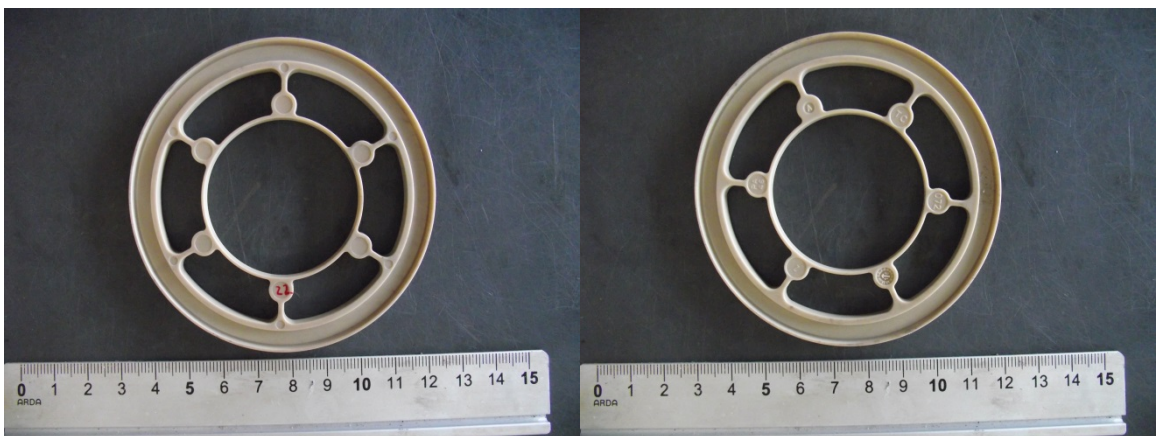


Figure 9.22: Sample LM502-17.

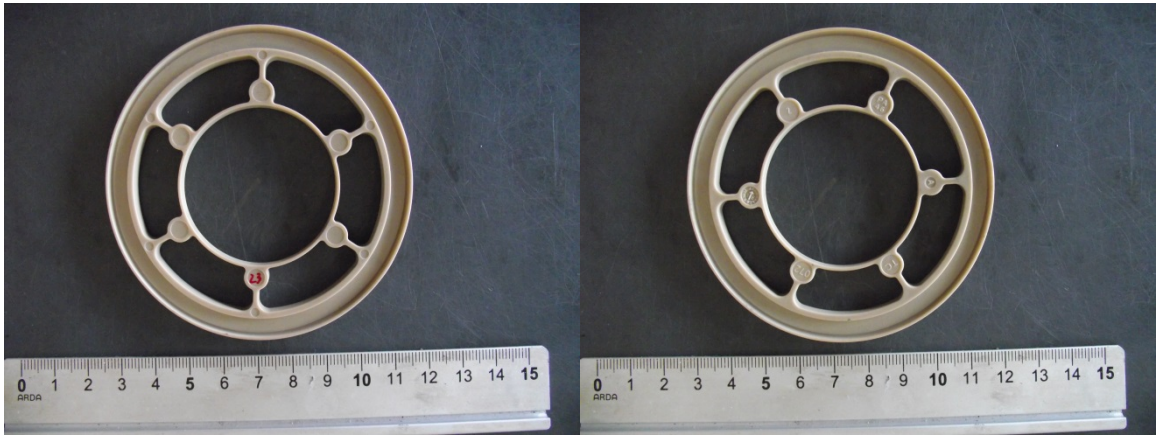


Figure 9.23: Sample LM503-17.



Figure 9.24: Sample LM504-17.

10. Appendix D



IMPAG AG - Feldeggstrasse 26 - Postfach - CH-8034 Zürich
Tel +41 43 499 25 00 - Fax +41 43 499 25 01 - info@impag.ch - www.impag.ch

QUALITÄTSZERTIFIKAT FÜR KALIBRIERMATERIALIEN
QUALITY ASSURANCE OF CALIBRATION MATERIALS
CERTIFICAT DE QUALITE DE MATERIAUX DE CALIBRAGE

Material:
Material: Indium Pills 99.999 %
Matériau:

Ihre Artikel Nr.:
Your Article No.: 00119442
Votre no d'article:

Literatur Schmelzpunkt:
Literature melting point: 156.6 °C
Point de fusion (littérature):

Charge Nr.:
Lot No.: WE 4649 / 7330
Charge no.:

Abpackdatum:
Date of Packing: January 2015
Date d'emballage:

Verfalldatum:
Expiry date: January 2021 (6 years of shelf-life)
Date d'expiration:

Ihre Referenz:
Your reference: Order No. 4600025234
Votre référence:

IMPAG Referenz:
IMPAG reference: 214081 / 673245
IMPAG référence:

Resultate der Analyse / Results of the analysis performed / Résultats d'analyse

Chemische Zusammensetzung in ppm / Chemical composition in ppm / Composition chimique en ppm:

As:		Zn:	< 2	Al:		Zn:		Ag:		Fe:	< 2
Sn:	3	Cr:		Hg:		Pb:	4	Cu:	< 2	Mg:	
Ti:	< 2	Bi:		Sb:		Au:		Cd:	< 2	Ni:	< 2

Messwerte in mm / Measurements in mm / Dimensions en mm:

Characteristics	Target Size	Tolerance								
Ø	1.5	± 0.1	1.4889	1.4951	1.4908	1.4871	1.4924	1.4872	1.4912	
Thickness	0.5	± 0.1	0.558	0.521	0.529	0.528	0.530	0.531	0.544	

Zurich, 4th March 2015 / ani

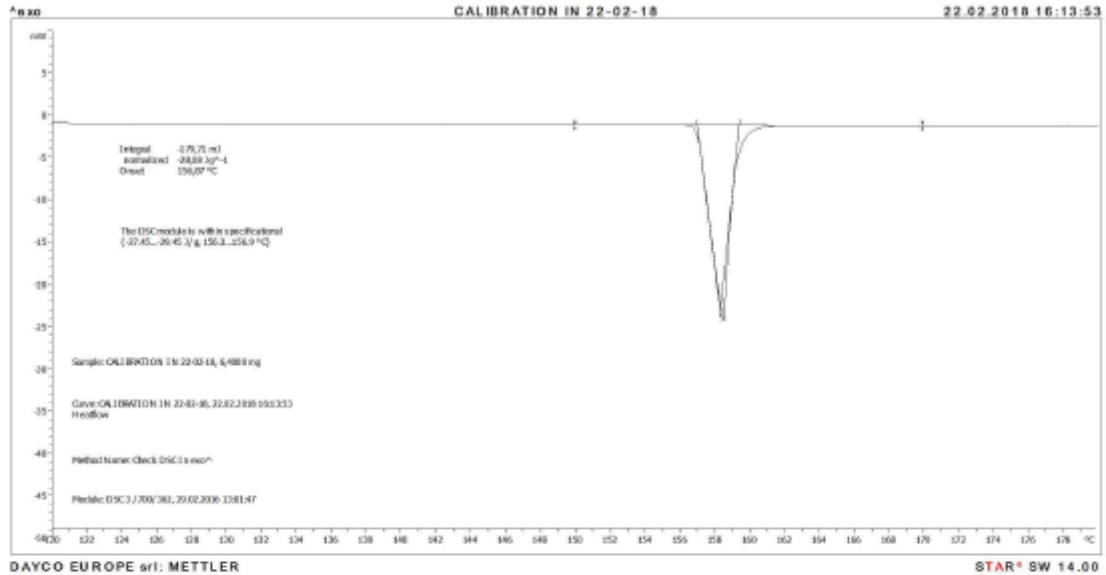
Figure 10.1: Quality assurance of Indium Pills 99,999% used in the DSC calibration.

CALIBRATION IN 22-02-18

Author: . .
Date: 22/02/2018
Database: STARe Default DB V14.00: METTLER



Evaluation: CALIBRATION IN 22-02-18, 22.02.2018 16:13:53



Curve: CALIBRATION IN 22-02-18, 22.02.2018 16:13:53

Sample: CALIBRATION IN 22-02-18, 6,4000 mg

Module: DSC 3 / 700/362, 29.02.2016 13:01:47

Sample Holder: Aluminum Standard 40ul
Weight : 0
Material: Aluminium

Method: Check DSC In exo^
dt 1,00 s
[1] 120,0..180,0 °C, 10,00 K/min
Synchronization enabled

User: METTLER

Results: Integral -179,71 mJ
normalized -28,08 Jg⁻¹
Onset 156,87 °C

Figure 10.2: Certificate of the DSC calibration performed with In on 22 February 2018

11. Appendix E

11.1. LM481-17

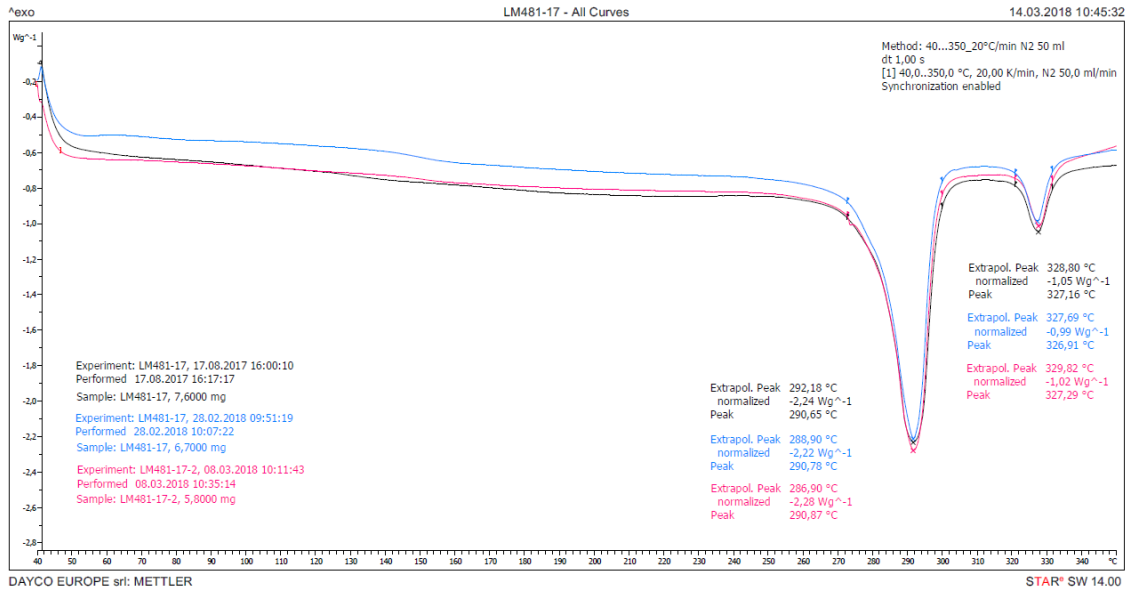


Figure 11.1: DSC measurements curves of spring bushing LM481-17 obtained from Analyses 1 (black), 2 (blue) and 3 (pink), using respectively samples from Groups 1, 2 and 3. All three curves exhibit two melting peaks and there aren't neither artifacts or other peaks that identify impurities. The first peak, with temperatures of 290,65°C, 290,78°C and 290,87°C, respectively, is compatible with PA46 (melting peak between 290 and 295°C); while the second peak, with temperatures of 327,16°C, 326,91°C and 327,29°C, is compatible with PTFE (melting peak between 325 and 335°C).

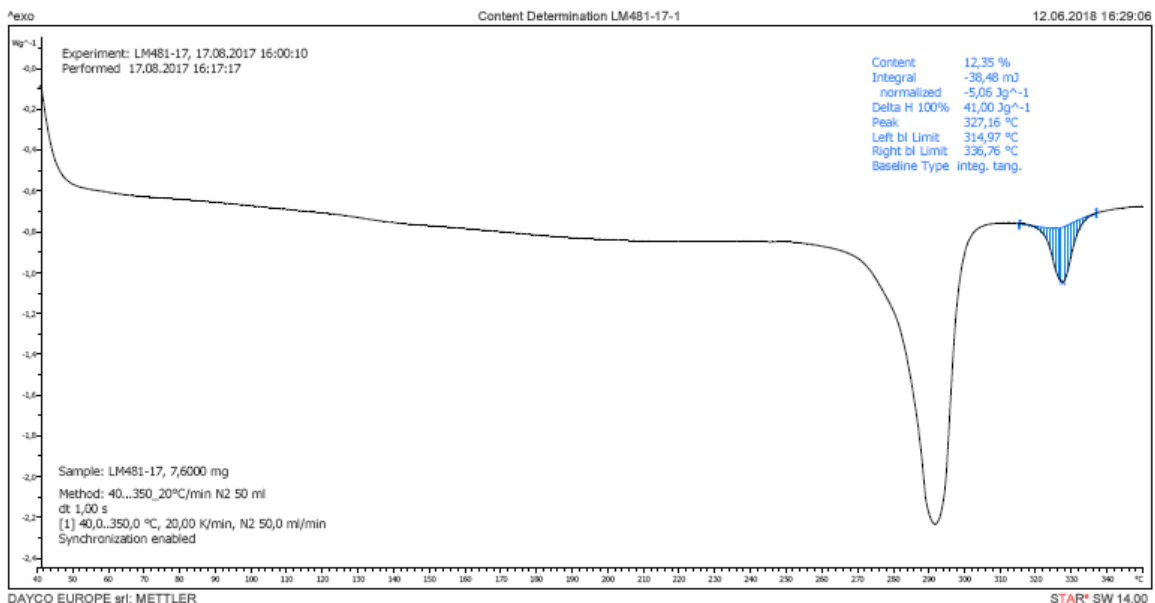


Figure 11.2: DSC measurement curve of sample LM481-17-1, from Group 1, obtained from Analysis 1, in which a content of 12,35% of PTFE was measured.

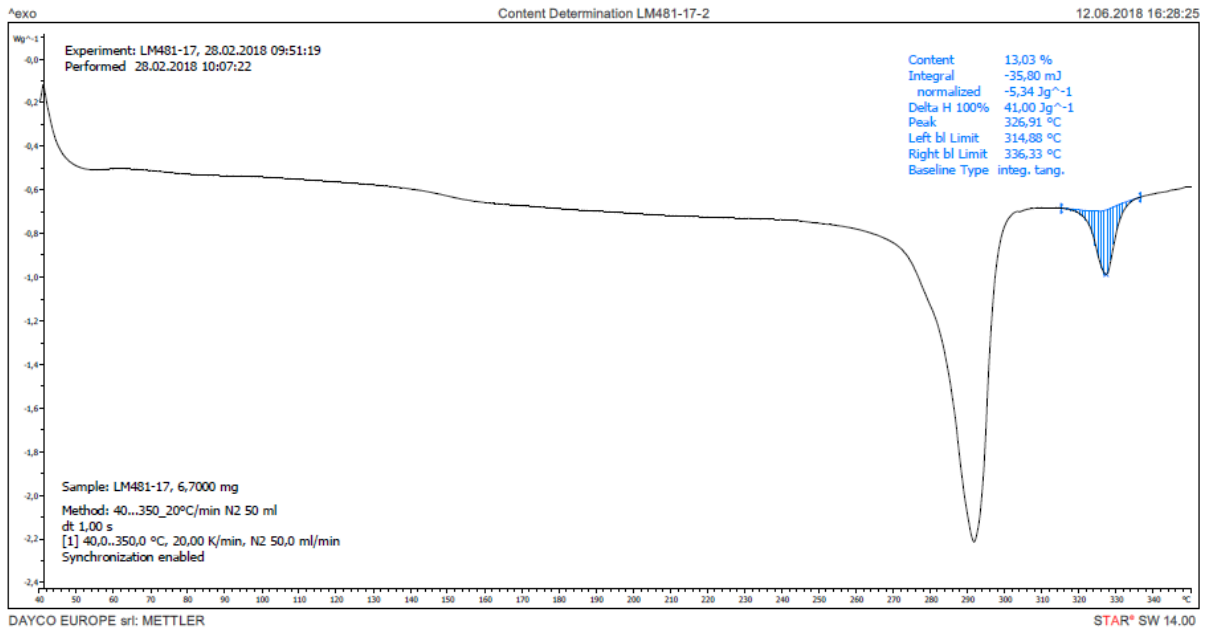


Figure 11.3: DSC measurement curve of sample LM481-17-2, from Group 2, obtained from Analysis 2, in which a content of 13,03% of PTFE was measured.

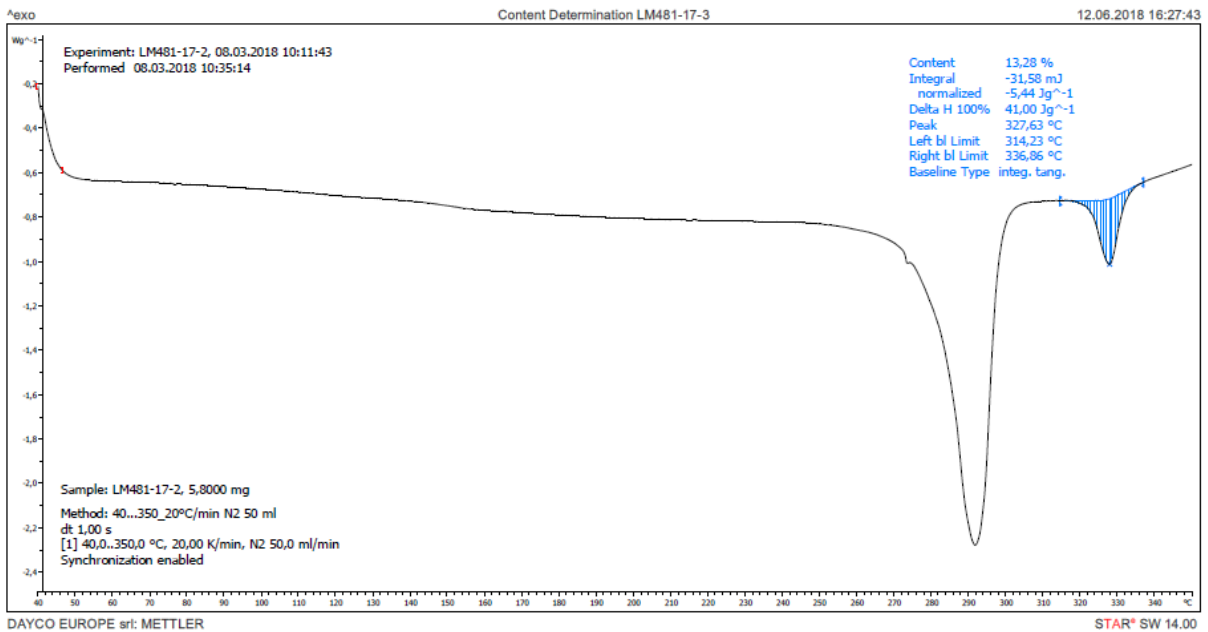


Figure 11.4: DSC measurement curve of sample LM481-17-3, from Group 3, obtained from Analysis 3, in which a content of 13,28% of PTFE was measured.

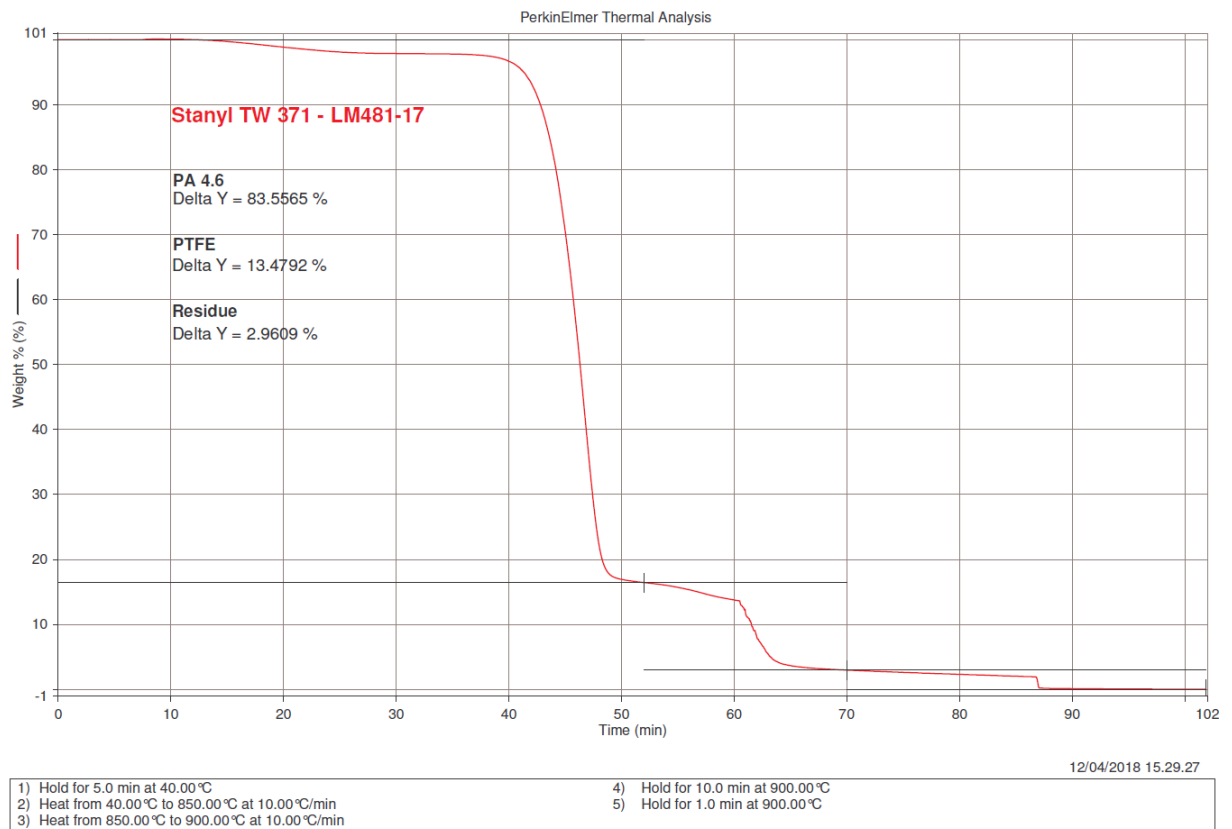


Figure 11.5: TGA measurement curve of sample LM481-17. The contents of PA46, PTFE and residue are, respectively, 83.5565%, 13.4792% and 2.9609%.

11.2. LM482-17

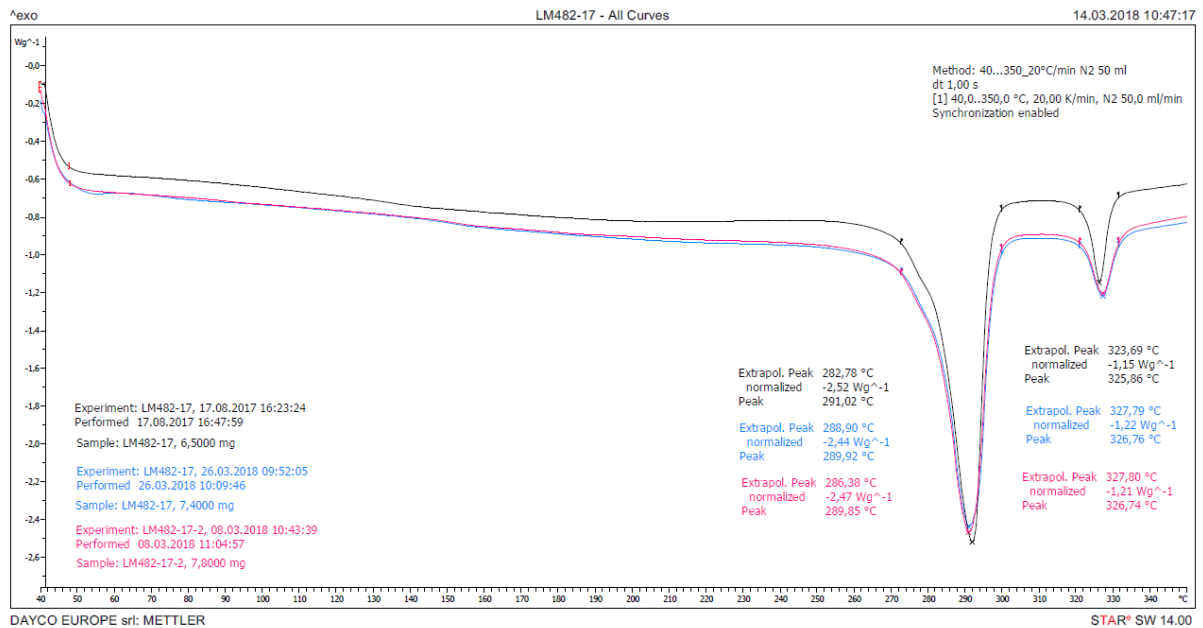


Figure 11.6: DSC measurements curves of spring bushing LM482-17 obtained from Analyses 1 (black), 2 (blue) and 3 (pink), using respectively samples from Groups 1, 2 and 3. All three curves exhibit two melting peaks and there aren't neither artifacts or other peaks that identify impurities. The first peak, with temperatures of 291,02°C, 289,92°C and 289,85°C, respectively, is compatible with PA46 (melting peak between 290 and 295°C) only in the 1st run, and it is slightly below in the 2nd and 3rd runs; while the second peak, with temperatures of 325,86°C, 326,76°C and 326,74°C, is compatible with PTFE (melting peak between 325 and 335°C).

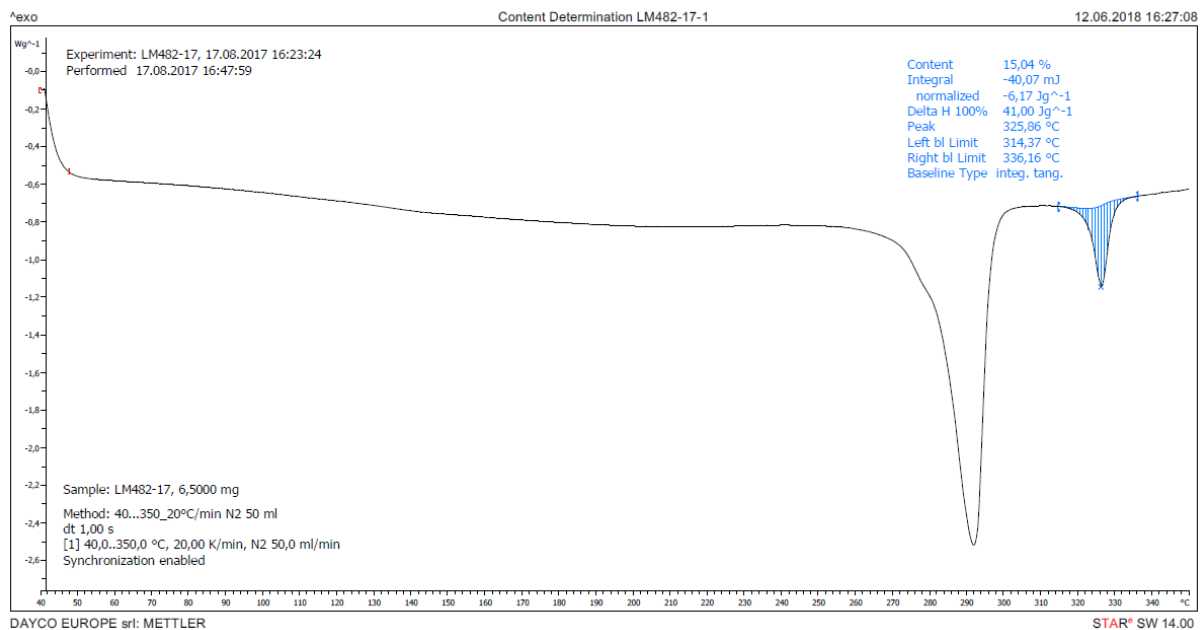


Figure 11.7: DSC measurement curve of sample LM482-17, from Group 1, obtained from Analysis 1, in which a content of 15,04% of PTFE was measured.

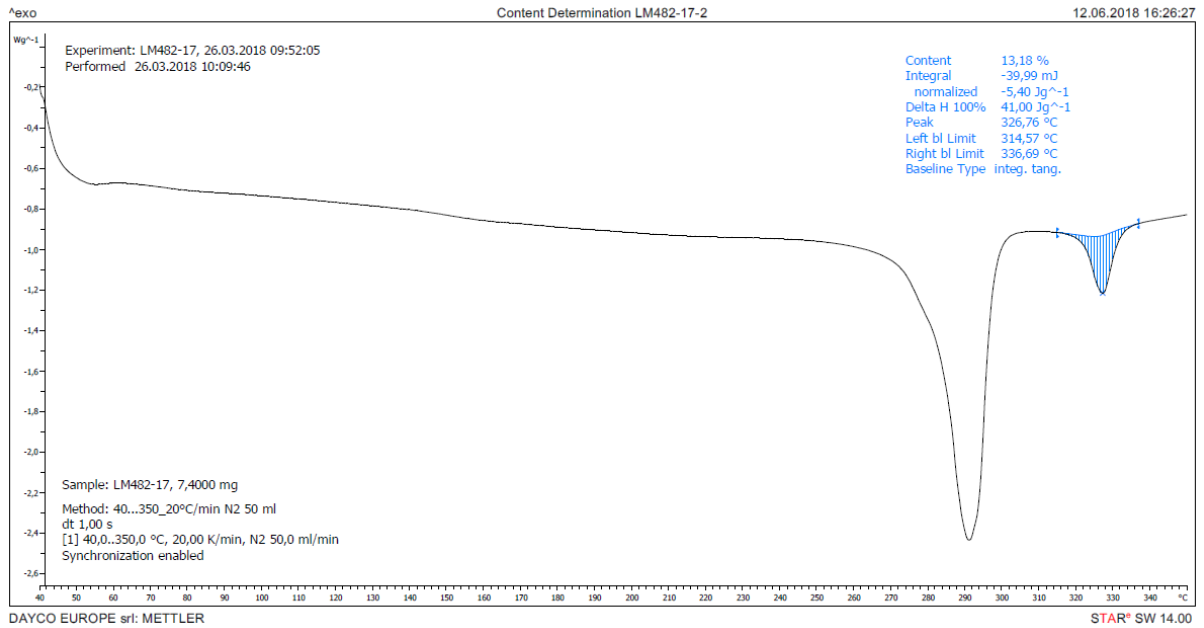


Figure 11.8: DSC measurement curve of sample LM482-17, from Group 2, obtained from Analysis 2, in which a content of 13,18% of PTFE was measured.

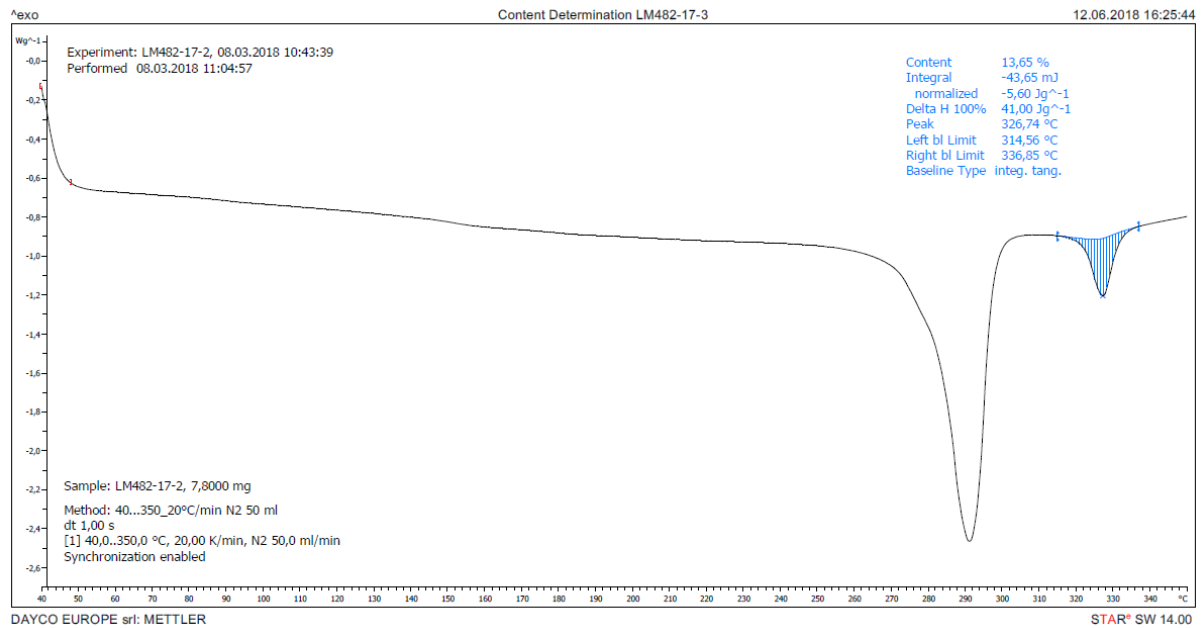


Figure 11.9: DSC measurement curve of sample LM482-17, from Group 3, obtained from Analysis 3, in which a content of 13,65% of PTFE was measured.

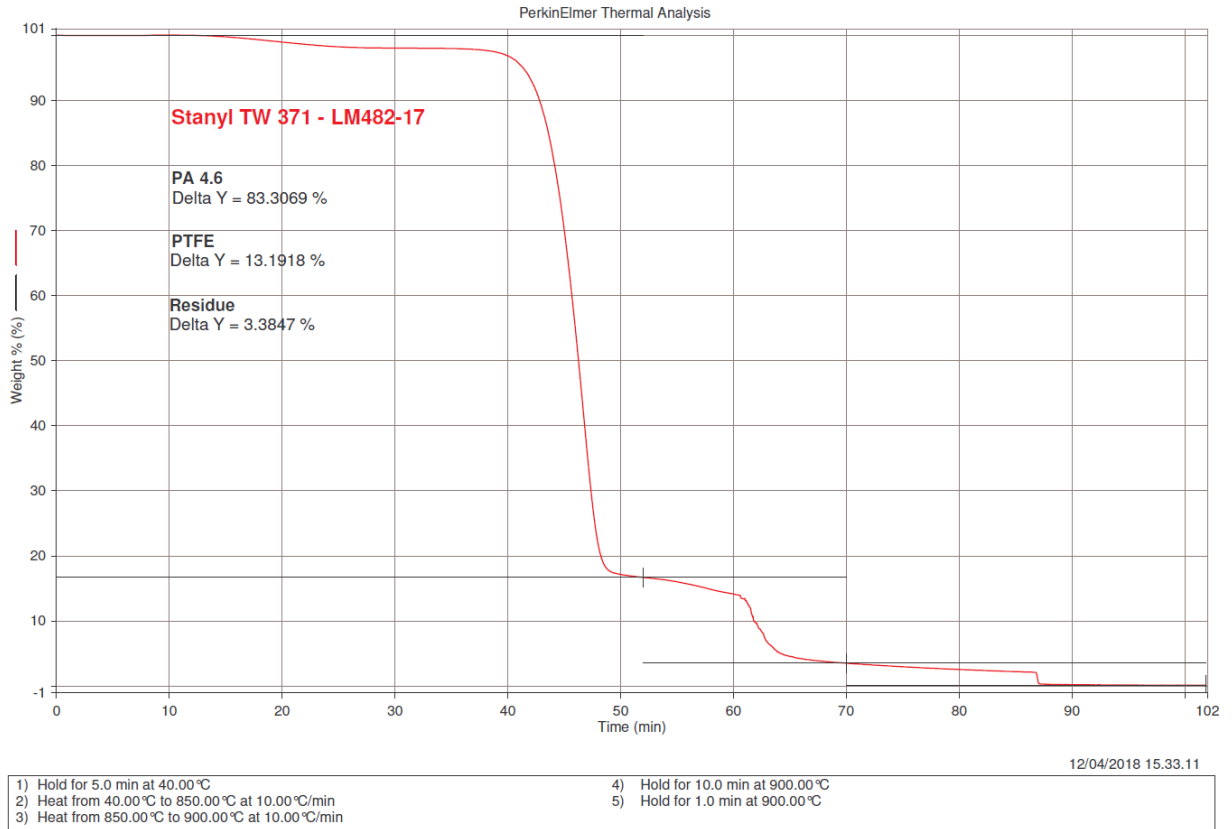


Figure 11.10: TGA measurement curve of sample LM482-17. The contents of PA46, PTFE and residue are, respectively, 83.3069%, 13.1918% and 3.3847%.

11.3. LM483-17

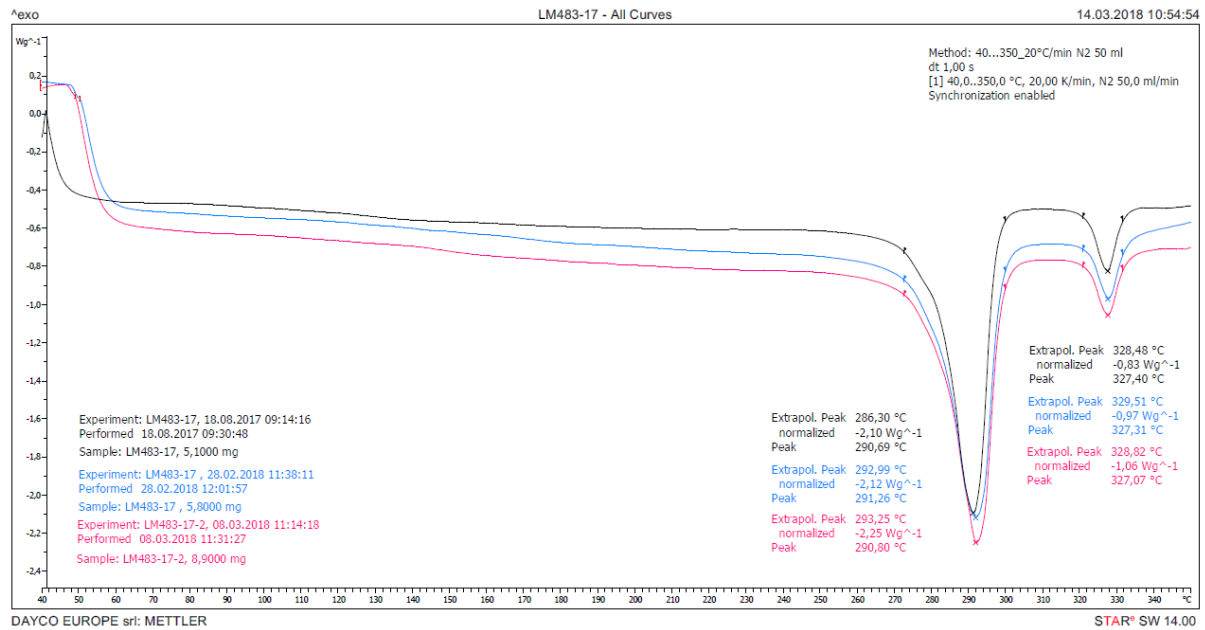


Figure 11.11: DSC measurements curves of spring bushing LM483-17 obtained from Analyses 1 (black), 2 (blue) and 3 (pink), using respectively samples from Groups 1, 2 and 3. All three curves exhibit two melting peaks and there aren't other peaks that identify impurities. The first peak, with temperatures of 290,69°C, 291,26°C and 290,80°C, respectively, is compatible with PA46 (melting peak between 290 and 295°C); while the second peak, with temperatures of 327,40°C, 326,31°C and 327,07°C, is compatible with PTFE (melting peak between 325 and 335°C).

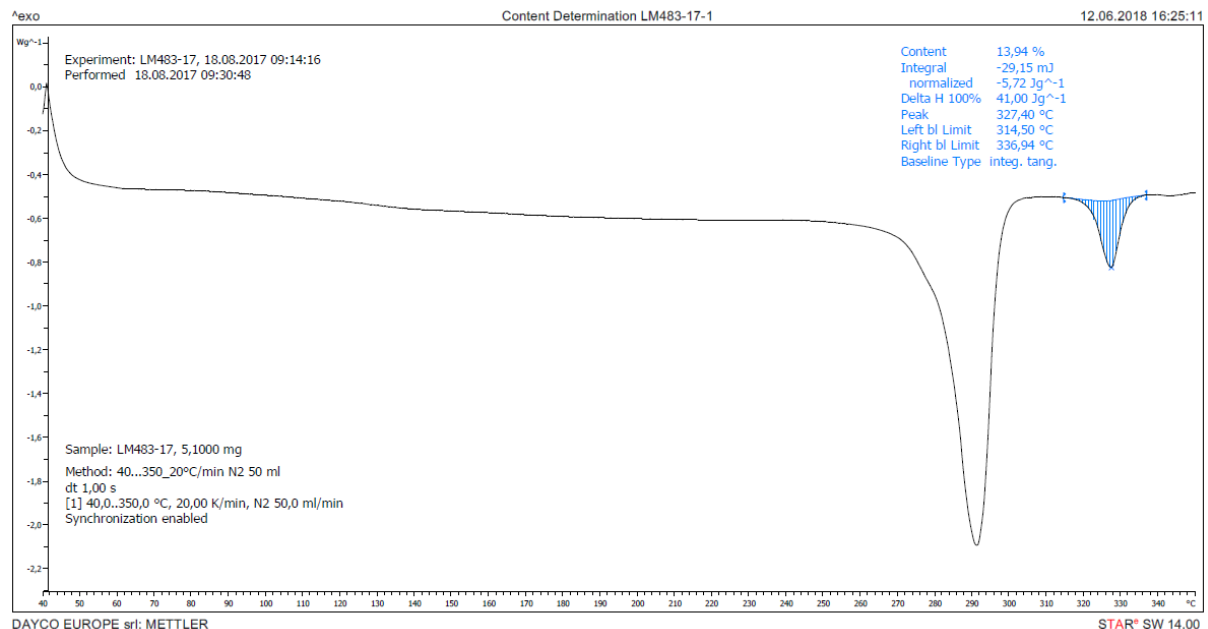


Figure 11.12: DSC measurement curve of sample LM483-17, from Group 1, obtained from Analysis 1, in which a content of 13,94% of PTFE was measured.

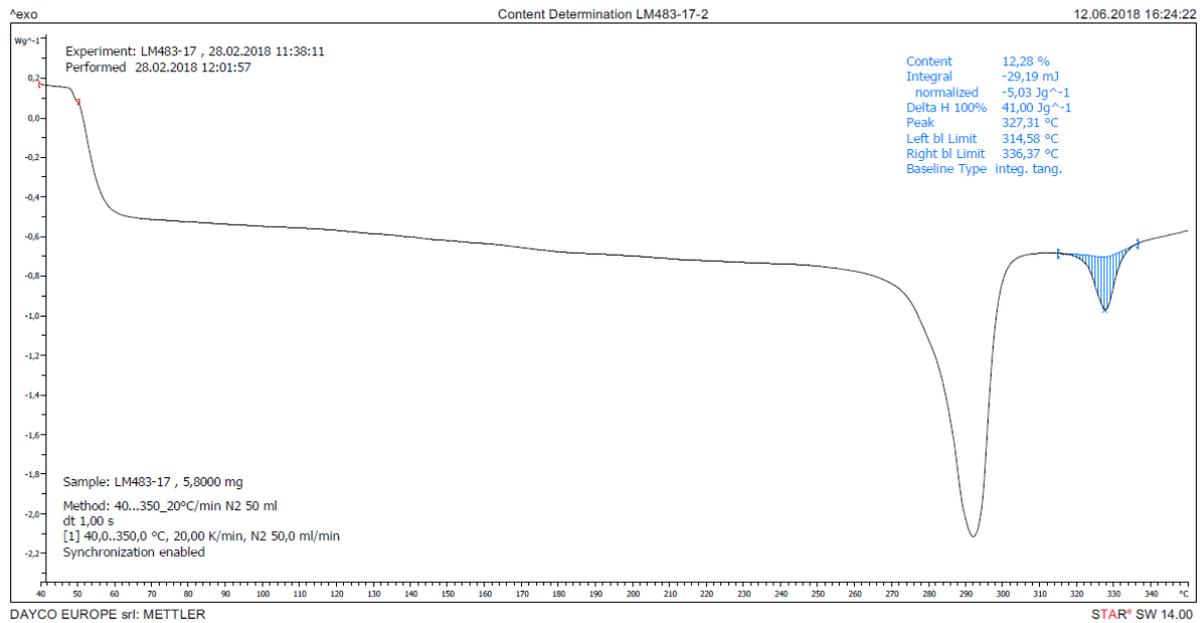


Figure 11.13: DSC measurement curve of sample LM483-17, from Group 2, obtained from Analysis 2, in which a content of 12,28% of PTFE was measured.

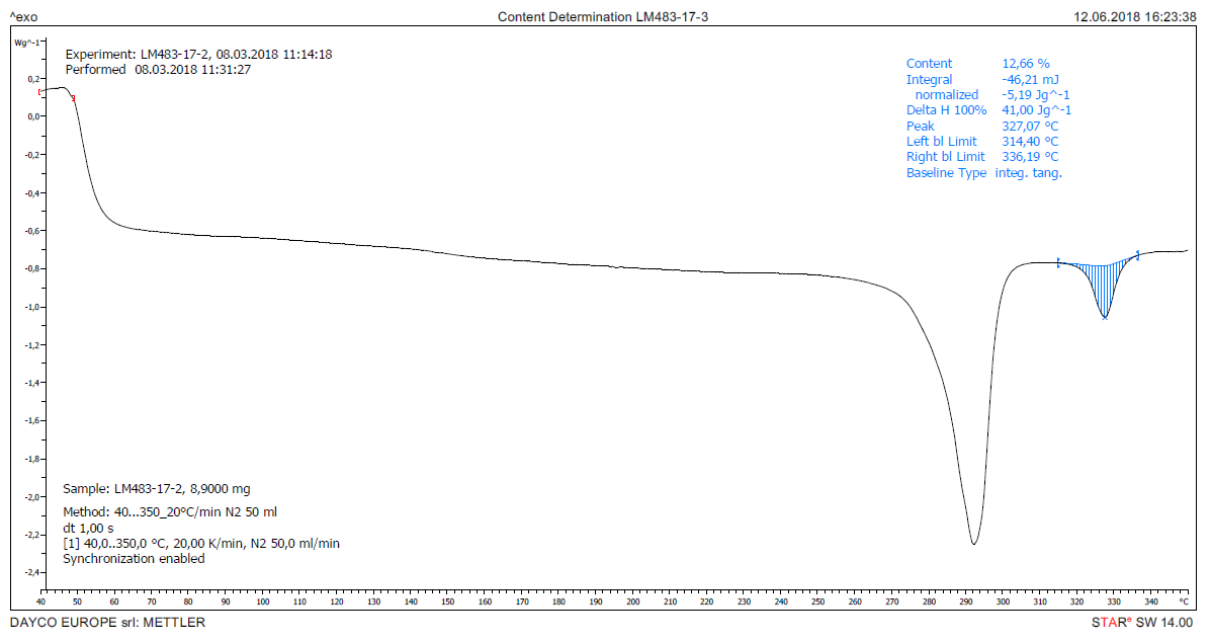


Figure 11.14: DSC measurement curve of sample LM483-17, from Group 3, obtained from Analysis 3, in which a content of 12,66% of PTFE was measured.

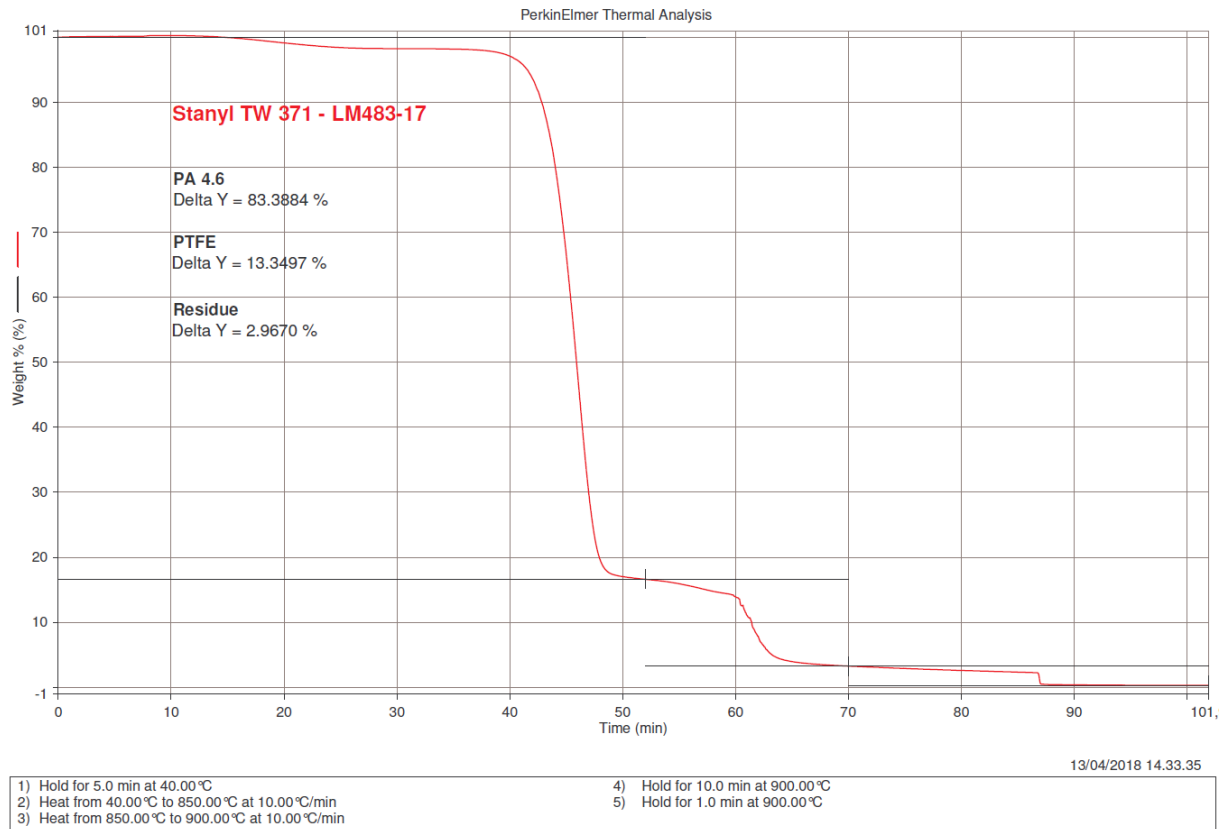


Figure 11.15: TGA measurement curve of sample LM483-17. The contents of PA46, PTFE and residue are, respectively, 83.3884%, 13.3497% and 2.9670%.

11.4. LM484-17

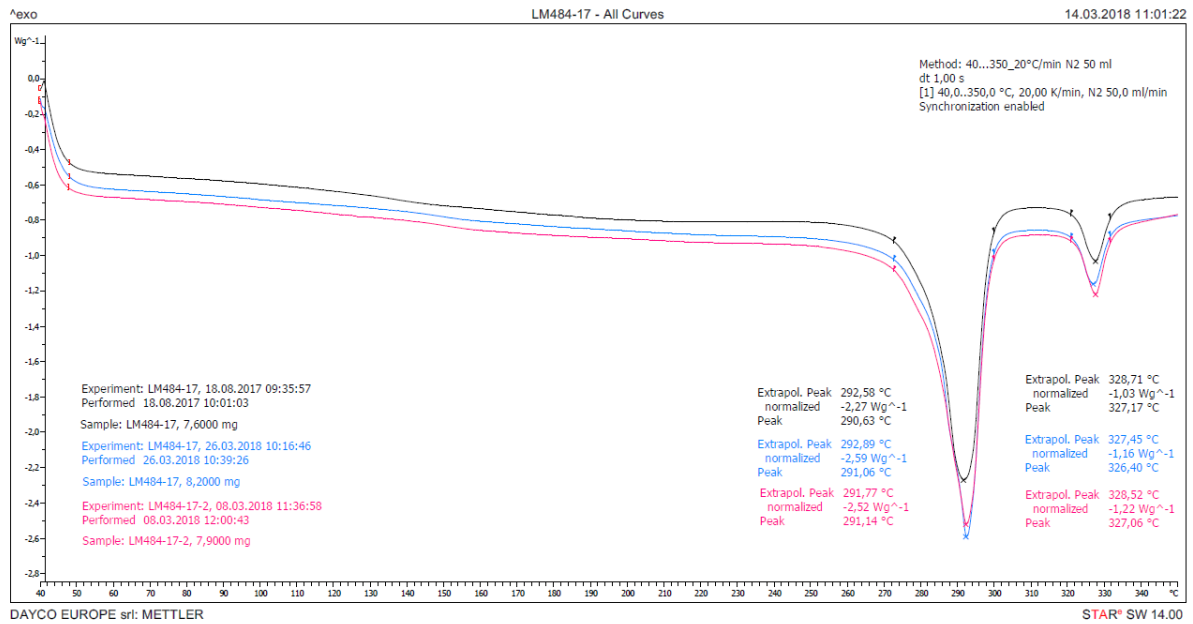


Figure 11.16: DSC measurements curves of spring bushing LM484-17 obtained from Analyses 1 (black), 2 (blue) and 3 (pink), using respectively samples from Groups 1, 2 and 3. All three curves exhibit two melting peaks and there aren't neither artifacts or other peaks that identify impurities. The first peak, with temperatures of 290,63°C, 291,06°C and 291,14°C, respectively, is compatible with PA46 (melting peak between 290 and 295°C); while the second peak, with temperatures of 327,17°C, 326,40°C and 327,06°C, is compatible with PTFE (melting peak between 325 and 335°C).

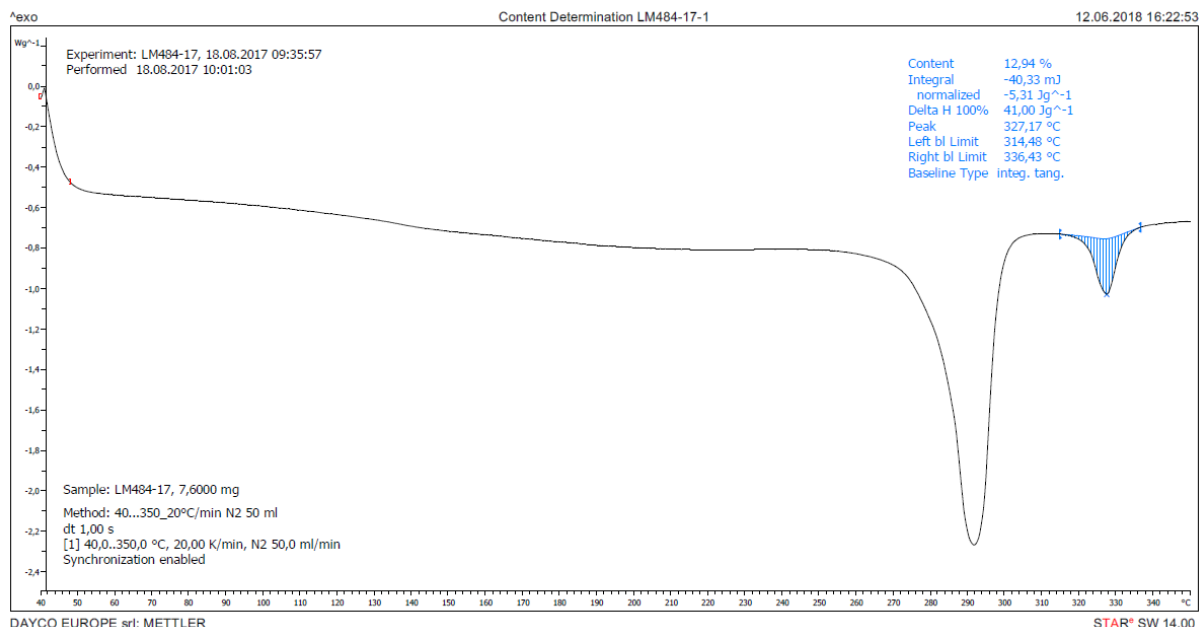


Figure 11.17: DSC measurement curve of sample LM484-17, from Group 1, obtained from Analysis 1, in which a content of 12,94% of PTFE was measured.

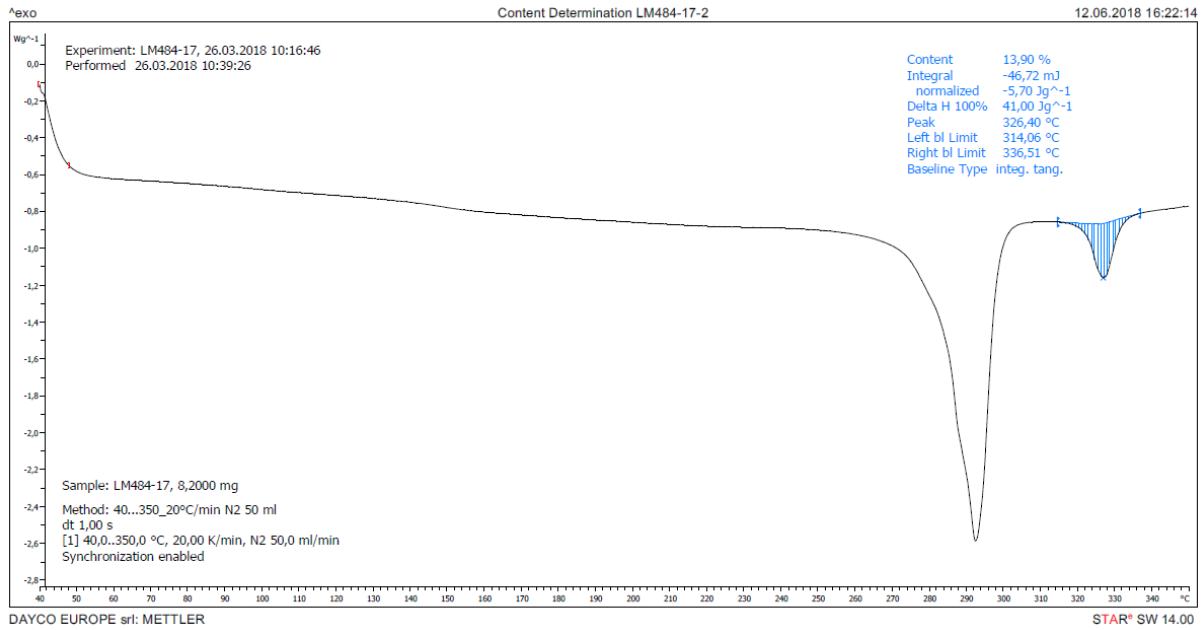


Figure 11.18: DSC measurement curve of sample LM484-17, from Group 2, obtained from Analysis 2, in which a content of 13,90% of PTFE was measured.

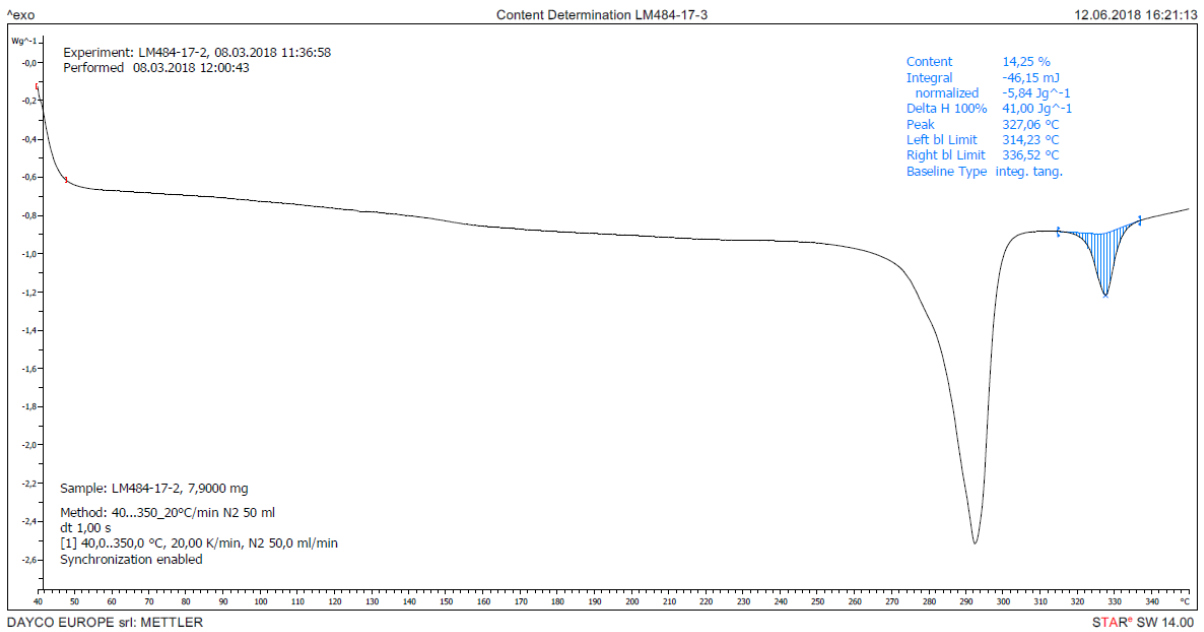


Figure 11.19: DSC measurement curve of sample LM484-17, from Group 3, obtained from Analysis 3, in which a content of 14,25% of PTFE was measured.

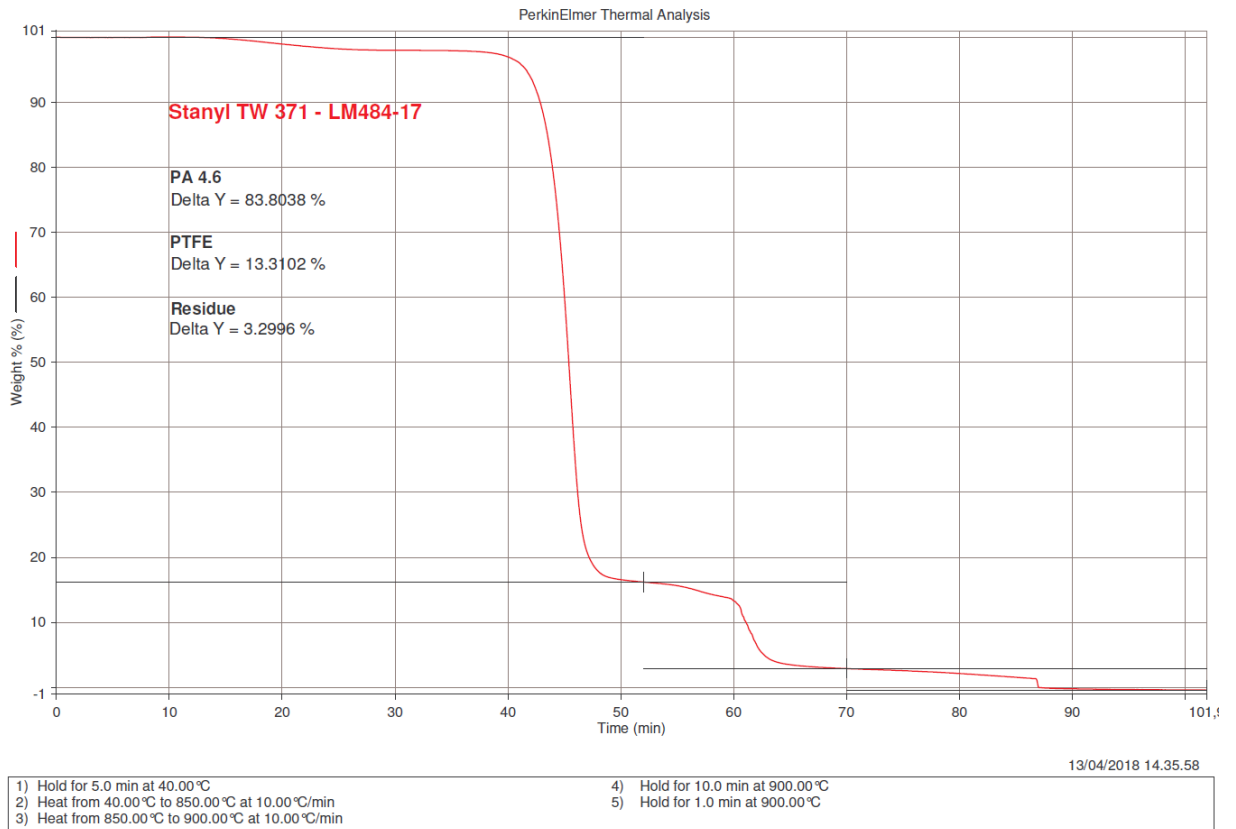


Figure 11.20: TGA measurement curve of sample LM484-17. The contents of PA46, PTFE and residue are, respectively, 83.8038%, 13.3102% and 3.2996%.

11.5. LM485-17

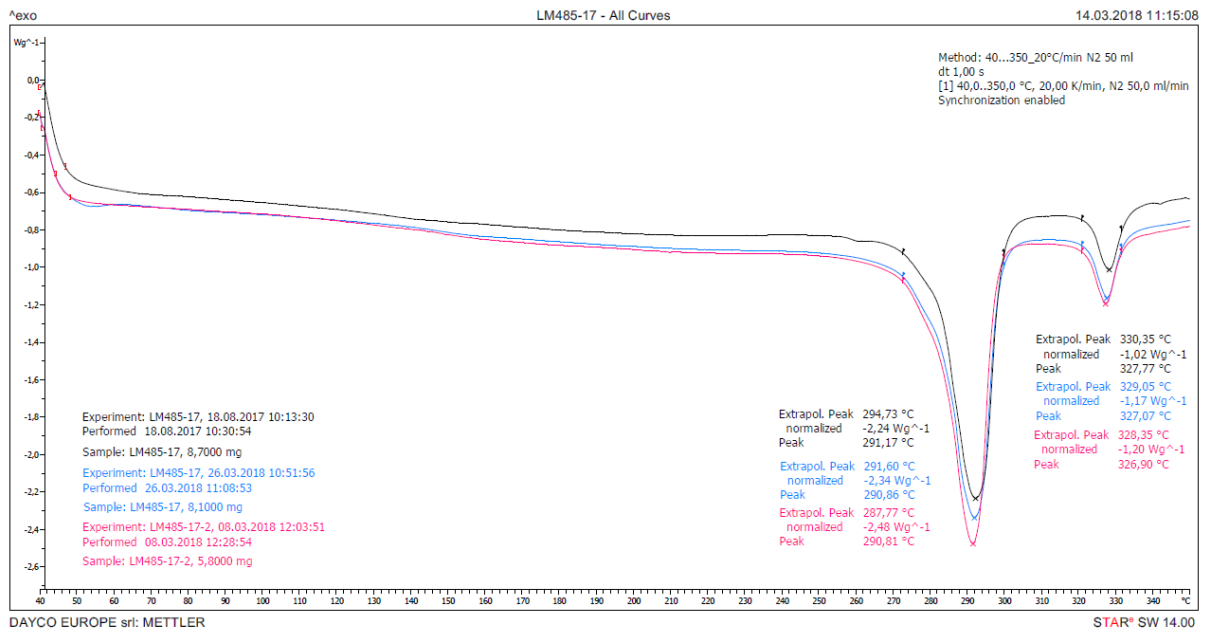


Figure 11.21: DSC measurements curves of spring bushing LM485-17 obtained from Analyses 1 (black), 2 (blue) and 3 (pink), using respectively samples from Groups 1, 2 and 3. All three curves exhibit two melting peaks and there aren't neither artifacts or other peaks that identify impurities. The first peak, with temperatures of 291,17°C, 290,86°C and 290,81°C, respectively, is compatible with PA46 (melting peak between 290 and 295°C); while the second peak, with temperatures of 327,77°C, 327,07°C and 326,90°C, is compatible with PTFE (melting peak between 325 and 335°C).

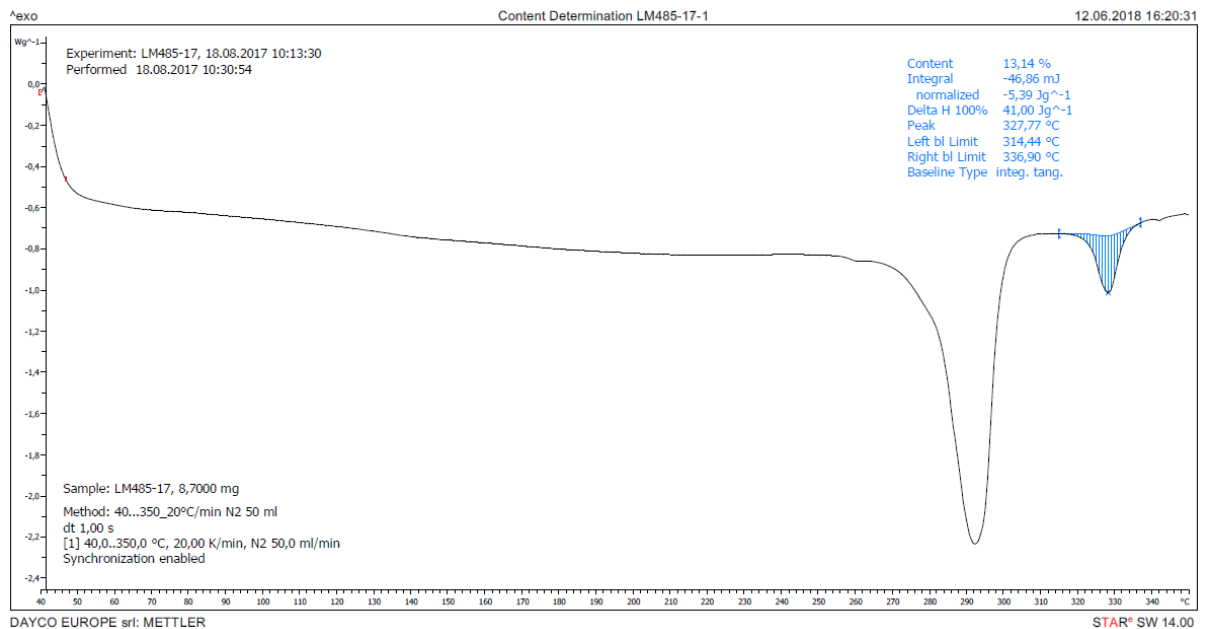


Figure 11.22: DSC measurement curve of sample LM485-17, from Group 1, obtained from Analysis 1, in which a content of 13,14% of PTFE was measured.

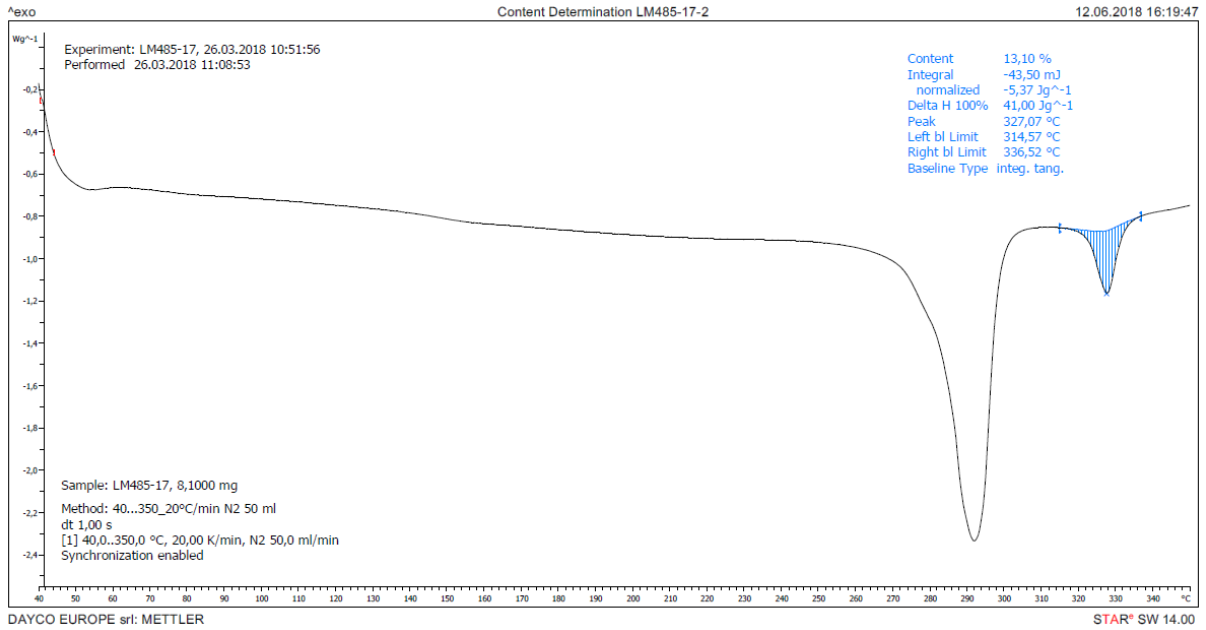


Figure 11.23: DSC measurement curve of sample LM485-17, from Group 2, obtained from Analysis 2, in which a content of 13,10% of PTFE was measured.

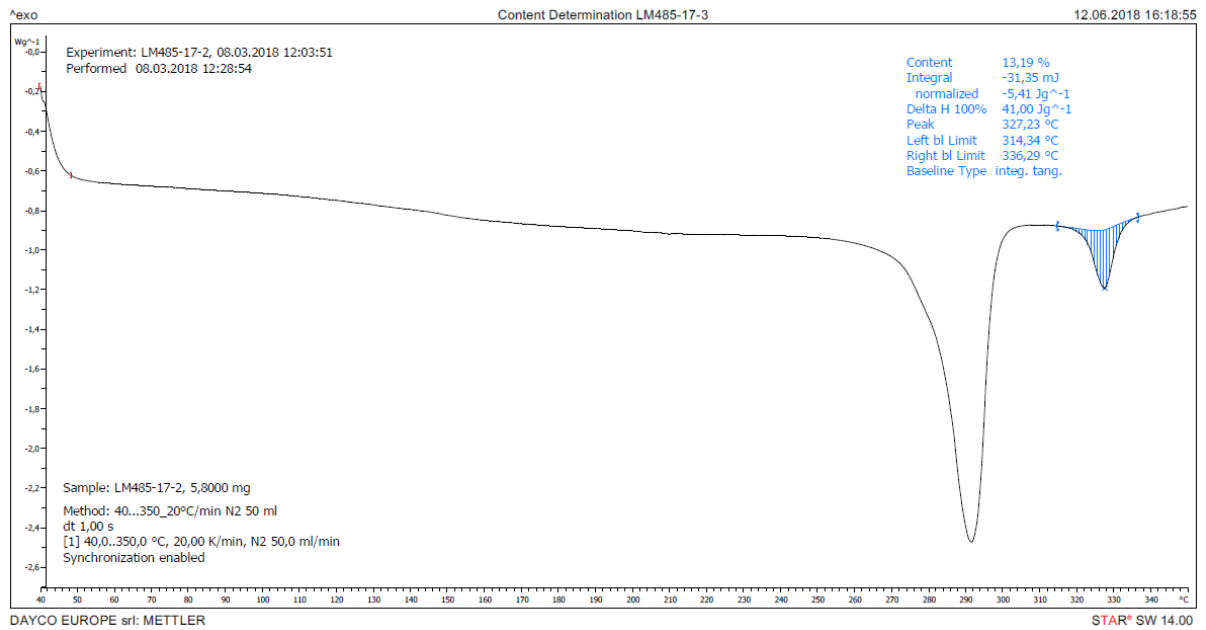


Figure 11.24: DSC measurement curve of sample LM485-17, from Group 3, obtained from Analysis 3, in which a content of 13,19% of PTFE was measured.

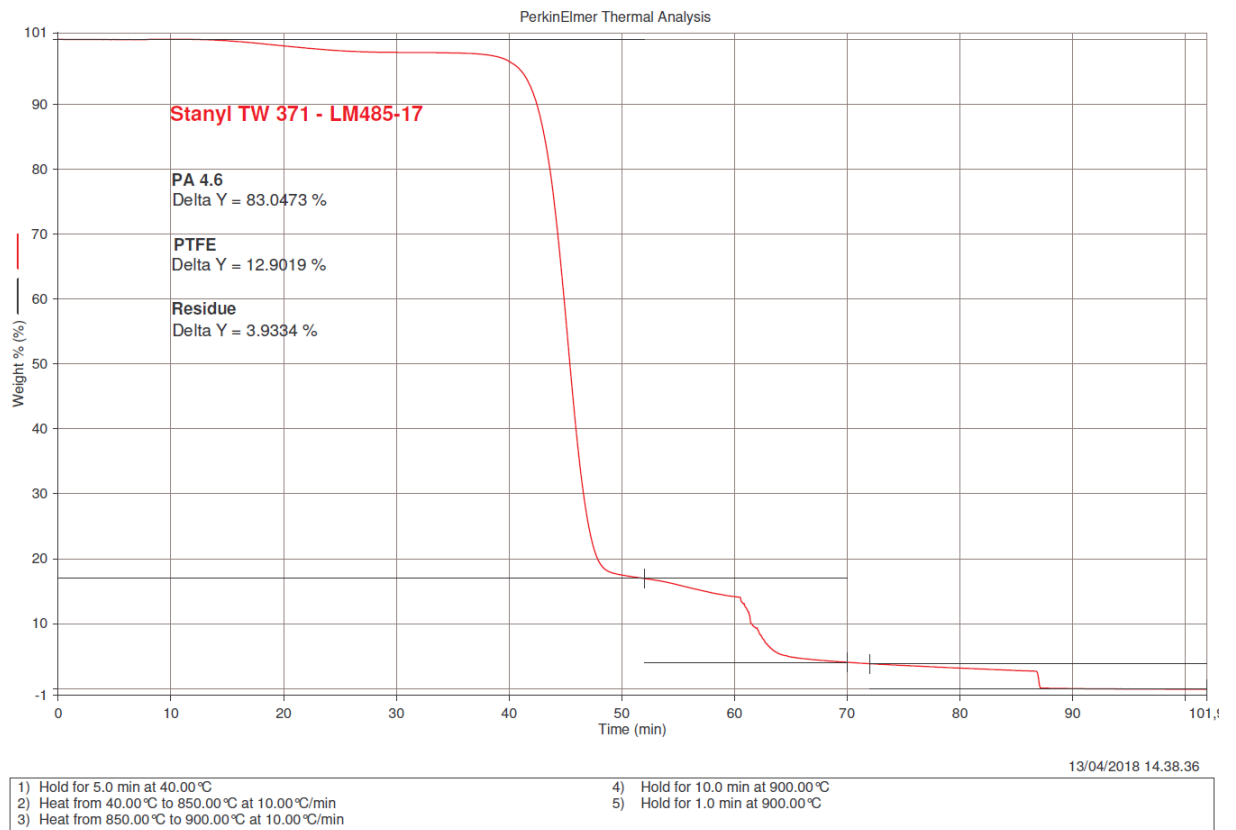


Figure 11.25: TGA measurement curve of sample LM485-17. The contents of PA46, PTFE and residue are, respectively, 83.0473%, 12.9019% and 3.9334%.

11.6. LM486-17

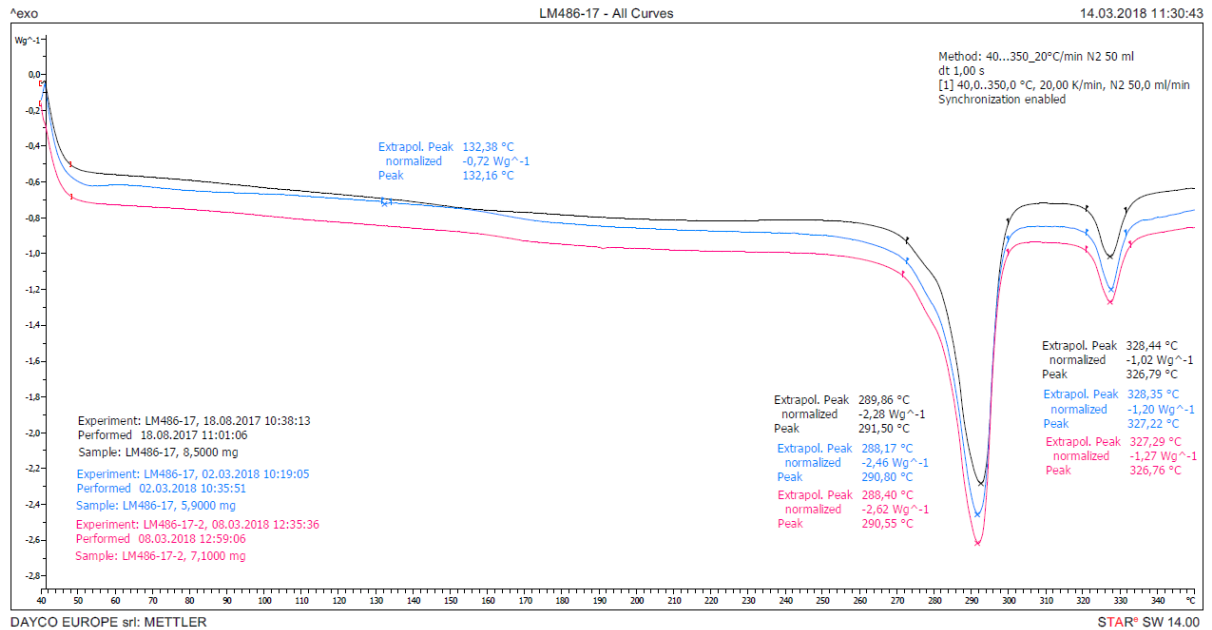


Figure 11.26: DSC measurements curves of spring bushing LM486-17 obtained from Analyses 1 (black), 2 (blue) and 3 (pink), using respectively samples from Groups 1, 2 and 3. All three curves exhibit two melting peaks and the one obtained from Analysis 2 presents also an endothermic peak with temperature of 132,16°C, caused by impurities. The first melting peak, with temperatures of 291,50°C, 290,80°C and 290,55°C, respectively, is compatible with PA46 (melting peak between 290 and 295°C); while the second peak, with temperatures of 326,79°C, 327,22°C and 326,76°C, is compatible with PTFE (melting peak between 325 and 335°C).

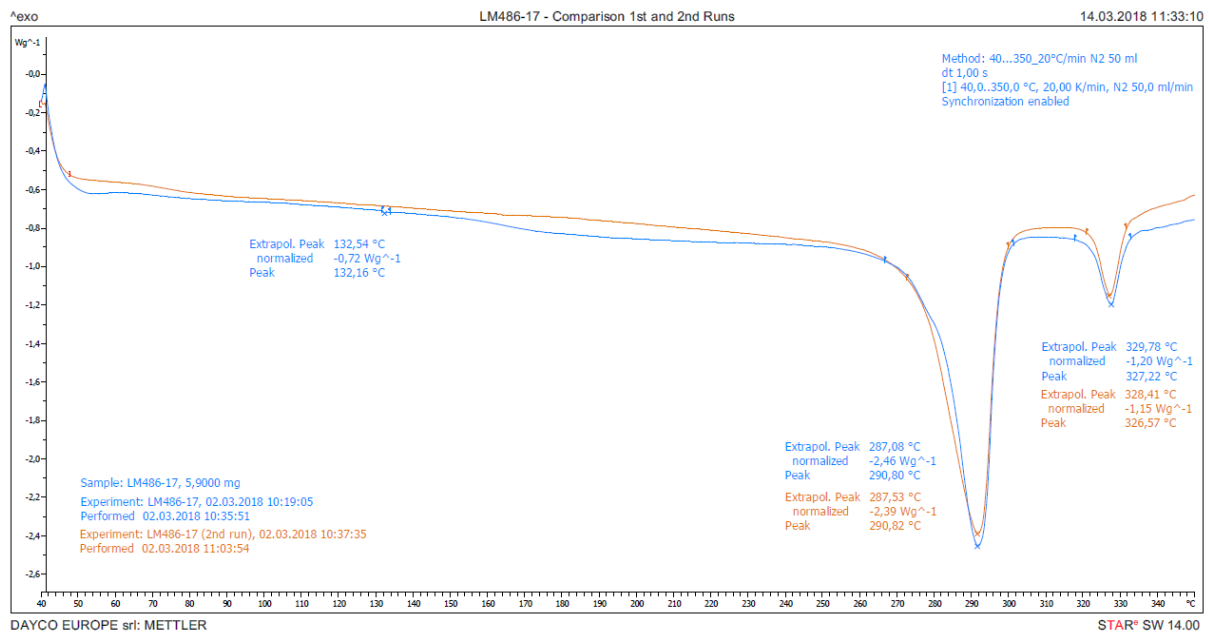


Figure 11.27: DSC measurement curves of spring bushing LM486-17 obtained in the first (blue) and second (orange) runs of Analysis 2. The second run was performed due to the presence of an endothermic peak with temperature of 132,16°C, caused by impurities in the first run. The curve obtained from the second run exhibits the two melting peaks, and there aren't neither artifacts or other peaks that identify impurities. The first peak, with temperatures of 290,80°C and 286,82°C, respectively, is compatible with PA46 (melting peak between 290 and 295°C); while the second peak, with temperatures of 327,22°C and 326,57°C, is compatible with PTFE (melting peak between 325 and 335°C).

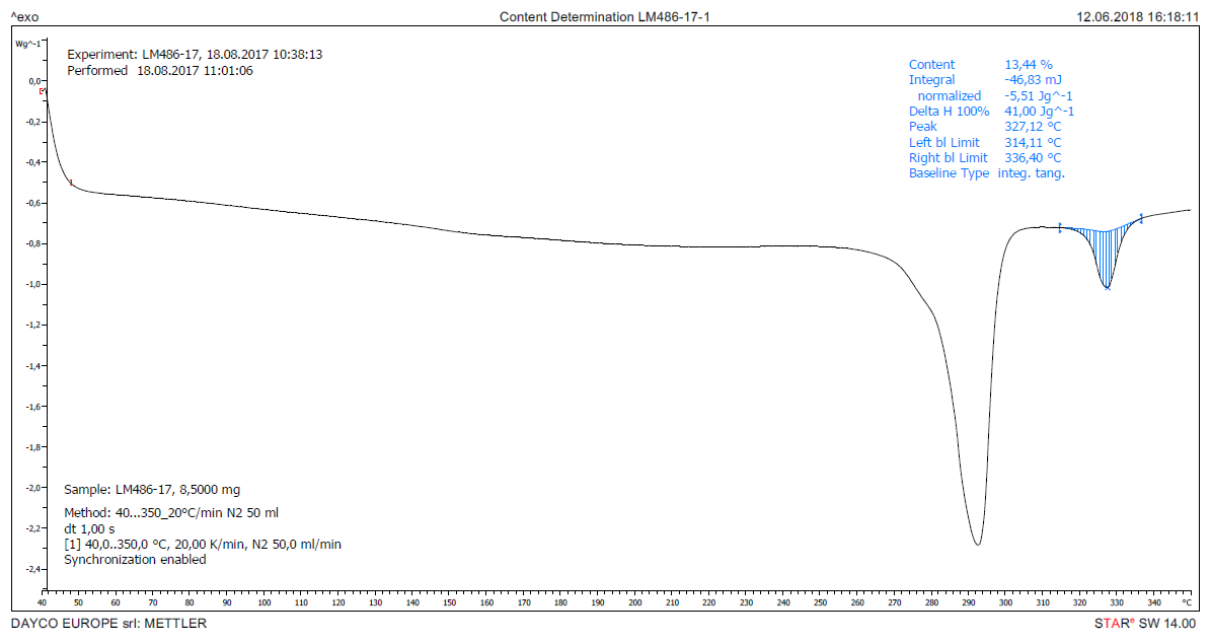


Figure 11.28: DSC measurement curve of sample LM486-17, from Group 1, obtained from Analysis 1, in which a content of 13,44% of PTFE was measured.

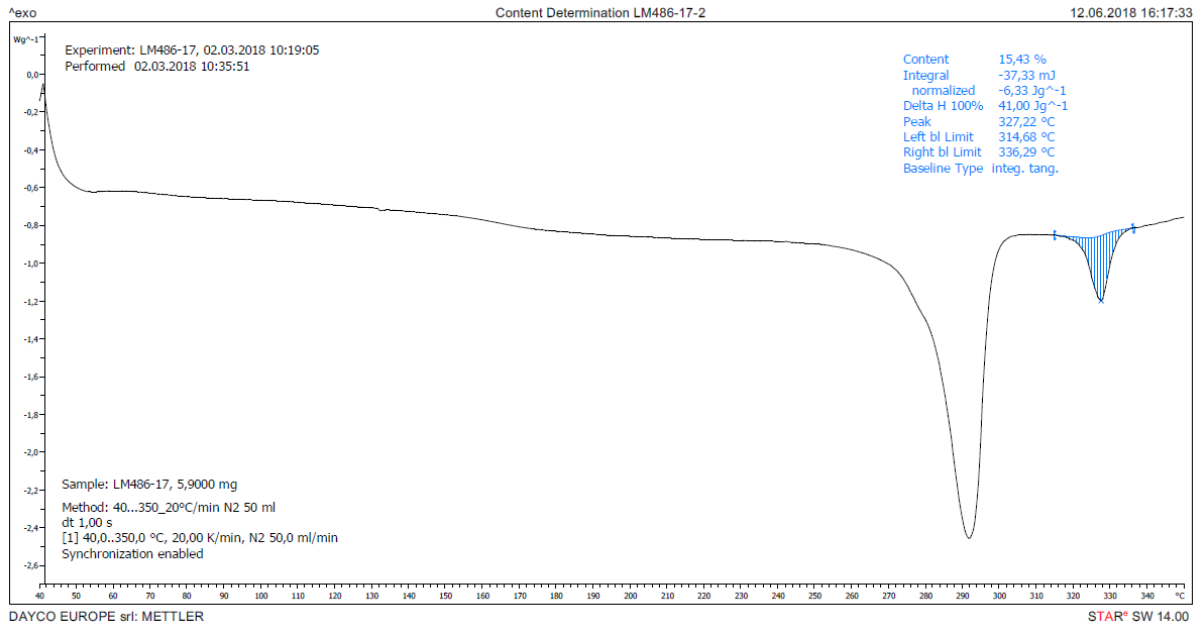


Figure 11.29: DSC measurement curve of sample LM486-17, from Group 2, obtained from Analysis 2, in which a content of 15,43% of PTFE was measured.

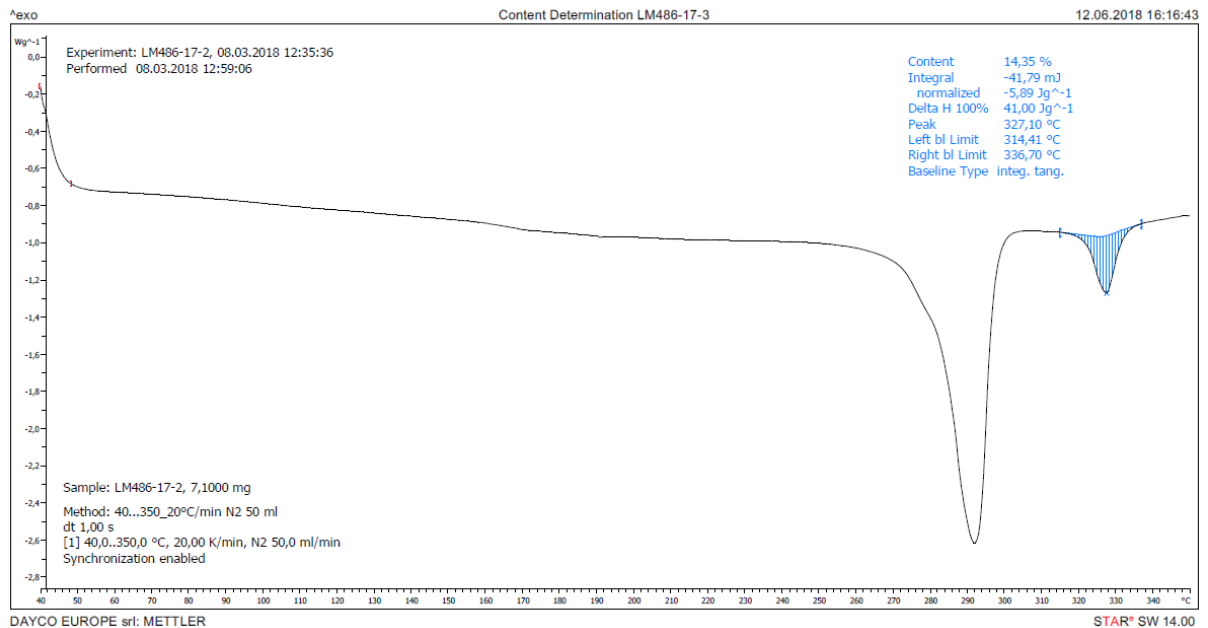


Figure 11.30: DSC measurement curve of sample LM486-17, from Group 3, obtained from Analysis 3, in which a content of 14,35% of PTFE was measured.

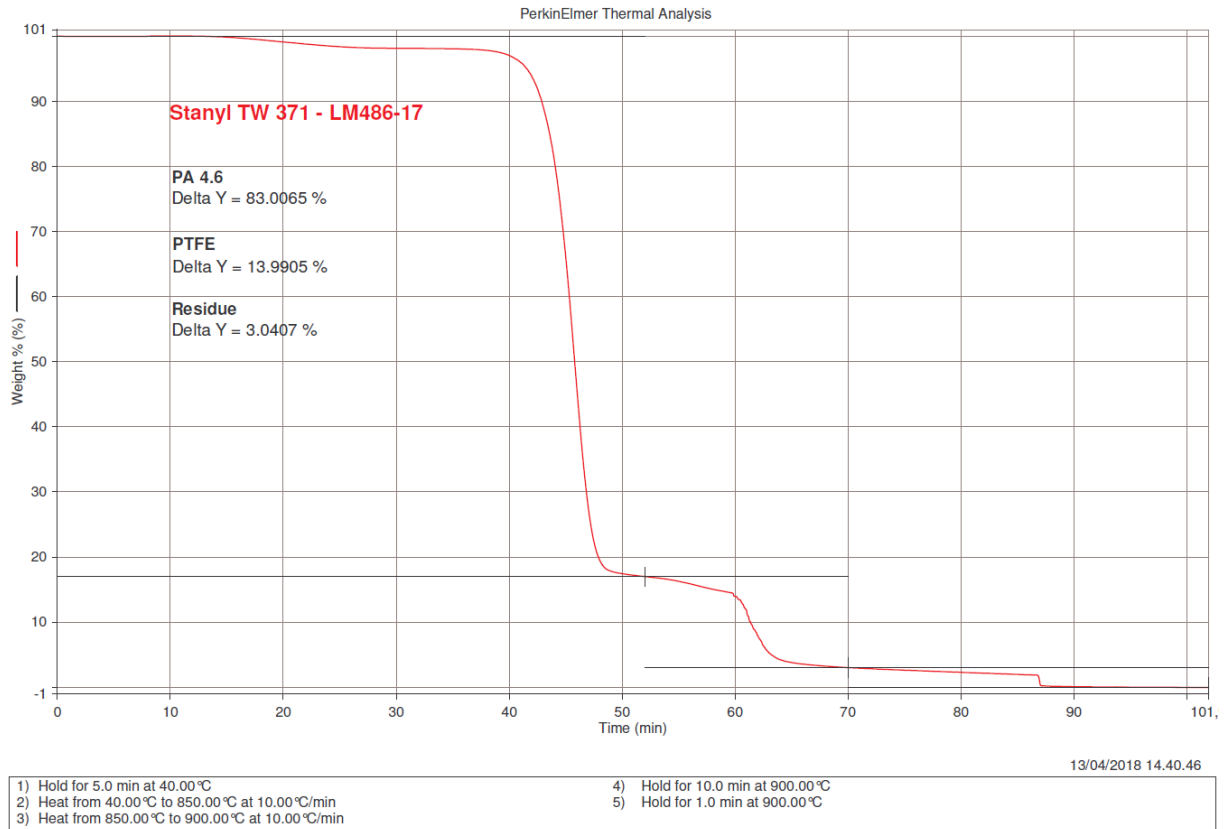


Figure 11.31: TGA measurement curve of sample LM486-17. The contents of PA46, PTFE and residue are, respectively, 83.0065%, 13.9905% and 3.0407%.

11.7. LM487-17

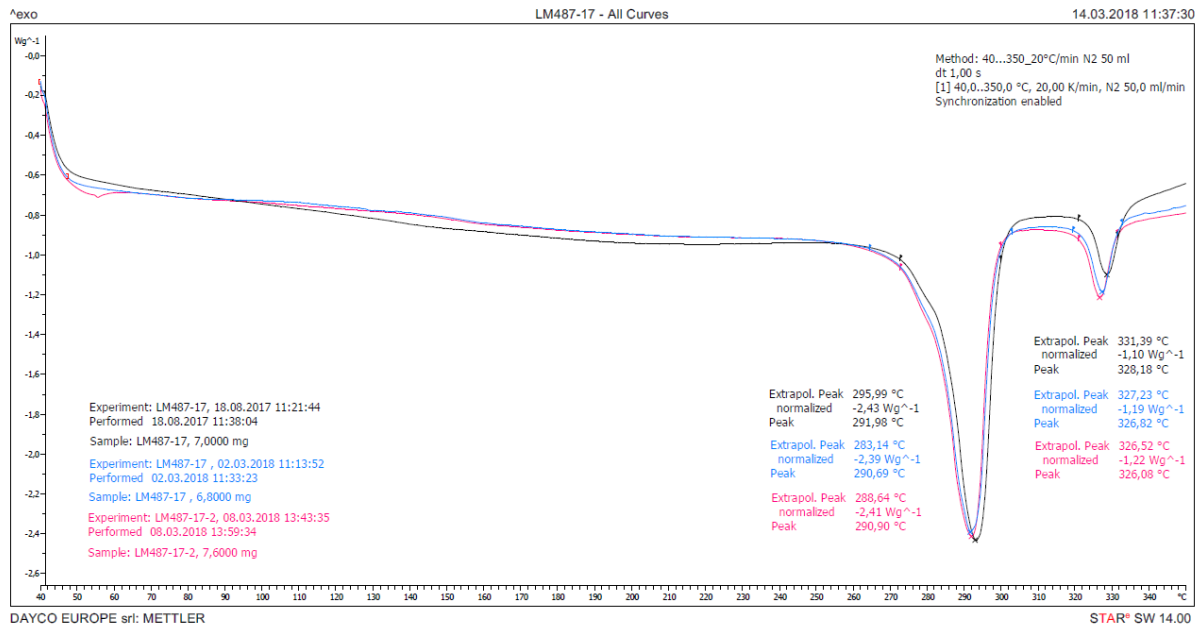


Figure 11.32: DSC measurements curves of spring bushing LM487-17 obtained from Analyses 1 (black), 2 (blue) and 3 (pink), using respectively samples from Groups 1, 2 and 3. All three curves exhibit two melting peaks and there aren't neither artifacts or other peaks that identify impurities. The first peak, with temperatures of 291,98°C, 290,69°C and 290,90°C, respectively, is compatible with PA46 (melting peak between 290 and 295°C); while the second peak, with temperatures of 328,18°C, 326,82°C and 326,08°C, is compatible with PTFE (melting peak between 325 and 335°C).

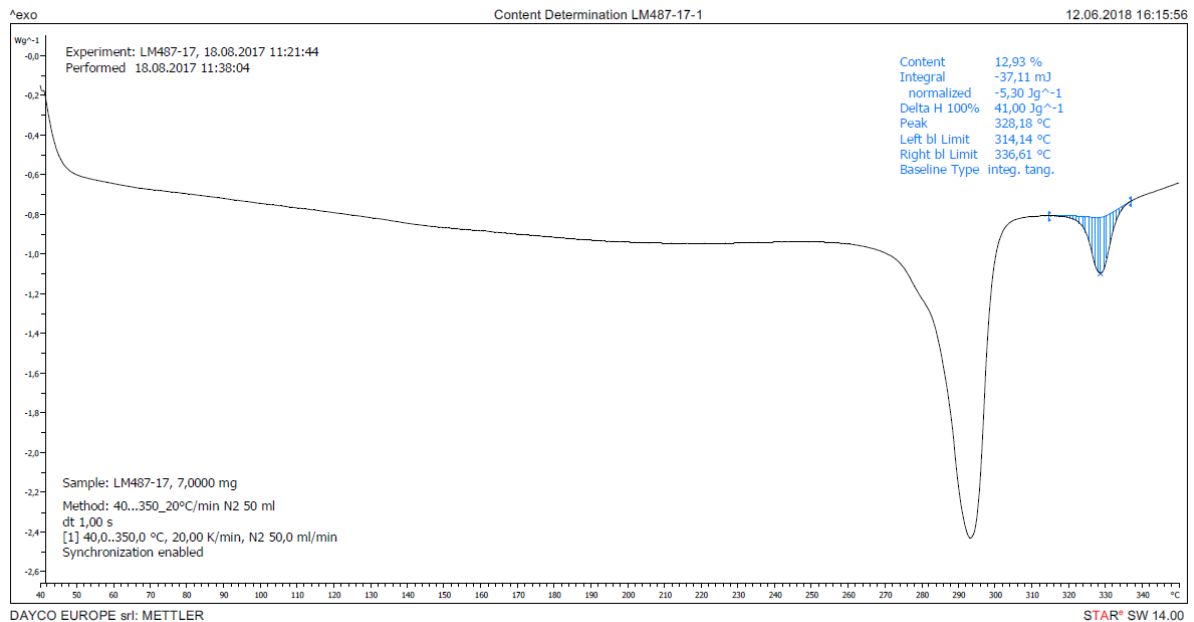


Figure 11.33: DSC measurement curve of sample LM487-17, from Group 1, obtained from Analysis 1, in which a content of 12,93% of PTFE was measured.

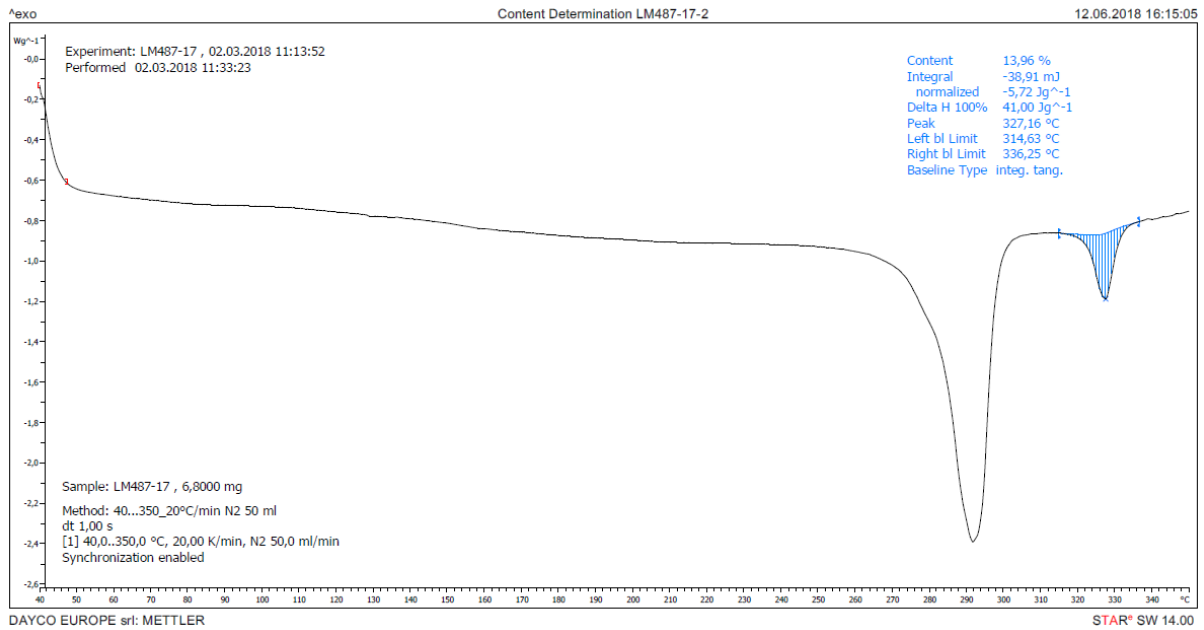


Figure 11.34: DSC measurement curve of sample LM487-17, from Group 2, obtained from Analysis 2, in which a content of 13,96% of PTFE was measured.

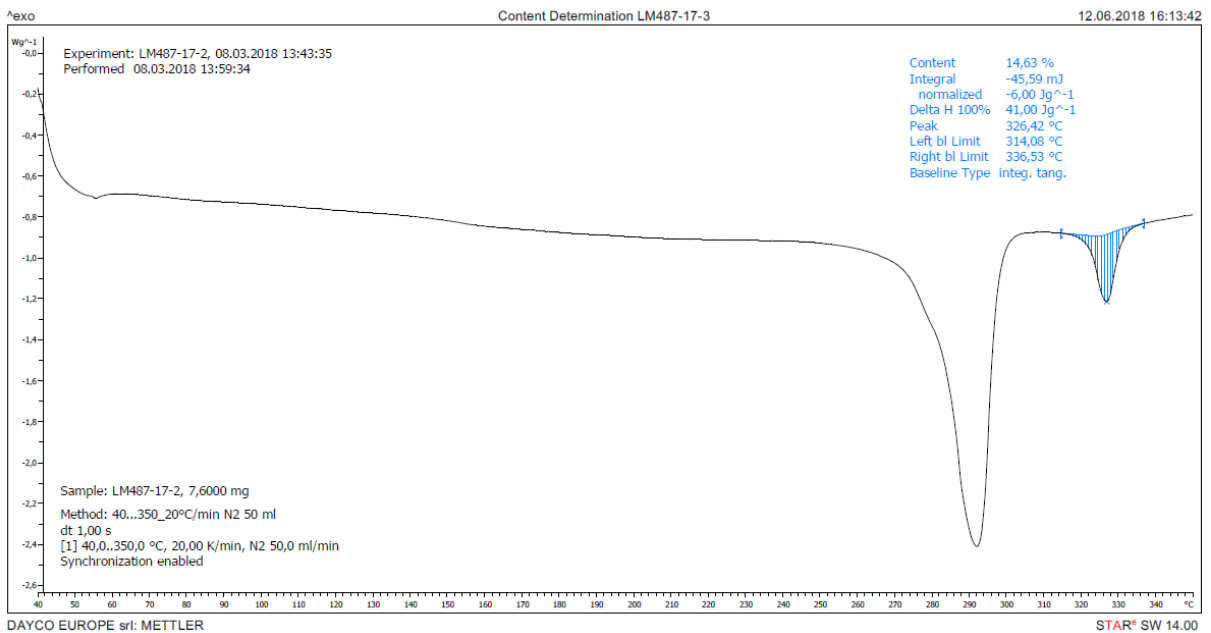


Figure 11.35: DSC measurement curve of sample LM487-17, from Group 3, obtained from Analysis 3, in which a content of 14,63% of PTFE was measured.

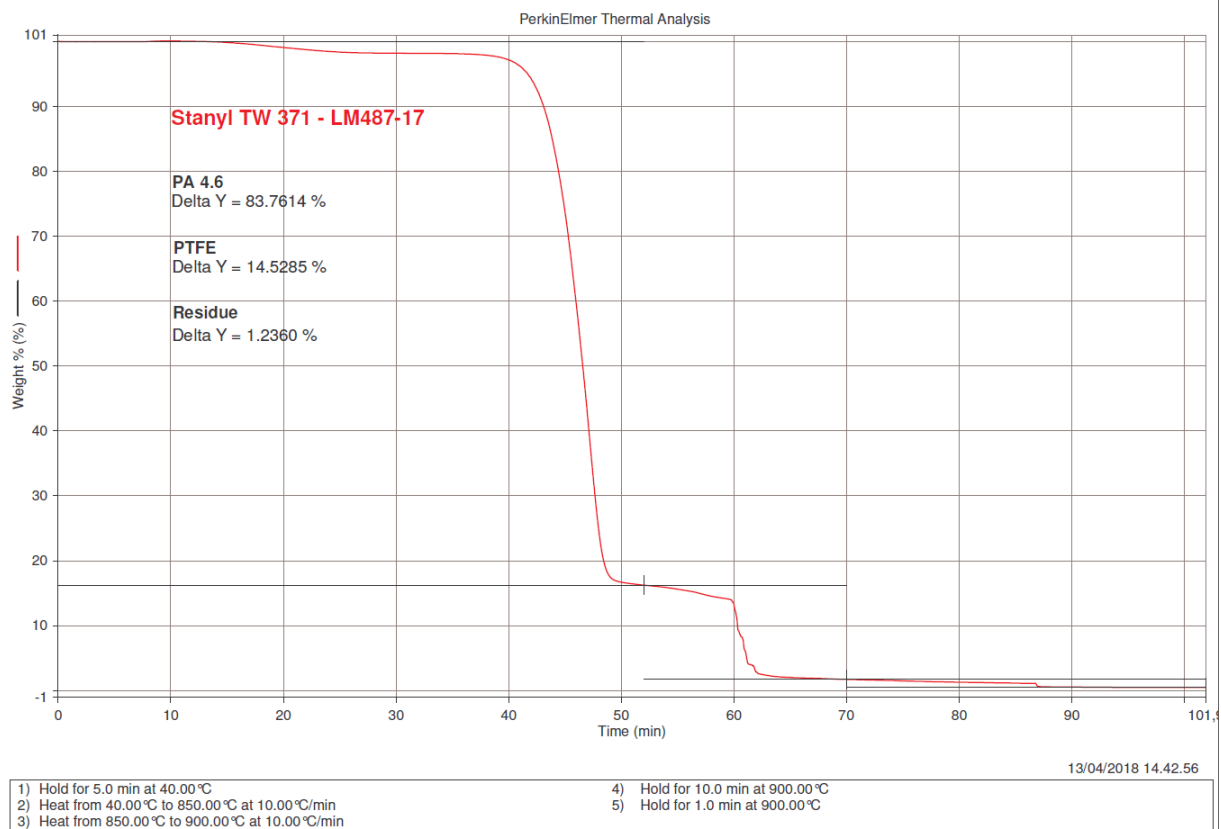


Figure 11.36: TGA measurement curve of sample LM487-17. The contents of PA46, PTFE and residue are, respectively, 83.7614%, 14.5285% and 1.2360%.

11.8. LM488-17

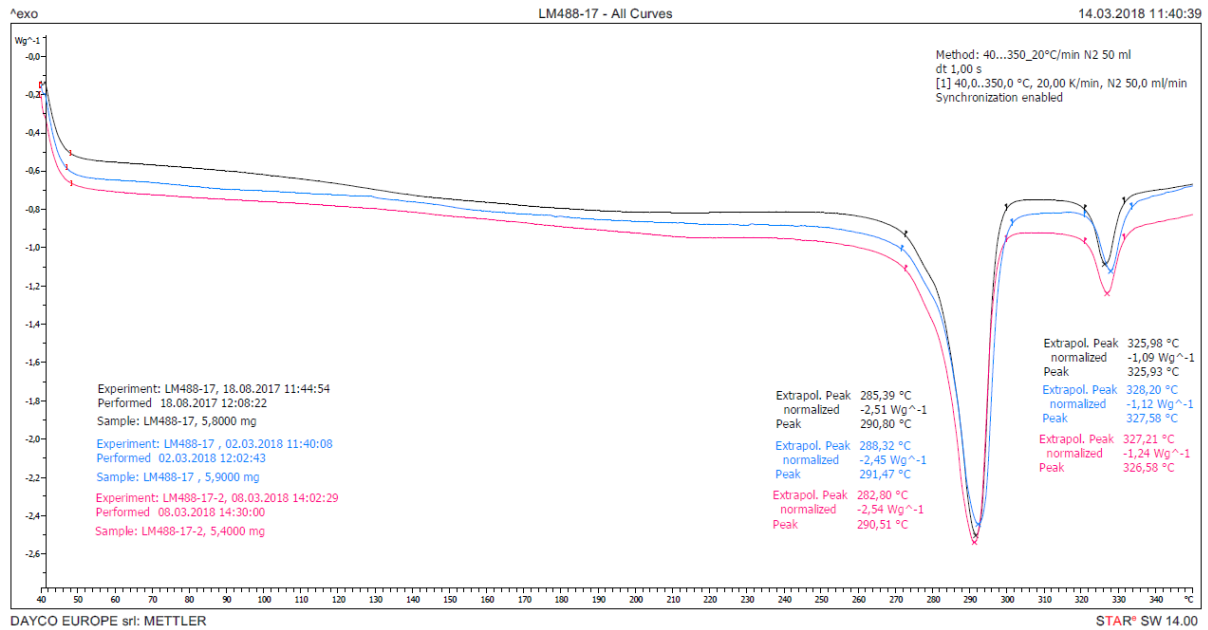


Figure 11.37: DSC measurements curves of spring bushing LM488-17 obtained from Analyses 1 (black), 2 (blue) and 3 (pink), using respectively samples from Groups 1, 2 and 3. All three curves exhibit two melting peaks and there aren't neither artifacts or other peaks that identify impurities. The first peak, with temperatures of 290,80°C, 291,47°C and 290,51°C, respectively, is compatible with PA46 (melting peak between 290 and 295°C); while the second peak, with temperatures of 325,93°C, 327,58°C and 326,58°C, is compatible with PTFE (melting peak between 325 and 335°C).

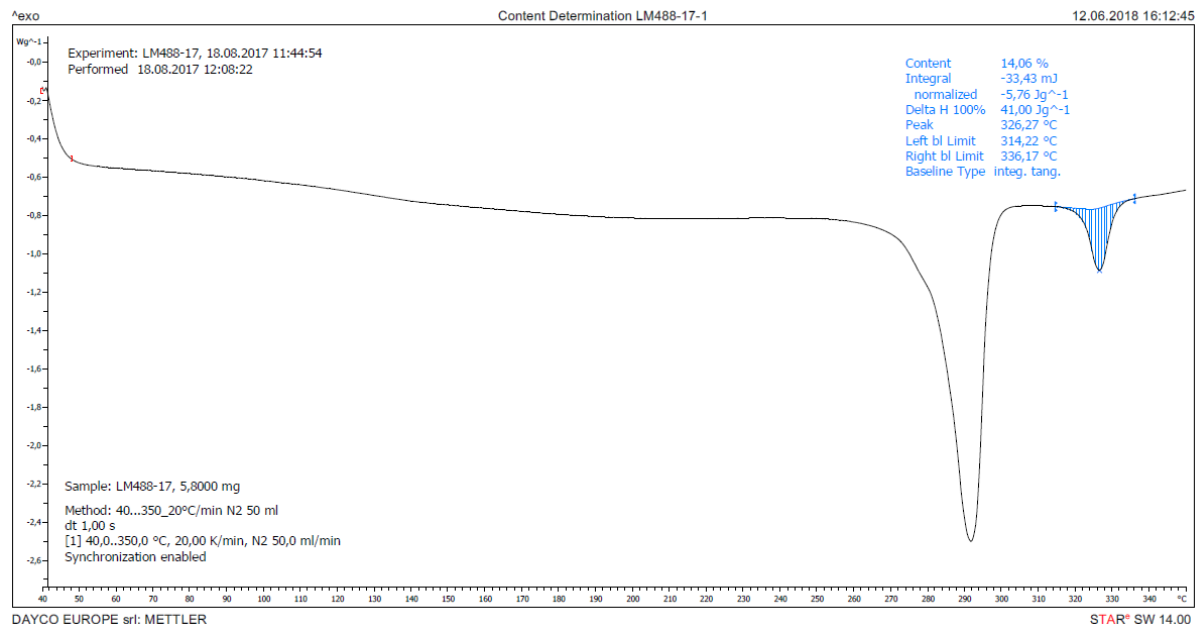


Figure 11.38: DSC measurement curve of sample LM488-17, from Group 1, obtained from Analysis 1, in which a content of 14,06% of PTFE was measured.

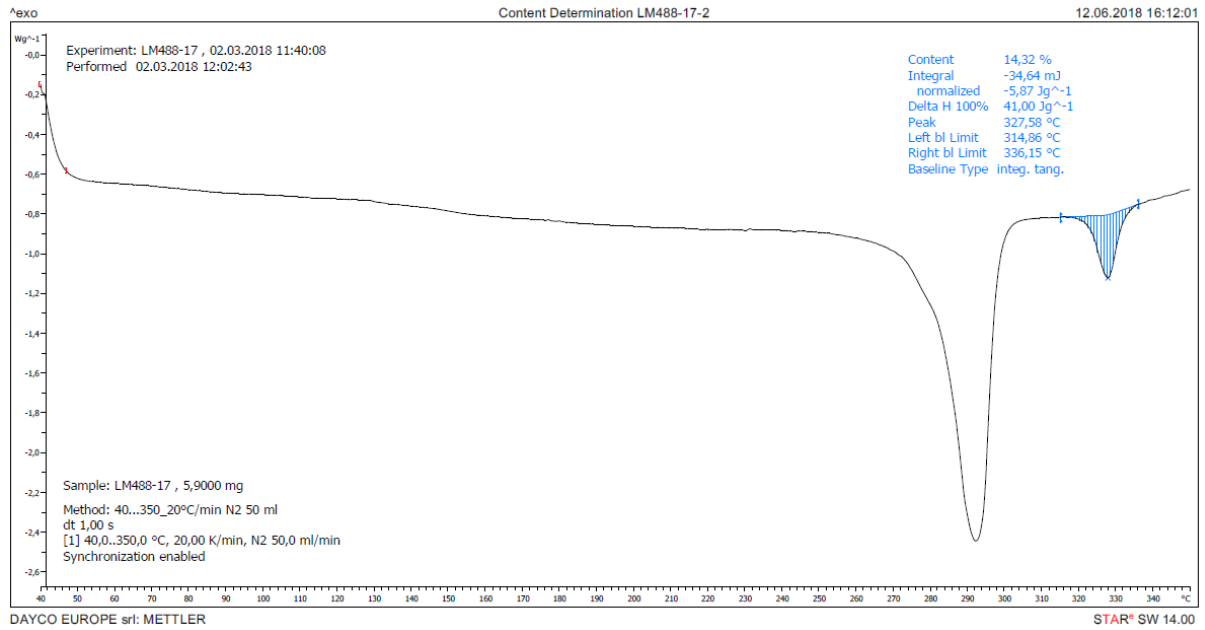


Figure 11.39: DSC measurement curve of sample LM488-17, from Group 2, obtained from Analysis 2, in which a content of 14,32% of PTFE was measured.

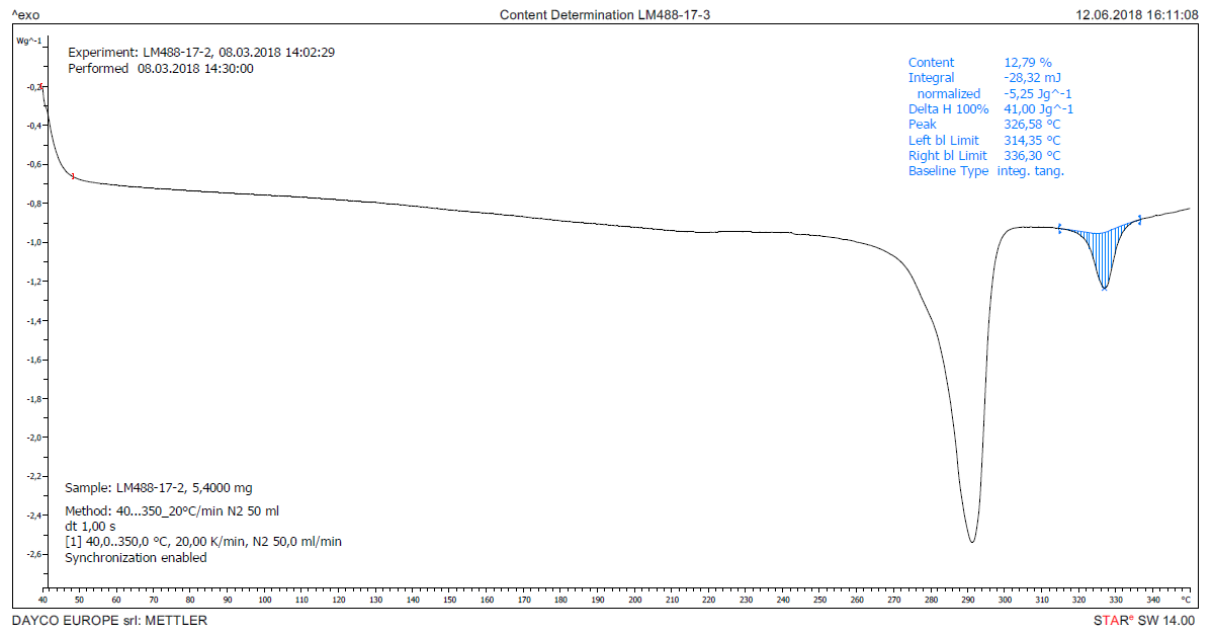


Figure 11.40: DSC measurement curve of sample LM488-17, from Group 3, obtained from Analysis 3, in which a content of 12,79% of PTFE was measured.

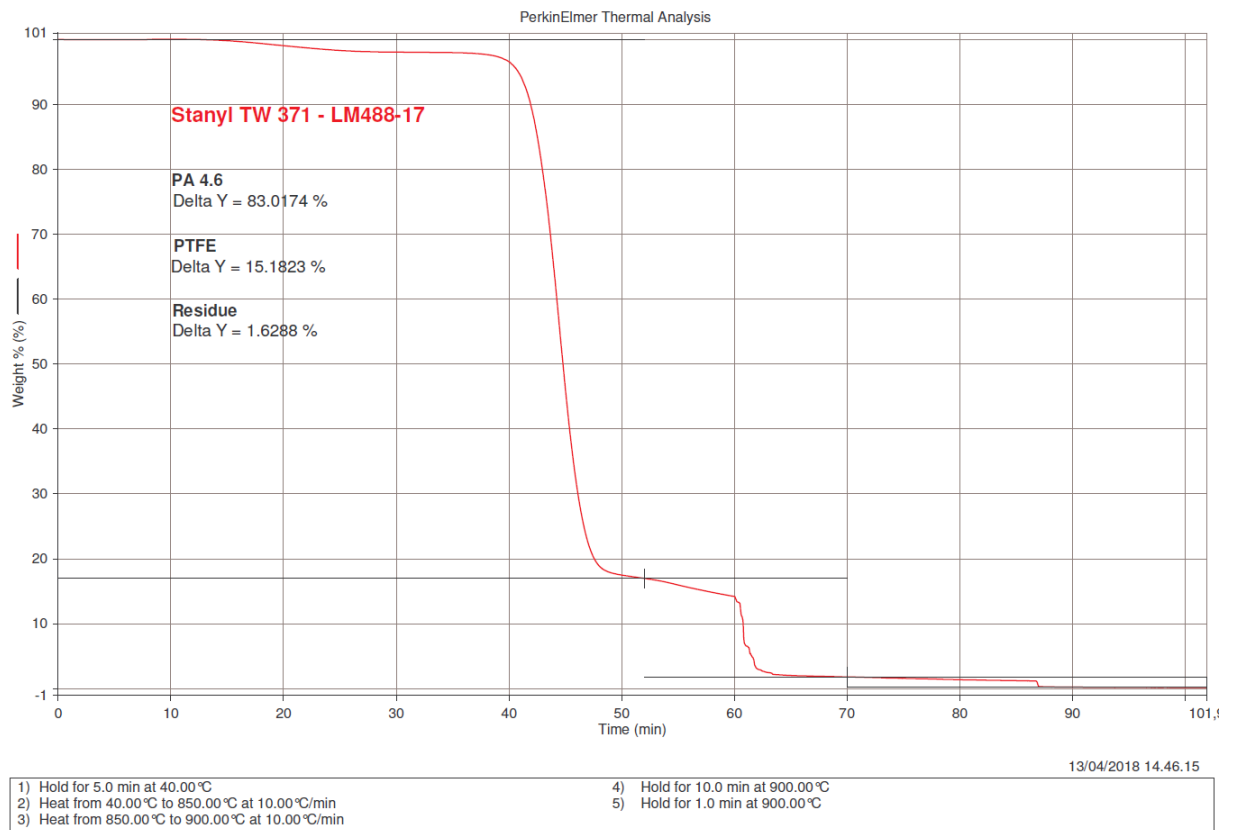


Figure 11.41: TGA measurement curve of sample LM488-17. The contents of PA46, PTFE and residue are, respectively, 83.0174%, 15.1823% and 1.6288%.

11.9. LM489-17

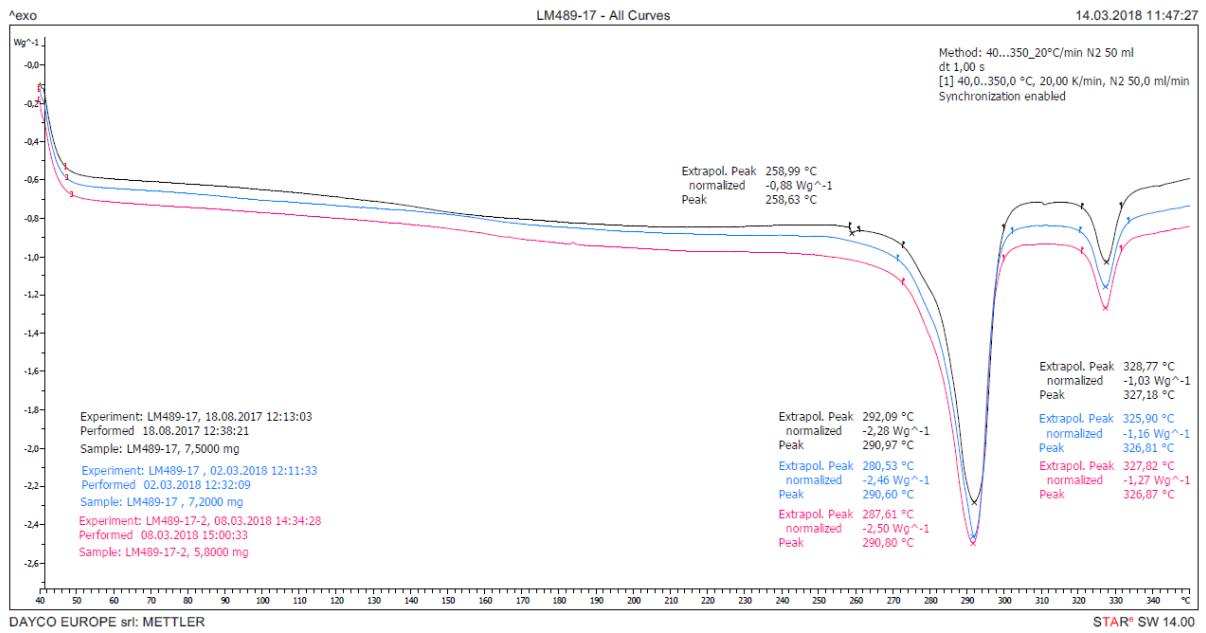


Figure 11.42: DSC measurements curves of spring bushing LM489-17 obtained from Analyses 1 (black), 2 (blue) and 3 (pink), using respectively samples from Groups 1, 2 and 3. All three curves exhibit two melting peaks and the one obtained from Analysis 1 presents also a peak that identifies impurities. The first peak, with temperatures of 290,97°C, 290,60°C and 290,80°C, respectively, is compatible with PA46 (melting peak between 290 and 295°C); while the second peak, with temperatures of 327,18°C, 326,81°C and 326,87°C, is compatible with PTFE (melting peak between 325 and 335°C).

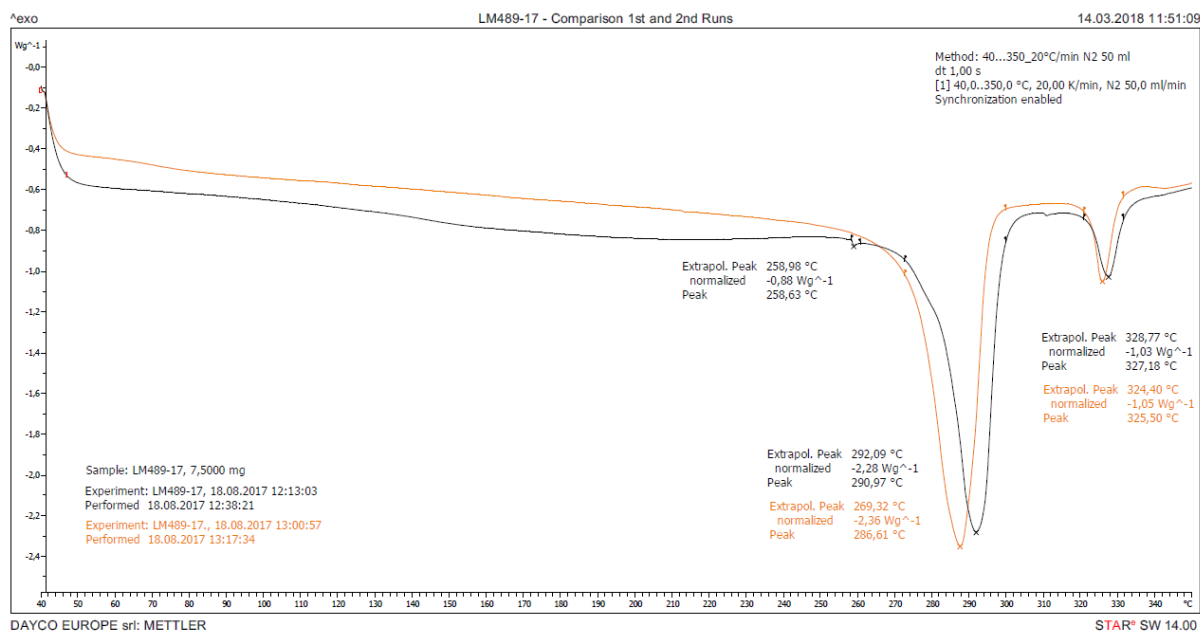


Figure 11.43: DSC measurement curves of spring bushing LM489-17 obtained in the first (blue) and second (orange) runs of Analysis 1. The second run was performed due to the presence of an endothermic peak with temperature of 258,63°C, caused by impurities in the first run. The curve obtained from the second run exhibits the two melting peaks, and there aren't neither artifacts or other peaks that identify impurities. The first peak, with temperatures of 290,97°C and 286,61°C, respectively, is compatible with PA46 (melting peak between 290 and 295°C) in the 1st run and slightly below in the 2nd run; while the second peak, with temperatures of 327,18°C and 325,50°C, is compatible with PTFE (melting peak between 325 and 335°C).

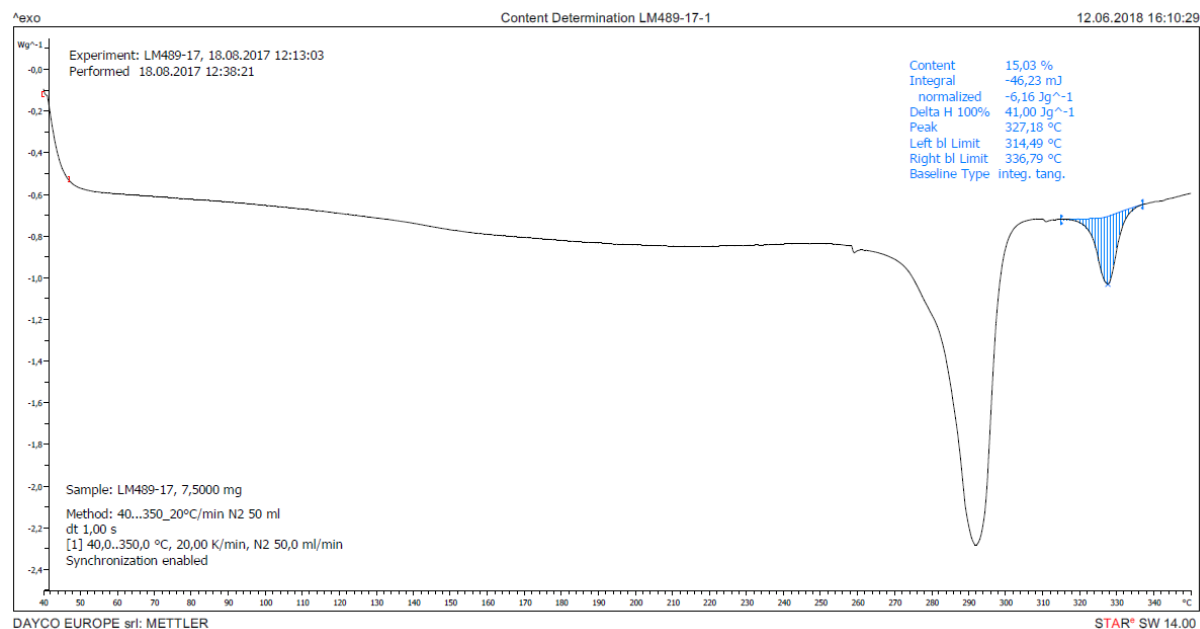


Figure 11.44: DSC measurement curve of sample LM489-17, from Group 1, obtained from Analysis 1, in which a content of 15,03% of PTFE was measured.

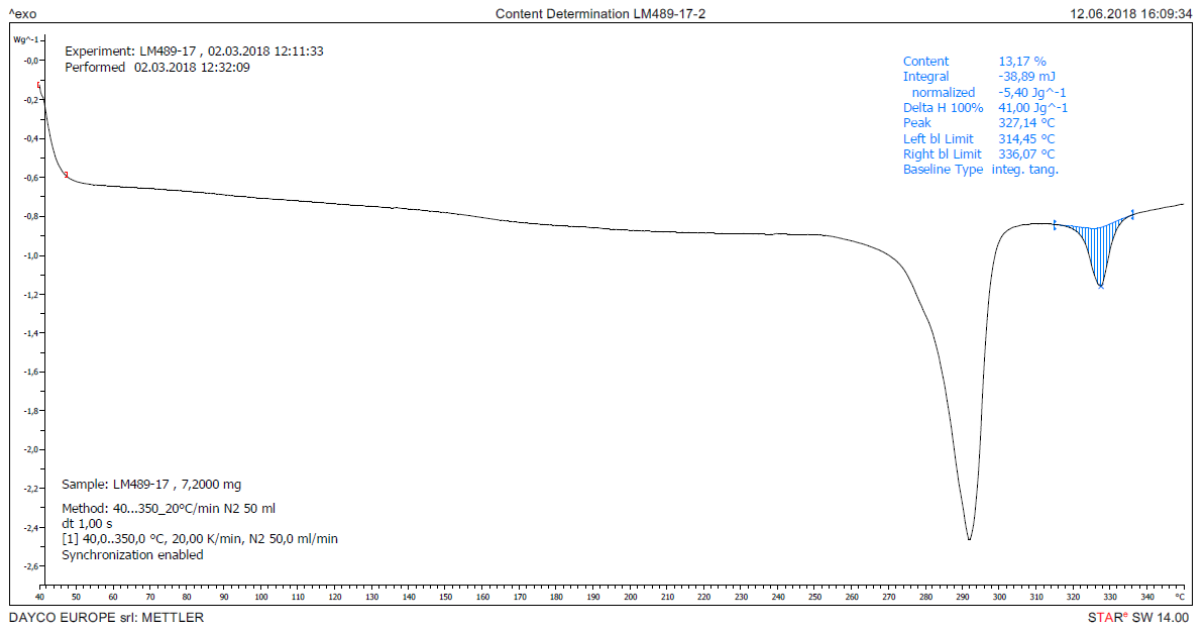


Figure 11.45: DSC measurement curve of sample LM489-17, from Group 2, obtained from Analysis 2, in which a content of 13,17% of PTFE was measured.

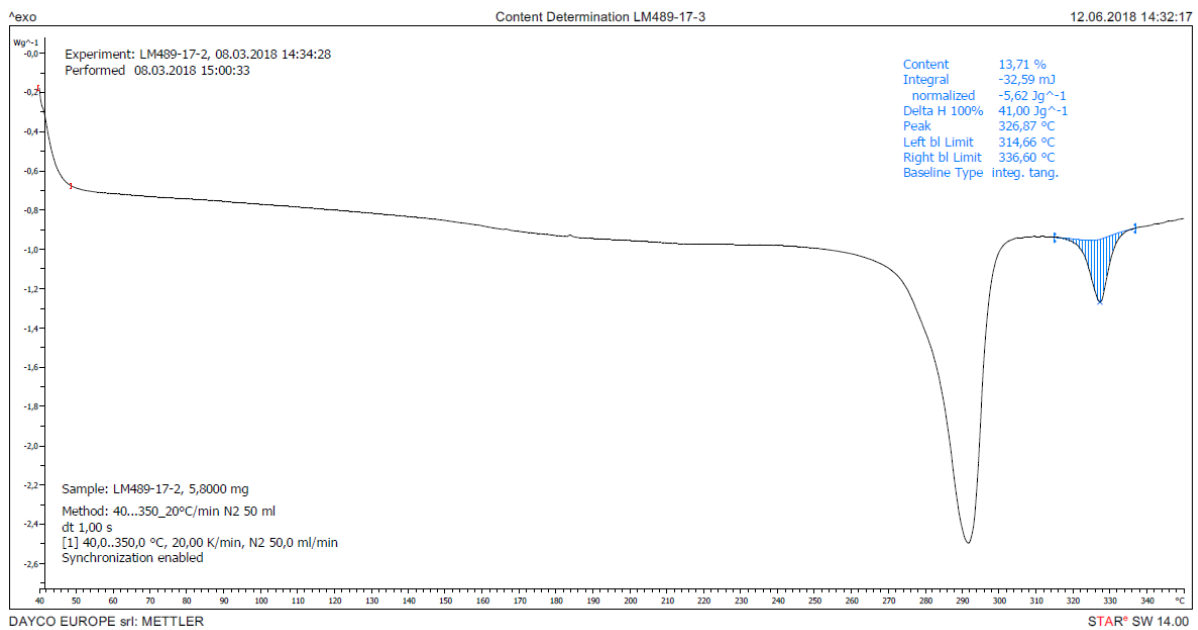


Figure 11.46: DSC measurement curve of sample LM489-17, from Group 3, obtained from Analysis 3, in which a content of 13,71% of PTFE was measured.

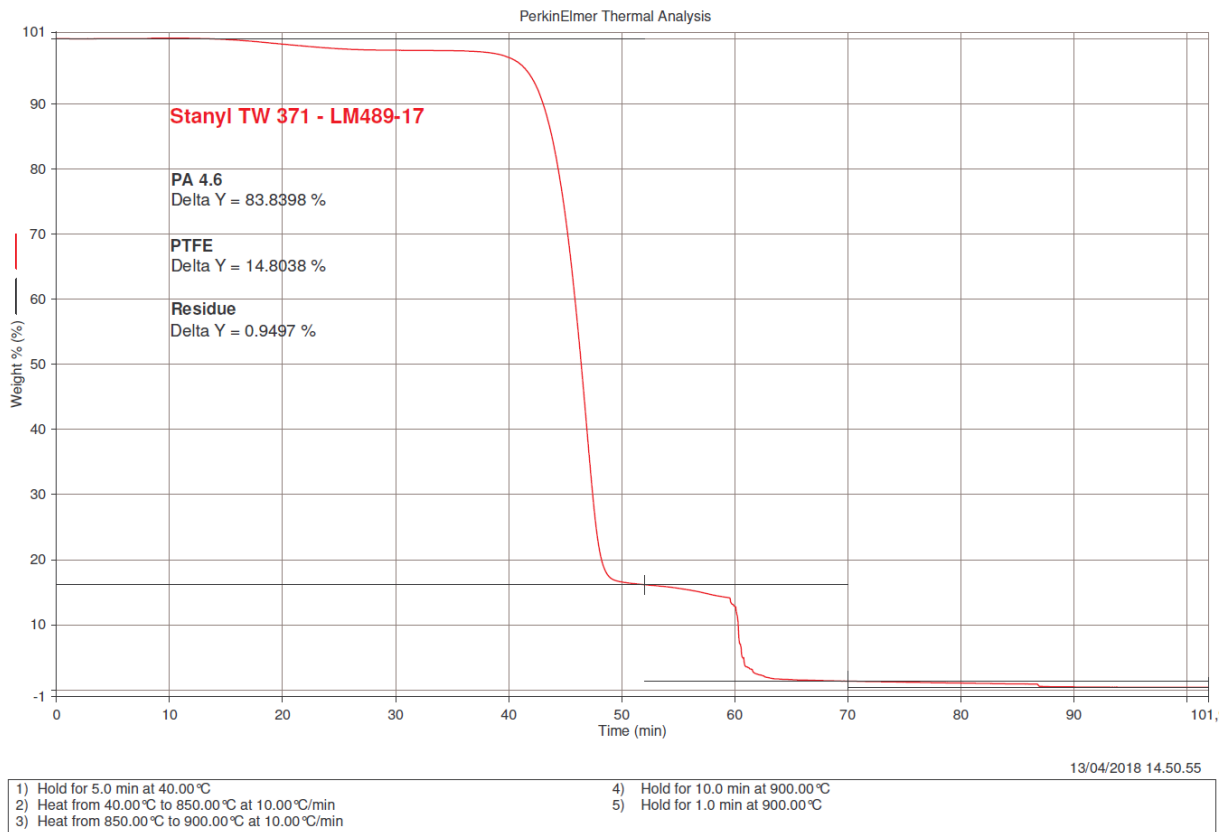


Figure 11.47: TGA measurement curve of sample LM489-17. The contents of PA46, PTFE and residue are, respectively, 83.8398%, 14.8038% and 0.9497%.

11.10. LM490-17

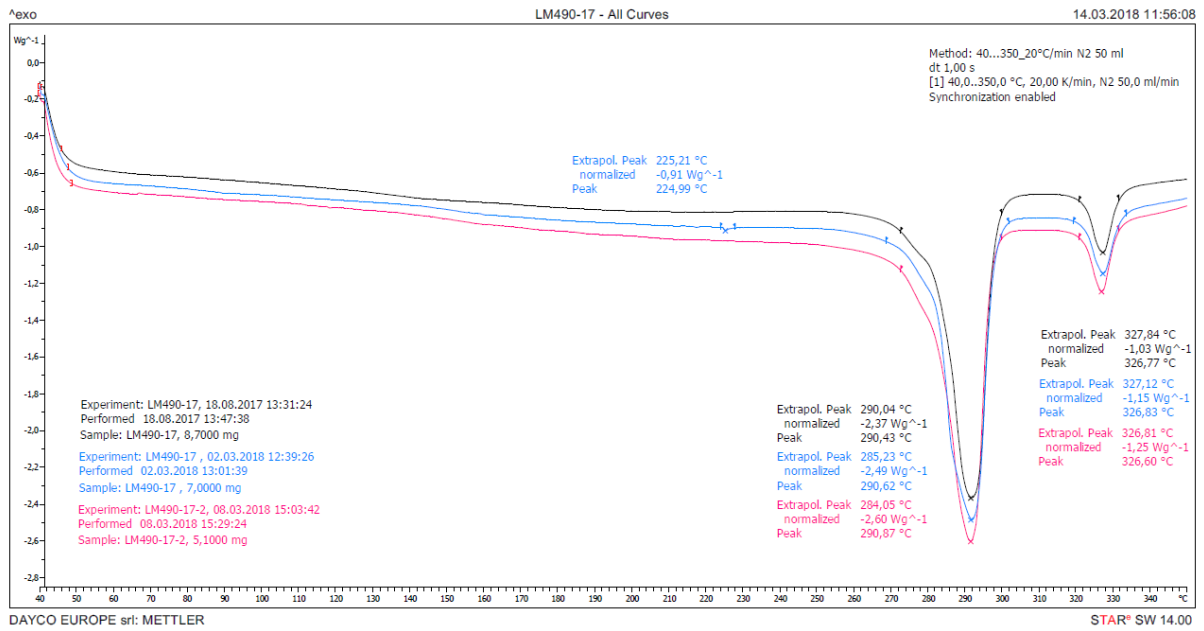


Figure 11.48: DSC measurements curves of spring bushing LM490-17 obtained from Analyses 1 (black), 2 (blue) and 3 (pink), using respectively samples from Groups 1, 2 and 3. All three curves exhibit two melting peaks and the one obtained from Analysis 2 presents also an endothermic peak with temperature of 224,99°C, caused by impurities. The first melting peak, with temperatures of 290,43°C, 290,62°C and 290,87°C, respectively, is compatible with PA46 (melting peak between 290 and 295°C); while the second peak, with temperatures of 326,77°C, 326,83°C and 326,60°C, is compatible with PTFE (melting peak between 325 and 335°C).

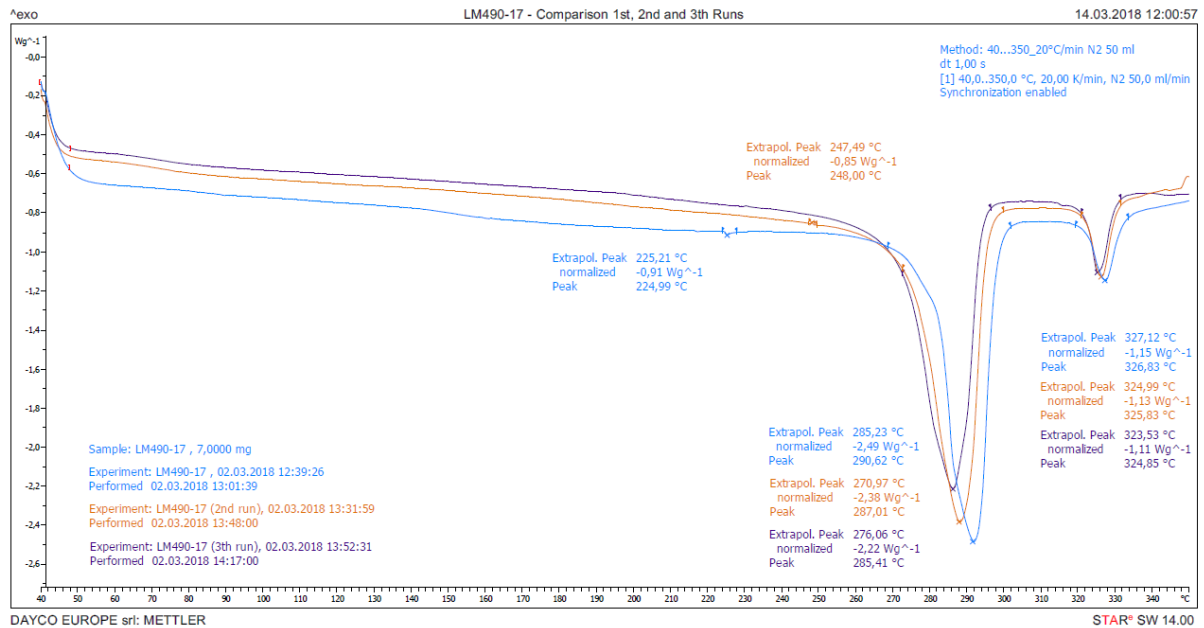


Figure 11.49: DSC measurement curves of spring bushing LM490-17 obtained in the first (blue), second (orange) and third (purple) runs of Analysis 2. The second run was performed due to the presence of an endothermic peak with temperature of 224,99°C, caused by impurities in the first run. And the third run was performed due to the presence of an exothermic peak with temperature of 248,00°C, caused by impurities in the second run. The curve obtained from the third run instead exhibits the two melting peaks, and there aren't neither artifacts or other peaks that identify impurities. The first peak, with temperatures of 290,62°C, 287,01°C and 285,41°C, respectively, is compatible with PA46 (melting peak between 290 and 295°C) in the 1st run and slightly below in the 2nd and 3rd runs; while the second peak, with temperatures of 326,83°C, 325,83°C and 324,85°C, is compatible with PTFE (melting peak between 325 and 335°C) in the 1st and 2nd runs and slightly below in the 3rd run.

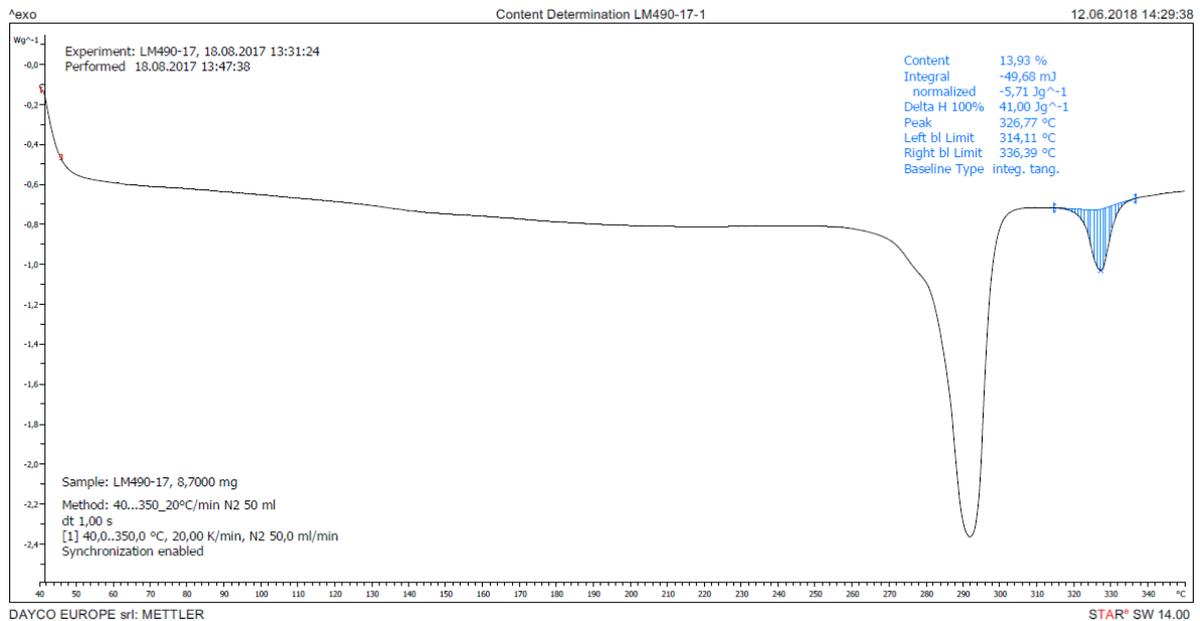


Figure 11.50: DSC measurement curve of sample LM490-17, from Group 1, obtained from Analysis 1, in which a content of 13,93% of PTFE was measured.

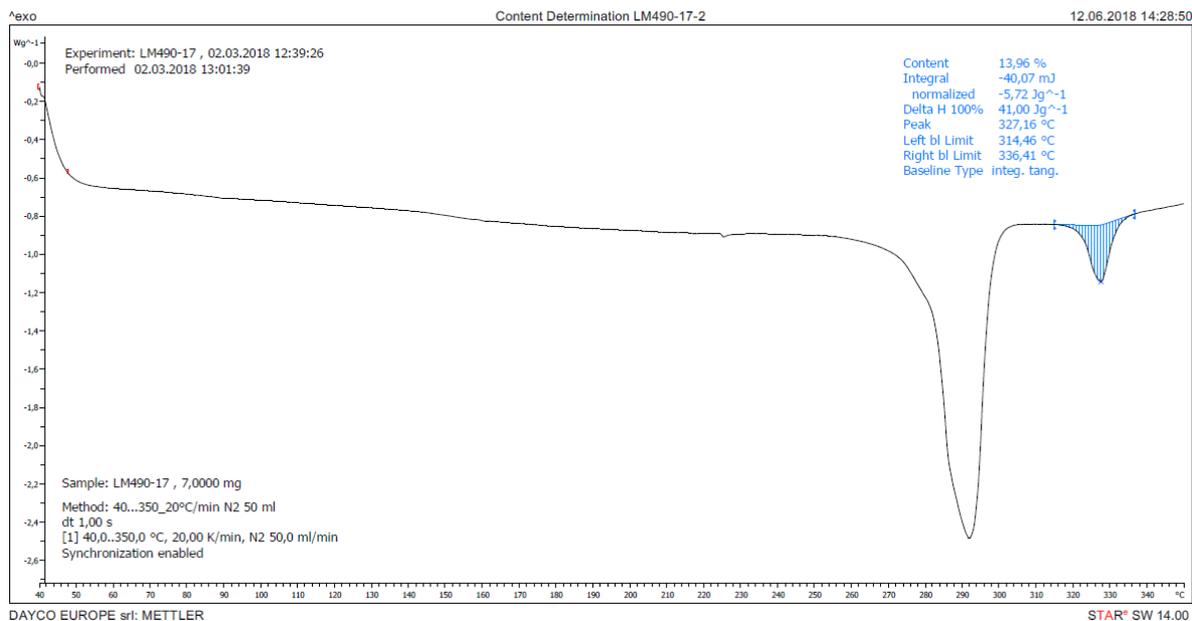


Figure 11.51: DSC measurement curve of sample LM490-17, from Group 2, obtained from Analysis 2, in which a content of 13,96% of PTFE was measured.

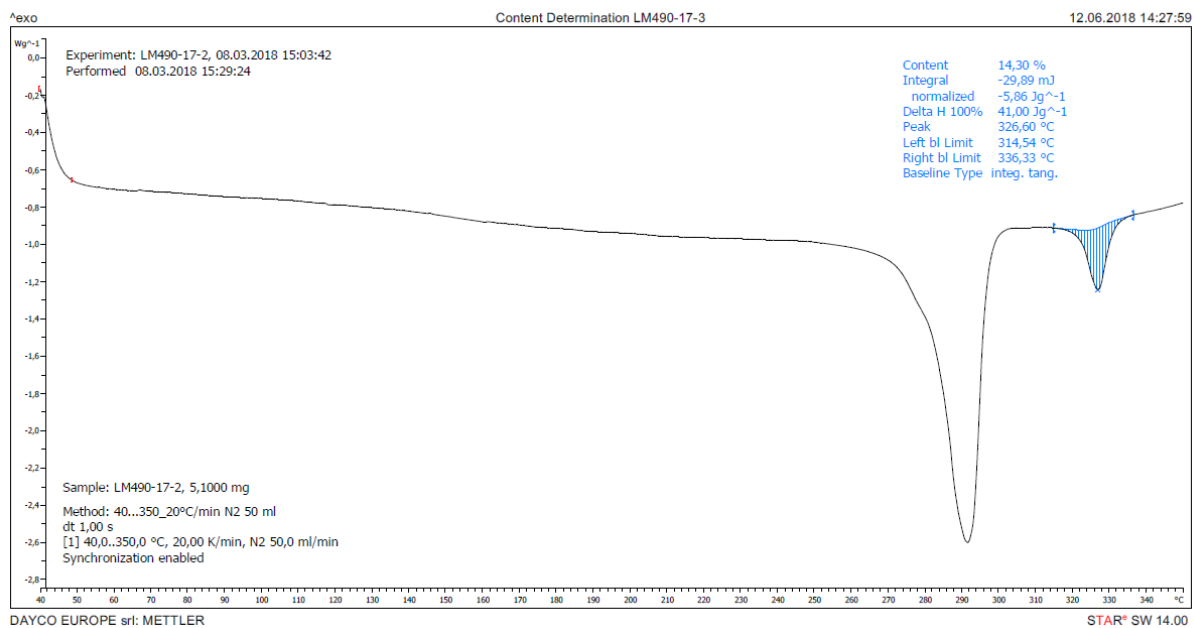


Figure 11.52: DSC measurement curve of sample LM490-17, from Group 3, obtained from Analysis 3, in which a content of 14,30% of PTFE was measured.

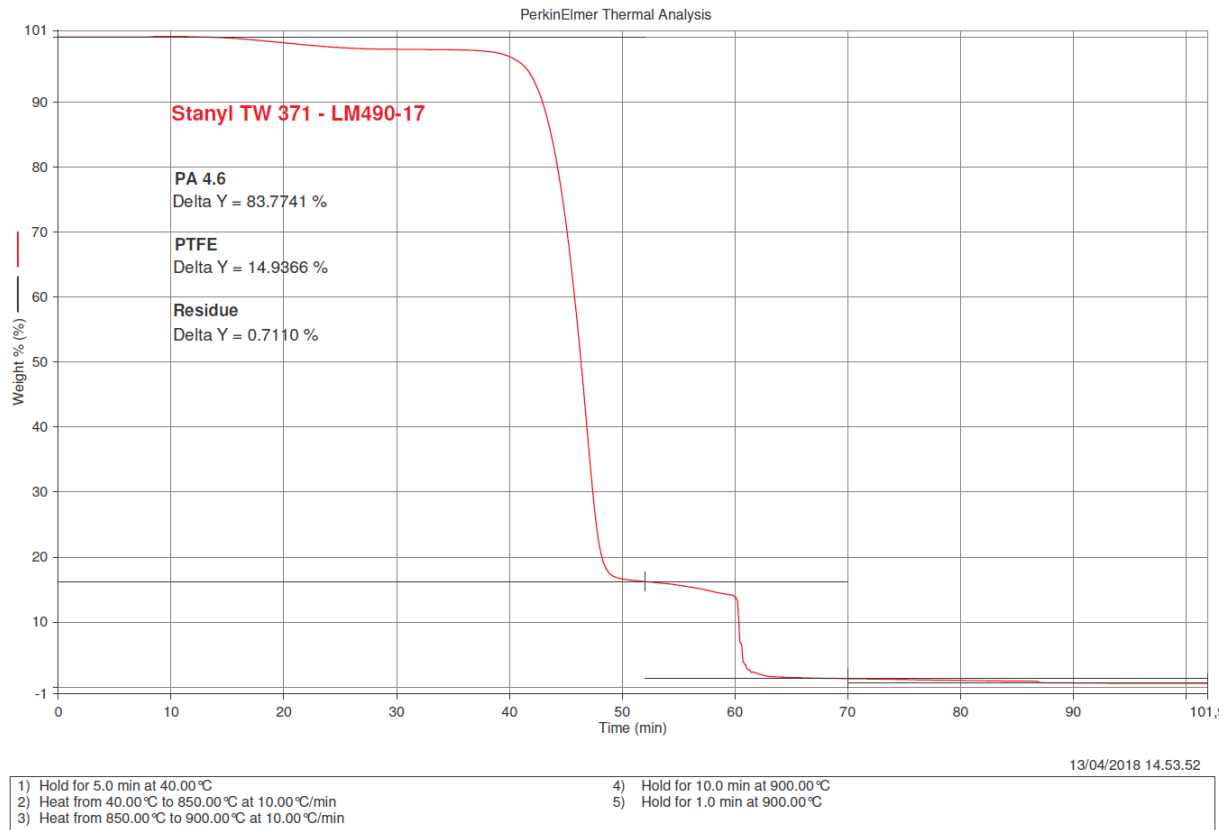


Figure 11.53: TGA measurement curve of sample LM490-17. The contents of PA46, PTFE and residue are, respectively, 83.7741%, 14.9366% and 0.7110%.

11.11. LM491-17

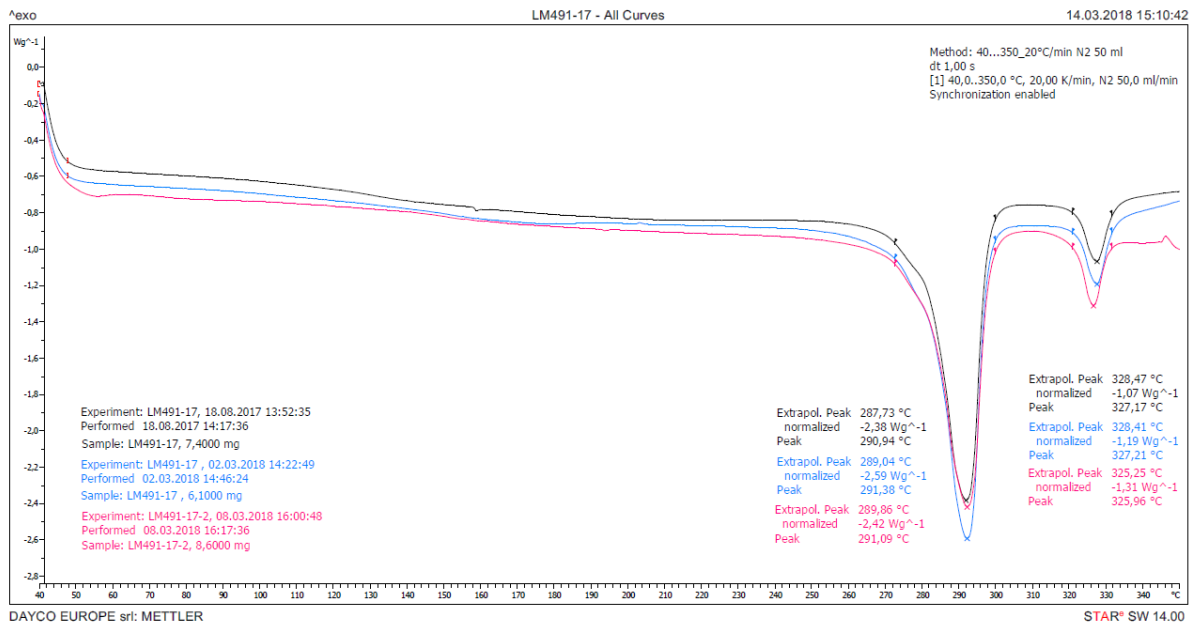


Figure 11.54: DSC measurements curves of spring bushing LM491-17 obtained from Analyses 1 (black), 2 (blue) and 3 (pink), using respectively samples from Groups 1, 2 and 3. All three curves exhibit two melting peaks and there aren't neither artifacts or other peaks that identify impurities. The first peak, with temperatures of 291,38°C, 290,94°C and 291,09°C, respectively, is compatible with PA46 (melting peak between 290 and 295°C); while the second peak, with temperatures of 327,21°C, 327,17°C and 325,96°C, is compatible with PTFE (melting peak between 325 and 335°C).

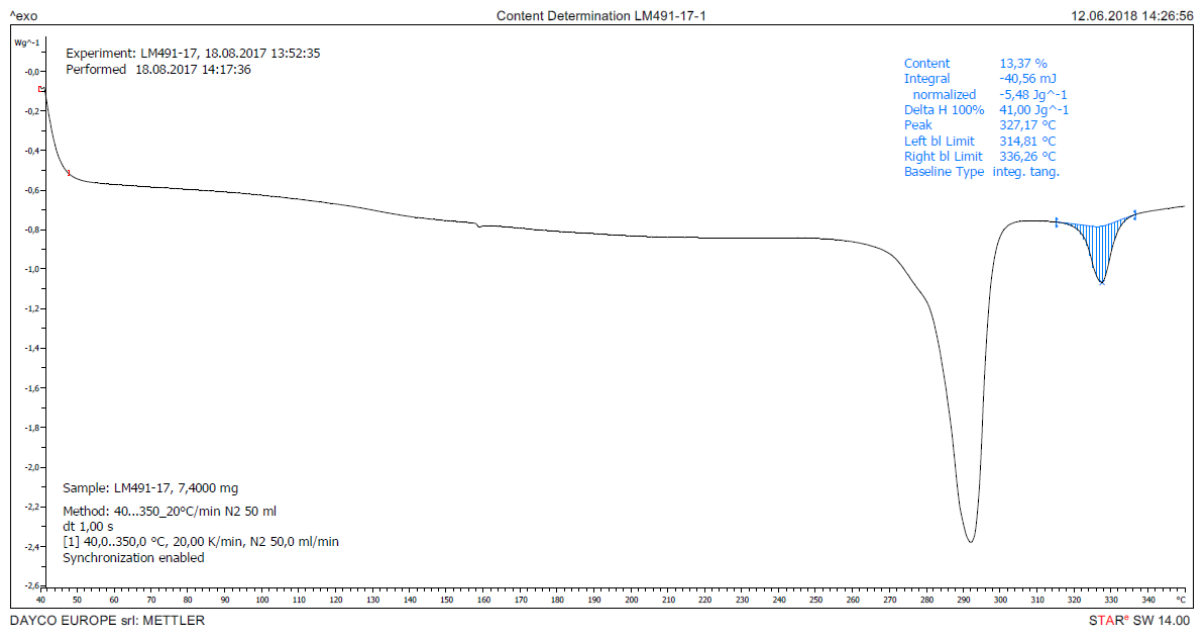


Figure 11.55: DSC measurement curve of sample LM491-17, from Group 1, obtained from Analysis 1, in which a content of 13,37% of PTFE was measured.

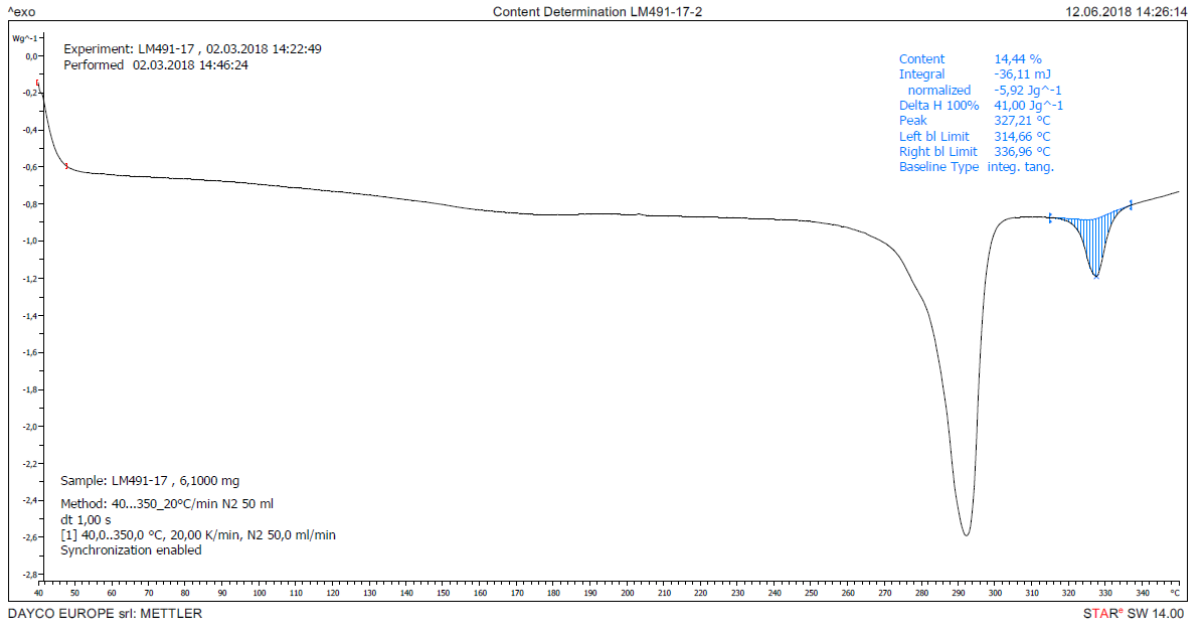


Figure 11.56: DSC measurement curve of sample LM491-17, from Group 2, obtained from Analysis 2, in which a content of 14,44% of PTFE was measured.

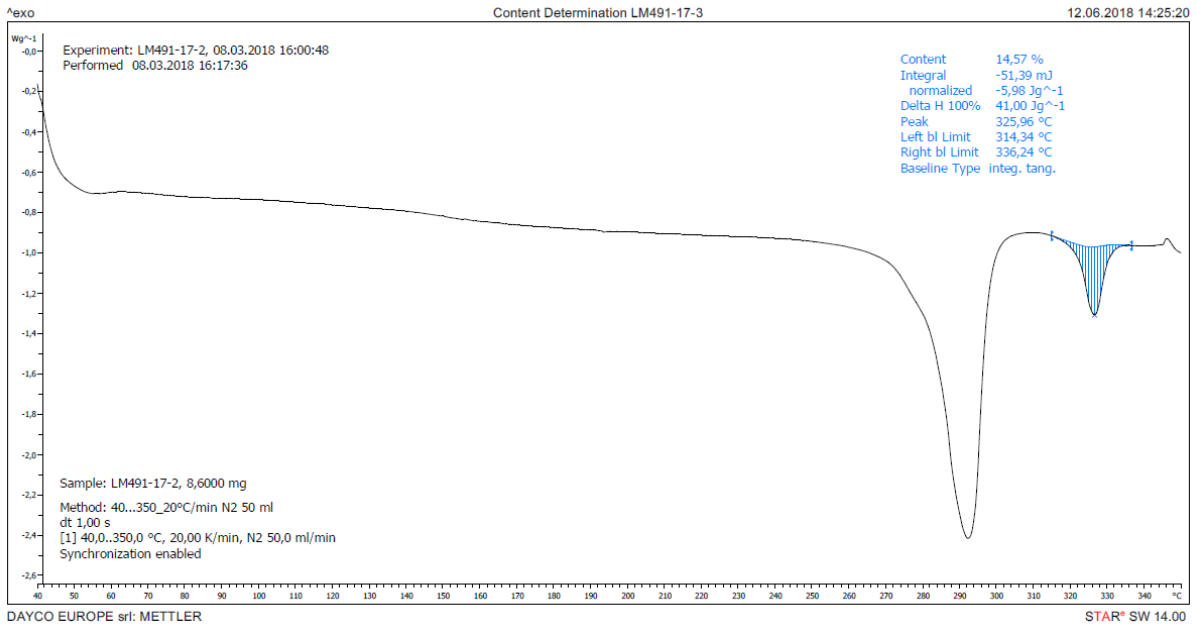


Figure 11.57: DSC measurement curve of sample LM491-17, from Group 3, obtained from Analysis 3, in which a content of 14,57% of PTFE was measured.

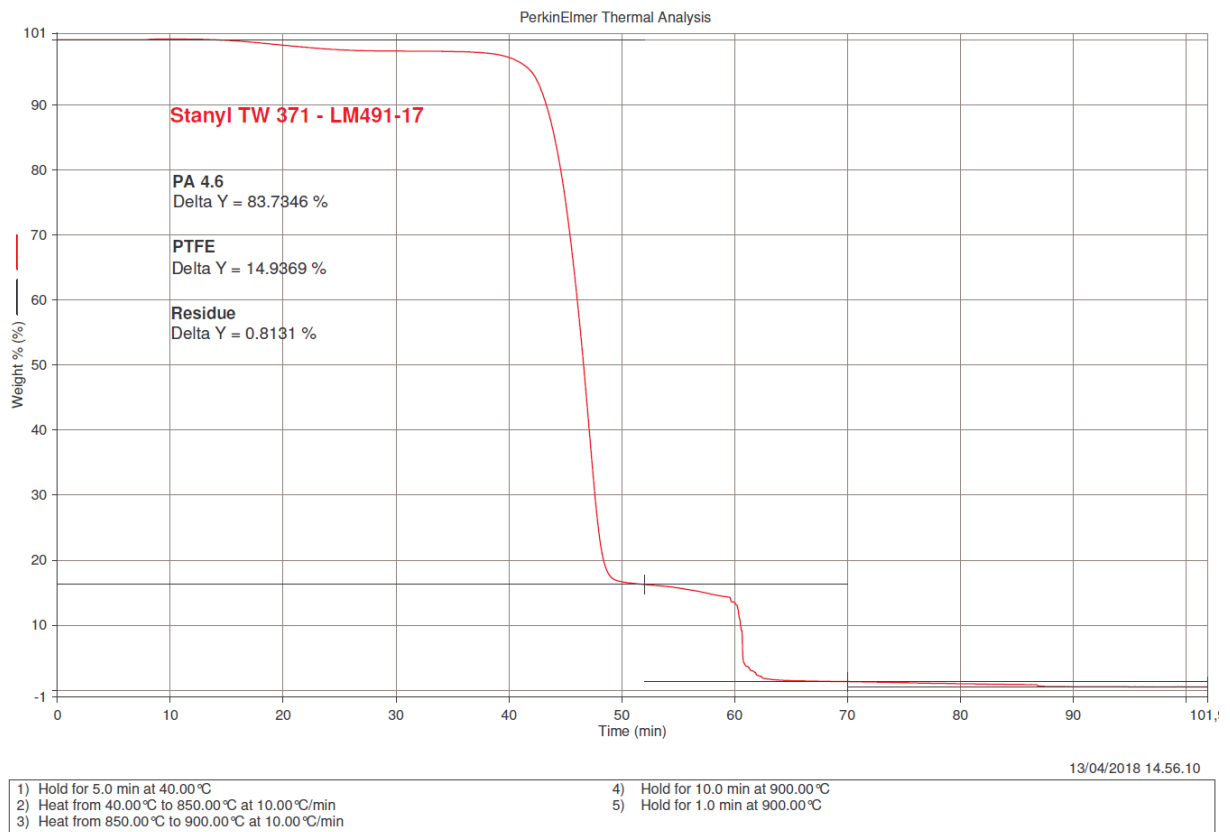


Figure 11.58: TGA measurement curve of sample LM491-17. The contents of PA46, PTFE and residue are, respectively, 83.7346%, 14.9369% and 0.8131%.

11.12. LM492-17

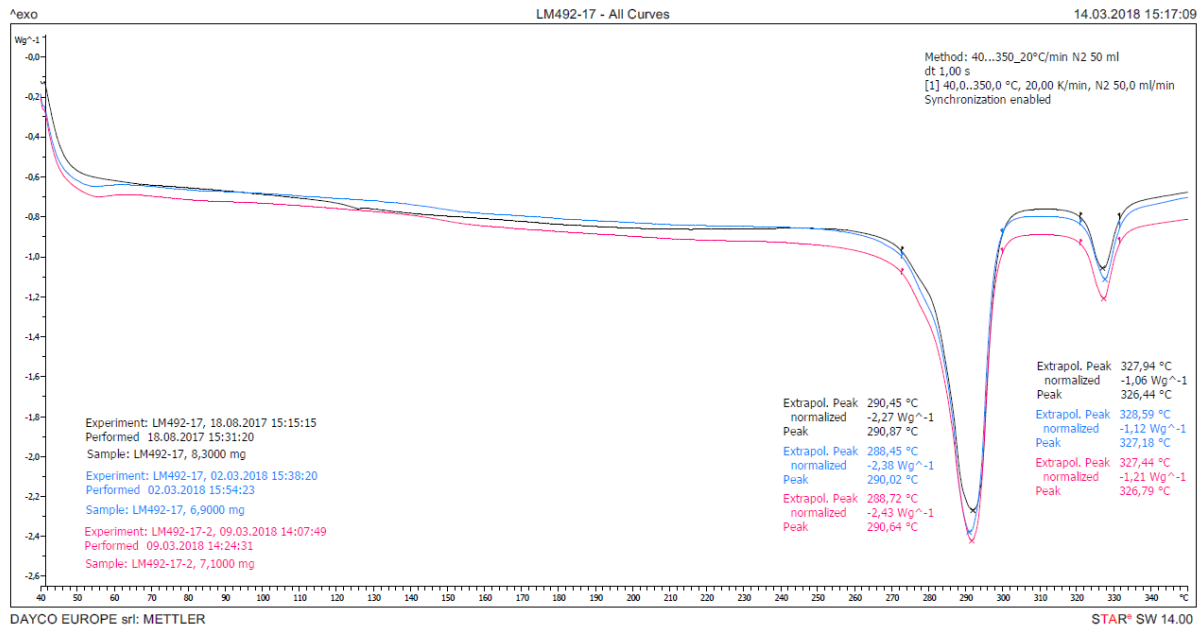


Figure 11.59: DSC measurements curves of spring bushing LM492-17 obtained from Analyses 1 (black), 2 (blue) and 3 (pink), using respectively samples from Groups 1, 2 and 3. All three curves exhibit two melting peaks and there aren't neither artifacts or other peaks that identify impurities. The first peak, with temperatures of 290,87°C, 290,02°C and 290,64°C, respectively, is compatible with PA46 (melting peak between 290 and 295°C); while the second peak, with temperatures of 326,44°C, 327,18°C and 326,79°C, is compatible with PTFE (melting peak between 325 and 335°C).

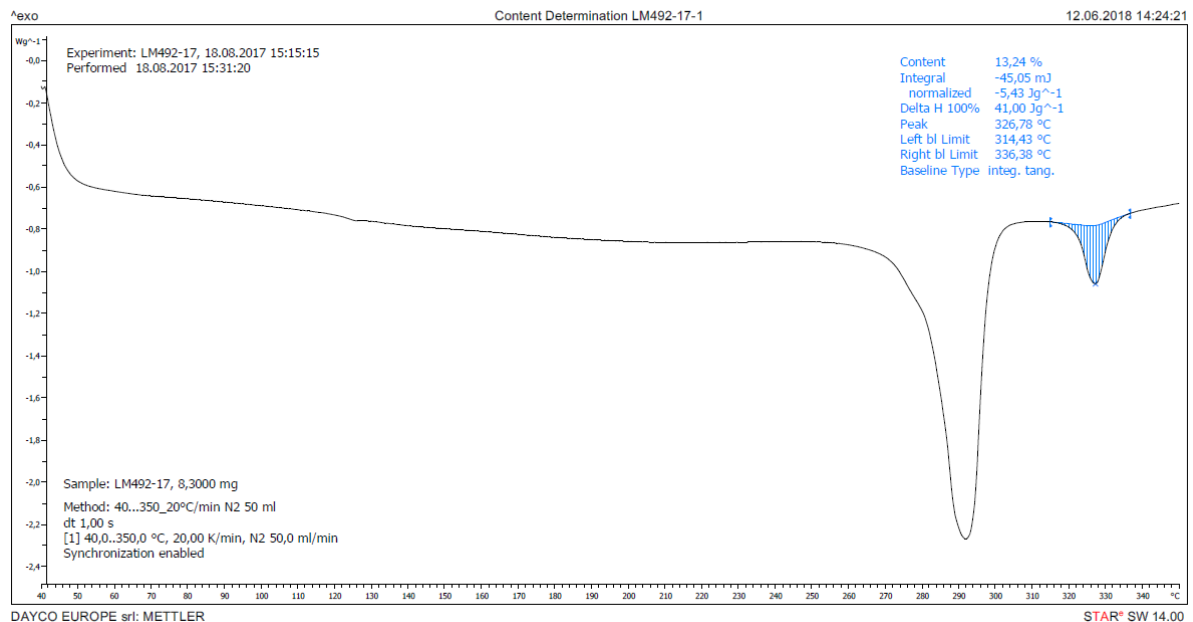


Figure 11.60: DSC measurement curve of sample LM492-17, from Group 1, obtained from Analysis 1, in which a content of 13,24% of PTFE was measured.

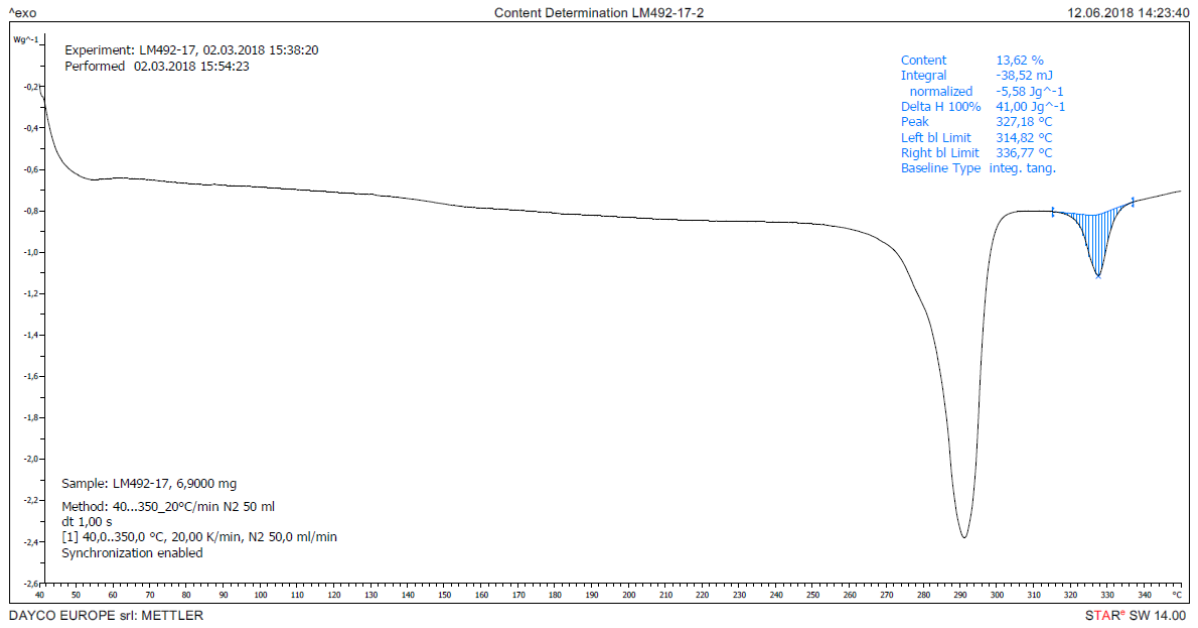


Figure 11.61: DSC measurement curve of sample LM492-17, from Group 2, obtained from Analysis 2, in which a content of 13,62% of PTFE was measured.

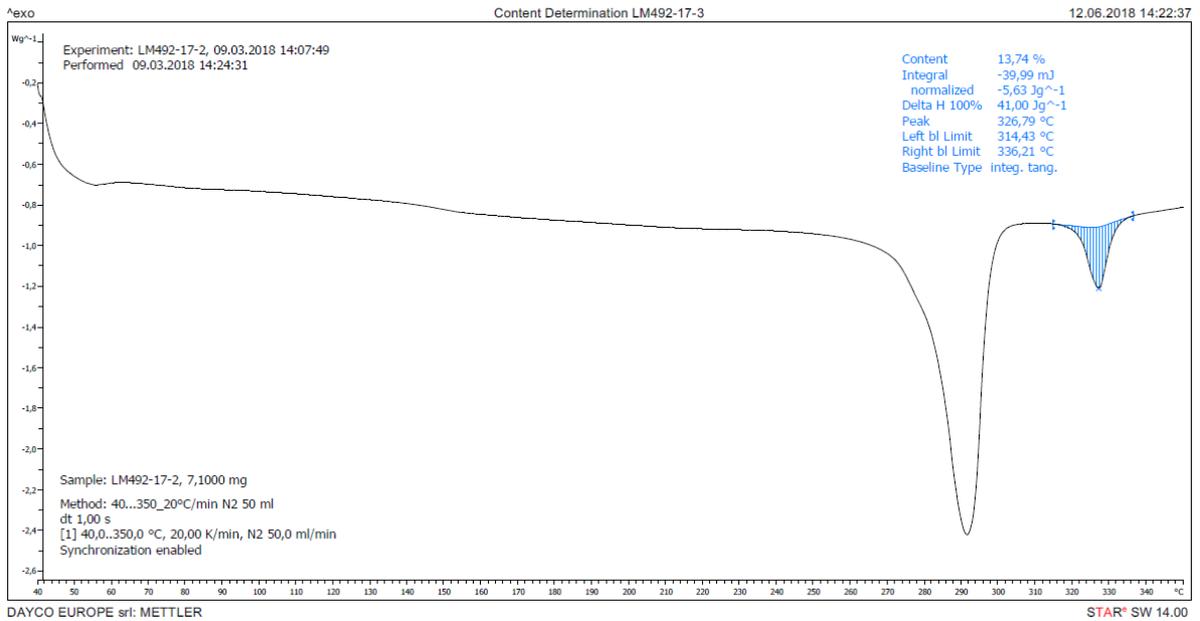


Figure 11.62: DSC measurement curve of sample LM492-17, from Group 3, obtained from Analysis 3, in which a content of 13,74% of PTFE was measured.

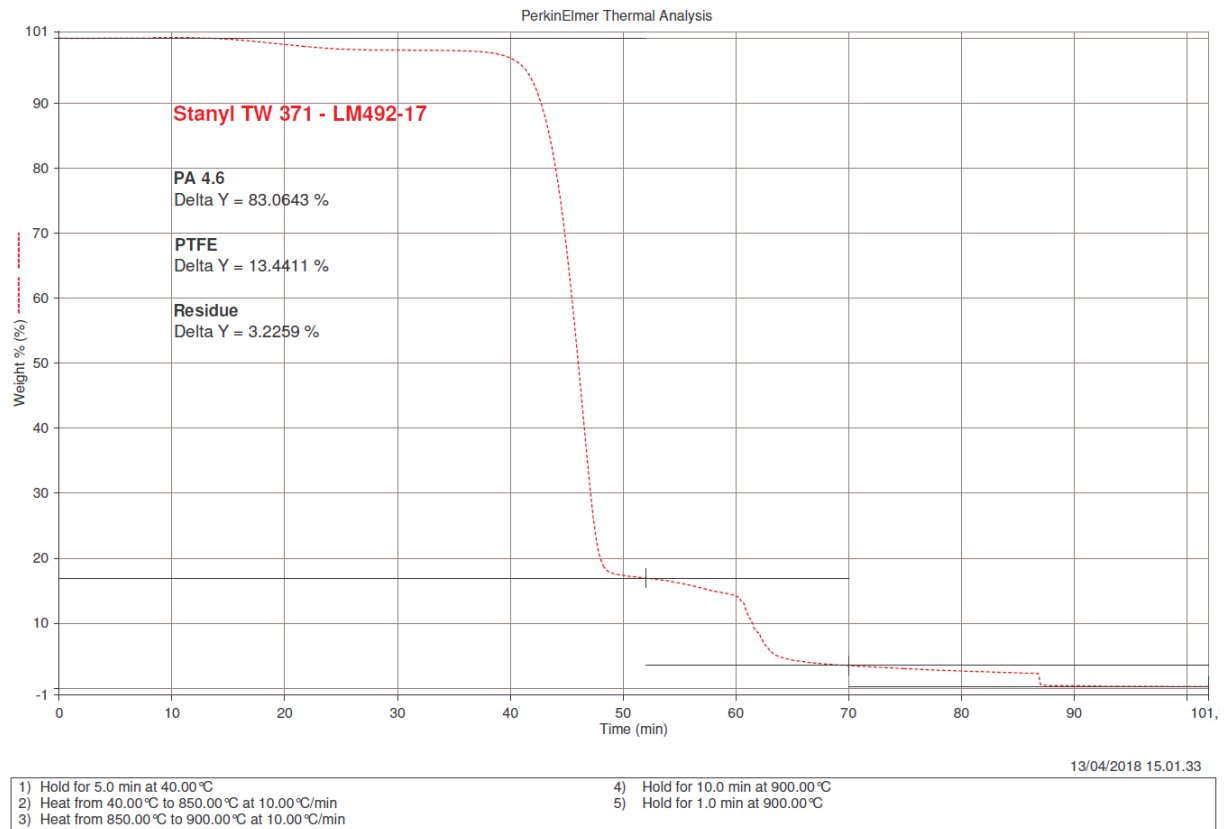


Figure 11.63: TGA measurement curve of sample LM492-17. The contents of PA46, PTFE and residue are, respectively, 83.0643%, 13.4411% and 3.2259%.

11.13. LM493-17

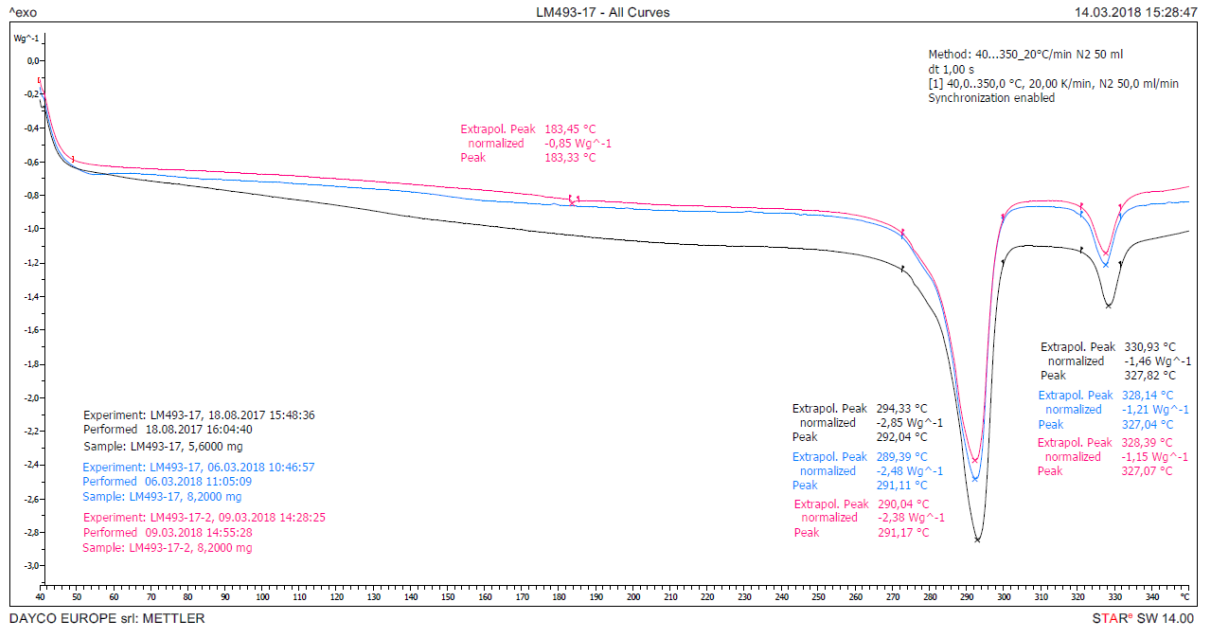


Figure 11.64: DSC measurements curves of spring bushing LM493-17 obtained from Analyses 1 (black), 2 (blue) and 3 (pink), using respectively samples from Groups 1, 2 and 3. All three curves exhibit two melting peaks and the one obtained from Analysis 3 presents also an endothermic peak with temperature of 183,33°C, caused by impurities. The first melting peak, with temperatures of 292,04°C, 291,11°C and 291,17°C, respectively, is compatible with PA46 (melting peak between 290 and 295°C); while the second peak, with temperatures of 327,82°C, 327,04°C and 327,07°C, is compatible with PTFE (melting peak between 325 and 335°C).

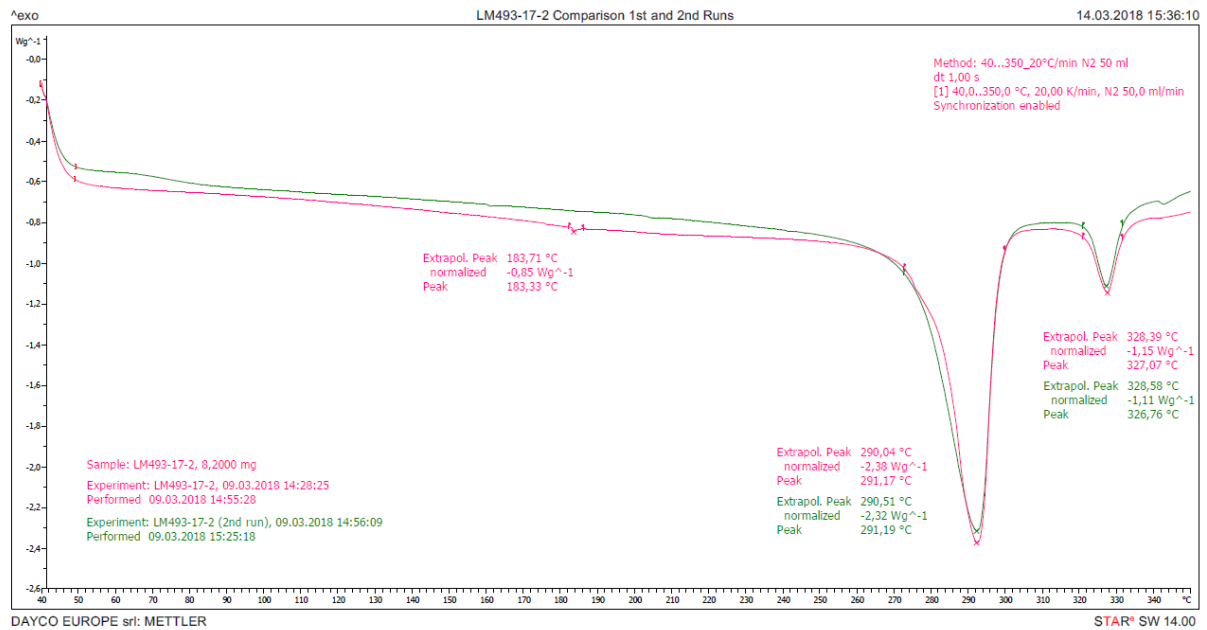


Figure 11.65: DSC measurement curves of spring bushing LM493-17 obtained in the first (pink) and second (green) runs of Analysis 3. The second run was performed due to the presence of an endothermic peak with temperature of 183,33°C, caused by impurities in the first run. The curve obtained from the second run exhibits the two melting peaks, and there aren't neither artifacts or other peaks that identify impurities. The first peak, with temperatures of 291,17°C and 291,19°C, respectively, is compatible with PA46 (melting peak between 290 and 295°C); while the second peak, with temperatures of 327,07°C and 326,76°C, is compatible with PTFE (melting peak between 325 and 335°C).

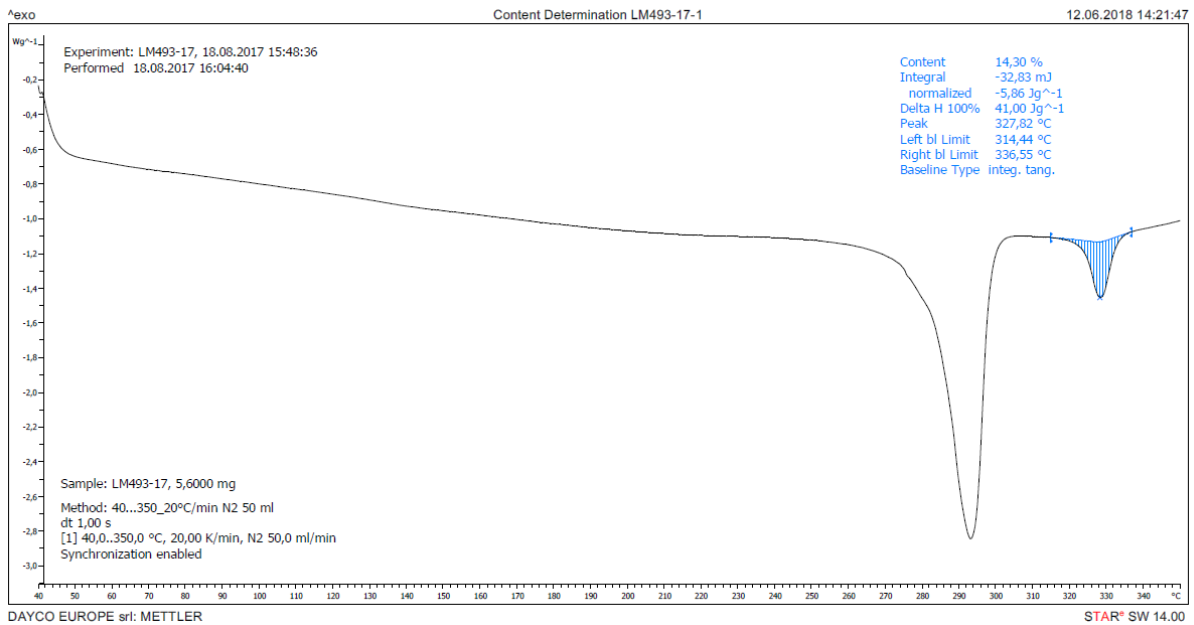


Figure 11.66: DSC measurement curve of sample LM493-17, from Group 1, obtained from Analysis 1, in which a content of 14,30% of PTFE was measured.

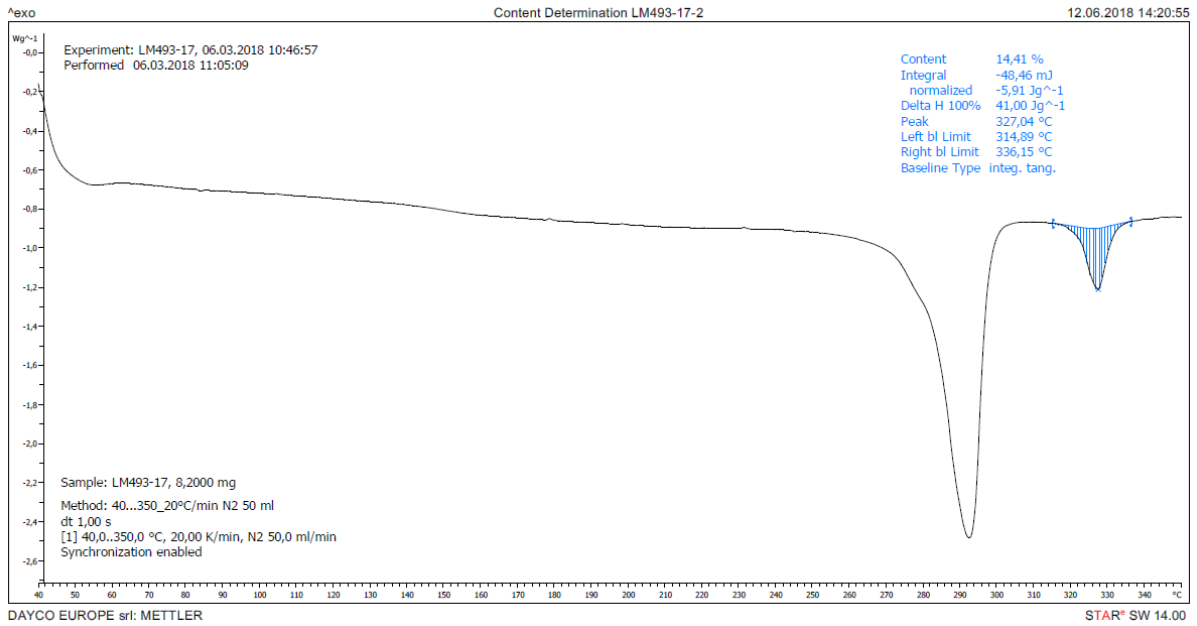


Figure 11.67: DSC measurement curve of sample LM493-17, from Group 2, obtained from Analysis 2, in which a content of 14,41% of PTFE was measured.

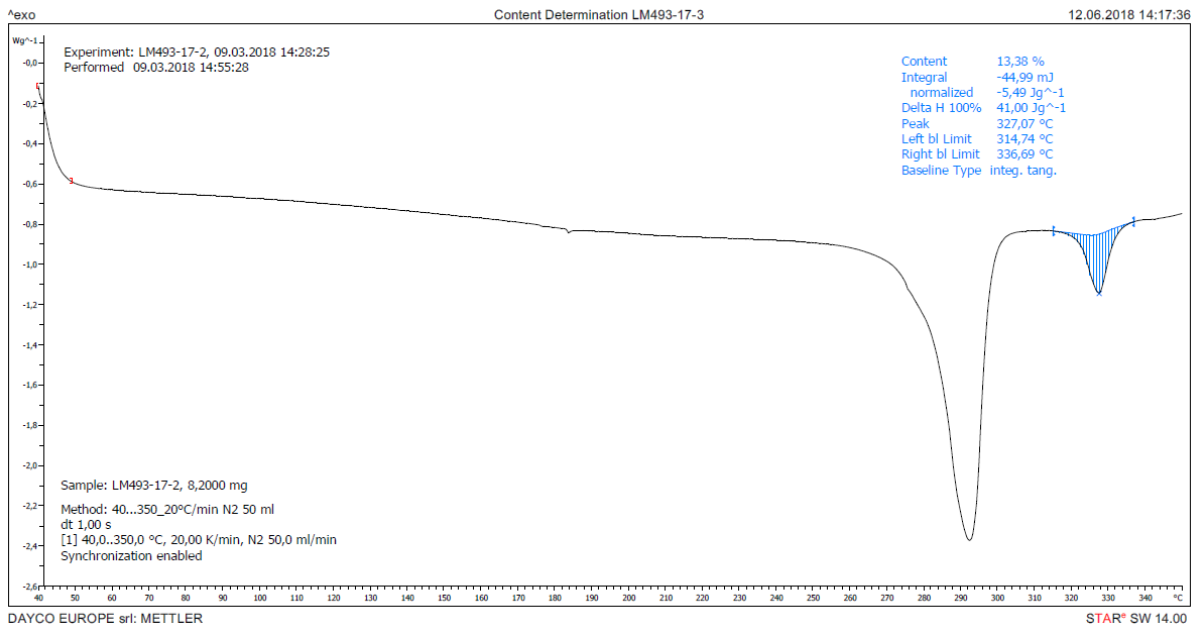


Figure 11.68: DSC measurement curve of sample LM493-17, from Group 3, obtained from Analysis 3, in which a content of 13,38% of PTFE was measured.

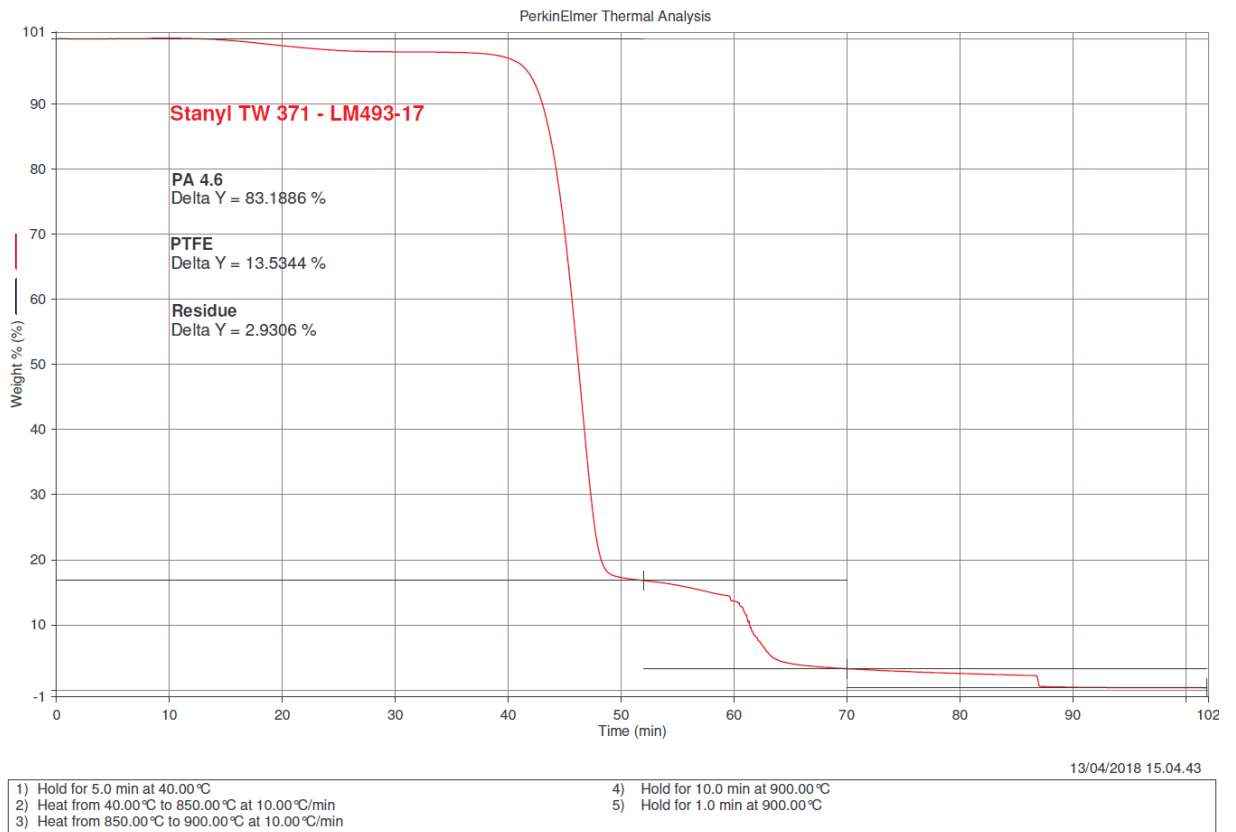


Figure 11.69: TGA measurement curve of sample LM493-17. The contents of PA46, PTFE and residue are, respectively, 83.1886%, 13.5344% and 2.9306%.

11.14. LM494-17

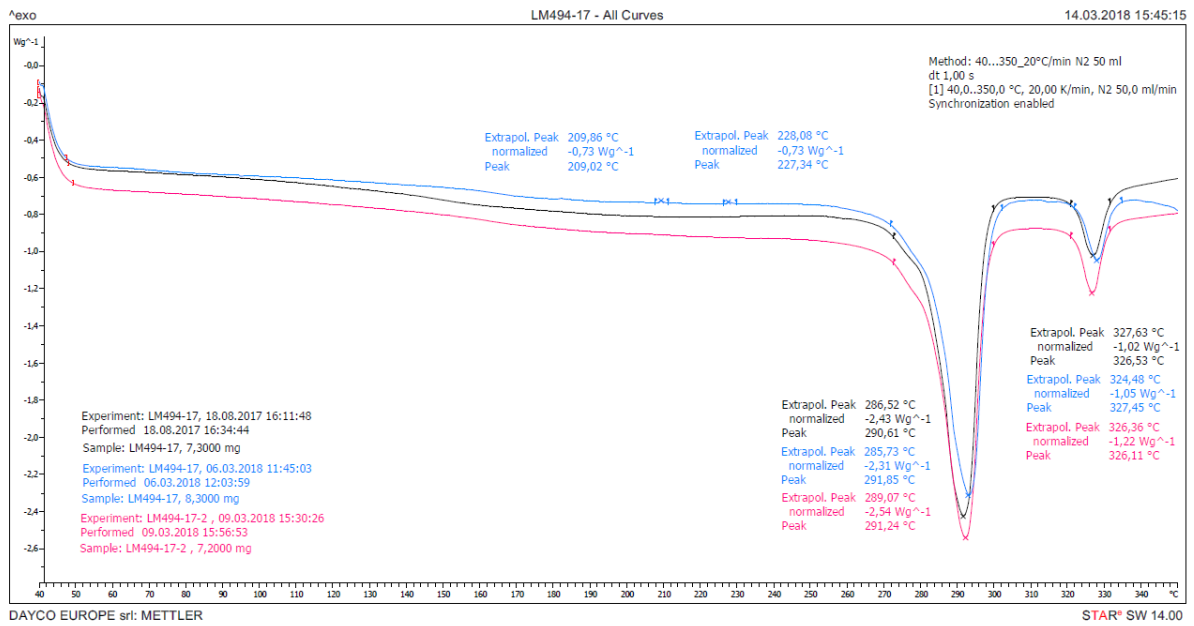


Figure 11.70: DSC measurements curves of spring bushing LM494-17 obtained from Analyses 1 (black), 2 (blue) and 3 (pink), using respectively samples from Groups 1, 2 and 3. All three curves exhibit two melting peaks and the one obtained from Analysis 2 presents also two exothermic peaks with temperatures of 209,02°C and 227,34°C, caused by impurities. The first melting peak, with temperatures of 290,61°C, 291,85°C and 291,24°C, respectively, is compatible with PA46 (melting peak between 290 and 295°C); while the second melting peak, with temperatures of 326,53°C, 327,45°C and 326,11°C, is compatible with PTFE (melting peak between 325 and 335°C).

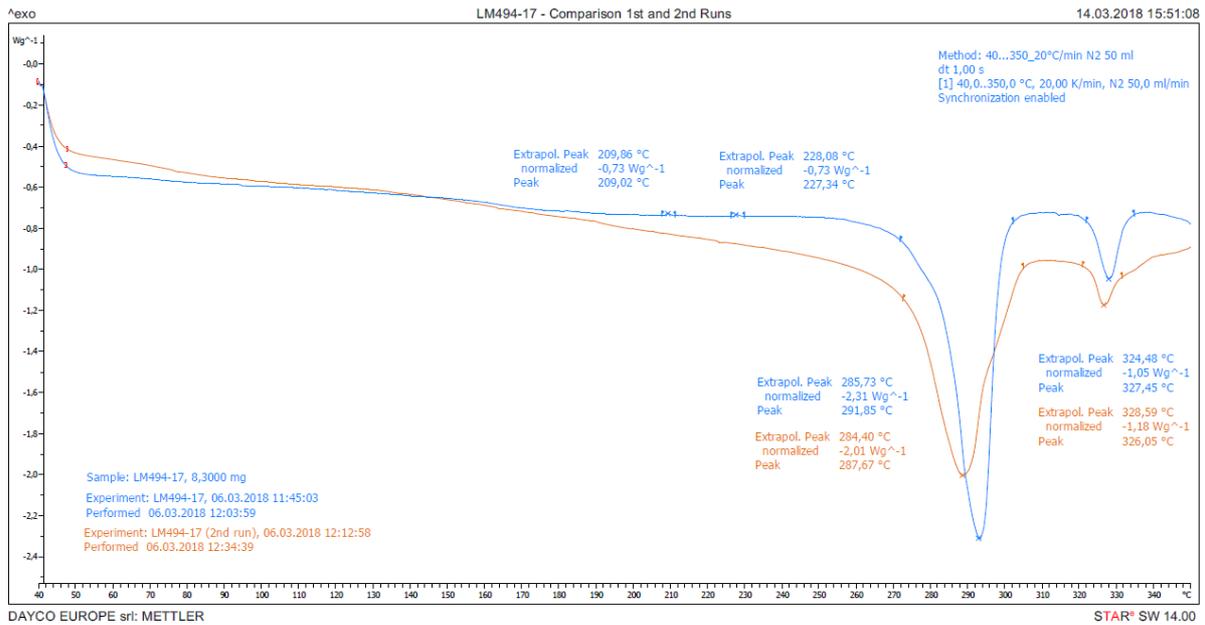


Figure 11.71: DSC measurement curves of spring bushing LM494-17 obtained in the first (blue) and second (orange) runs of Analysis 2. The second run was performed due to the presence of two exothermic peaks with temperatures of 209,02°C and 227,34°C, caused by impurities in the first run. The curve obtained from the second run exhibits the two melting peaks, and there aren't neither artifacts or other peaks that identify impurities, however its baseline shifts towards the endothermic zone due to the scape of the sample from the crucible through the hole on the lid. The first peak, with temperatures of 291,85°C and 287,67°C, respectively, is compatible with PA46 (melting peak between 290 and 295°C) in the 1st run and slightly below in the 2nd run; while the second peak, with temperatures of 327,45°C and 326,05°C, is compatible with PTFE (melting peak between 325 and 335°C).

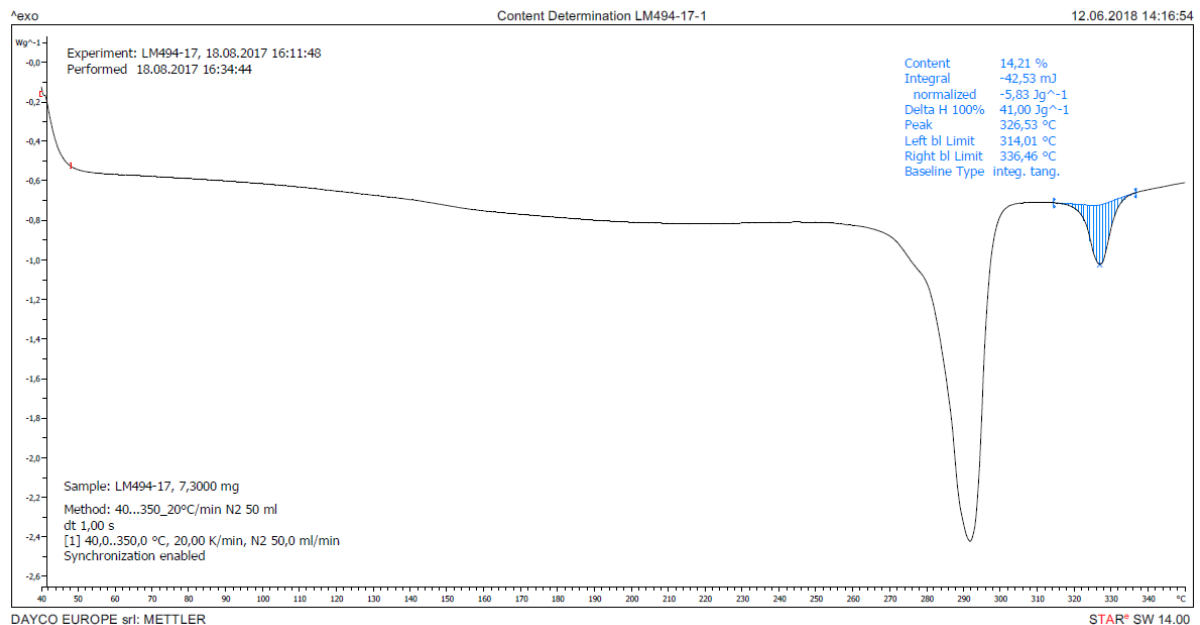


Figure 11.72: DSC measurement curve of sample LM494-17, from Group 1, obtained from Analysis 1, in which a content of 14,21% of PTFE was measured.

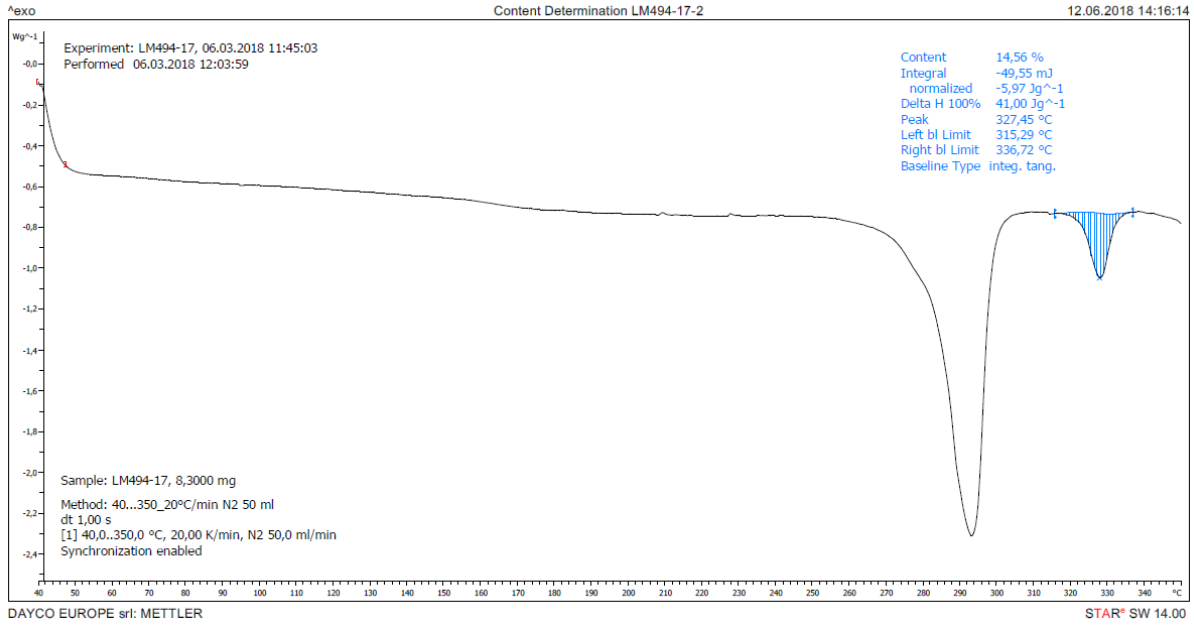


Figure 11.73: DSC measurement curve of sample LM494-17, from Group 2, obtained from Analysis 2, in which a content of 14,56% of PTFE was measured.

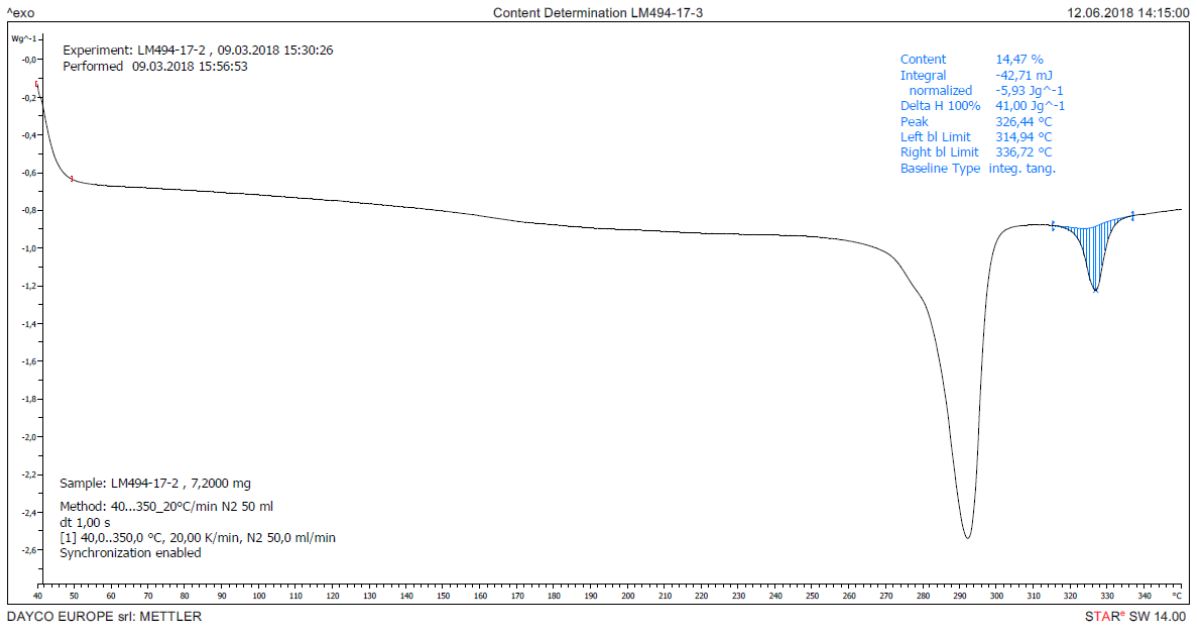


Figure 11.74: DSC measurement curve of sample LM494-17, from Group 3, obtained from Analysis 3, in which a content of 14,47% of PTFE was measured.

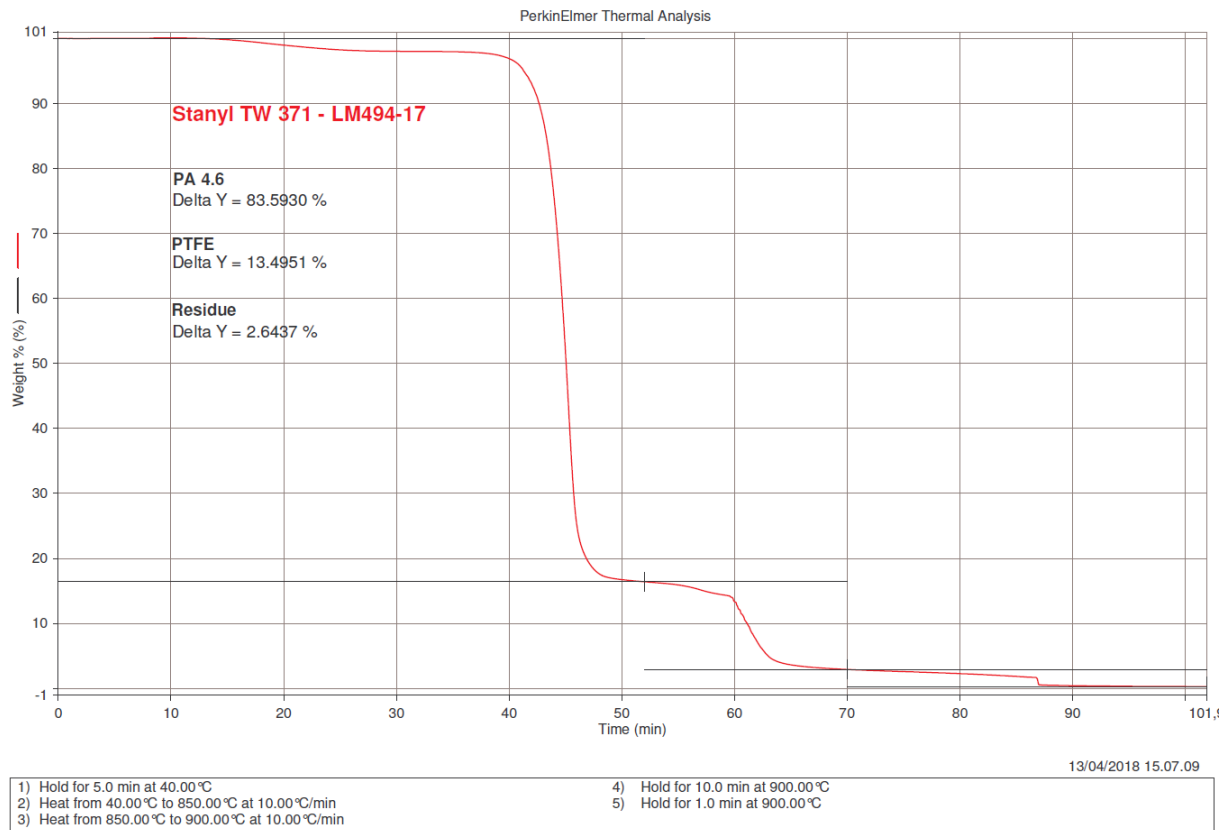


Figure 11.75: TGA measurement curve of sample LM494-17. The contents of PA46, PTFE and residue are, respectively, 83.5930%, 13.4951% and 2.6437%.

11.15. LM495-17

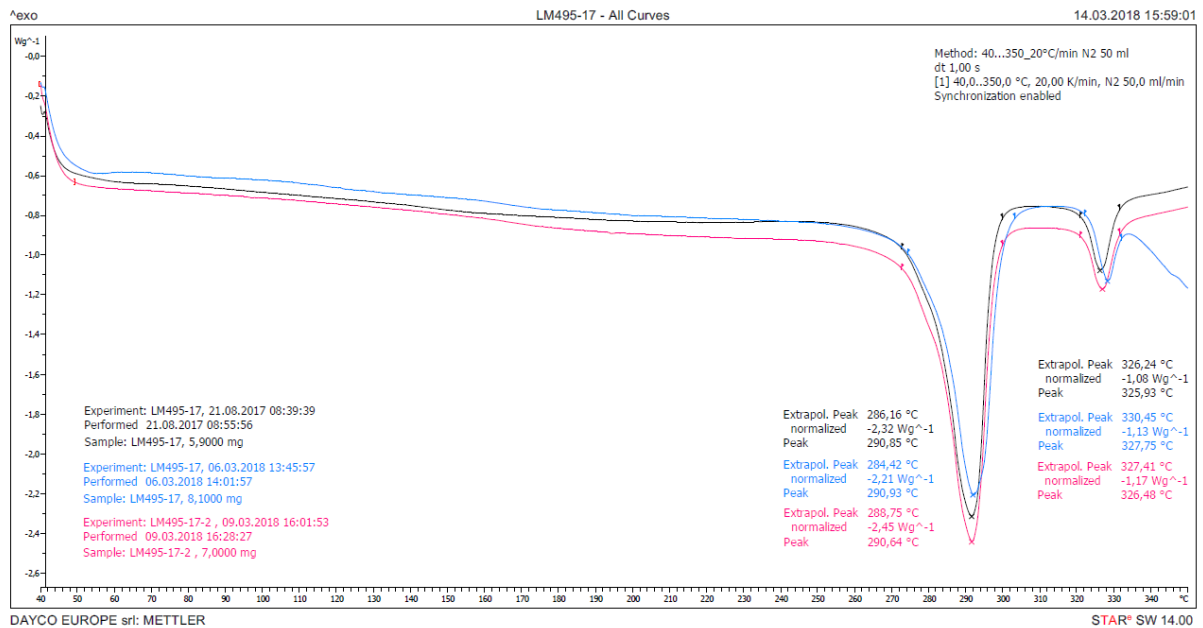


Figure 11.76: DSC measurements curves of spring bushing LM495-17 obtained from Analyses 1 (black), 2 (blue) and 3 (pink), using respectively samples from Groups 1, 2 and 3. All three curves exhibit two melting peaks and there aren't other peaks that identify impurities. However, the curve from Analysis 2 exhibits some irregularities at the final part due to the scape of the material from the crucible through the hole on the lid. The first peak, with temperatures of 290,85°C, 290,93°C and 290,64°C, respectively, is compatible with PA46 (melting peak between 290 and 295°C); while the second peak, with temperatures of 325,93°C, 327,75°C and 326,48°C, is compatible with PTFE (melting peak between 325 and 335°C).

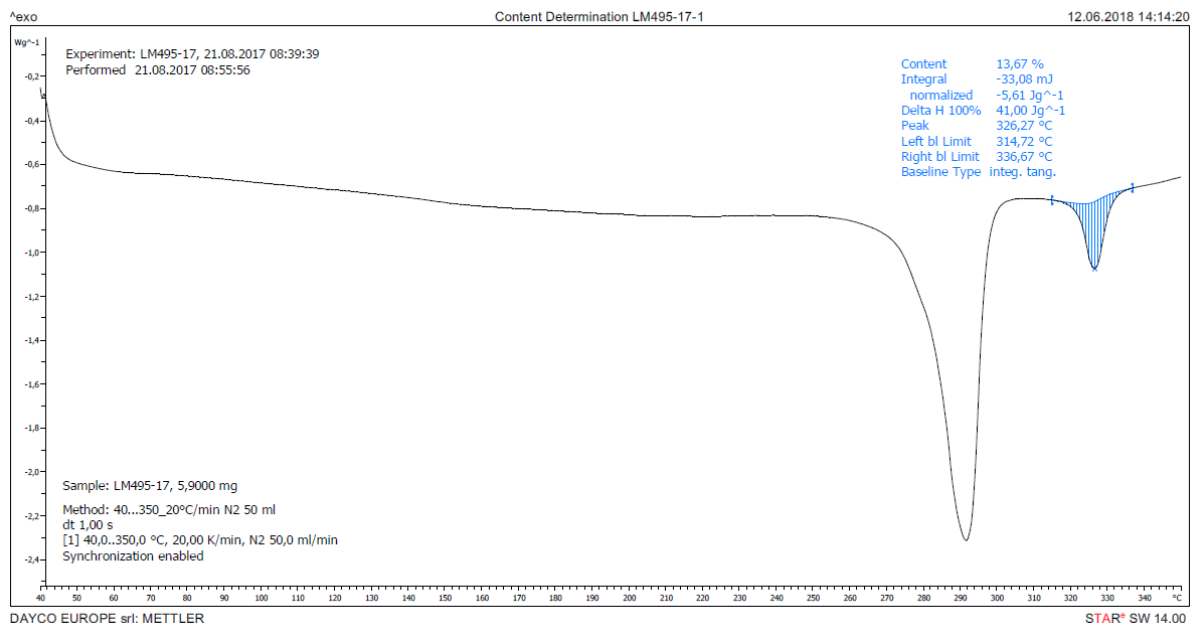


Figure 11.77: DSC measurement curve of sample LM495-17, from Group 1, obtained from Analysis 1, in which a content of 13,67% of PTFE was measured.

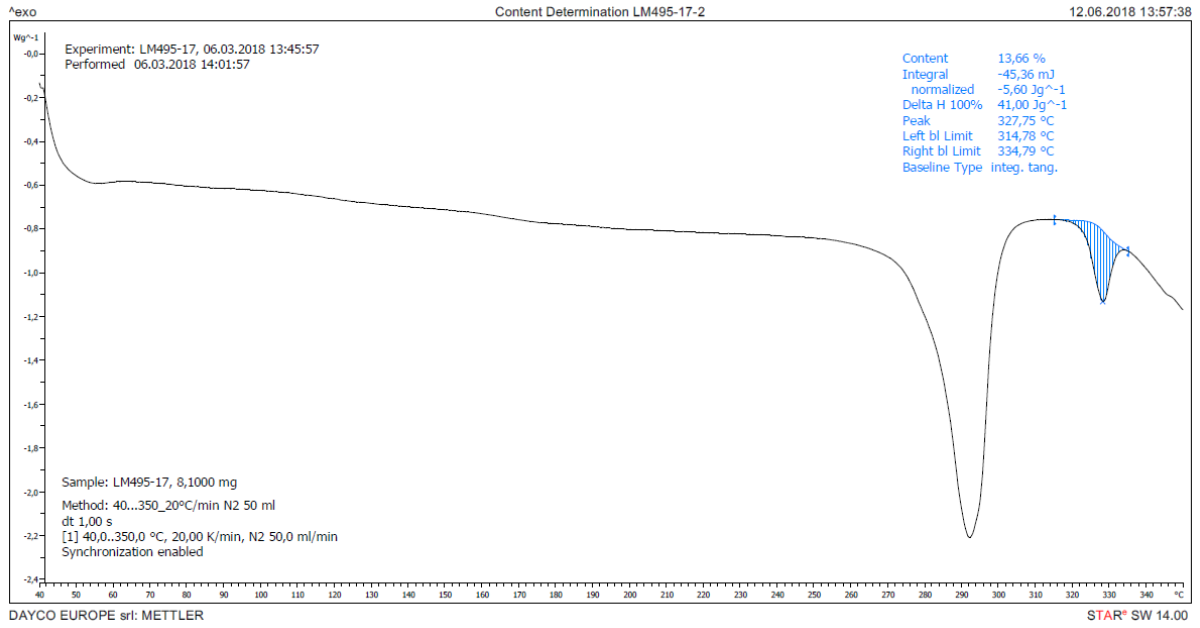


Figure 11.78: DSC measurement curve of sample LM495-17, from Group 2, obtained from Analysis 2, in which a content of 13,66% of PTFE was measured.

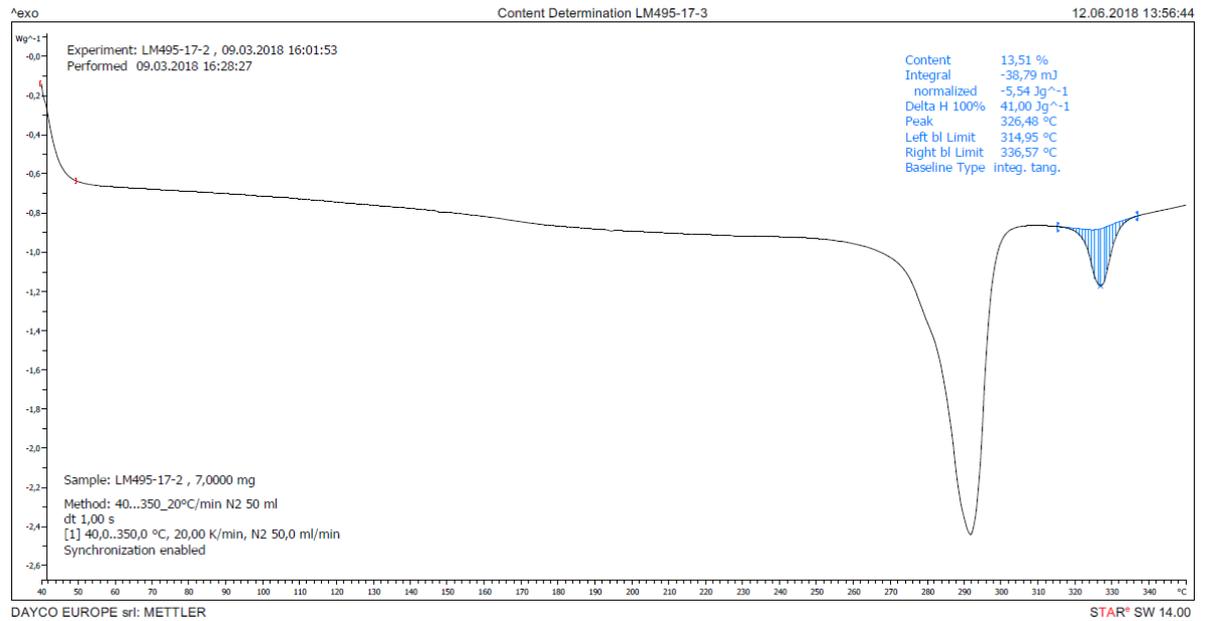


Figure 11.79: DSC measurement curve of sample LM495-17, from Group 3, obtained from Analysis 3, in which a content of 13,51% of PTFE was measured.

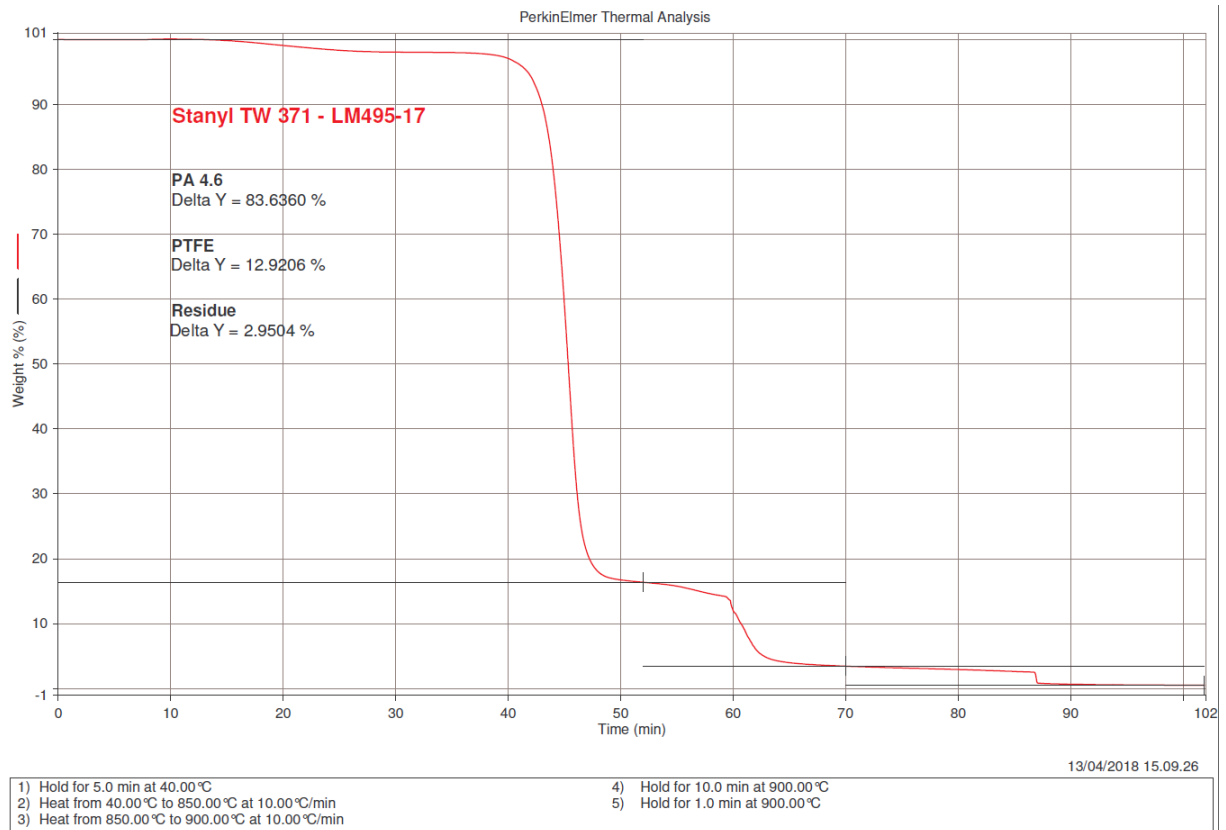


Figure 11.80: TGA measurement curve of sample LM495-17. The contents of PA46, PTFE and residue are, respectively, 83.6360%, 12.9206% and 2.9504%.

11.16. LM496-17

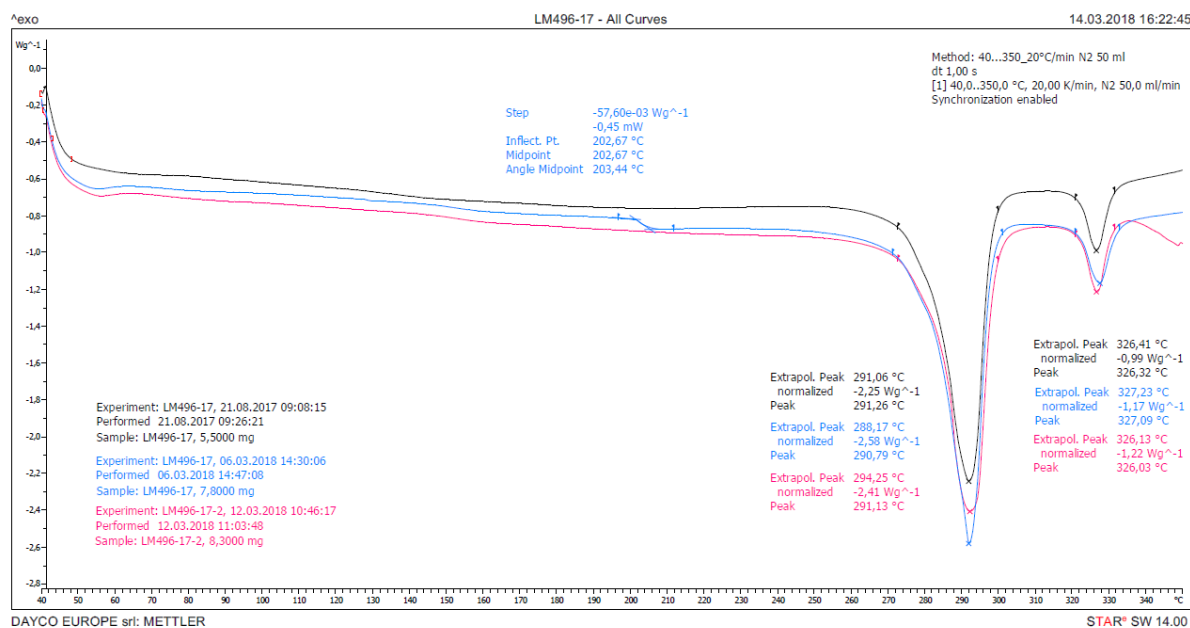


Figure 11.81: DSC measurements curves of spring bushing LM496-17 obtained from Analyses 1 (black), 2 (blue) and 3 (pink), using respectively samples from Groups 1, 2 and 3. All three curves exhibit two melting peaks and there aren't other peaks that identify impurities. However, the curve from Analysis 2 exhibits a step like effect with a midpoint temperature of 202,67°C, that is not compatible with the T_g range of PA46 and PTFE. This step may be an artifact due to a deformation of the crucible caused by the vapor pressure of the sample. In addition, there are some irregularities at the final part of the curve obtained from Analysis 3, caused by the scape of the material from the crucible through the hole on the lid. The first melting peak, with temperatures of 291,26°C, 290,79°C and 291,13°C, respectively, is compatible with PA46 (melting peak between 290 and 295°C); while the second peak, with temperatures of 326,32°C, 327,09°C and 326,03°C, is compatible with PTFE (melting peak between 325 and 335°C).

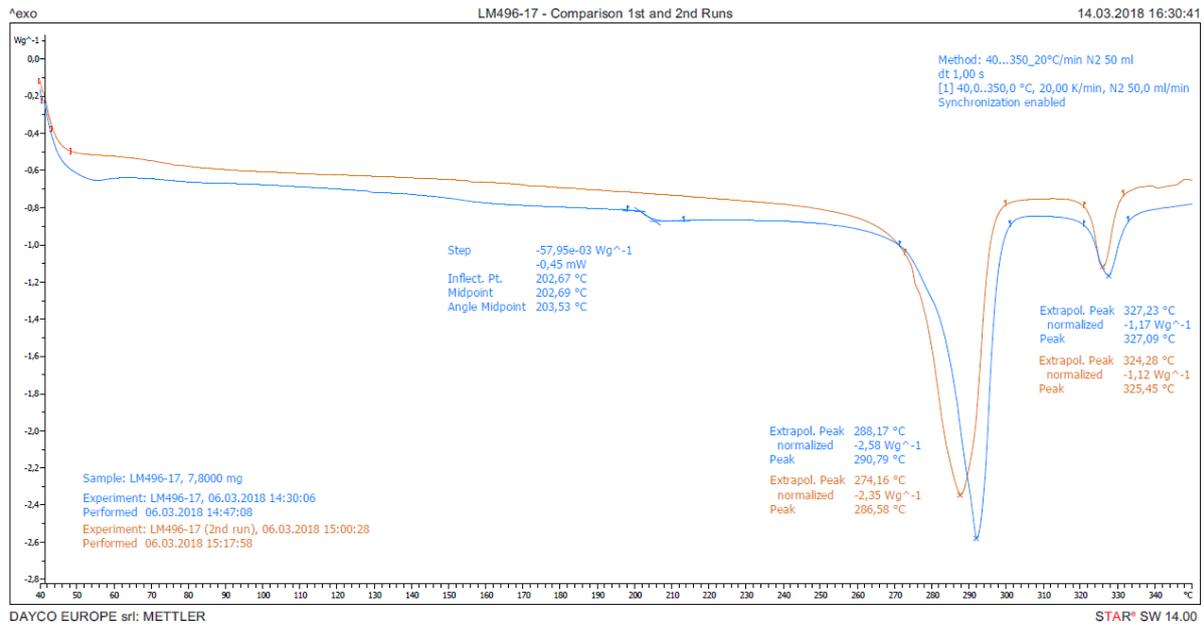


Figure 11.82: DSC measurement curves of spring bushing LM496-17 obtained in the first (blue) and second (orange) runs of Analysis 2. The second run was performed due to the presence of a step like effect with a midpoint temperature of 202,69 $^{\circ}C$ in the first run, that was interpreted as an artifact caused by the deformation of the crucible due to the vapor pressure of the sample. In the second run, it is possible to see only the two melting peaks, that shift significantly to lower temperatures. The first peak, with temperatures of 290,79 $^{\circ}C$ and 286,58 $^{\circ}C$, respectively, is compatible with PA46 (melting peak between 290 and 295 $^{\circ}C$) only in the 1st run, and it is slightly below in the 2nd one; while the second peak, with temperatures of 327,09 $^{\circ}C$ and 325,45 $^{\circ}C$, is compatible with PTFE (melting peak between 325 and 335 $^{\circ}C$).

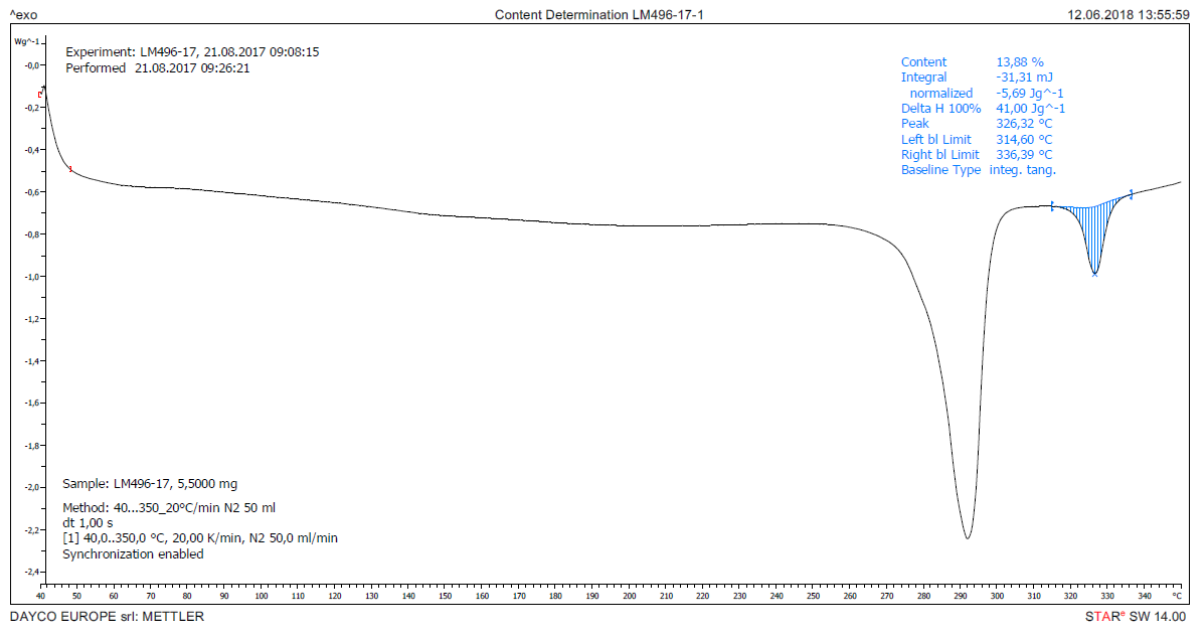


Figure 11.83: DSC measurement curve of sample LM496-17, from Group 1, obtained from Analysis 1, in which a content of 13,88% of PTFE was measured.

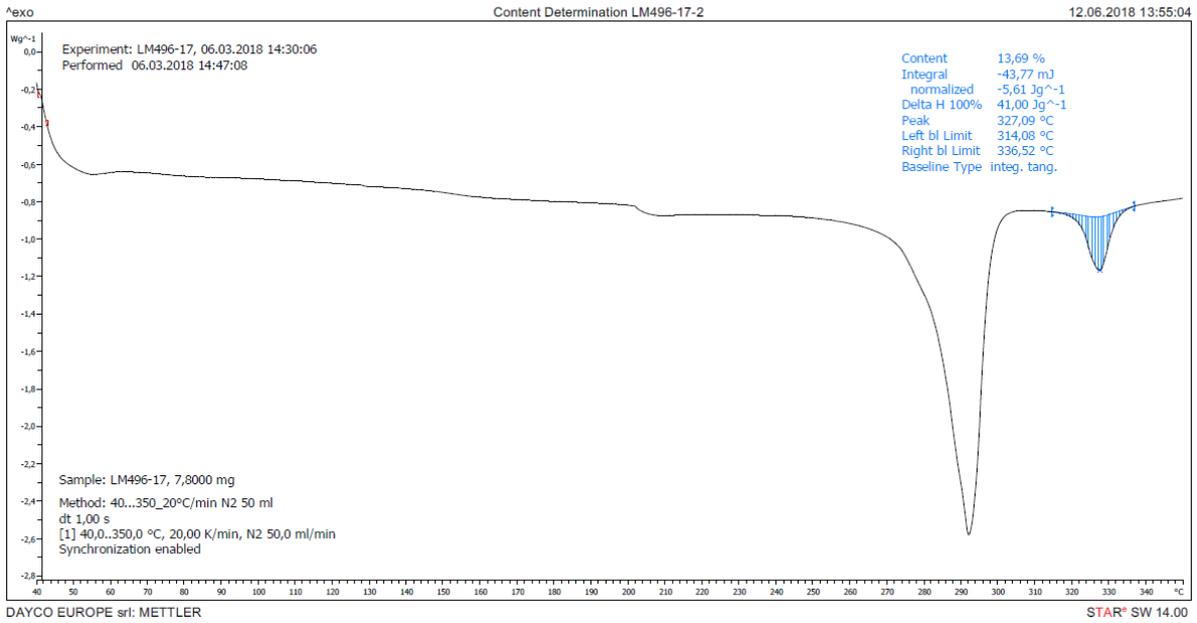


Figure 11.84: DSC measurement curve of sample LM496-17, from Group 2, obtained from Analysis 2, in which a content of 13,69% of PTFE was measured.

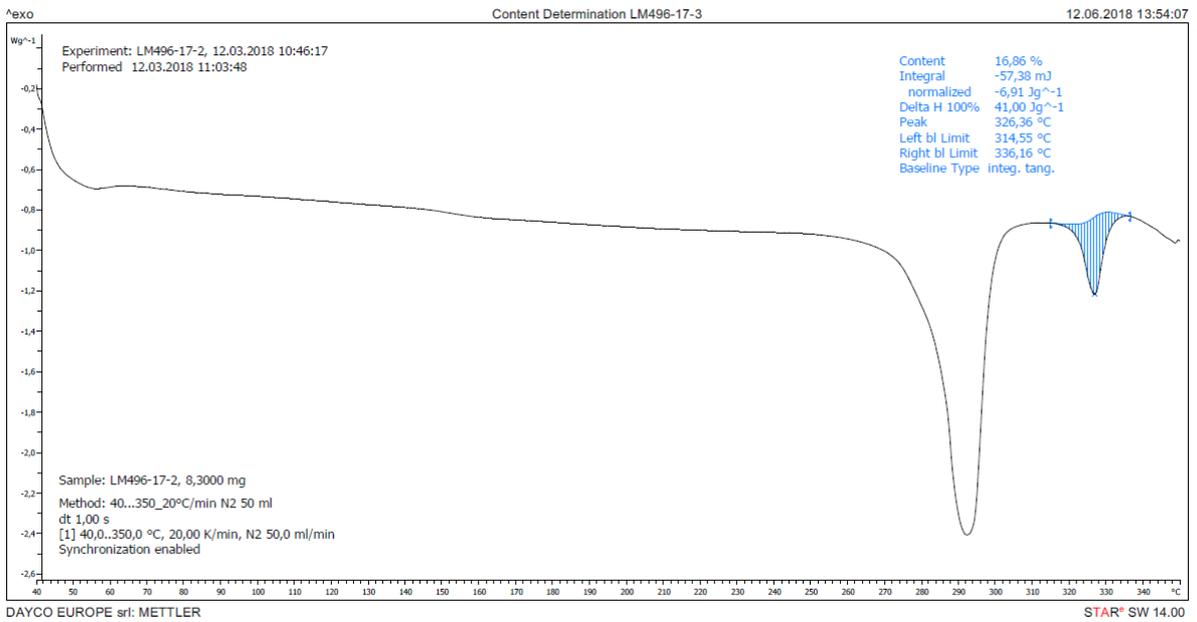


Figure 11.85: DSC measurement curve of sample LM496-17, from Group 3, obtained from Analysis 3, in which a content of 16,86% of PTFE was measured.

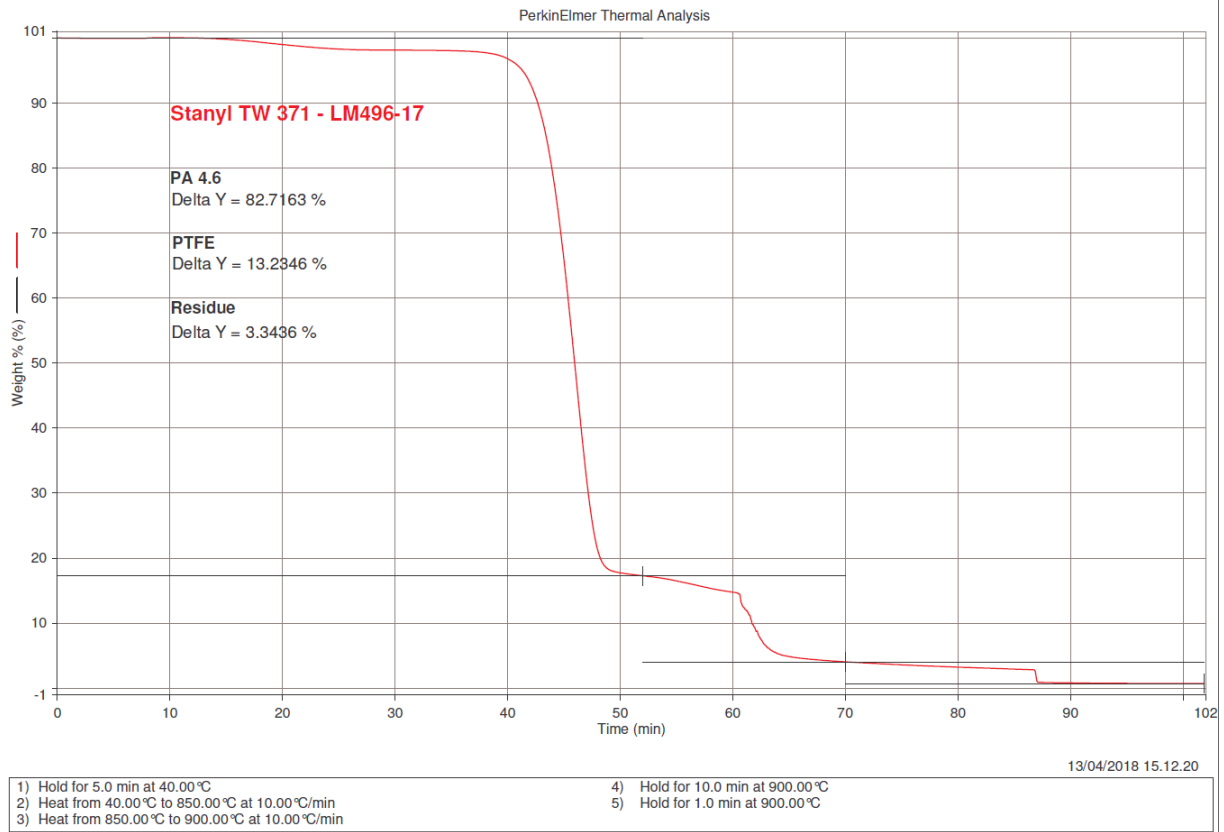


Figure 11.86: TGA measurement curve of sample LM496-17. The contents of PA46, PTFE and residue are, respectively, 82.7163%, 13.2346% and 3.3436%.

11.17. LM497-17

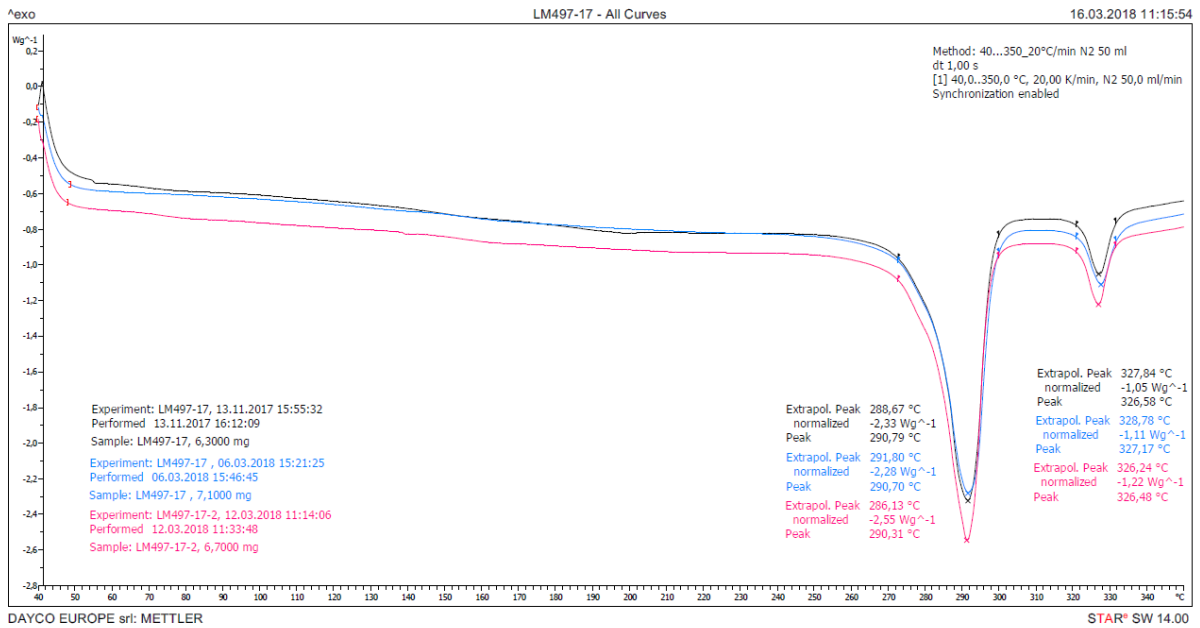


Figure 11.87: DSC measurements curves of spring bushing LM497-17 obtained from Analyses 1 (black), 2 (blue) and 3 (pink), using respectively samples from Groups 1, 2 and 3. All three curves exhibit two melting peaks and there aren't neither artifacts or other peaks that identify impurities. The first peak, with temperatures of 290,79°C, 290,70°C and 290,31°C, respectively, is compatible with PA46 (melting peak between 290 and 295°C); while the second peak, with temperatures of 326,58°C, 327,17°C and 326,48°C, is compatible with PTFE (melting peak between 325 and 335°C).

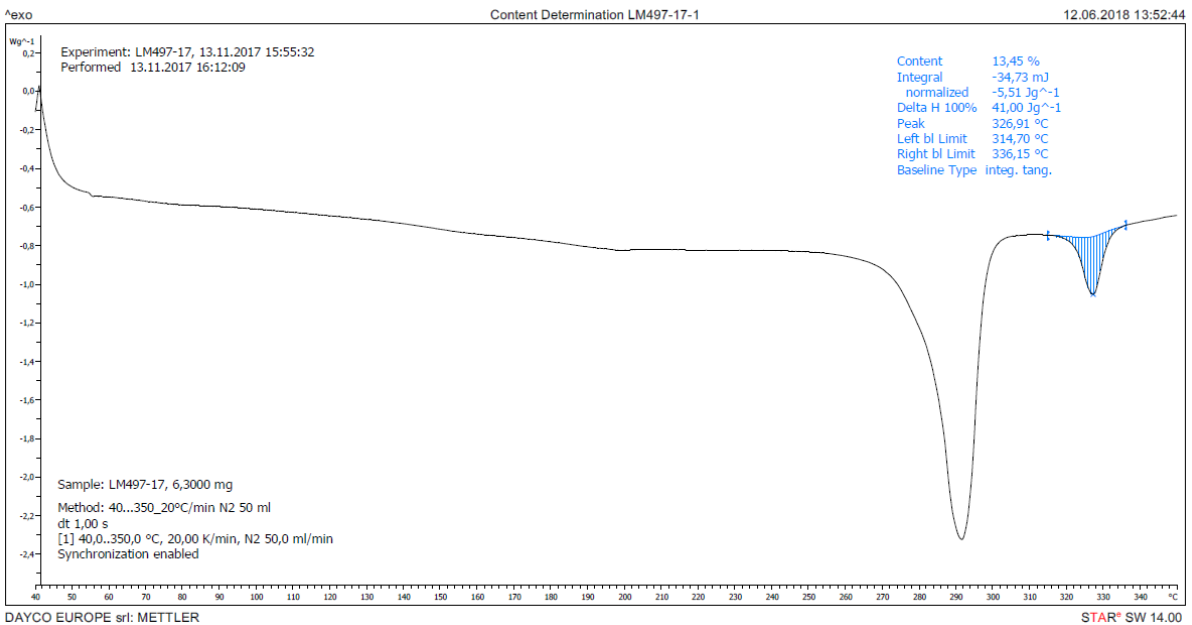


Figure 11.88: DSC measurement curve of sample LM497-17, from Group 1, obtained from Analysis 1, in which a content of 13,45% of PTFE was measured.

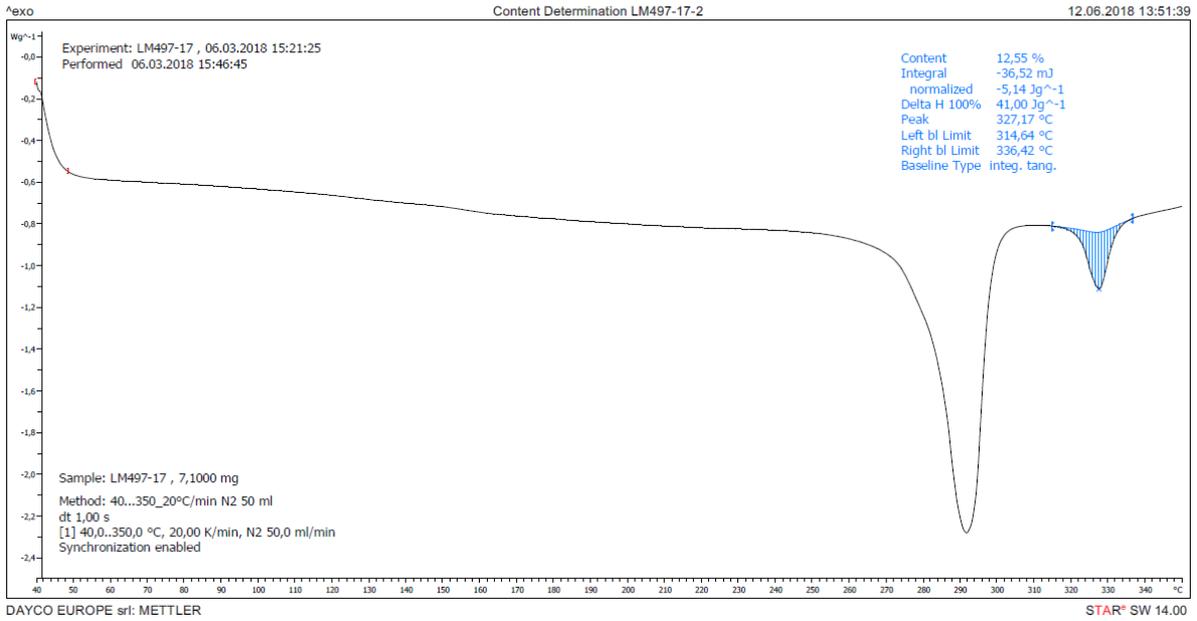


Figure 11.89: DSC measurement curve of sample LM497-17, from Group 2, obtained from Analysis 2, in which a content of 12,55% of PTFE was measured.

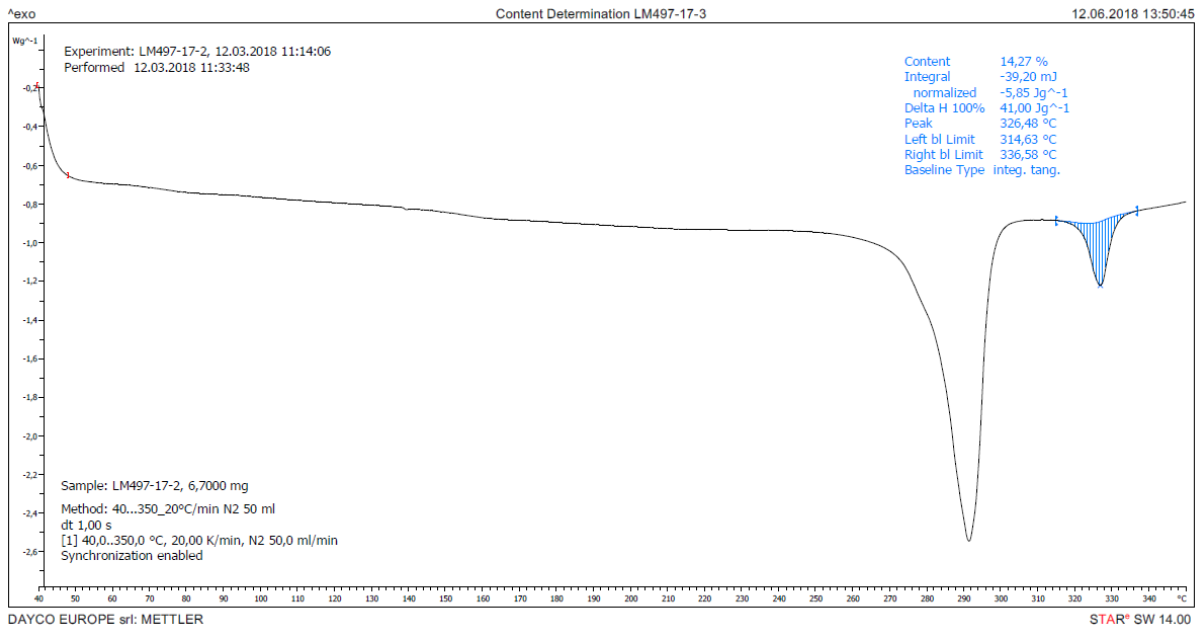


Figure 11.90: DSC measurement curve of sample LM497-17, from Group 3, obtained from Analysis 3, in which a content of 14,27% of PTFE was measured.

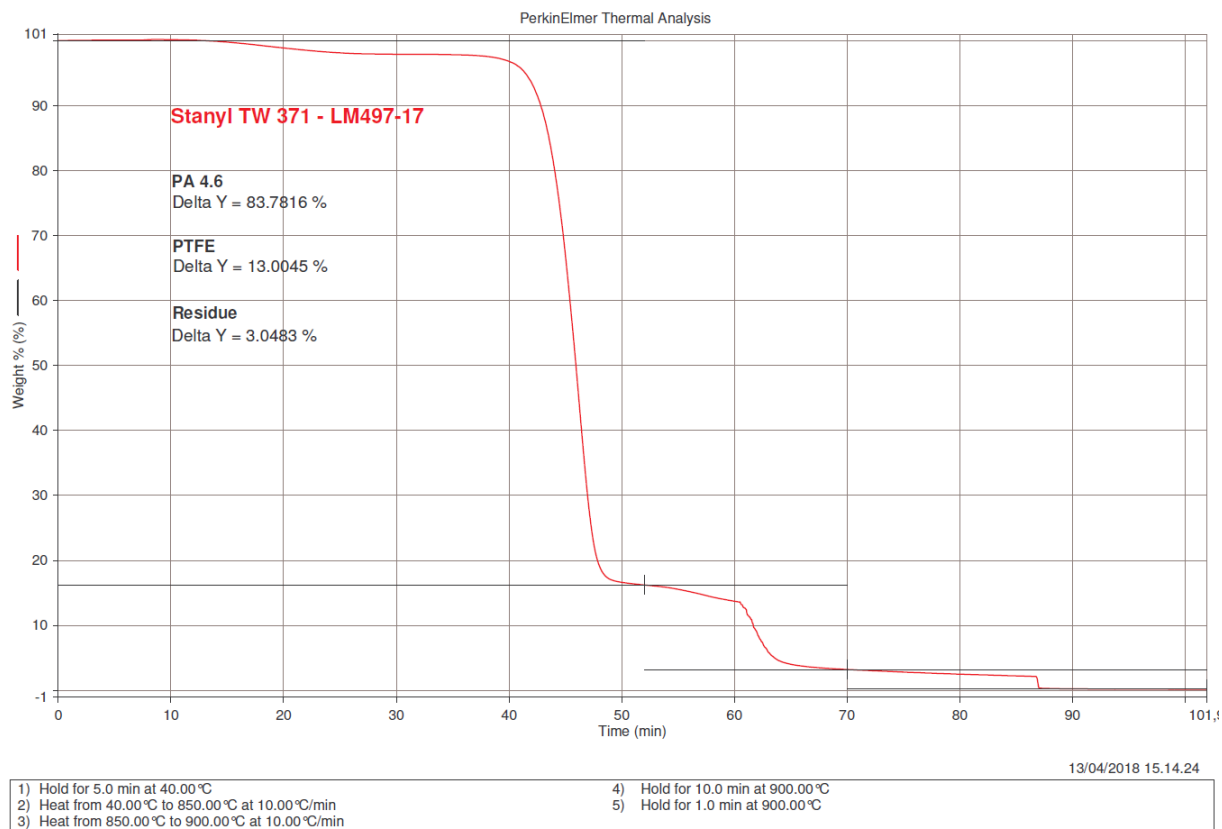


Figure 11.91: TGA measurement curve of sample LM497-17. The contents of PA46, PTFE and residue are, respectively, 83.7816%, 13.0045% and 3.0483%.

11.18. LM498-17

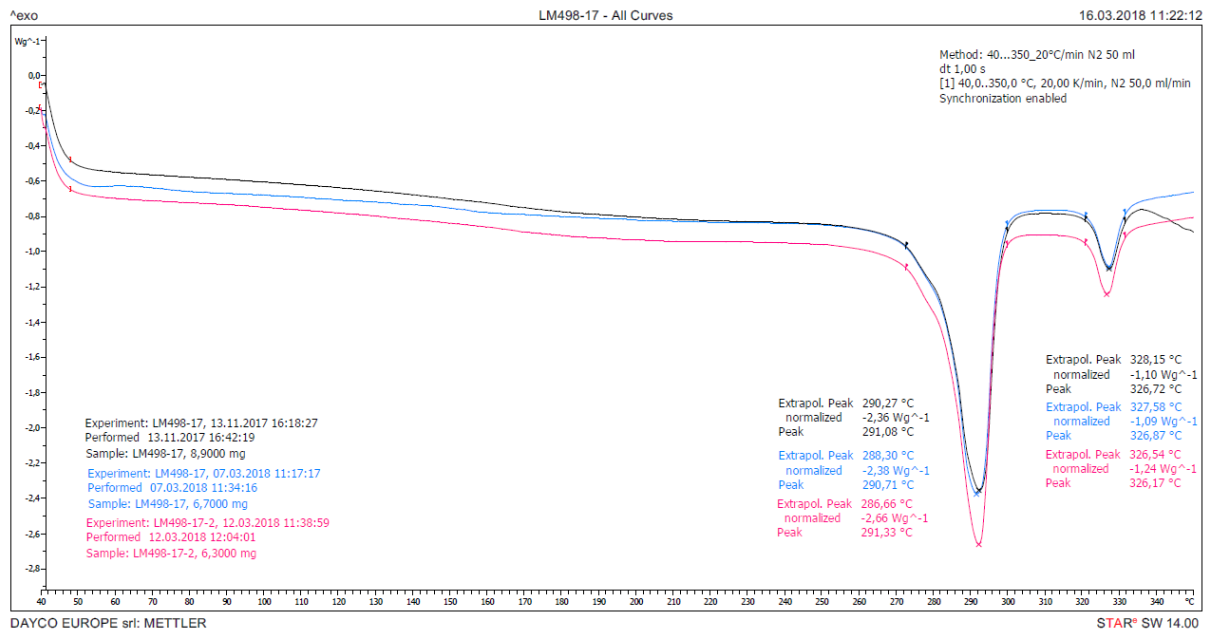


Figure 11.92: DSC measurements curves of spring bushing LM498-17 obtained from Analyses 1 (black), 2 (blue) and 3 (pink), using respectively samples from Groups 1, 2 and 3. All three curves exhibit two melting peaks and there aren't other peaks that identify impurities. However, the curve from Analysis 1 exhibits some irregularities at the final part due to the scape of the material from the crucible through the hole on the lid. The first peak, with temperatures of 291,08°C, 290,71°C and 291,33°C, respectively, is compatible with PA46 (melting peak between 290 and 295°C); while the second peak, with temperatures of 326,72°C, 326,87°C and 326,17°C, is compatible with PTFE (melting peak between 325 and 335°C).

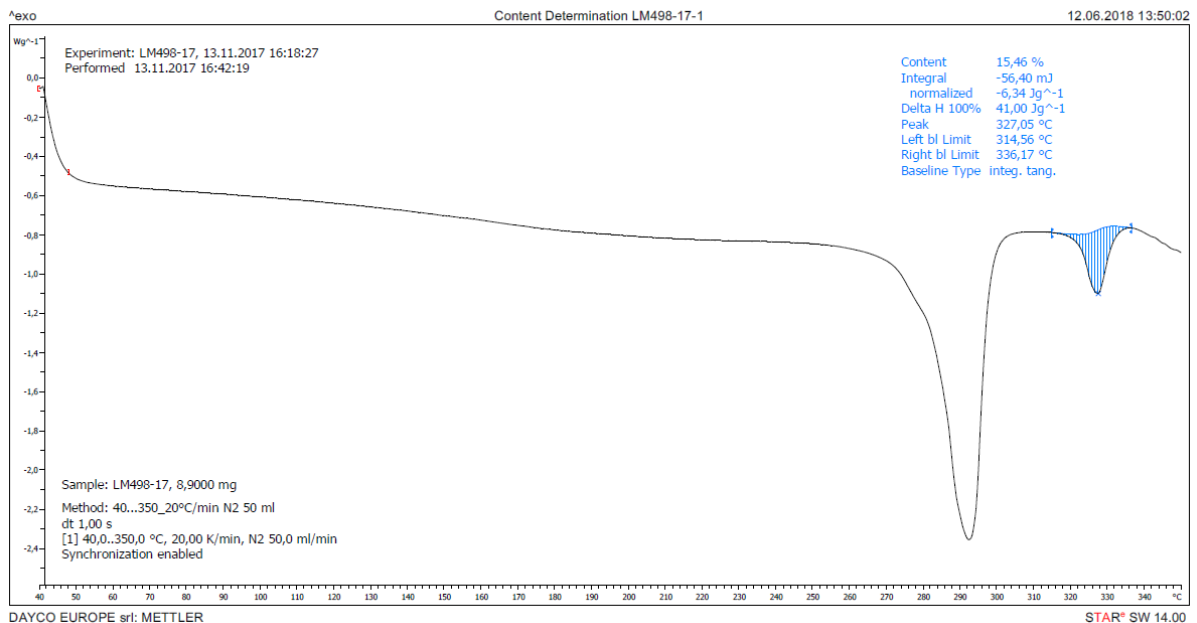


Figure 11.93: DSC measurement curve of sample LM498-17, from Group 1, obtained from Analysis 1, in which a content of 15,46% of PTFE was measured.

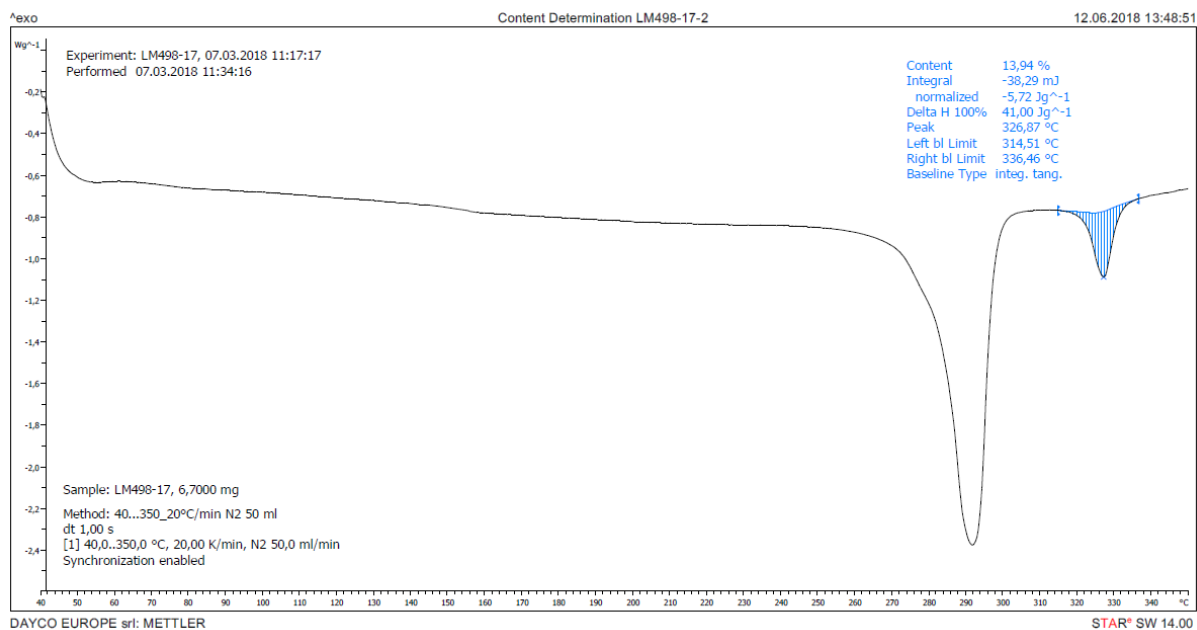


Figure 11.94: DSC measurement curve of sample LM498-17, from Group 2, obtained from Analysis 2, in which a content of 13,94% of PTFE was measured.

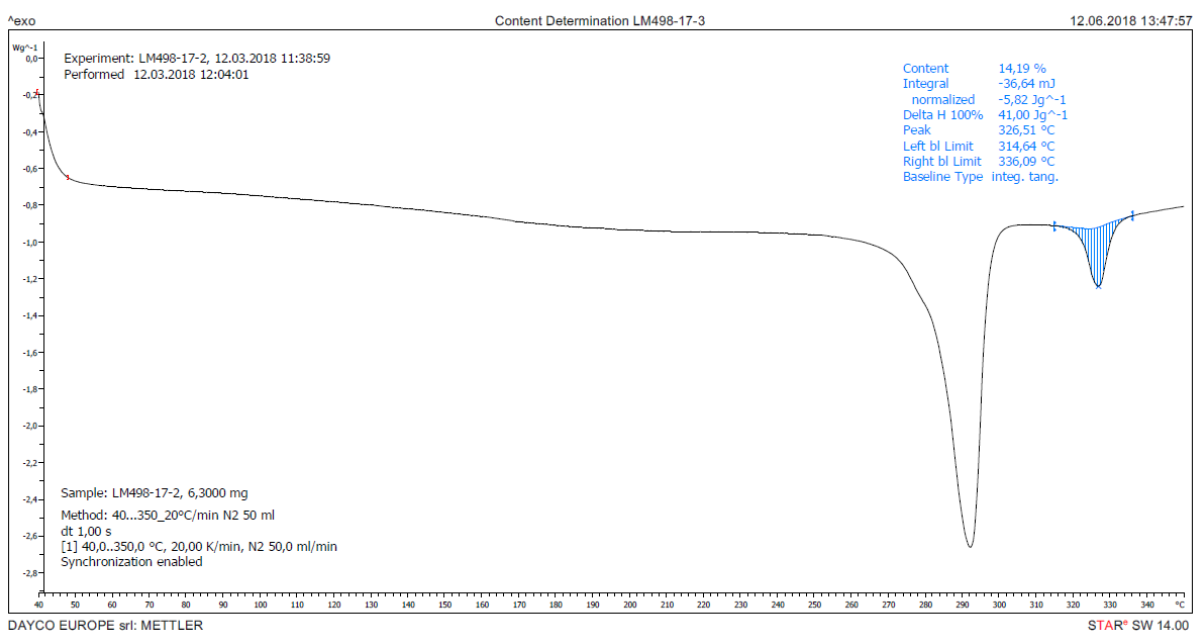


Figure 11.95: DSC measurement curve of sample LM498-17, from Group 3, obtained from Analysis 3, in which a content of 14,19% of PTFE was measured.

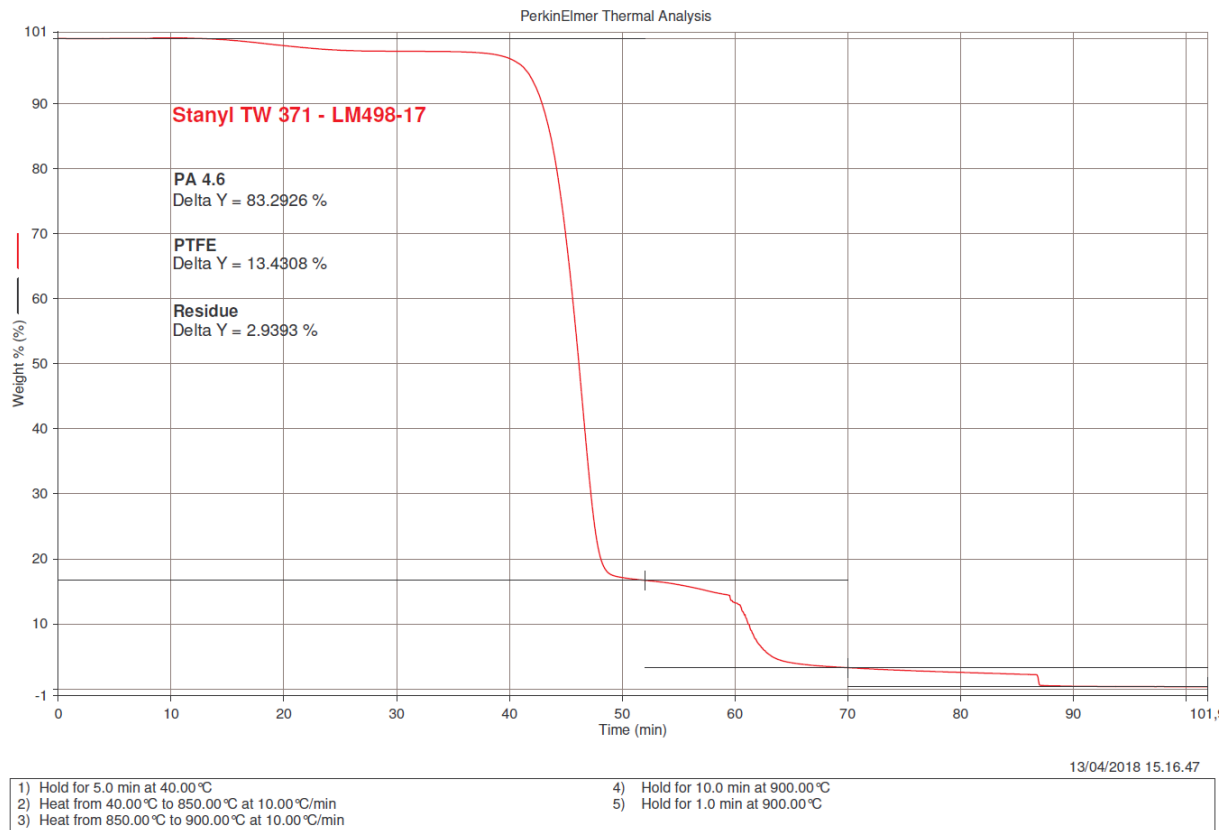


Figure 11.96: TGA measurement curve of sample LM498-17. The contents of PA46, PTFE and residue are, respectively, 83.2926%, 13.4308% and 2.9393%.

11.19. LM499-17

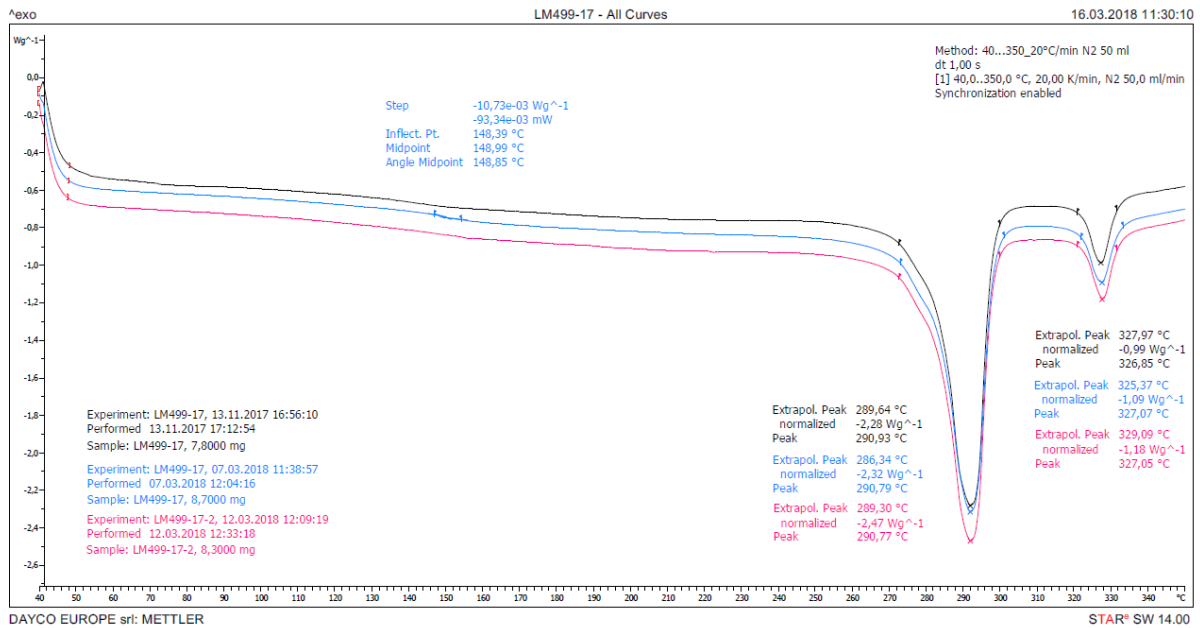


Figure 11.97: DSC measurements curves of spring bushing LM499-17 obtained from Analyses 1 (black), 2 (blue) and 3 (pink), using respectively samples from Groups 1, 2 and 3. All three curves exhibit two melting peaks and there aren't other peaks that identify impurities. However, the curve from Analysis 2 exhibits a step like effect with a midpoint temperature of 148,99°C, that is not compatible with the Tg range of PA46 and PTFE. This step may be an artifact due to a deformation of the crucible caused by the vapor pressure of the sample. The first melting peak, with temperatures of 290,93°C, 290,79°C and 290,77°C, respectively, is compatible with PA46 (melting peak between 290 and 295°C); while the second peak, with temperatures of 326,85°C, 327,07°C and 327,05°C, is compatible with PTFE (melting peak between 325 and 335°C).

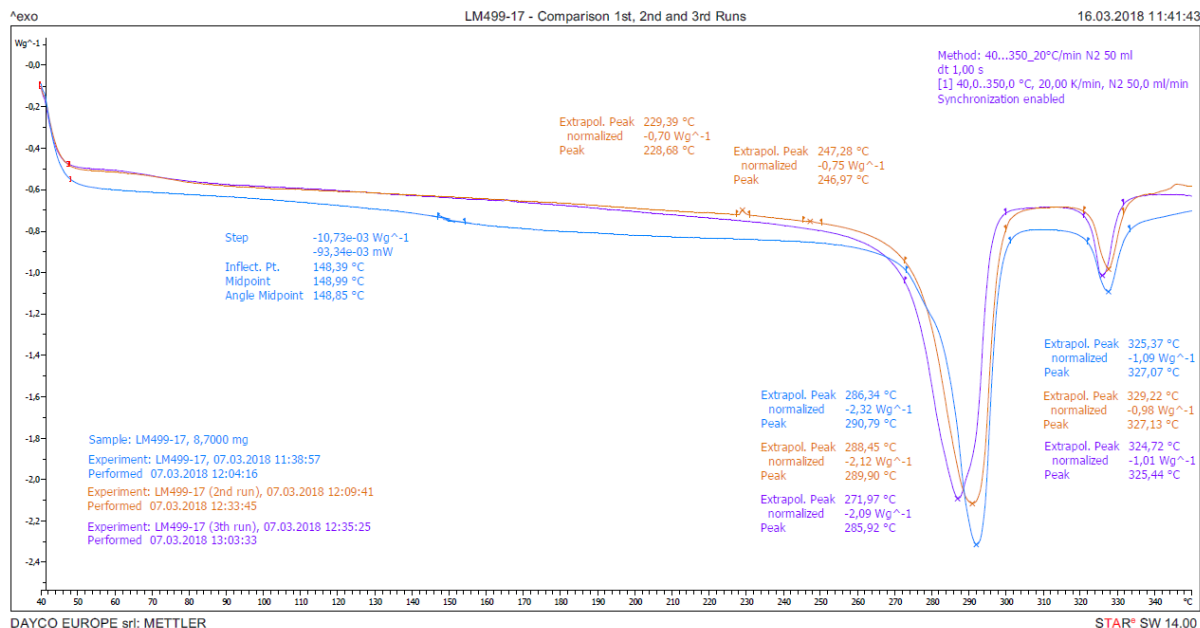


Figure 11.98: DSC measurement curves of spring bushing LM499-17 obtained in the first (blue), second (orange) and third (purple) runs of Analysis 2. The second run was performed due to the presence of a step like effect with a midpoint temperature of 148,99°C in the first run, that was interpreted as an artifact caused by the deformation of the crucible due to the vapor pressure of the sample. While the third run was performed due to the presence, in the second run, of two exothermic peaks with temperatures of 228,68°C and 246,97°C, caused by impurities. In the third run, instead, it is possible to see only the two melting peaks, that shift significantly to lower temperatures. The first peak, with temperatures of 290,79°C, 289,90 and 285,92°C, respectively, is compatible with PA46 (melting peak between 290 and 295°C) only in the 1st run, and it is slightly below in the 2nd and 3rd runs; while the second peak, with temperatures of 327,07°C, 327,13°C and 325,44°C, is compatible with PTFE (melting peak between 325 and 335°C).

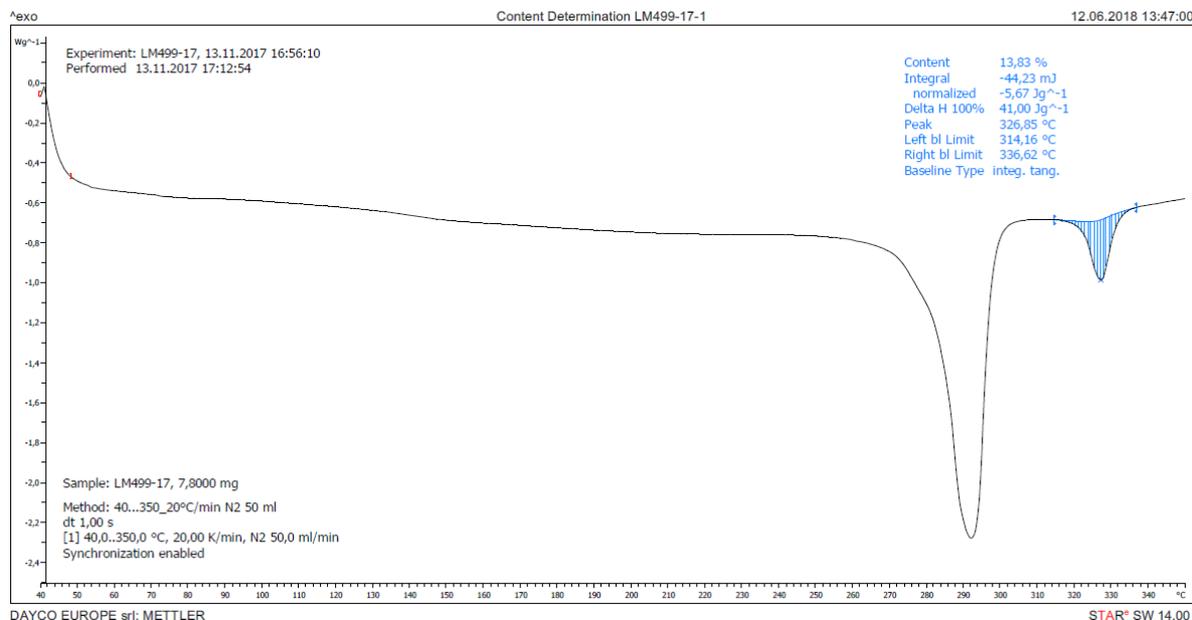


Figure 11.99: DSC measurement curve of sample LM499-17, from Group 1, obtained from Analysis 1, in which a content of 13,83% of PTFE was measured.

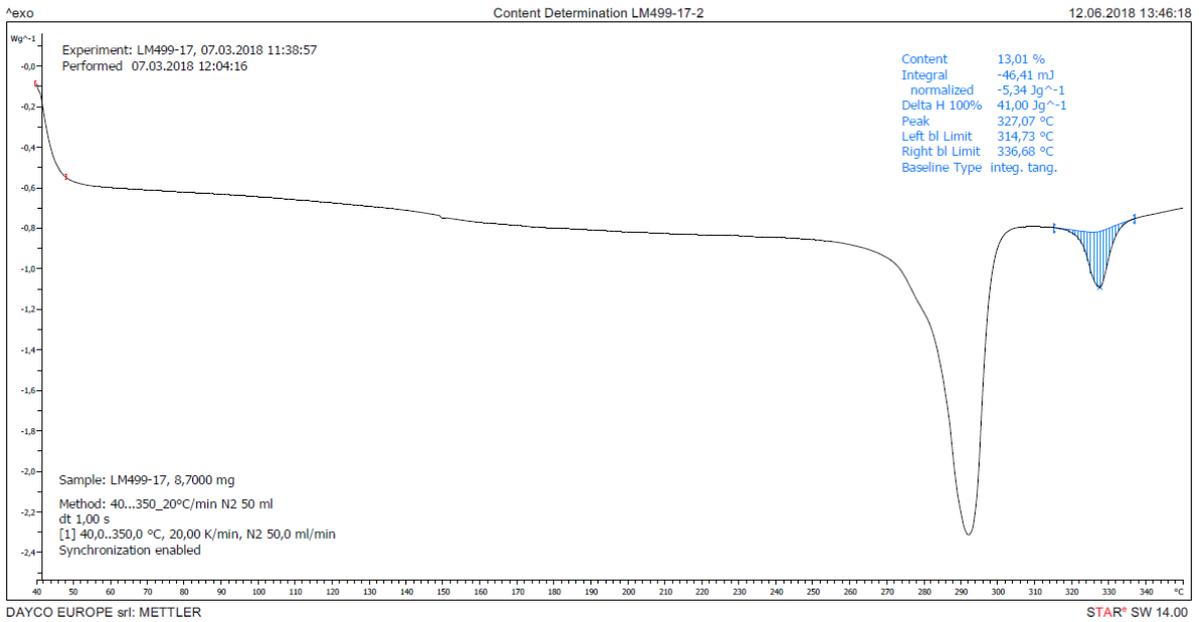


Figure 11.100: DSC measurement curve of sample LM499-17, from Group 2, obtained from Analysis 2, in which a content of 13,01% of PTFE was measured.

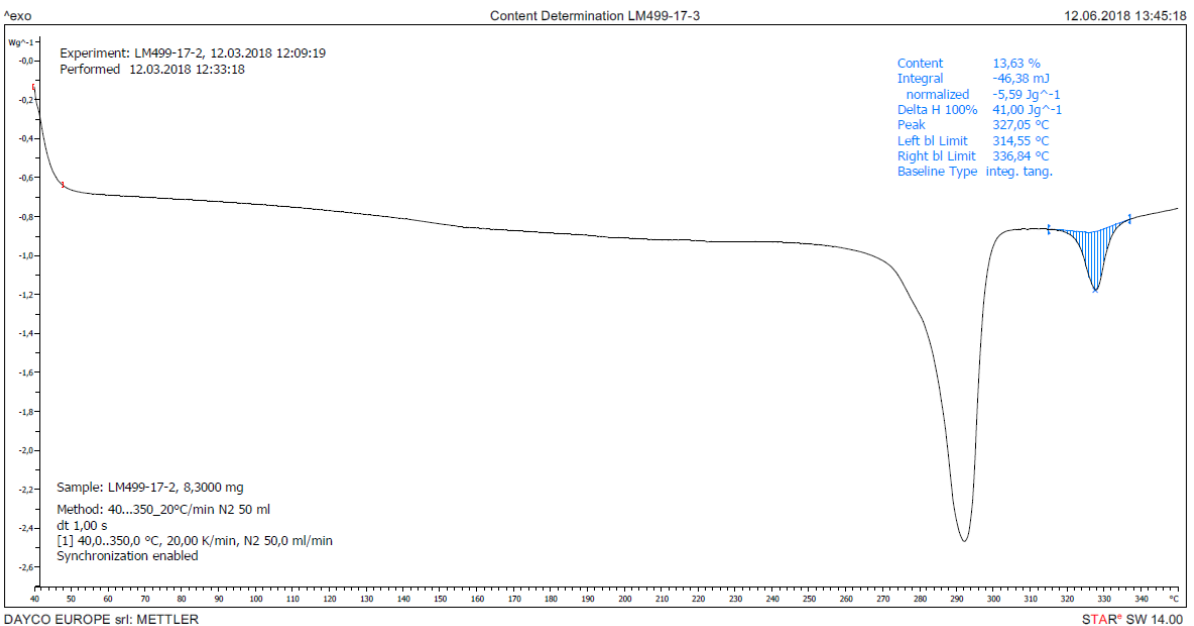


Figure 11.101: DSC measurement curve of sample LM499-17, from Group 3, obtained from Analysis 3, in which a content of 13,63% of PTFE was measured.

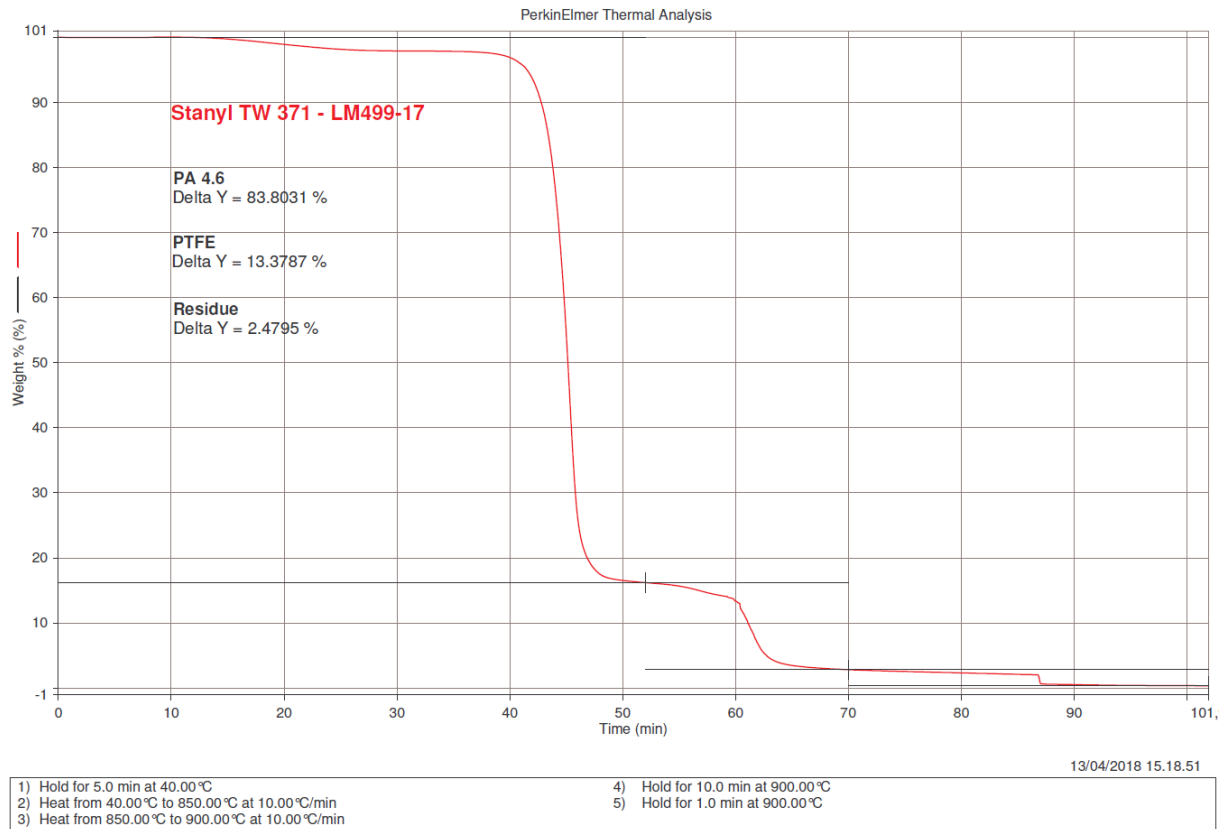


Figure 11.102: TGA measurement curve of sample LM499-17. The contents of PA46, PTFE and residue are, respectively, 83.8031%, 13.3787% and 2.4795%.

11.20. LM500-17

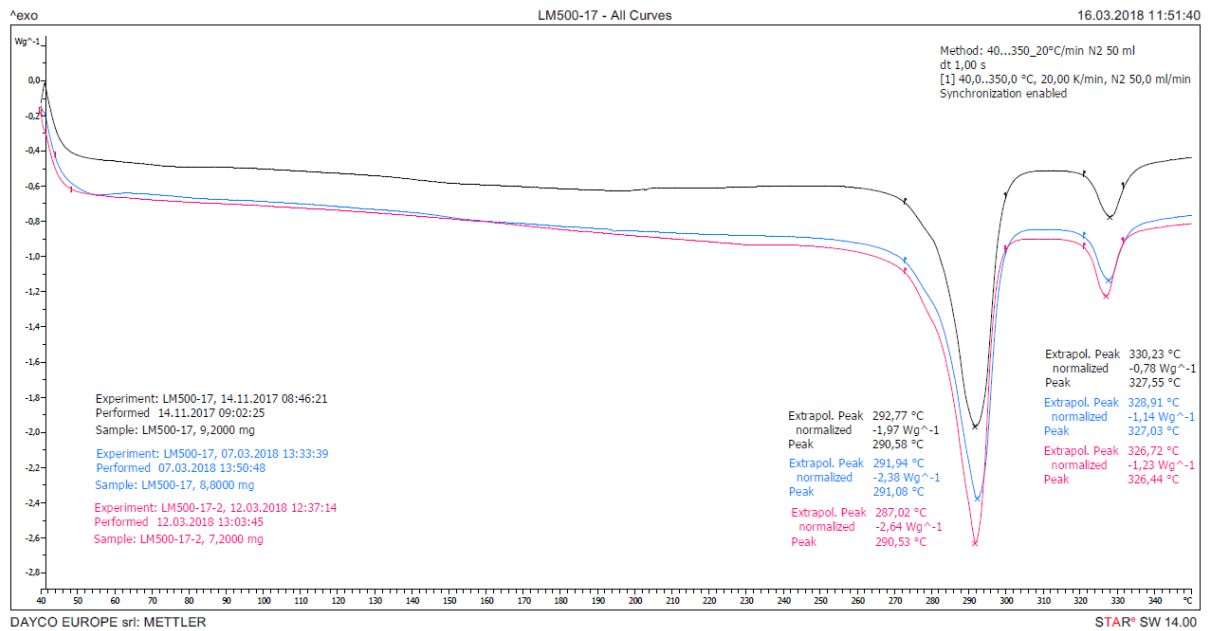


Figure 11.103: DSC measurements curves of spring bushing LM500-17 obtained from Analyses 1 (black), 2 (blue) and 3 (pink), using respectively samples from Groups 1, 2 and 3. All three curves exhibit two melting peaks and there aren't neither artifacts or other peaks that identify impurities. The first peak, with temperatures of 290,58°C, 291,08°C and 290,53°C, respectively, is compatible with PA46 (melting peak between 290 and 295°C); while the second peak, with temperatures of 327,55°C, 327,03°C and 326,44°C, is compatible with PTFE (melting peak between 325 and 335°C).

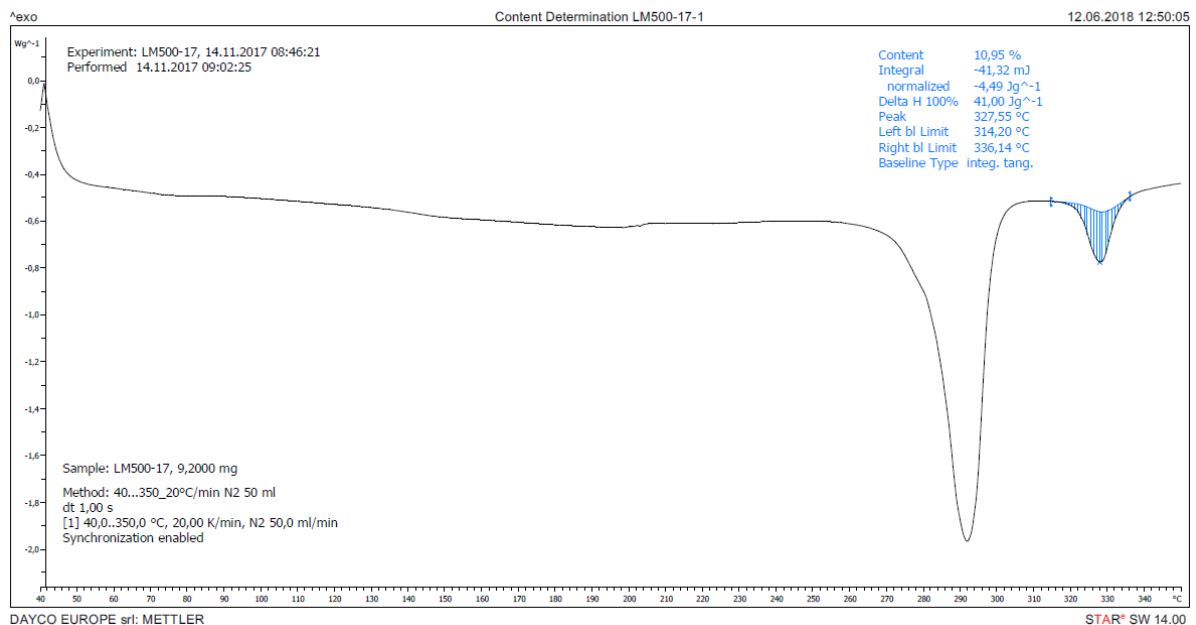


Figure 11.104: DSC measurement curve of sample LM500-17, from Group 1, obtained from Analysis 1, in which a content of 10,95% of PTFE was measured.

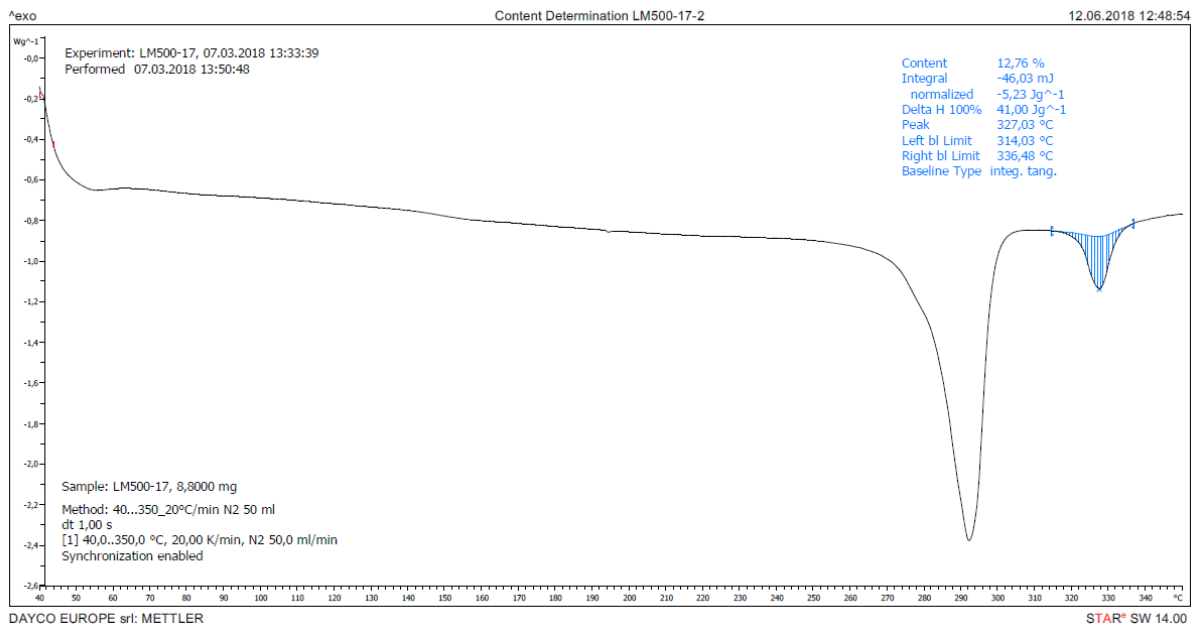


Figure 11.105: DSC measurement curve of sample LM500-17, from Group 2, obtained from Analysis 2, in which a content of 12,76% of PTFE was measured.

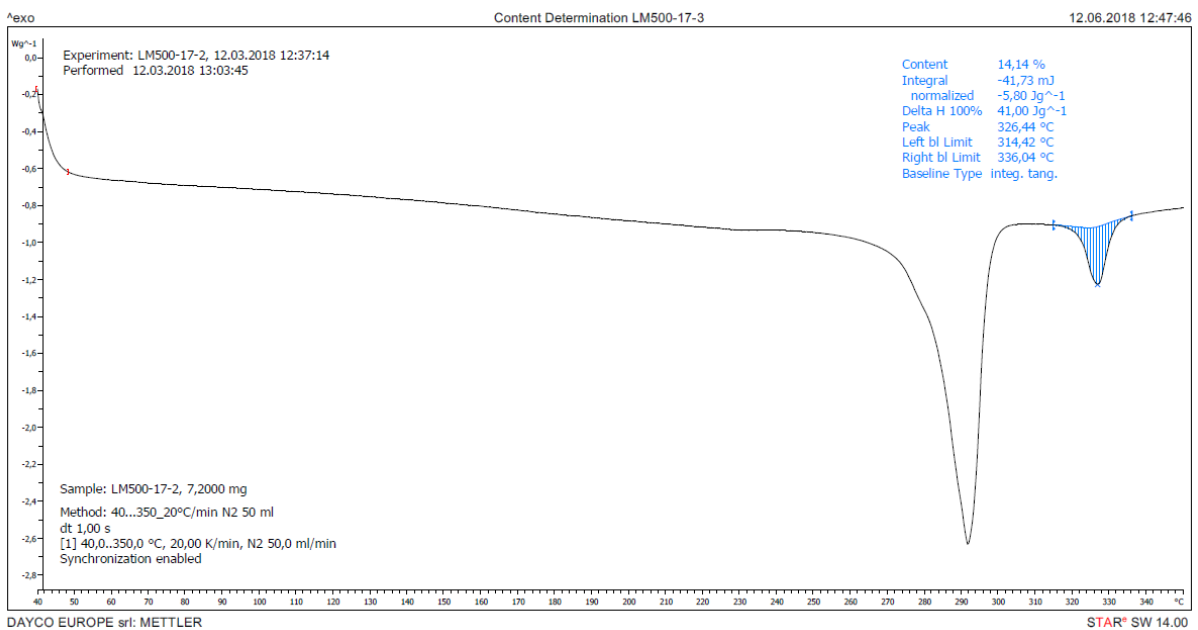


Figure 11.106: DSC measurement curve of sample LM500-17, from Group 3, obtained from Analysis 3, in which a content of 14,14% of PTFE was measured.

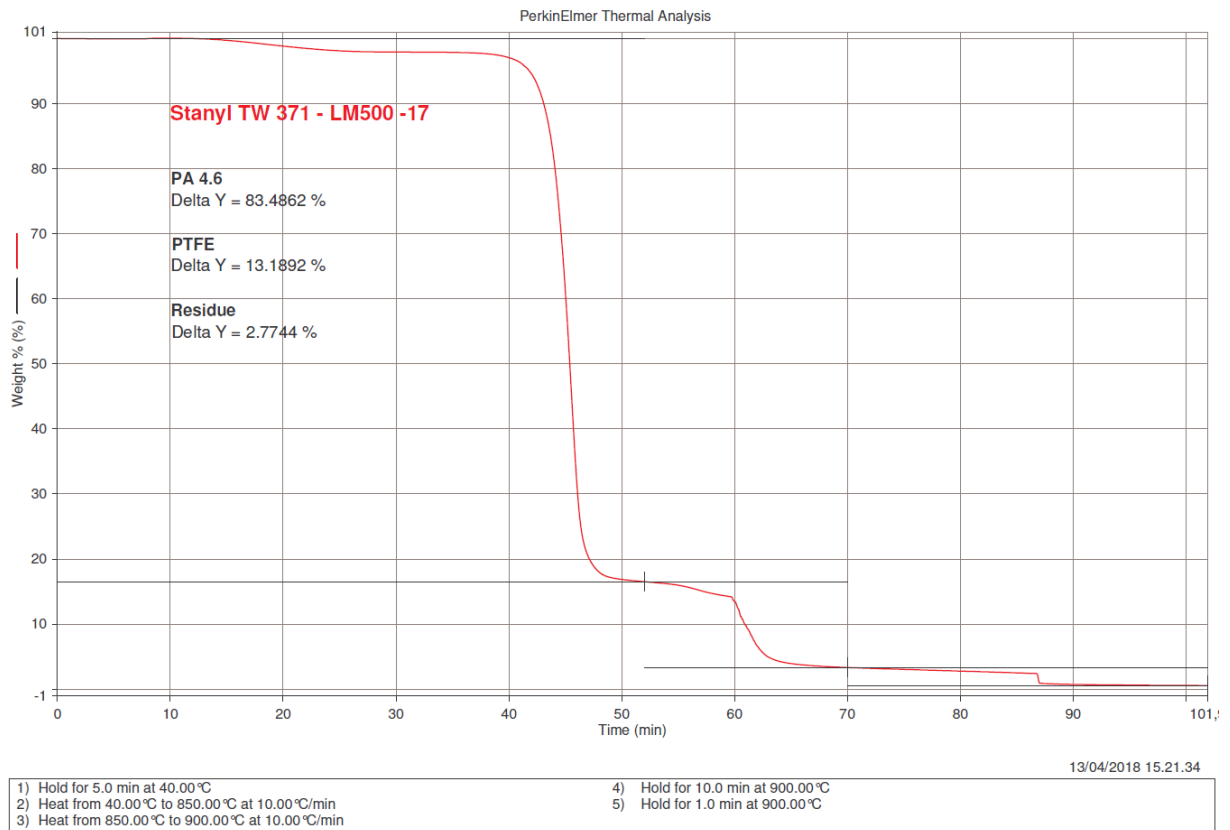


Figure 11.107: TGA measurement curve of sample LM500-17. The contents of PA46, PTFE and residue are, respectively, 83.4862%, 13.1892% and 2.7744%.

11.21. LM501-17

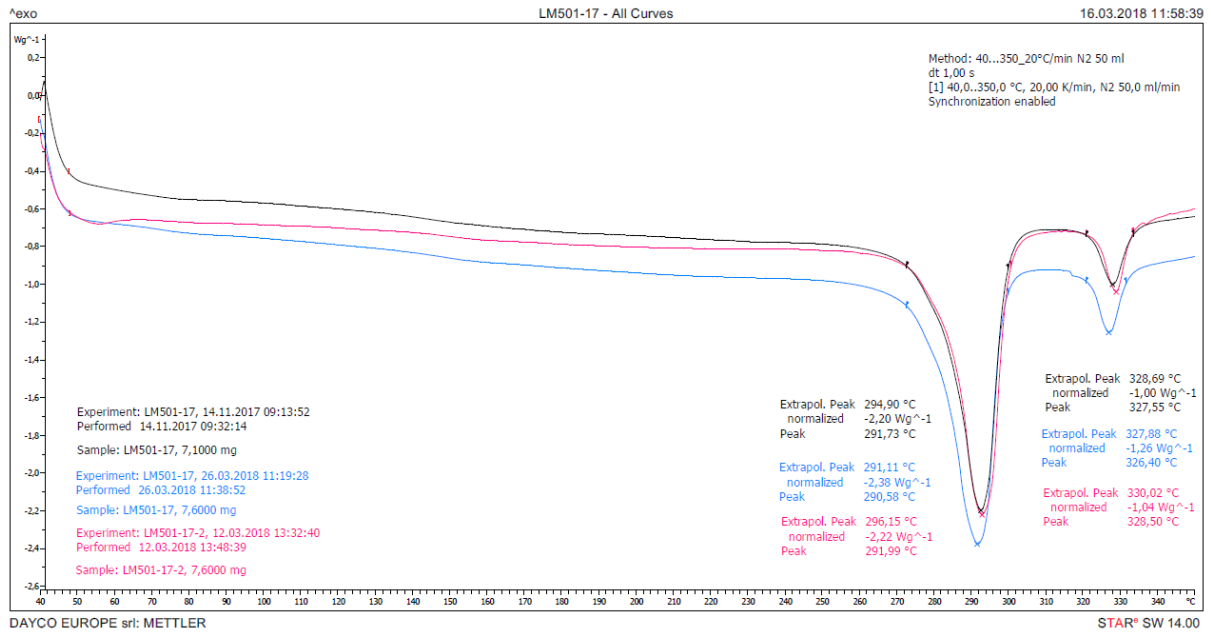


Figure 11.108: DSC measurements curves of spring bushing LM501-17 obtained from Analyses 1 (black), 2 (blue) and 3 (pink), using respectively samples from Groups 1, 2 and 3. All three curves exhibit two melting peaks and there aren't neither artifacts or other peaks that identify impurities. The first peak, with temperatures of 291,73°C, 290,58°C and 291,99°C, respectively, is compatible with PA46 (melting peak between 290 and 295°C); while the second peak, with temperatures of 327,55°C, 326,40°C and 328,50°C, is compatible with PTFE (melting peak between 325 and 335°C).

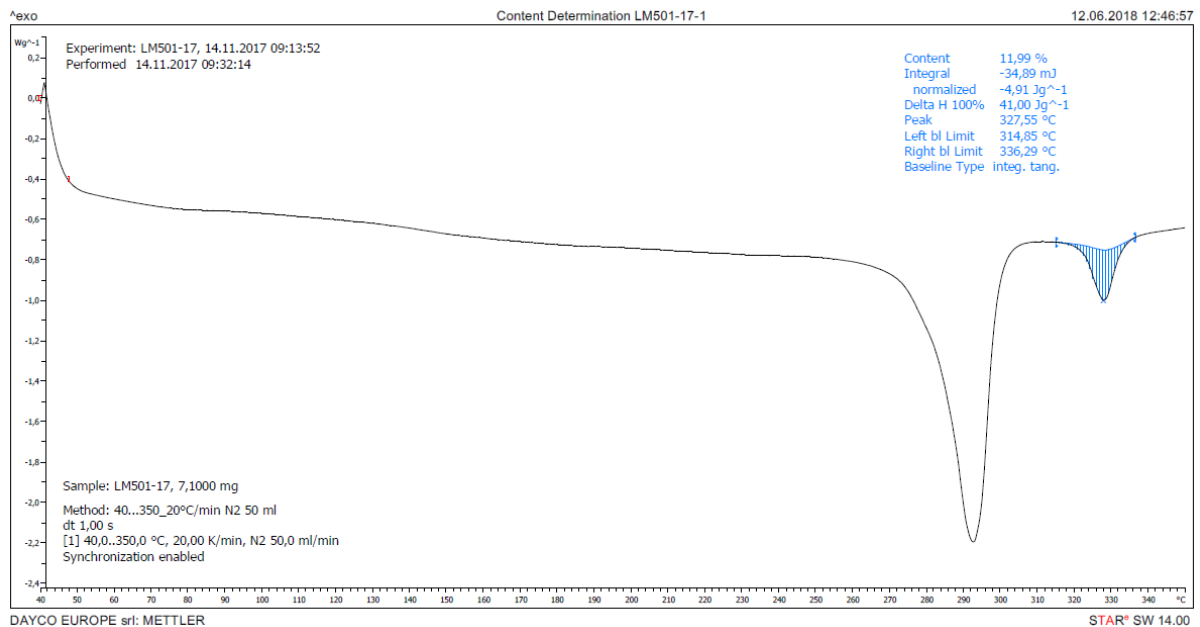


Figure 11.109: DSC measurement curve of sample LM501-17, from Group 1, obtained from Analysis 1, in which a content of 11,99% of PTFE was measured.

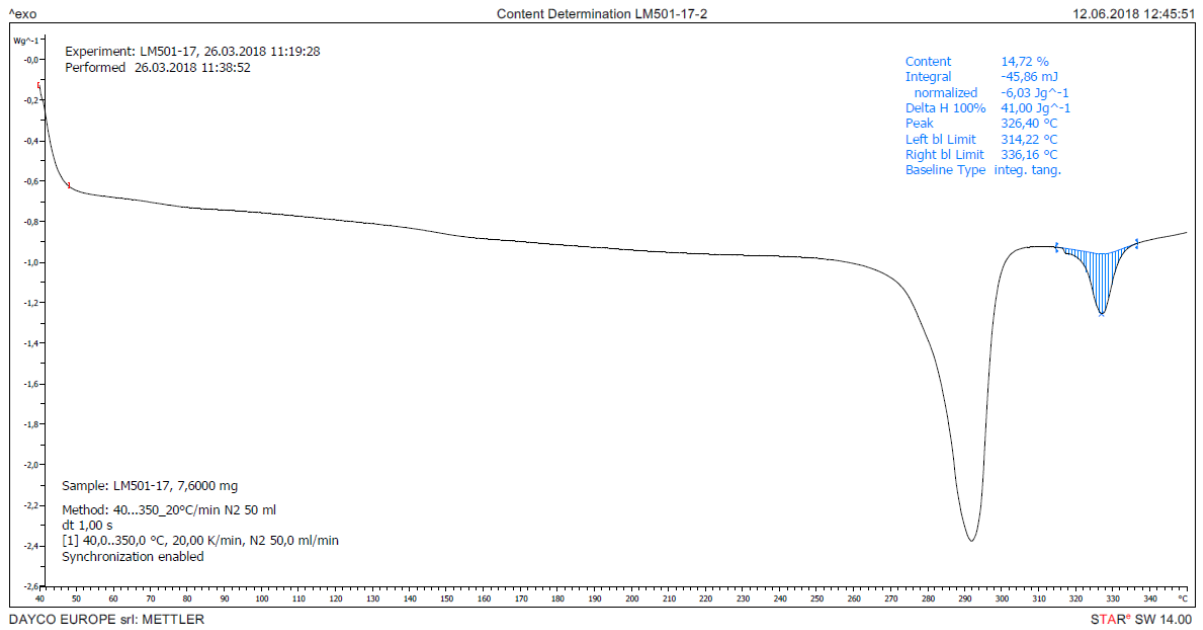


Figure 11.110: DSC measurement curve of sample LM501-17, from Group 2, obtained from Analysis 2, in which a content of 14,72% of PTFE was measured.

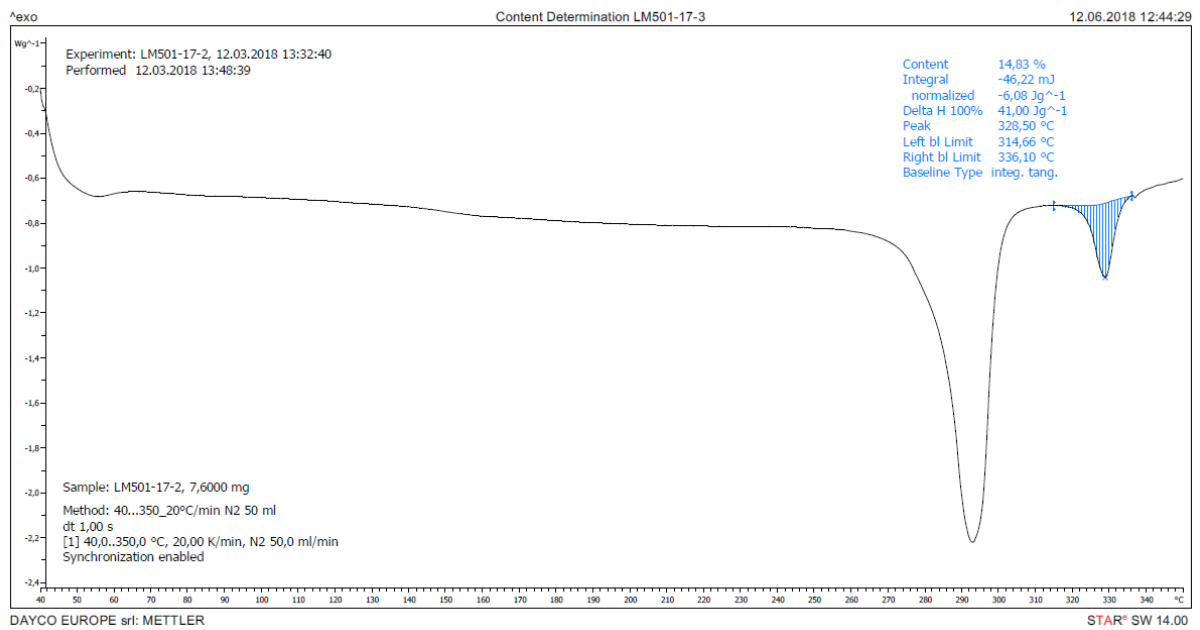


Figure 11.111: DSC measurement curve of sample LM501-17, from Group 3, obtained from Analysis 3, in which a content of 14,83% of PTFE was measured.

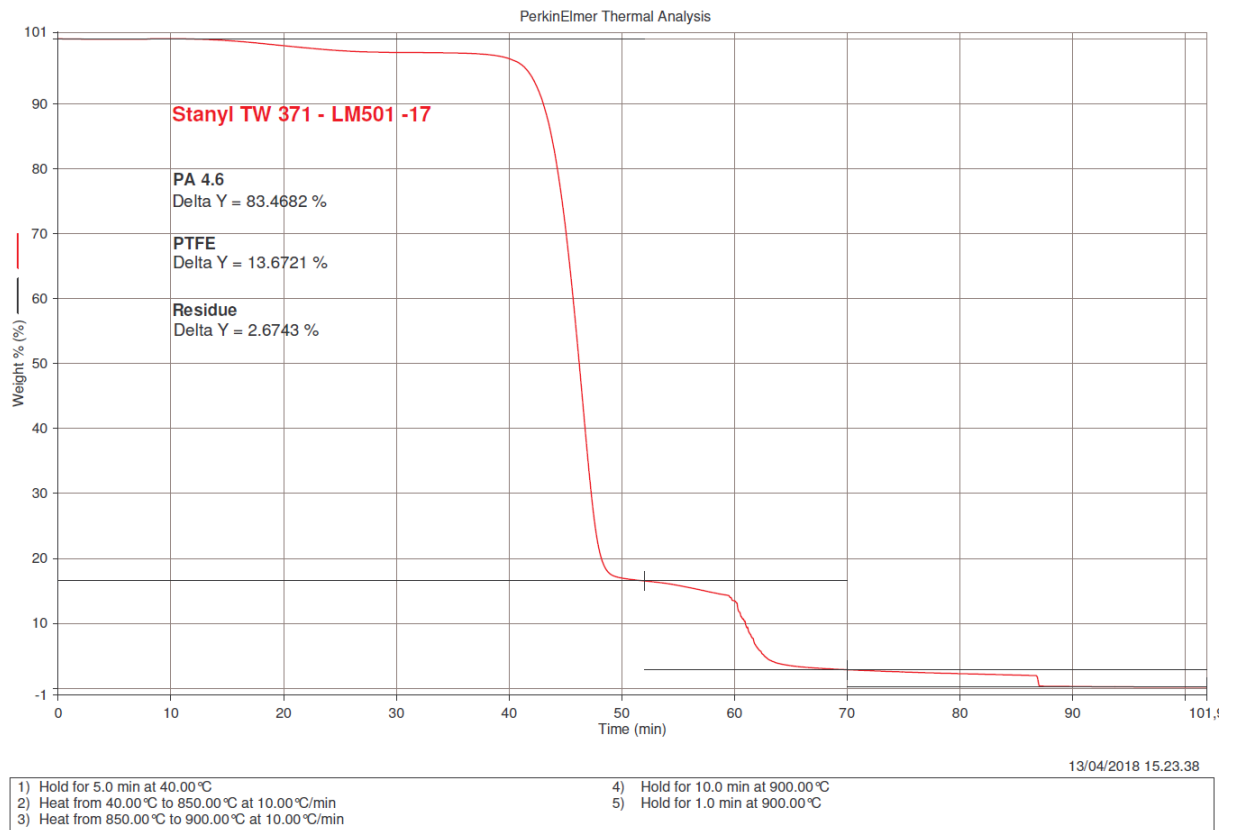


Figure 11.112: TGA measurement curve of sample LM501-17. The contents of PA46, PTFE and residue are, respectively, 83.4682%, 13.6721% and 2.6743%.

11.22. LM502-17

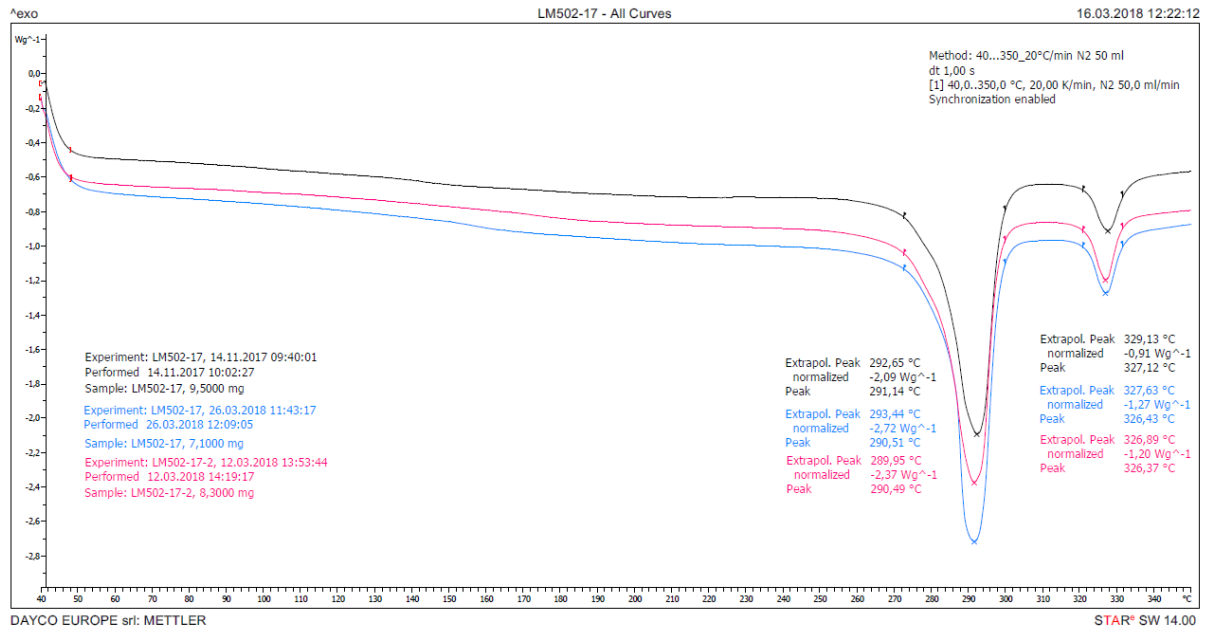


Figure 11.113: DSC measurements curves of spring bushing LM501-17 obtained from Analyses 1 (black), 2 (blue) and 3 (pink), using respectively samples from Groups 1, 2 and 3. All three curves exhibit two melting peaks and there aren't neither artifacts or other peaks that identify impurities. The first peak, with temperatures of 291,14°C, 290,51°C and 290,49°C, respectively, is compatible with PA46 (melting peak between 290 and 295°C); while the second peak, with temperatures of 327,12°C, 326,43°C and 326,37°C, is compatible with PTFE (melting peak between 325 and 335°C).

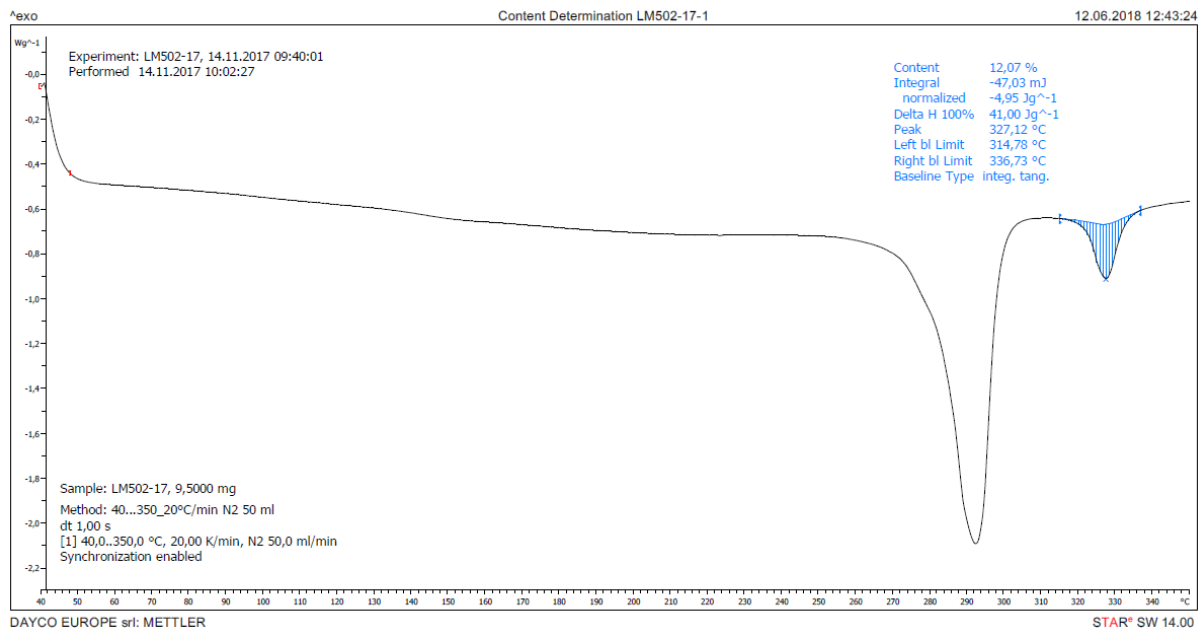


Figure 11.114: DSC measurement curve of sample LM502-17, from Group 1, obtained from Analysis 1, in which a content of 12,07% of PTFE was measured.

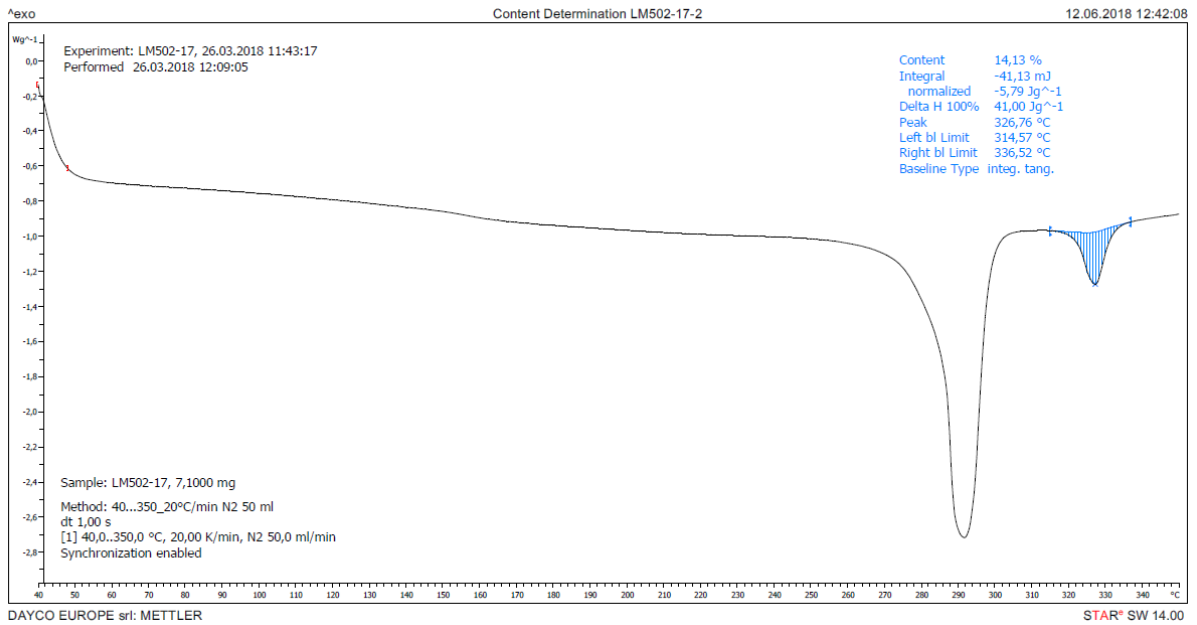


Figure 11.115: DSC measurement curve of sample LM502-17, from Group 2, obtained from Analysis 2, in which a content of 14,13% of PTFE was measured.

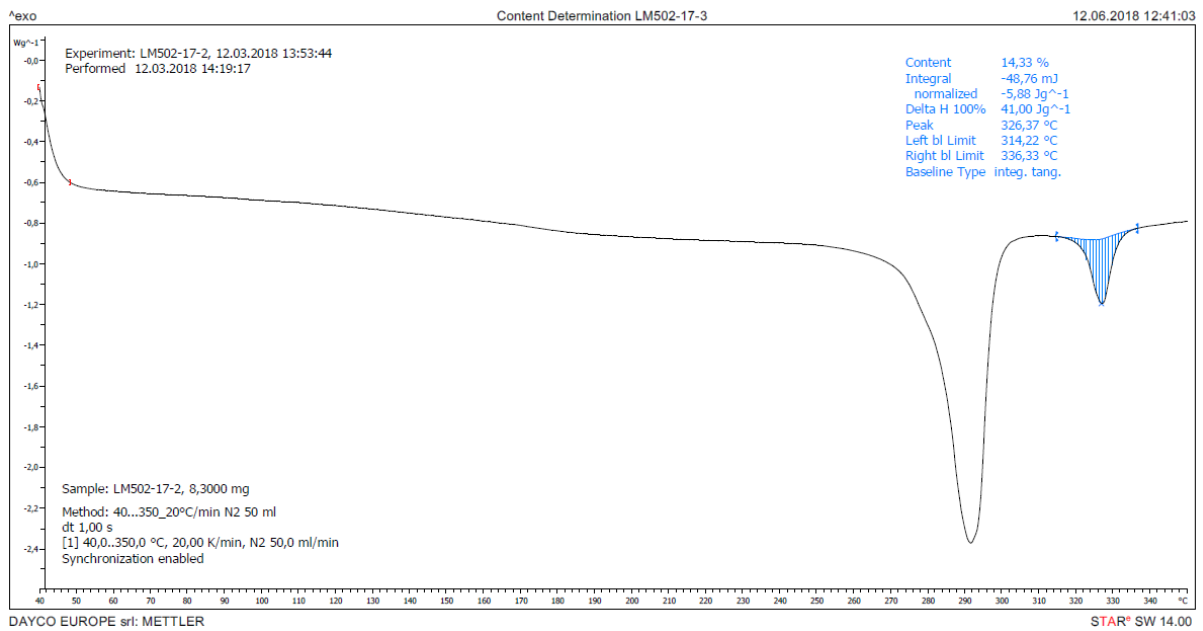


Figure 11.116: DSC measurement curve of sample LM502-17, from Group 3, obtained from Analysis 3, in which a content of 14,33% of PTFE was measured.

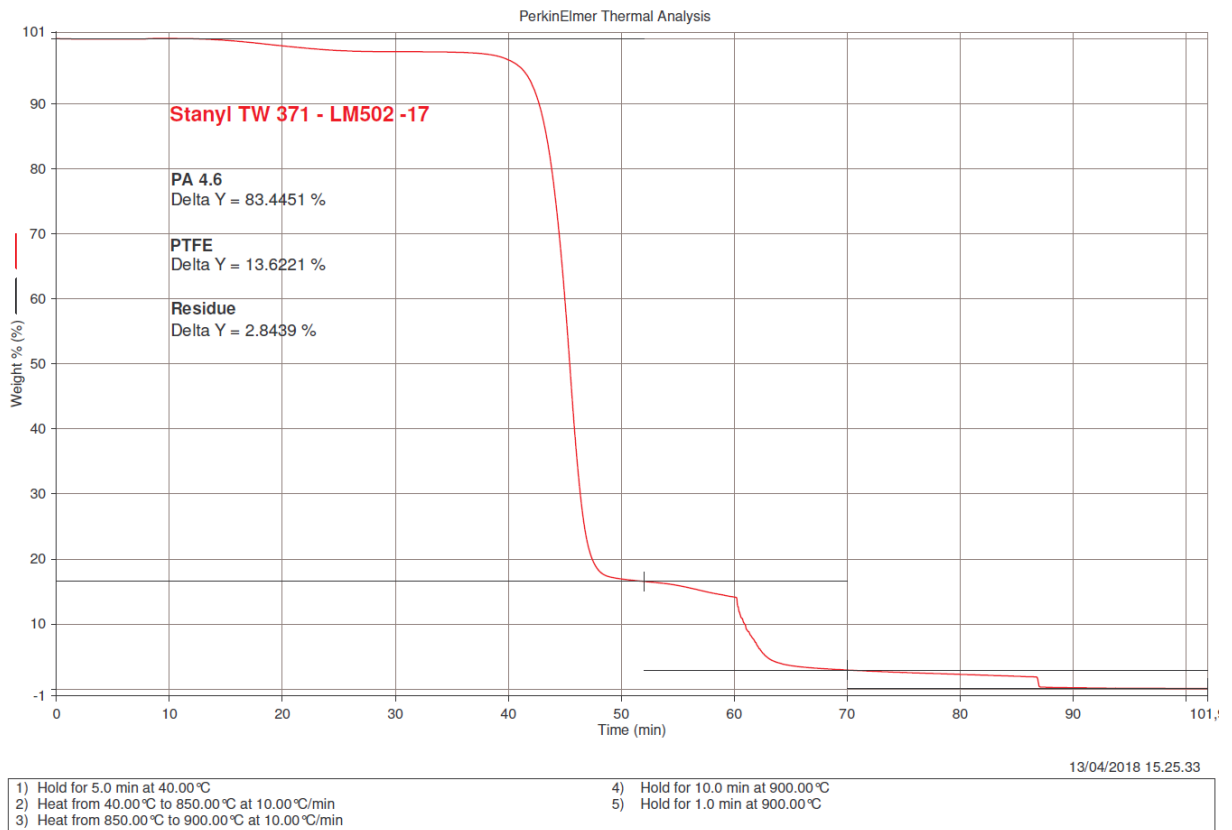


Figure 11.117: TGA measurement curve of sample LM502-17. The contents of PA46, PTFE and residue are, respectively, 83.4451%, 13.6221% and 2.8439%.

11.23. LM503-17

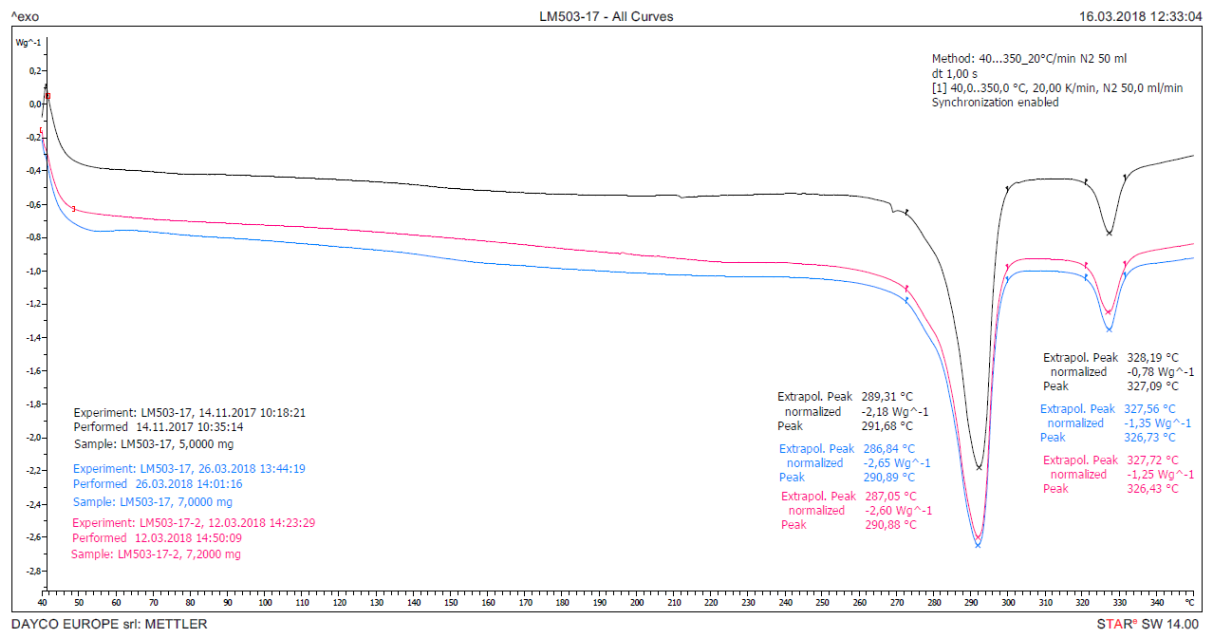


Figure 11.118: DSC measurements curves of spring bushing LM503-17 obtained from Analyses 1 (black), 2 (blue) and 3 (pink), using respectively samples from Groups 1, 2 and 3. All three curves exhibit two melting peaks and there aren't neither artifacts or other peaks that identify impurities. The first peak, with temperatures of 291,68°C, 290,89°C and 290,88°C, respectively, is compatible with PA46 (melting peak between 290 and 295°C); while the second peak, with temperatures of 327,09°C, 326,73°C and 326,43°C, is compatible with PTFE (melting peak between 325 and 335°C).

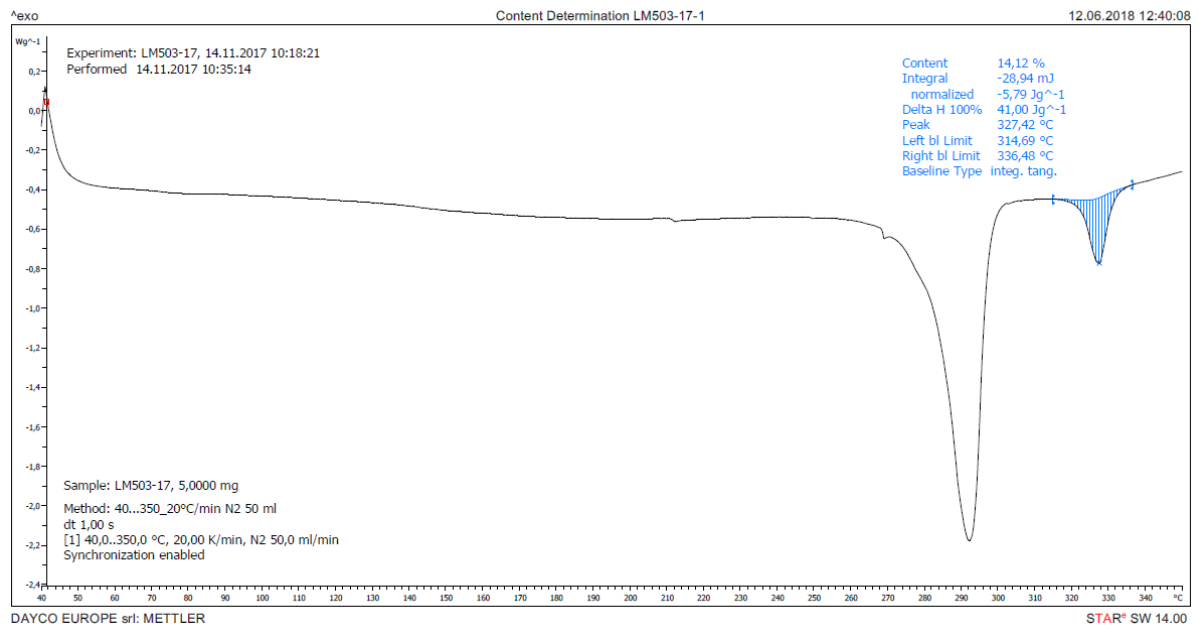


Figure 11.119: DSC measurement curve of sample LM503-17, from Group 1, obtained from Analysis 1, in which a content of 14,12% of PTFE was measured.

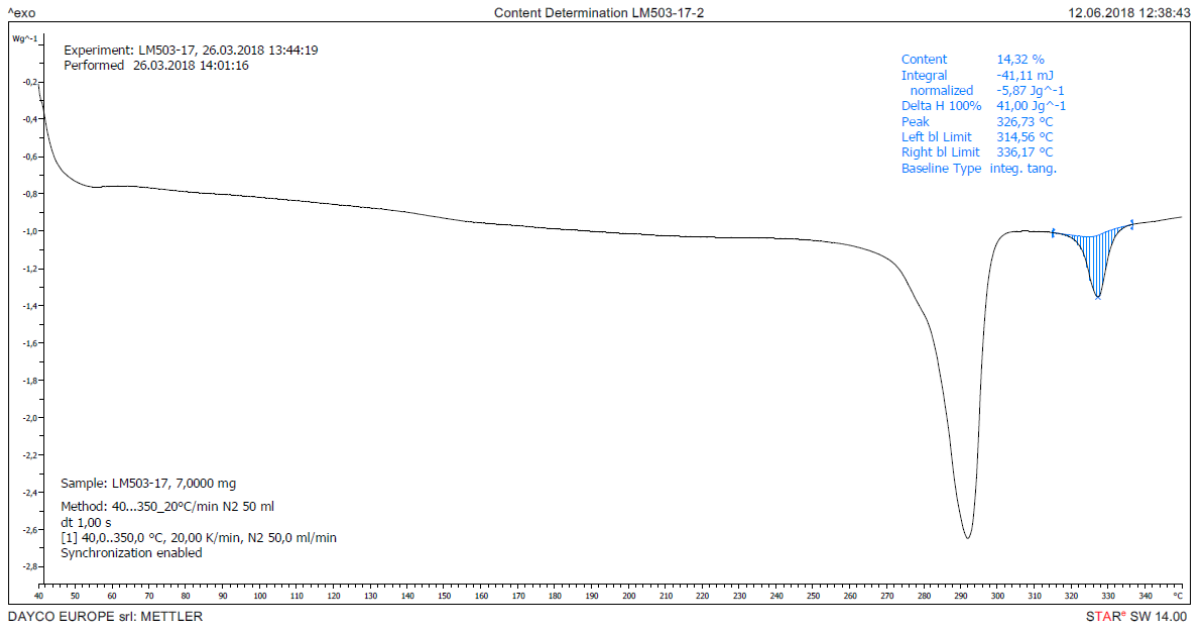


Figure 11.120: DSC measurement curve of sample LM503-17, from Group 2, obtained from Analysis 2, in which a content of 14,32% of PTFE was measured.

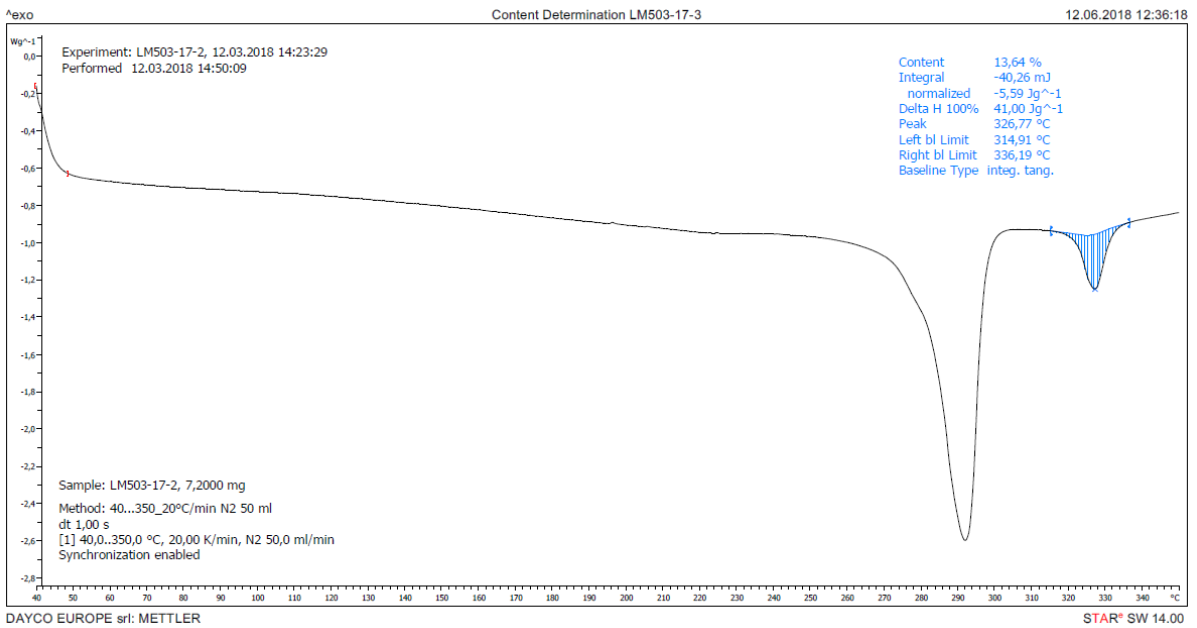


Figure 11.121: DSC measurement curve of sample LM503-17, from Group 3, obtained from Analysis 3, in which a content of 13,64% of PTFE was measured.

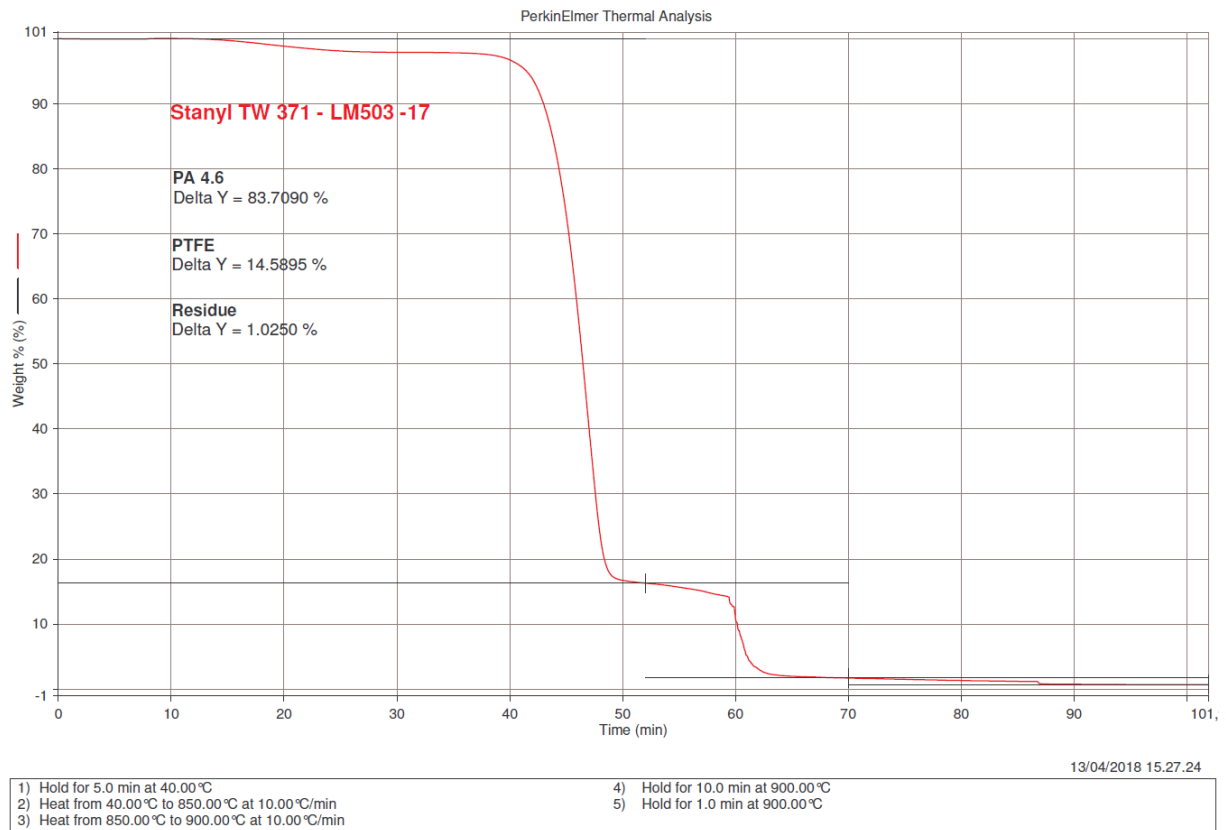


Figure 11.122: TGA measurement curve of sample LM503-17. The contents of PA46, PTFE and residue are, respectively, 83.7090%, 14.5895% and 1.0250%.

11.24. LM504-17

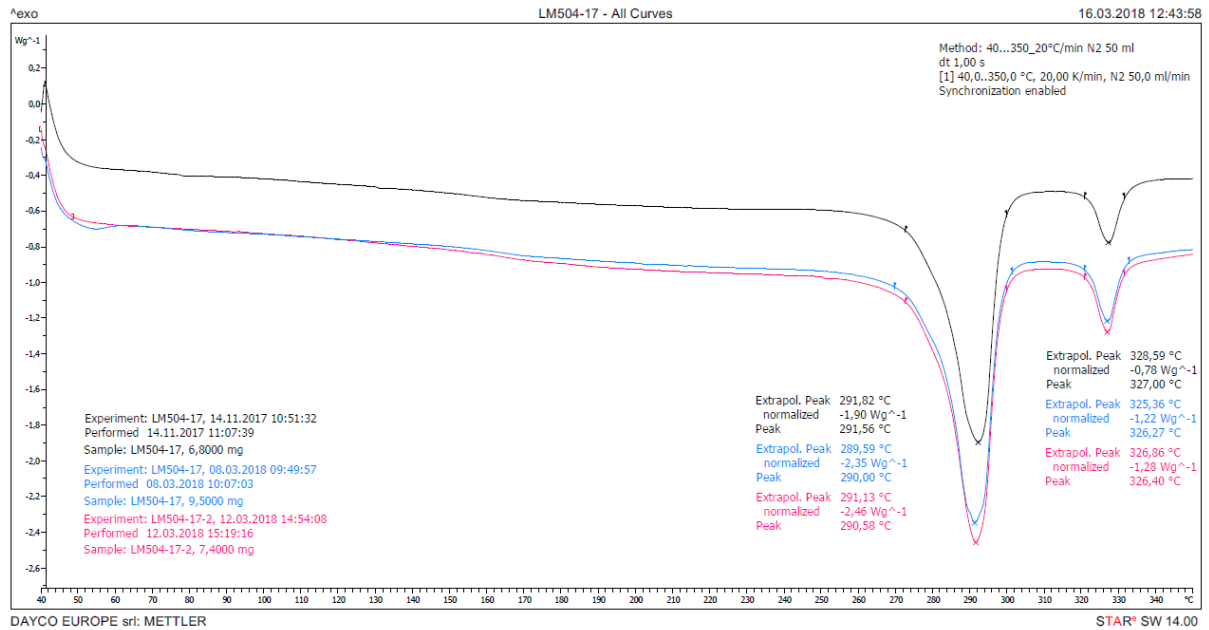


Figure 11.123: DSC measurements curves of spring bushing LM504-17 obtained from Analyses 1 (black), 2 (blue) and 3 (pink), using respectively samples from Groups 1, 2 and 3. All three curves exhibit two melting peaks and there aren't neither artifacts or other peaks that identify impurities. The first peak, with temperatures of 291,56°C, 290,00°C and 290,55°C, respectively, is compatible with PA46 (melting peak between 290 and 295°C); while the second peak, with temperatures of 327,00°C, 326,27°C and 326,40°C, is compatible with PTFE (melting peak between 325 and 335°C).

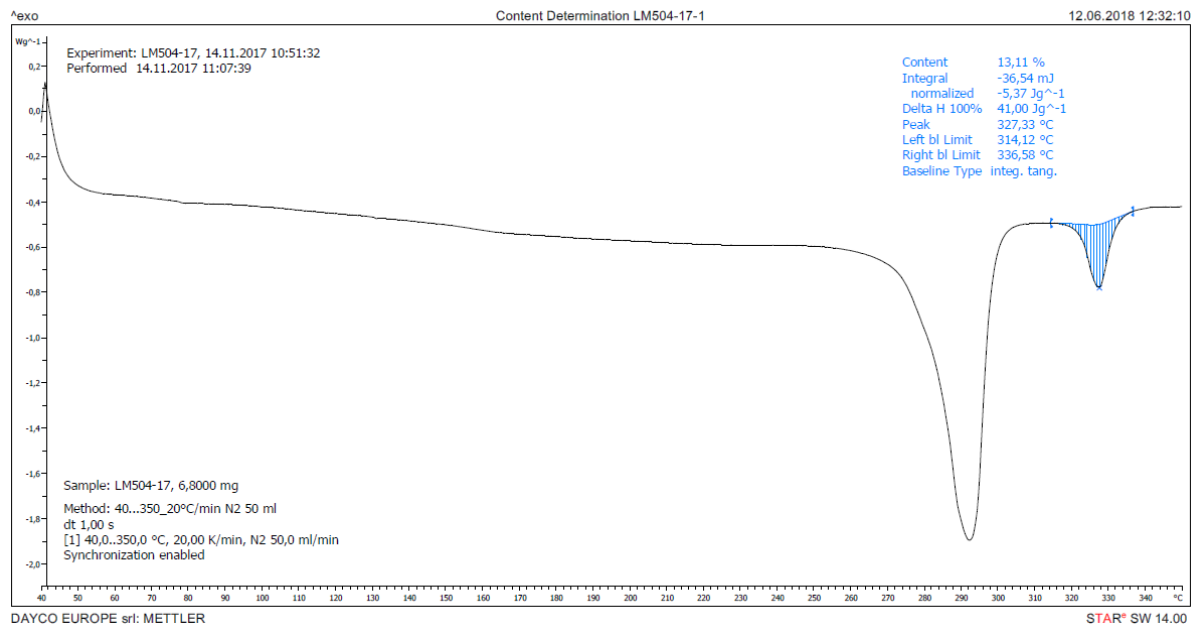


Figure 11.124: DSC measurement curve of sample LM504-17, from Group 1, obtained from Analysis 1, in which a content of 13,11% of PTFE was measured.

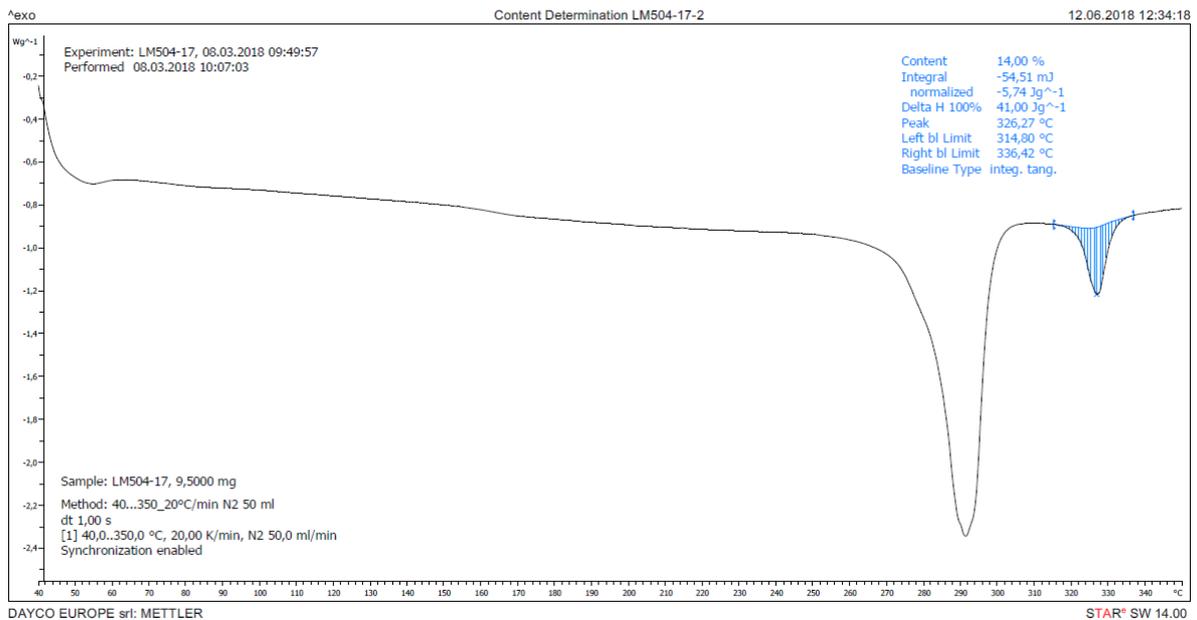


Figure 11.125: DSC measurement curve of sample LM504-17, from Group 2, obtained from Analysis 2, in which a content of 14,00% of PTFE was measured.

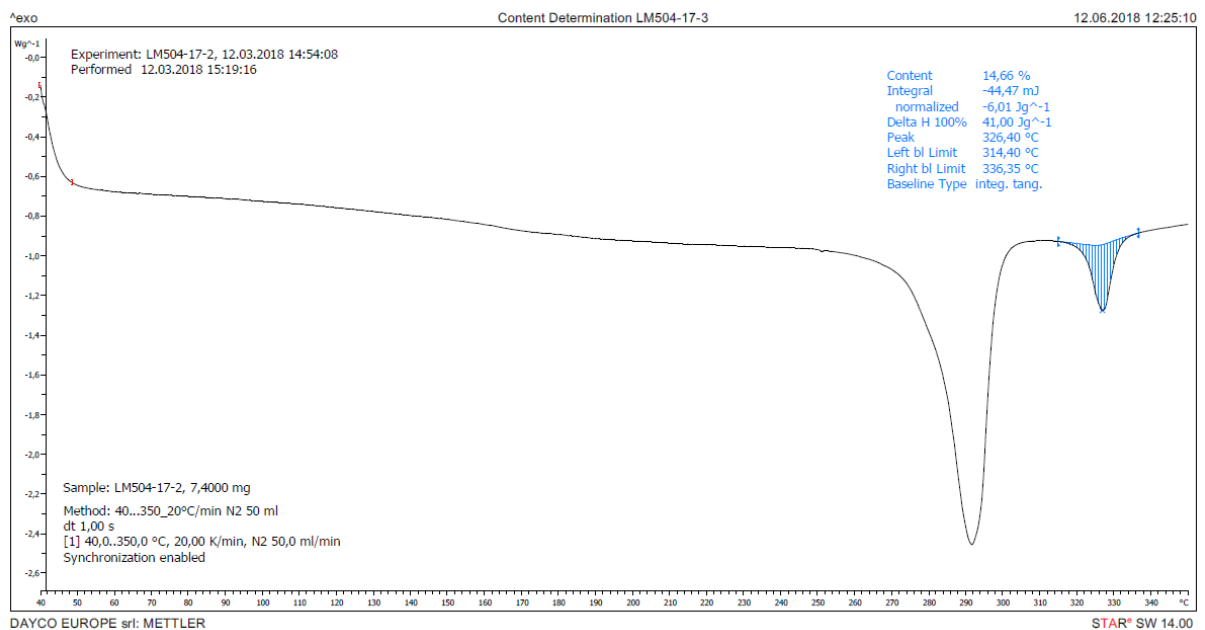


Figure 11.126: DSC measurement curve of sample LM504-17, from Group 3, obtained from Analysis 3, in which a content of 14,66% of PTFE was measured.

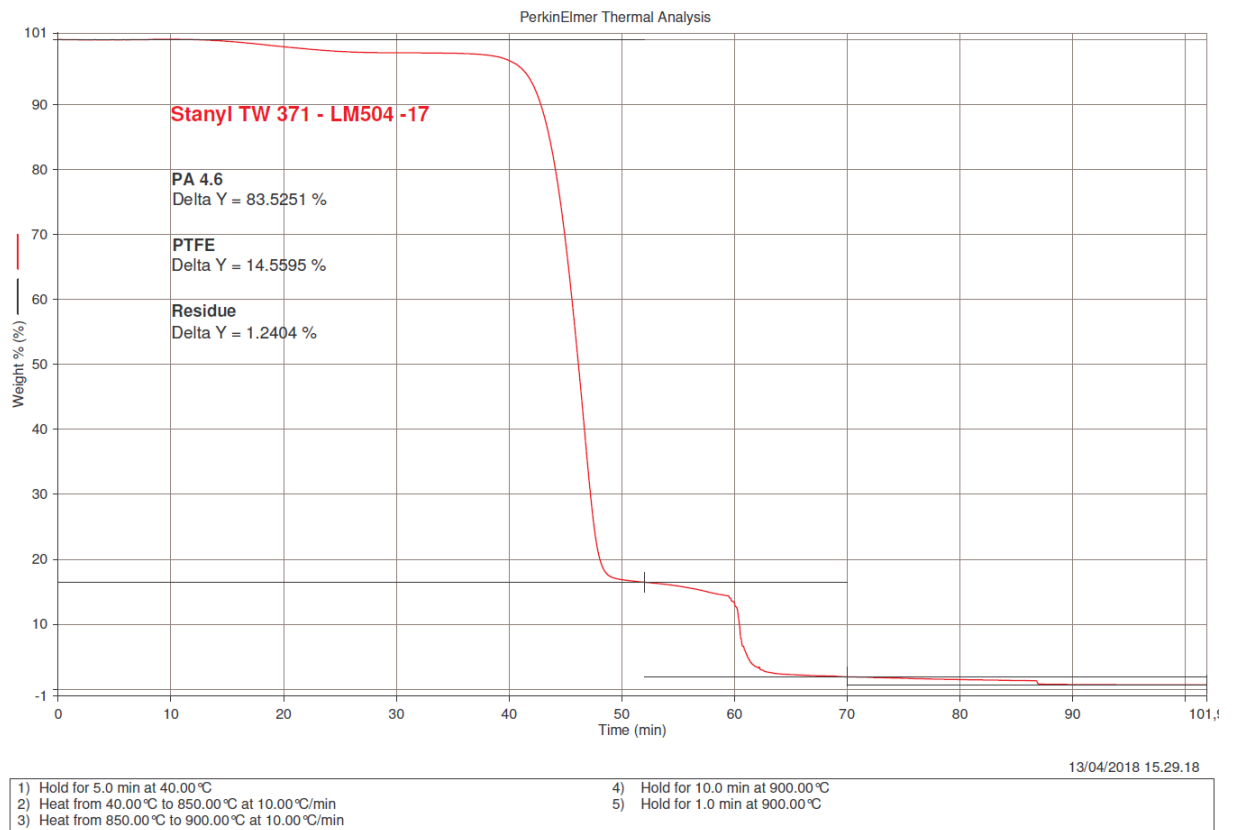


Figure 11.127: TGA measurement curve of sample LM504-17. The contents of PA46, PTFE and residue are, respectively, 83.5251%, 14.5595% and 1.2404%.